DEVELOPING CMMCA FLIGHT PROFILES FOR CRUISE MISSILE TRACKING

THESIS

Andrew C. Hachman
Captain, USAF

AFIT/GOR/ENS/92M-13

DEPARTMENT OF THE AIR FORCE
AIR UNIVERSITY
AIR FORCE INSTITUTE OF TECHNOLOGY

Wright-Patterson Air Force Base, Ohio

REPORT DOCUMENTATION PAGE

Form Approved
OMB No. 0704-0188

1. AGENCY USE ONLY (Leave blank)	2. REPORT DATE	3. REPORT TYPE AND DATES COVERED
	March 1992	Master's Thesis

4. TITLE AND SUBTITLE
DEVELOPING CMMCA FLIGHT PROFILES FOR CRUISE MISSILE TRACKING

5. FUNDING NUMBERS

6. AUTHOR(S)
Andrew C. Hachman, Captain, USAF

7. PERFORMING ORGANIZATION NAME(S) AND ADDRESS(ES)
Air Force Institute of Technology, WPAFB OH 45433-6583

8. PERFORMING ORGANIZATION REPORT NUMBER
AFIT/GOR/ENS/92M-13

9. SPONSORING/MONITORING AGENCY NAME(S) AND ADDRESS(ES)
4950 Test Wing/FFE
Wright Patterson AFB, OH 45433

10. SPONSORING/MONITORING AGENCY REPORT NUMBER

11. SUPPLEMENTARY NOTES

12a. DISTRIBUTION/AVAILABILITY STATEMENT
Approved for public release; distribution unlimited

12b. DISTRIBUTION CODE

13. ABSTRACT *(Maximum 200 words)*

The Air Force has recently acquired two aircraft dedicated for cruise missile tracking. These aircraft, known as the Cruise Missile Mission Control Aircraft (CMMCA), are responsible for collecting data from the missile and tracking and positively controlling the missile during live fire testing over the western United States. Due to the limited tracking radar range and the flight characteristics of the CMMCA, tracking cruise missiles through complex maneuvers is not always possible. A FORTRAN optimization, based on flight simulation and optimal control theory, was written in a prior thesis effort in order to determine optimal CMMCA flight profiles for tracking cruise missiles through certain maneuvers. The primary emphasis of this research effort was to conduct an analysis of the previously written optimization program, and to make the appropriate modifications to improve the performance and efficiency of the program. The program was tested over several different missile flight paths, using a variety of different initial program conditions and input parameters, in order to find the program modifications and parameter settings that produced the best CMMCA flight profiles in response to the given cruise missile flight path.

14. SUBJECT TERMS	15. NUMBER OF PAGES
Radar tracking; Control theory; Guided missiles; Flight Simulation; Computerized Simulation; Guidance	277
	16. PRICE CODE

17. SECURITY CLASSIFICATION OF REPORT	18. SECURITY CLASSIFICATION OF THIS PAGE	19. SECURITY CLASSIFICATION OF ABSTRACT	20. LIMITATION OF ABSTRACT
Unclassified	Unclassified	Unclassified	UL

THESIS APPROVAL

STUDENT: Captain Andrew C. Hachman CLASS: GOR 92-M

THESIS TITLE: Developing CMMCA Flight Profiles For Cruise Missile Tracking

DEFENSE DATE: 4 MAR 92

COMMITTEE:	NAME/DEPARTMENT	SIGNATURE
Advisor	Colonel Thomas F. Schuppe/ENS	
Reader	Major Dennis C. Dietz/ENS	

AFIT/GOR/ENS/92M-13

DEVELOPING CMMCA FLIGHT PROFILES FOR CRUISE MISSILE TRACKING

THESIS

Presented to the Faculty of the School of Engineering
of the Air Force Institute of Technology
Air University
In Partial Fulfillment of the
Requirements for the Degree of
Master of Science in Operations Research

Andrew C. Hachman, B.S.
Captain, USAF

March, 1992

Preface

The purpose of this research was to extend the work that was previously done by two other AFIT students on the CMMCA cruise missile tracking problem. The primary effort here was the critical analysis and modification of an optimization program that was written by Capt Tony Garton, and based on a penalty function and algorithm originally proposed by Lt Col William Baker.

I am indebted to my advisor Col Thomas Schuppe for suggesting the problem to me and for providing me a great amount of assistance and the occasional push in the proper direction when required. I would like to thank my reader, Maj Dennis Dietz for his insight and perception of the problem. I also wish to thank Lt Col Baker for his mathematical expertise and taking time from his schedule to answer my questions. I would also like to thank Capt Tony Garton for his interest in the problem and supplying me with the right information when needed. Finally I wish to thank my wife Shelley for allowing me to spend the first five months of our married life finishing my thesis and finishing school.

Andrew C. Hachman

Table of Contents

List of Figures

List of Tables

Abstract

The Air Force has recently acquired two aircraft dedicated for cruise missile tracking. These aircraft, known as the Cruise Missile Mission Control Aircraft (CMMCA), are responsible for collecting data from the missile and tracking and positively controlling the missile during live fire testing over the western United States. Due to the limited tracking radar range and the flight characteristics of the CMMCA, tracking cruise missiles through complex maneuvers is not always possible. A FORTRAN optimization, based on flight simulation and optimal control theory, was written in a prior thesis effort in order to determine optimal CMMCA flight profiles for tracking cruise missiles through certain maneuvers.

The primary emphasis of this research effort was to conduct an analysis of the previously written optimization program, and to make the appropriate modifications to improve the performance and efficiency of the program. The program was tested over several different missile flight paths, using a variety of different initial program conditions and input parameters, in order to find the program modifications and parameter settings that produced the best CMMCA flight profiles in response to the given cruise missile flight path.

DEVELOPING CMMCA FLIGHT PROFILES FOR CRUISE MISSILE TRACKING

I. Introduction

1.1 Background

The 4950th Test Wing at Wright-Patterson AFB will soon acquire two aircraft dedicated to supporting cruise missile flight tests. These aircraft, EC-18s known as the Cruise Missile Mission Control Aircraft (CMMCA), are designed to perform many different tasks during cruise missile flight tests, which take place across the western United States and Canada.

The primary role of the CMMCA is receiving and processing telemetry data from the missile. The CMMCA is responsible for tracking and positively controlling the missile, and also tracking any nearby aircraft intruding into the airspace of the cruise missile and of the CMMCA. Missile tracking and airspace control are accomplished using a modified AN/APG-63 auto-track radar system. The CMMCA also contains a remote command and control/flight termination system (RCC/FTS) which allows the CMMCA flight crew to take control of the missile if the missile strays from the intended course or in any situation of imminent danger to the missile or the surrounding environment (4).

During previous cruise missile flight tests, EC-135s from the 4950th Test Wing, which did not have the missile tracking capability of the CMMCA, received and processed telemetry data from the missile. The roles of tracking and maintaining control of the missile and the surrounding airspace were performed by a combination of fighter and other support aircraft. The CMMCA was designed to combine the roles of all these aircraft into one platform (5:1-3).

1.2 Problem Statement

Tracking cruise missiles is not a problem when the missile is flying a relatively straight path. However, during most cruise missile flight tests, the missile follows a complex route to test terrain masking and other deception techniques and to test the flight characteristics of the missile. The missile must also maneuver in order to stay within the confines of the restricted airspace of the test range. The difference in flight characteristics between the CMMCA and the cruise missile, combined with the difference in altitude between the two aircraft (the cruise missile flies at an altitude less than 1000 feet above ground level, while the CMMCA maintains an altitude of approximately 29,000 feet) makes tracking the missile through these maneuvers an extremely difficult problem, even though the CMMCA crew knows the planned flight path of the missile (19).

There have been at least two previous attempts at solving the cruise missile tracking problem. The first attempt was a thesis by Heavner, who investigated the use of, and applied, dynamic programming to solve the missile tracking problem. In his research, he found the optimal flight paths for the CMMCA for a particular set of simple missile maneuvers. However, this method proved to be too complex and computer intensive to solve the problem for anything more than a single maneuver (7:36-38).

Garton took another approach to solving this problem. In his thesis, Garton used a continuous simulation model to set up a flight path for a cruise missile maneuver, and also to find an initial guess for a CMMCA flight path to track the missile. He then used a FORTRAN program to improve upon the initial guess. This method found the optimal CMMCA flight path given the particular missile flight profile and a starting point for the CMMCA relative to the missile. This method also worked well for some simple missile maneuvers, but produced infeasible CMMCA flight paths for some of the more complex maneuvers (5:4). A more detailed description of Garton's research effort is found in Chapter 2.

Two considerable problems exist in attempting to find optimum CMMCA flight paths for cruise missile tracking. The first problem occurs when the entire cruise missile flight path (or a large portion of the flight path) is broken down into individual maneuvers, and the CMMCA flight path is optimized for each individual maneuver. The position of the CMMCA relative to the cruise missile at the end of the optimal flight path for one particular maneuver may not be the optimal starting point for the next cruise missile maneuver; it may not even be a feasible starting point for the next maneuver.

The second problem is that the modified AN/APG-63 radar system has a much shorter useful range than the telemetry system, and is therefore the limiting factor in the effective telemetry and tracking range from the CMMCA to the cruise missile. Also, the telemetry system of the CMMCA has a shorter range than the telemetry system on the EC-135s (4). Previously, the EC-135s could 'stand-off' while the cruise missile flew complex maneuvers and still receive good telemetry data. Performing these stand-off routines with the CMMCA will result in the tracking radar losing radar lock on the missile and a possible loss of telemetry data, and is therefore no longer an acceptable method of collecting data from the cruise missile during complex maneuvers. However, due to the limitations imposed by the flight characteristics of the CMMCA, following the same flight path as the cruise missile through these complex maneuvers is quite often not possible.

1.3 Research Objective

The objective of this research is to develop optimal CMMCA flight profiles for cruise missile tracking. A methodology will be produced that will find the optimal flight profiles for tracking cruise missiles through a series of complex maneuvers or over a large distance, given a particular missile flight path and the flight characteristics of the CMMCA. This research will extend the research already done by Garton and Heavner.

1.4 Assumptions and Limitations

Several assumptions and limitations must be made in order to narrow the scope of this thesis effort. Many of these assumptions were also valid for the research previously done by Garton and Heavner. These assumptions and limitations are the following:

- For this research effort, the slant range from the CMMCA to the cruise missile will be discounted. The CMMCA and cruise missile will be assumed to remain at constant altitudes during the entire flight path, and therefore any representation of the two aircraft will be in two dimensions.
- Due to the performance limitations of the tracking radar system, the feasible distance from the CMMCA to the cruise missile will be restricted to a range of five to fifteen nautical miles. The feasible azimuth deviation from the centerline of the CMMCA to the cruise missile will be restricted to a range of -60 to 60 degrees.
- Due to physical limitations of the CMMCA, the maximum true air speed (TAS) will be 480 knots and the minimum TAS will be 320 knots. The maximum desired bank angle will be 30 degrees.
- No wind conditions will be incurred by the cruise missile, but the wind conditions for the CMMCA are variable. This allows for different CMMCA headings caused by high altitude wind conditions.
- Although the movements of the CMMCA and cruise missile are continuous processes in time, numerical solution techniques used by the computer to solve the tracking problem require the flight paths to be expressed as discrete processes. The discrete time interval assumed for this research effort is 0.10 minutes.

1.5 Overview

Chapter 2 of this thesis provides an overview of the current literature that is pertinent to solving this cruise missile tracking problem. This includes information required for a better understanding of previous research efforts in this area, such as control theory, dynamic programming, and simulation. Chapter 2 also includes a development of Garton's approach to solving this problem. It covers the concepts and methodologies Garton used to develop his FORTRAN simulation program. Chapter 3 covers the initial modifications made to Garton's FORTRAN program, and proceeds into the experimental design methodologies developed for this research effort. Chapter 3 also includes all computer code and other material used in the development of the work. Chapter 4 is a presentation of the results of this research effort, and the recommendations and conclusions are presented in Chapter 5.

II. Literature Review

2.1 Introduction

In order to properly investigate the problem of tracking cruise missiles with the cruise missile mission control aircraft (CMMCA), this research must include a review of the current literature on information relating to the cruise missile tracking problem. This chapter begins with sections on the basics of missile tracking and optimal control theory. These are followed by a thorough description of the work done by Garton. Next, proportional navigation is briefly discussed as a possible alternate solution technique to this problem. The final section discusses simulation techniques, with an emphasis on verification and validation, which will constitute a significant portion of this research.

2.2 Cruise Missile Tracking

During cruise missile flight tests, the CMMCA flight crew has the responsibility of keeping the cruise missile within the tracking radar system's radar cone over the entire flight of the missile, or over the greatest percentage of the missile's flight if 100 percent coverage is not possible. As was previously mentioned in Chapter 1, the assumed limits of the tracking radar for this research are 5 to 15 nautical miles in range and -60 to 60 degrees in azimuth. Figure 1 shows the azimuth and range limits of the tracking radar. In order to further simplify the cruise missile tracking problem, the cruise missile is assumed to be positively tracked by the CMMCA when the missile is anywhere within the tracking radar's coverage pattern. Establishing a nominal cruise missile position near the center of the CMMCA's radar coverage allows the flight crew to let the missile's position vary slightly in any direction with respect to the CMMCA without losing radar contact.

Cruise missile tracking must be accomplished without violating the physical constraints of the CMMCA. As discussed in Chapter 1, the airspeed limitations are a

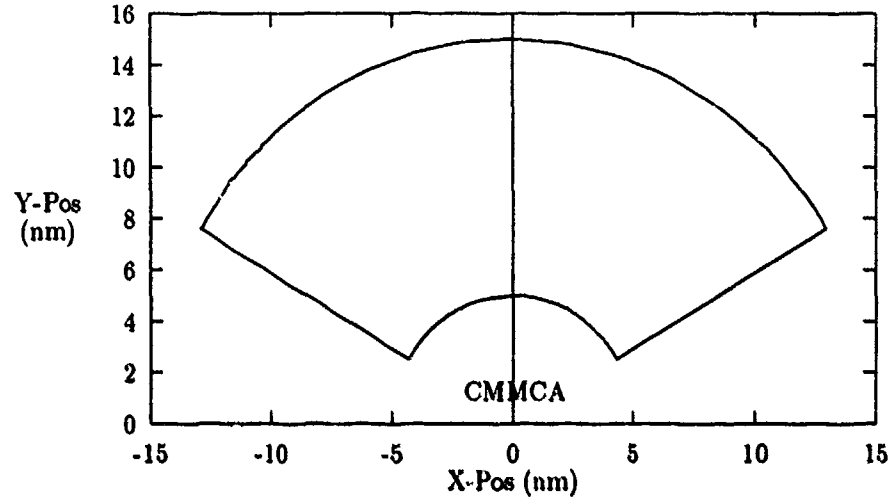

Figure 1. Range and Azimuth Limits of Tracking Radar

minimum of 320 knots and a maximum of 480 knots, while the bank angle is limited to 30 degrees. Sustaining bank angles greater than 30 degrees places physical strain and fatigue on the mission crew members on board the aircraft, many of whom are performing their jobs while standing up the entire mission (4). To allow for the greatest flexibility in cruise missile tracking without violating the aircraft's physical constraints, the nominal airspeed and bank angle should be at the center of the performance limitations, or 400 knots and 0 degrees respectively.

2.3 Optimal Control Theory

The objective of optimal control theory, as defined by Kirk, is "to determine the control signals that will cause a process to satisfy the physical constraints and at the same time minimize (or maximize) some performance criterion" (8:3). The cruise missile tracking problem of attempting to maximize the percentage of the cruise missile flight path that the CMMCA can track, while staying within the physical performance limits of the aircraft, can be viewed as an optimal control problem.

Garton used a combination of optimal control theory and simulation to model the flight paths of the CMMCA and the cruise missile (5:5). In setting up the equations to model the flight path of the two aircraft, Garton followed the three steps for formulating an optimal control problem as outlined by Kirk:

1. A mathematical description (or model) of the process to be controlled.
2. A statement of the physical constraints.
3. Specification of a performance criterion. (8:4)

The movements of the CMMCA and the cruise missile conform to physical laws, and therefore can be described by mathematical equations. Since the CMMCA and the cruise missile are both airborne vehicles, they can change their flight path in three independent directions and also rotate about three separate axes. This gives both aircraft six degrees of freedom (14:235). However, for the scope of this research, both the CMMCA and the cruise missile are assumed to maintain constant altitude (12). Therefore, their flight paths can be described in terms of a two-dimensional (North-South and East-West) coordinate system.

Defining the flight path of the CMMCA in mathematical form is the first step in solving the cruise missile tracking problem by any solution method and is also the first phase of formulating an optimal control problem. In his research, Garton defined the flight path of the CMMCA in the form of three differential equations (5:7-8). These equations, which describe a two- dimensional flight path for the CMMCA, are the following:

$$\frac{dx}{dt} = TAS * \sin(HDG) + WV_x \tag{1}$$

$$\frac{dy}{dt} = TAS * \cos(HDG) + WV_y \tag{2}$$

$$\frac{dHDG}{dt} = \frac{g * \tan(\alpha)}{TAS} \tag{3}$$

The independent variables in these equations are the aircraft heading (HDG), the true airspeed (TAS), the CMMCA bank angle (α), and the two components of wind velocity (WV_x and WV_y). The constant g in equation (3) represents the gravitational constant. Here, North is the positive y-direction, and East is the positive x-direction (5:8-9).

The choice of independent and dependent variables depends on what information is needed about the system being evaluated. Since the object of this research is to derive information about the position of the CMMCA relative to the cruise missile, the above equations are applicable.

The next phase of formulating a control theory solution is determining the physical limitations of the systems. The CMMCA has limitations on its maximum and minimum operating speeds and maximum bank angle. These limitations restrict the set of possible flight paths that the CMMCA could follow. Therefore, these limitations must also be included in the control theory formulation of the CMMCA flight path. In his research Garton solved the three differential equations which describe the flight path of the CMMCA (equations 1 - 3), changed them from a continuous to a discrete form (since the cruise missile tracking problem must be in a discrete form for a numerical solution), and transformed variables in the equations so that the control variables are the true airspeed and bank angle at each discrete time point. The final forms of these equations are as follows: (5:59)

$$x_i = x_0 + \sum_{j=0}^{i} TAS_j \sin[HDG_j] W_j^i \Delta t + WV_x(t - t_0) \tag{4}$$

$$y_i = y_0 + \sum_{j=0}^{i} TAS_j \cos[HDG_j] W_j^i \Delta t + WV_y(t - t_0) \tag{5}$$

$$HDG_i = HDG_0 + \sum_{j=0}^{i} C \frac{\tan[\alpha_j]}{TAS_j} W_j^i \Delta t \tag{6}$$

The previous equations can thus describe the position of the CMMCA at any discrete point along its flight path, based on the initial position of the CMMCA (x_0 and y_0), the initial heading of the CMMCA (HDG_0), the true airspeed and bank angle values up to that point (TAS_j and α_k), the heading values up to that point (which are functions of initial position, airspeed, and bank angle), and the wind conditions. The W_j^i values are quadrature weights, which are necessary for solving these equations numerically using the trapezoidal rule for numerical integration.

The final step in formulating an optimal control theory problem is selecting an appropriate performance criteria. Kirk defines an optimal control as "one that minimizes (or maximizes) the performance measure" (8:10). For the cruise missile tracking problem, the appropriate performance measure is maximizing the percentage of the cruise missile flight path over which the CMMCA can successfully track the missile.

2.4 Garton's Solution Method

As discussed earlier, in his attempt to solve this problem Garton used optimal control theory, which was implemented in a FORTRAN simulation program to find optimal CMMCA flight paths for tracking cruise missiles (5:18). At the heart of the FORTRAN program is an objective functional originally developed by Baker and later adapted to this particular solution method (2).

2.4.1 Objective Functional. The FORTRAN simulation program developed by Garton finds an optimal CMMCA flight path by means of iteratively performing a modified gradient search in order to minimize an objective functional (5:18-19). The objective functional describes the position of the CMMCA relative to a nominal position determined to be the best position for the CMMCA for tracking the cruise

missile. The objective functional is based on the following four independent variables: distance from the CMMCA to the cruise missile, the cruise missile azimuth angle relative to the CMMCA, the CMMCA true airspeed (TAS), and the CMMCA bank angle. The objective functional calculates a value at each discrete point in the CMMCA flight path, based on the difference between the variables and their nominal values. This 'penalty' increases as a function of the difference between the variable and its nominal value. Figure 2 shows the basic shape of the penalty curve for each of the objective functional variables. Therefore, the goal of the optimization program is to minimize the penalty imposed at each discrete point in the CMMCA flight path.

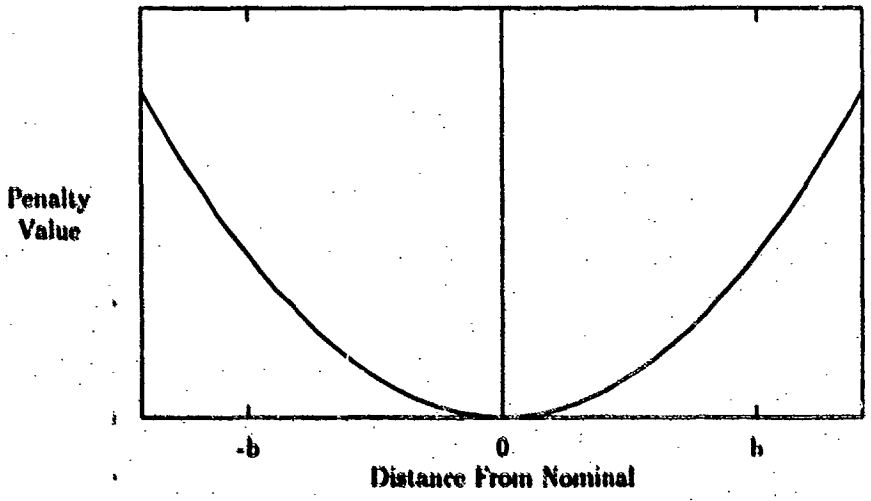

Figure 2. Penalty Function Shape

The first two variables are included in the objective functional in order to keep the cruise missile within the limits of the CMMCA's tracking radar system. As was previously mentioned in Chapter 1, the limits of the tracking radar are 5 to 15 nautical miles (nm) in range, and -60 to 60 degrees in azimuth. Figure 1 showed the azimuth and range limits of the tracking radar. The last two variables are included in the objective functional to ensure that the CMMCA does not exceed its airspeed

and bank angle limitations. The airspeed limitations assumed for this research are 320 to 480 knots, and the assumed bank angle limitation is 30 degrees.

The penalty induced by the current position error is described by the following equation:

$$J(r,\theta) = [r_i - r_0]^2 + W_1[\theta_i - \theta_0]^2 \tag{7}$$

where r_0 is the nominal desired range from the CMMCA to the cruise missile, θ_0 is the nominal desired azimuth angle between the two aircraft, and W_1 is a weighting factor used to scale the penalties between the range and azimuth angle deviations.

The penalty induced by CMMCA control inputs comes from the airspeed and bank angle. The airspeed penalty is of the form:

$$J_{TAS} = W_2 \left[\frac{V(t) - U_0}{\mu}\right]^{2*K_3} \tag{8}$$

where U_0 is the nominal desired true airspeed, μ is an allowable variance from the nominal true airspeed value, and K_3 is an integer value that affects the steepness of the penalty function. W_2 is another weighting factor used to scale the penalties.

The final part of the induced penalty comes from the bank angle. The bank angle penalty is of the form:

$$J_\phi = W_3 \left[\frac{\alpha_i}{\beta_0}\right]^{2*K_4} \tag{9}$$

where β_0 is the nominal desired bank angle and K_4 is an integer value that affects the steepness of the penalty function. W_3 is the final weighting factor used to scale the penalties.

The overall discrete form of the objective functional thus becomes:

$$J[\vec{V},\vec{\alpha}] = \sum_{i=0}^{N} W_i J_i \tag{10}$$

where

$$J_i = [r_i - r_0]^2 + W_1[\theta_i - \theta_0]^2 + W_2\left[\frac{V_i - U_0}{\mu}\right]^{2*K_3} + W_3\left[\frac{\alpha_i}{\beta_0}\right]^{2*K_4} \qquad (11)$$

The Wt_i values again are quadrature weights used to numerically calculate the objective functional penalty value using the trapezoidal rule.

Since the only two variables that can be controlled by the CMMCA flight crew are airspeed and bank angle, the distance and azimuth angle from the CMMCA to the cruise missile must be expressed in terms of the true airspeed and bank angle. Garton used equations (4) through (6) to express the current position (r_i and θ_i) in terms of true airspeed and bank angle, thereby describing the flight path using only the initial conditions and the two control inputs.

With the objective functional completed, Garton then constructed a FORTRAN program designed to find the optimal CMMCA flight path based upon the given cruise missile flight path and the CMMCA flight characteristics. Given an initial CMMCA flight path, this program evaluates the overall penalty value of the current CMMCA flight path by calculating the penalty induced at each discrete point in the flight path, and then calculates the changes to the true airspeed and bank angle necessary to produce a flight path with a smaller overall penalty.

The program uses a gradient search method to reduce the penalty value. It calculates the gradient of the objective functional with respect to each airspeed and bank angle in the maneuver (5:25-31). The opposite direction of the gradient indicates the direction of steepest decent, and thus the direction of maximum reduction of the objective functional. The program then computes the penalty value at two points along the direction of steepest decent, and using the current penalty value as a third point along the gradient, fits a parabola to these points. The point at which this fitted parabola is minimized is assumed to be close to the actual minimum

penalty value along the gradient, and is thus used as the next starting point for the minimization routine (1).

The penalty induced by the new flight path is then calculated and again changes are made to the airspeed and bank angle. These steps are performed iteratively until a solution determined to be the optimal solution is found. The solution is declared optimal if a minimum desired penalty value is achieved. If the program cannot produce a flight path with less penalty than the desired penalty value within a certain number of program iterations, the program is terminated.

The next two subsections describe the input files needed to make Garton's program work, and the output files produced by the program.

2.4.2 Optimization Program Inputs. The first input file to the optimization program is the file INPUT.DAT. This input file must contain the cruise missile x- and y- positions for each discrete time point in the cruise missile maneuver, and also an initial vector of CMMCA speeds and bank angles for each point. From an initial effort at solving this problem, Garton had designed a SLAM II simulation model designed to replicate the flight characteristics of both the cruise missile and the CMMCA (5:31). He modified this model, to produce as output, cruise missile x- and y-positions (relative to the initial CMMCA position) at discrete time intervals for a given cruise missile maneuver. This output file also included an initial guess for the CMMCA bank angle and speed necessary to pursue the missile. Therefore, the output file from this SLAM II program produced the necessary input flight profile for the FORTRAN optimization program (5:31-33).

Other input files required to run the FORTRAN program contain the nominal values for distance and azimuth from the CMMCA to the missile and true airspeed and bank angle, weights for each of the objective functional components, wind conditions for the CMMCA, and data to calculate the quadrature values needed for the numerical integrations.

2.4.3 Optimization Program Output. Garton's simulation program produces two output files for each cruise missile maneuver. The first output file, labeled RESULTS.OUT, lists the CMMCA bank angle, airspeed, range to the cruise missile, and azimuth angle from the CMMCA to the cruise missile for each discrete time point in the cruise missile manuever. RESULTS.OUT also includes the final JSTOP value and the number of iterations performed by the program to obtain the final solution. An example of the output file RESULTS.OUT, illustrating the results for a 90 degree right turn by the cruise missile, is shown in Table 1 below.

The other output file obtained from the optimization program is the cruise missile and CMMCA x- and y- positions for each discrete time point during the missile maneuver. This data can be used to produce plots of the cruise missile and the optimal CMMCA flight path for following the cruise missile maneuver. The plot for the 90 degree cruise missile turn example is shown in Figure 3.

2.4.4 FORTRAN Program Performance. Garton ran his optimization program for the following cruise missile flight paths: a straight flight with the CMMCA 8 nautical miles directly behind the missile, a straight flight with the CMMCA starting with a 5 nautical mile horizontal offset and 8 nautical miles behind the missile, and 90, 180, and 270 degree turns each with the CMMCA starting 8 nm directly behind the missile. The CMMCA was able to track the cruise missile through the straight flights and 90 degree turn with 100 percent radar coverage, but radar coverage fell dramatically for the 180 and 270 degree turns. The output results for each run are summarized in Table 2.

2.5 Proportional Navigation

Proportional navigation is a technique that is commonly used by airplanes and missiles in pursuit of other airborne vehicles. Proportional navigation, as stated by Guelman, is "a homing guidance technique in which the missile turn rate is directly

Table 1. Data From File RESULTS.OUT, 90 Degree Cruise Missile Turn

JSTOP = 7.691867 NUMBER OF ITERATIONS = 150				
Time	BANK (deg)	SPEED (kTAS)	RANGE (nm)	THETA (deg)
0.1	-9.3	400.4	8.0	1.4
0.2	-7.5	399.0	8.0	4.0
0.3	-5.9	397.8	8.0	6.3
0.4	-4.3	396.7	8.0	8.3
0.5	-2.9	395.7	8.0	10.0
0.6	-1.4	394.7	8.0	11.3
0.7	0.0	393.8	8.1	12.8
0.8	1.4	392.9	8.1	14.3
0.9	2.8	391.9	8.1	16.0
1.0	4.2	391.0	8.1	17.6
1.1	5.7	390.1	8.1	19.2
1.2	7.2	389.1	8.1	20.8
1.3	8.8	388.3	8.1	22.1
1.4	10.4	387.4	8.1	23.3
1.5	12.0	386.7	8.1	24.2
1.6	13.5	386.0	8.1	24.9
1.7	15.0	385.6	8.0	25.2
1.8	16.2	385.3	7.9	25.3
1.9	17.3	385.4	7.9	25.1
2.0	17.9	385.8	7.9	24.7
2.1	18.2	386.5	7.8	23.9
2.2	18.0	387.5	7.8	22.7
2.3	17.4	388.8	7.8	21.2
2.4	16.5	390.1	7.8	19.6
2.5	15.4	391.5	7.8	18.0
2.6	14.2	392.8	7.9	16.3
2.7	12.9	394.0	7.9	14.7
2.8	11.5	395.2	7.9	13.2
2.9	10.2	396.2	7.9	11.8
3.0	8.9	397.1	7.9	10.6
3.1	7.7	397.8	7.9	9.6
3.2	6.6	398.4	7.9	8.7
3.3	5.5	398.9	7.9	8.0
3.4	4.5	399.3	7.9	7.5
3.5	3.5	399.6	8.0	7.1
3.6	2.7	399.8	8.0	6.9
3.7	1.9	399.9	8.0	6.9
3.8	1.2	400.0	8.0	7.0

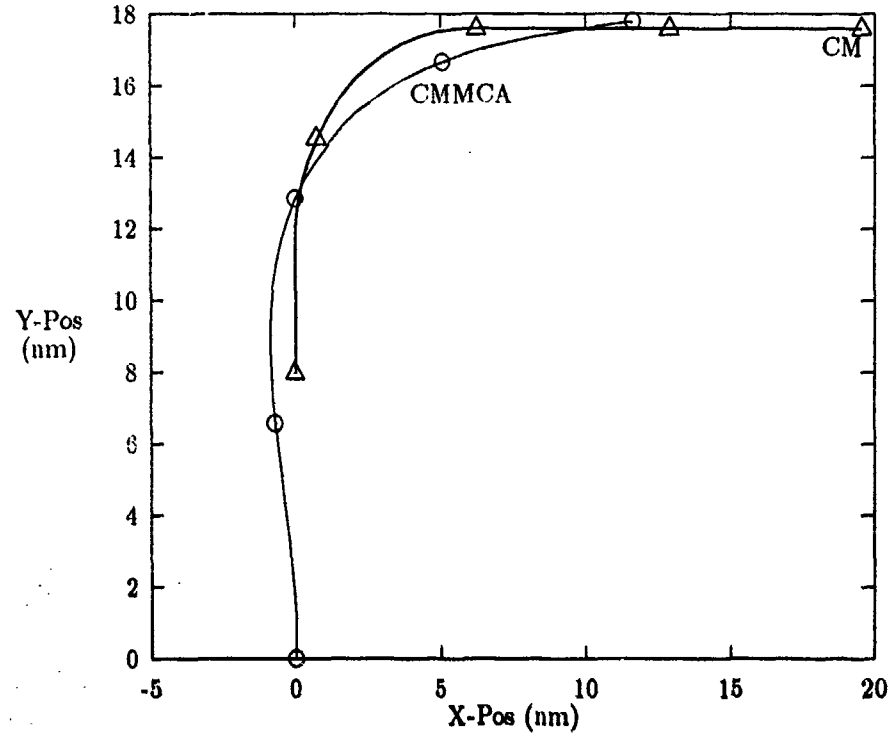

Figure 3. Graphical Output of 90 Degree Cruise Missile Turn

Table 2. Preliminary Results of Garton's Optimization Program

Flight Path	Percent Coverage
Straight	100
Straight w/ Offset	100
90 Degree Turn	100
180 Degree Turn	34.3
270 Degree Turn	58.7

proportional to the turn rate in space of the line of sight [to the pursued vehicle]" (6:364). In proportional navigation, the missile reacts to the movements of the vehicle being pursued and follows a flight path that is dependent on the the physical limitations of the missile and on the flight path of the other vehicle. The flight path of the missile becomes a function of the current heading and location of the maneuvering target.

The laws governing the proportional navigation flight paths for vehicles in pursuit of maneuvering targets are represented by non-linear differential equations, with the independent variables being the velocity and acceleration of the target vehicle (9:81-82). The complexity of these equations makes solving them in closed form computationally intractable. However, recent work by Mahapatra and Shukla has led to a quasilinear closed-form solution for the proportional navigation equations. Mahapatra and Shukla have shown this solution to be very accurate by comparing it to current linear approximation and numerical solution techniques (9:88).

With this quasilinear solution technique, a computer could be used to determine the proportional navigation flight path of a CMMCA, given a particular set of CMMCA and cruise missile velocity and acceleration conditions. Since the missile flight path is known prior to each cruise missile flight test, the cruise missile and CMMCA flight paths could be simulated with the CMMCA following proportional navigation laws to pursue the cruise missile through various maneuvers. By adjusting the starting point and the navigation rules of the CMMCA, a set of flight paths could be developed and analyzed to find the optimal CMMCA flight path.

2.6 Simulation

Computer simulation is one of the possible techniques available to aid in determining optimal CMMCA flight paths for tracking cruise missiles. Simulation has previously been used on this problem and also on similar problems. Garton used simulation to determine flight paths obtained through control theory methods (5:31).

Simulation was successfully used in a similar situation, when it was used to model the motion of the Orbital Maneuvering Vehicle during the performance of required duties in space. This simulation helped determine the expected capabilities of the planned Orbital Maneuvering Vehicle, even though that vehicle will not be built for many years (15:98-99).

Simulation is the process of designing and building a computer model of a system and then using that model to draw inferences about the modeled system (10:6). The purpose of simulation, as described by Bekey, is "either to yield insight into the behavior of the process being simulated or to make predictions of performance" (3:57). If simulation is to be useful, it must simplify the description of the system while still accurately representing the system conditions to be studied.

The simulation process can be broken down into ten distinct steps. Pritsker describes these steps as the following:

1. Problem Formulation.
2. Model Building.
3. Data Acquisition.
4. Model Translation.
5. Verification.
6. Validation.
7. Strategic and Tactical Planning.
8. Experimentation.
9. Analysis of Results.
10. Implementation and Documentation. (10:10-11)

The most important steps of this model building procedure are the verification and validation. Verification of a simulation model ensures that the system simulation performs exactly as the model-builder intended. Validation of a model ensures that the simulation represents the system well enough to gain useful information about the system. The underlying problem is that validity is not a deterministic condition; a model cannot be viewed as either valid or not valid. The validity of a model is

more of a stochastic process, and is actually a measure of the degree to which the model represents the system (13:177-178).

Sargent describes the validation process as consisting of "performing test and evaluation within the model development process to determine whether a model is valid or not" (11:33). Sargent goes on to describe several validation techniques, including comparison to other models, validity based on expected events, and comparison to historical data (11:33-34). The validity of the simulation of CMMCA flight paths can be ensured by two of these three methods. The simulation can be compared to historical data gathered during previous cruise missile tests, and the simulation can also be checked for events that are expected to take place during the cruise missile flight testing (such as CMMCA reaction to certain cruise missile maneuvers). Another method of validating the simulation is comparing the results of the modified code to Garton's original code. Any modifications to the simulation should show some improvement to the simulation, or should not be included in the modifications. Therefore, any simulation model built during this research can be effectively validated by more than one method.

2.7 Summary

Through optimal control theory, Garton and Baker developed an equation that describes the flight path of the CMMCA in discrete time points relative to the flight path of the cruise missile and assigns a penalty value if the flight path is not optimal. Garton then used this equation as the basis for a FORTRAN program which is designed to find optimal flight paths for cruise missile tracking. Garton's research went a long way towards solving the cruise missile tracking problem, but the premliminary results presented in section 2.4.4 show that there is still much room for improvement. This chapter presented a summary of Garton's work and the mathematical formulation leading up to his FORTRAN program, and also presented information necessary for continuing his work toward finding optimal solutions.

III. Methodology

3.1 Introduction

This chapter describes the steps taken in the analysis and modification of Garton's optimization code. The first section explains the modifications made to the output files in order to better analyze the performance of the simulation. The second section discusses the changes made to the weighting factors of the individual components of the objective functional. Next, the four cruise missile flight paths used to test the program are presented and discussed, followed by a section describing an alternate initial CMMCA flight path. The next section of this chapter discusses the experimental design techniques used to analyze the performance of the optimization program and determine the weight settings for optimal tracking performance. Following that is a discussion of three different methods which were used to improve the performance of the program over the last flight profile. The final section of this chapter discusses the analysis of the program in an attempt to determine the conditions necessary for convergence of the algorithm to a single optimal solution.

3.2 Output Modifications to Optimization Program

Originally, Garton's optimization program printed out the CMMCA bank angle, airspeed, range to the cruise missile, and azimuth angle to the cruise missile for every time point in the maneuver. This information was printed to the file RESULTS.OUT. The program also output the x and y coordinates of both the CMMCA and cruise missile at every discrete point of the entire maneuver into the file PLOT.DAT. An example of this output for a 90 degree turn was seen in Figure 3. This information is very beneficial to CMMCA mission planners and crew members when attempting to figure out how to track cruise missiles, but does not present enough information in order to perform a rigorous analysis of the performance of the program.

In order to properly evaluate the performance of the optimization program, several changes needed to be made to the output files. These changes inlude modification of existing output files, and also creating an additional output file.

3.2.1 RESULTS.OUT Modifications. The most needed performance criterion missing from the output of the optimization program is the percentage of the cruise missile maneuver that the cruise missile was in the radar cone of the CMMCA's tracking radar system. The percentage of radar coverage through the given cruise missile maneuver is really the key point in the optimization of the CMMCA flight path, since the CMMCA flight crew seeks to maximize ths percentage. The proper FORTRAN code was added to the program so that the optimization program determines the percentage of radar coverage over the entire cruise missile maneuver. This is accomplished by evaluating at each discrete time point whether the cruise missile is within the CMMCA's radar limits, and then calculating the percentage of radar coverage for the entire run.

Another missing criterion is the percentage of the cruise missile maneuver that the CMMCA is within its bank angle and airspeed constraints. The CMMCA airspeed and bank angle at each point are calculated by the optimization program and printed out in the file RESULTS.OUT, but the percentage of the flight path that the CMMCA is within these constraints is not calculated. The program was modified to calculate the percentage of the missile maneuver that the CMMCA is within its constraints. This value is found by calculating at each time point whether the CMMCA is within its constraints, and then calculating the percentage over the entire maneuver.

An example of the modified RESULTS.OUT for the 90 degree turn example of Chapter 2, indicating the additions made to the output file RESULTS.OUT, is shown in Table 3. Two columns were added to the output file. The first column added, labeled RADAR, indicates at each discrete point whether or not the cruise missile

was within the CMMCA's radar cone. The second column added, labeled STRUCT, indicates at each discrete point whether or not the CMMCA was within the physical limits of the aircraft. One item to note is that the percentage of radar coverage, the points at which radar coverage does not occur, the percentage of satisfying the physical constraints, and the points at which the constraints are not satisfied, are calculated only for the CMMCA flight path determined by the program as having the minimum penalty value. The coverage and constraint percentages are not used by the program to evaluate the optimal flight path. The program still determines the optimal path by the minimized value of the objective functional.

3.2.2 Penalty Source Calculations. Another output modification determined as necessary for properly analyzing the optimization routine is the evaluation of the source of the induced penalty at each point in the flight path. This will show the points in the CMMCA flight path which are inducing the penalty into the objective functional, and which penalty function components (i.e. range, bank angle) are inducing the penalty. Knowing the source of the penalty, along with the 'trouble spots' in the CMMCA flight path, should show where the program is failing or having problems, and will help indicate the 'route' to be taken towards producing a better algorithm.

The objective functional values for each objective functional variable at each discrete time point were added to the CMMCA program output as a separate file, called JCALC.OUT. The output file JCALC.OUT is shown in Table 4 for the 90 degree turn example of Chapter 2. This table shows the penalty value induced by each objective functional component at each discrete time point, and also shows the points where the missile was out of the radar cone and where the CMMCA exceeded its physical constraints.

The graphical output of the file JCALC.OUT is shown in Figures 4 through 7. These plots indicate very clearly the source of the final penalty value, and where

Table 3. Modified File RESULTS.OUT Output, 90 Degree Missile Turn

JSTOP = 7.691867
NUMBER OF ITERATIONS = 150

Time	BANK	SPEED	RANGE	THETA	RADAR	STRUCT
0.1	-9.6	400.0	8.0	1.4	1	1
0.2	-7.8	398.9	8.0	4.2	1	1
0.3	-6.1	397.9	8.0	6.6	1	1
0.4	-4.5	397.1	8.0	8.7	1	1
0.5	-3.0	396.3	8.0	10.4	1	1
0.6	-1.5	395.5	8.1	11.7	1	1
0.7	0.0	394.8	8.1	13.2	1	1
0.8	1.5	394.0	8.1	14.8	1	1
0.9	2.9	393.3	8.1	16.4	1	1
1.0	4.4	392.5	8.1	18.1	1	1
1.1	5.9	391.8	8.1	19.7	1	1
1.2	7.5	391.1	8.1	21.1	1	1
1.3	9.0	390.4	8.1	22.5	1	1
1.4	10.6	389.7	8.1	23.6	1	1
1.5	12.2	389.1	8.1	24.5	1	1
1.6	13.7	388.7	8.1	25.1	1	1
1.7	15.1	388.3	8.0	25.4	1	1
1.8	16.3	388.2	8.0	25.5	1	1
1.9	17.3	388.3	7.9	25.4	1	1
2.0	17.9	388.6	7.9	25.1	1	1
2.1	18.1	389.2	7.8	24.3	1	1
2.2	18.0	390.0	7.8	23.2	1	1
2.3	17.5	391.0	7.8	21.8	1	1
2.4	16.6	392.1	7.8	20.2	1	1
2.5	15.6	393.2	7.8	18.5	1	1
2.6	14.4	394.2	7.9	16.9	1	1
2.7	13.1	395.2	7.9	15.2	1	1
2.8	11.8	396.2	7.9	13.7	1	1
2.9	10.5	397.0	7.9	12.2	1	1
3.0	9.2	397.7	7.9	10.9	1	1
3.1	7.9	398.3	7.9	9.8	1	1
3.2	6.7	398.8	7.9	8.9	1	1
3.3	5.6	399.2	7.9	8.1	1	1
3.4	4.6	399.5	8.0	7.5	1	1
3.5	3.6	399.7	8.0	7.0	1	1
3.6	2.7	399.9	8.0	6.8	1	1
3.7	1.9	400.0	8.0	6.7	1	1
3.8	1.2	400.0	8.0	6.9	1	1

CM IN RADAR CONE 100.00 PERCENT
CMMCA IN STURCTURAL LIMITS 100.00 PERCENT

Table 4. File JCALC.OUT Output, 90 Degree Missile Turn

JRANGE	JTHETA	JSPEED	JBANK	RADAR	STRUCT
0.0000	0.0006	0.0000	0.1038	1	1
0.0000	0.0053	0.0000	0.0683	1	1
0.0001	0.0132	0.0000	0.0419	1	1
0.0003	0.0228	0.0000	0.0229	1	1
0.0010	0.0328	0.0000	0.0100	1	1
0.0026	0.0420	0.0000	0.0025	1	1
0.0054	0.0534	0.0000	0.0000	1	1
0.0092	0.0669	0.0000	0.0024	1	1
0.0134	0.0824	0.0001	0.0097	1	1
0.0170	0.0996	0.0001	0.0220	1	1
0.0191	0.1178	0.0001	0.0397	1	1
0.0199	0.1361	0.0002	0.0630	1	1
0.0184	0.1537	0.0003	0.0921	1	1
0.0154	0.1695	0.0004	0.1269	1	1
0.0109	0.1824	0.0004	0.1669	1	1
0.0060	0.1917	0.0005	0.2106	1	1
0.0017	0.1970	0.0006	0.2558	1	1
0.0000	0.1982	0.0006	0.2990	1	1
0.0040	0.1960	0.0006	0.3357	1	1
0.0176	0.1918	0.0005	0.3608	1	1
0.0292	0.1805	0.0004	0.3706	1	1
0.0348	0.1641	0.0003	0.3642	1	1
0.0348	0.1448	0.0002	0.3434	1	1
0.0313	0.1245	0.0001	0.3119	1	1
0.0263	0.1047	0.0001	0.2740	1	1
0.0210	0.0865	0.0000	0.2336	1	1
0.0163	0.0705	0.0000	0.1938	1	1
0.0123	0.0569	0.0000	0.1567	1	1
0.0092	0.0456	0.0000	0.1235	1	1
0.0069	0.0365	0.0000	0.0949	1	1
0.0052	0.0293	0.0000	0.0708	1	1
0.0040	0.0239	0.0000	0.0511	1	1
0.0030	0.0198	0.0000	0.0355	1	1
0.0024	0.0169	0.0000	0.0234	1	1
0.0018	0.0151	0.0000	0.0145	1	1
0.0014	0.0141	0.0000	0.0081	1	1
0.0011	0.0138	0.0000	0.0040	1	1
0.0008	0.0143	0.0000	0.0015	1	1
0.0005	0.0155	0.0000	0.0003	1	1
0.0002	0.0086	0.0000	0.0000	1	1

the cruise missile was out of the radar system's coverage area. The penalty source information in this graphical form will clearly benefit the analysis of the optimization program.

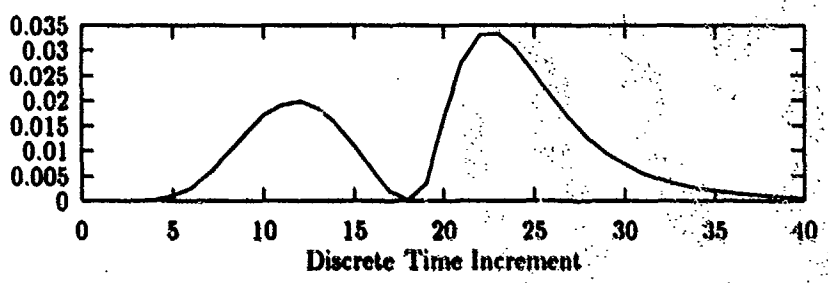

Figure 4. Penalty Incurred From Range Error, 90 Degree Missile Turn

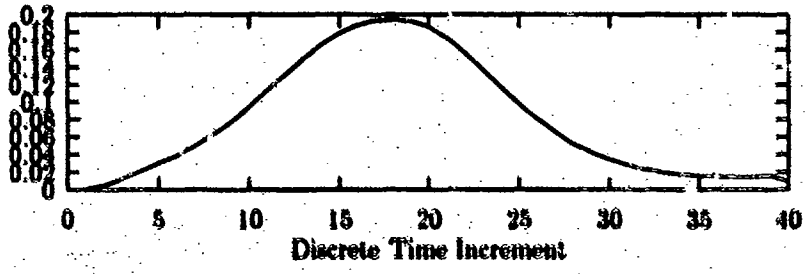

Figure 5. Penalty Incurred From Azimuth Error, 90 Degree Missile Turn

3.3 Normalization of Objective Function Weights

The next phase of program modification involves the individual components of the objective functional. Recall the discrete objective functional was given by:

$$J[\vec{V}, \vec{a}] \approx \sum_{i=0}^{N} W t_i J_i \qquad (12)$$

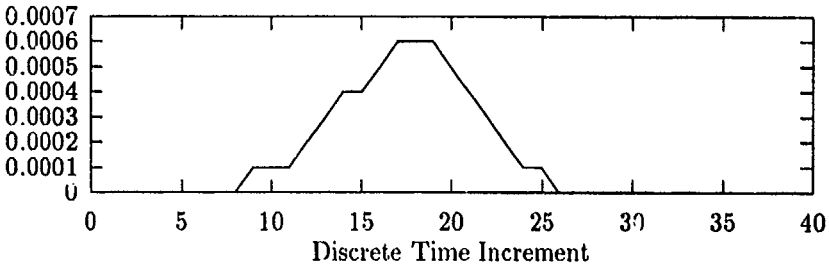

Figure 6. Penalty Incurred From Airspeed Error, 90 Degree Missile Turn

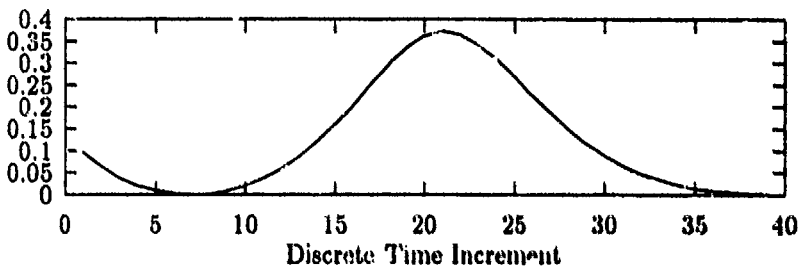

Figure 7. Penalty Incurred From Bank Angle Error, 90 Degree Missile Turn

where

$$J_i = [r_i - r_0]^2 + W_1[\theta_i - \theta_0]^2 + W_2\left[\frac{V_i - U_0}{\mu}\right]^{2*K_3} + W_3\left[\frac{\alpha_i}{\beta_0}\right]^{2*K_4} \qquad (13)$$

The objective function penalty value J_i at each discrete time point becomes greater than zero when one or more of the variables of the functional are not at their nominal values. The value of J_i incurred depends on the difference between the variable and its nominal value.

As seen in Table 3, most of the total J value for the 90 degree turn example was generated from the bank angle and azimuth angle components of the objective functional, whereas the penalty imposed by the range component was one order of magnitude smaller and the penalty imposed by the airspeed component was three orders of magnitude smaller. Therefore, in evaluating the optimal CMMCA flight path for the 90 degree cruise missile turn, the most important components as seen by the program were the bank angle and azimuth angle. This is due primarily to the differences in units between the objective functional components. Therefore, the components of the objective functional must be scaled with respect to each other, so that a particular range error produces the same penalty as some particular azimuth angle error, airspeed error, and bank angle error.

Since the range limits of the CMMCA are 5 to 15 nautical miles (nm) and the nominal range was set by Garton at 8 nm from the CMMCA to the cruise missile, a penalty of $(15 - 8)^2$ or 49 is incurred when the missile is at the outer limit of the CMMCA's radar cone, and a penalty of $(5 - 8)^2$ or 9 is incurred when the missile is at the inner radar limit. By adjusting the nominal range value to 10 nm, the same penalty value (25) is incurred when the missile is at either the inner or outer limit of the radar cone. (The nominal range from the CMMCA to the cruise missile is one of the variables that will be adjusted during the experimenting with the program.)

This adjustment provides a logical basis for comparing the range penalty to the other penalties.

Logically, the same penalty should be assigned when the cruise missile is at the range limit as when the missile is at the azimuth limit of the radar cone. The azimuth limits of the CMMCA's radar cone are -60 to 60 degrees, or -1.047 to 1.047 radians since the program performs all angle computations in radians. Therefore, at the azimuth limits of the radar, the penalty imposed is $(1.047 - 0)^2$ or 1.097. This means that the range penalty is 22.797 times greater at the radar limits than the azimuth penalty. Therefore, the azimuth scaling factor required to equate the range and azimuth errors is $S_1 = 22.797$.

Similarly, scaling factors can be applied to the airspeed and bank angle errors. The nominal airspeed is currently 400 KTAS, or because the program calculates airspeed in nm/min, 6.667 nm/min. The airspeed limitations are 320 to 480 KTAS, or 5.333 to 8 nm/min. Garton previously set the other airspeed constants μ and K_3 set to 1.25 and 2 respectively, and at these settings the upper (and lower) airspeed limit imposed a penalty of $((8 - 6.667)/1.25)^4$, or 1.2945. Therefore, the scaling factor required to equate the radar range and azimuth limits to the airspeed limit is $S_2 = 19.312$.

The CMMCA bank angle limit is 30 degrees, or 0.524 radians. With the current values of β_0 and K_4 set and 0.524 and 1 respectively, the objective functional imposes a penalty of 1 when the bank angle is at its 30 degree limit. Therefore, the scaling factor required to equate the bank angle limit to the range, azimuth, and airspeed limits is $S_3 = 25$.

With all these scaling factors included, the final form of the objective functional is the following:

$$J[\vec{V}, \vec{\alpha}] = \sum_{i=0}^{N} W t_i J_i \qquad (14)$$

where

$$J_i = [r_i - r_0]^2 + 22.797W_1[\theta_i - \theta_0]^2 + 19.312W_2\left[\frac{V_i - U_0}{\mu}\right]^{2*K_3} + 25W_3\left[\frac{\alpha_i}{\beta_0}\right]^{2*K_4} \quad (15)$$

This final form of the objective functional became the starting point for the analysis performed on the optimization program. With all necessary program modifications completed, the next phase of the research was analyzing the performance of the algorithm and attempting to adjust the objective function variables to achieve the best possible performance of the algorithm, regardless of the cruise missile maneuver being tracked.

3.4 Cruise Missile Flight Paths

In order to test the optimization program's response to cruise missile maneuvers of varying lengths and complexity, four distinctly different cruise missile flight paths were constructed. These flight paths also provided a basis over which the program could be run in order to test for improvements in the algorithm. These improvements were obtained from altering the variables of the objective functional and also varying the initial CMMCA flight path. The four initial CMMCA flight paths, and the reasons for choosing each particular path, are discussed below.

The first flight path was a 180 degree cruise missile turn. This was the first maneuver for which Garton's program previously could not find a feasible CMMCA flight path to successfully follow the missile. This was the simplest maneuver attempted, because any improved optimization program was expected to be able to replicate Garton's success for the straight cruise missile path and also the 90 degree turn. Previously, the program could achieve about 38 percent radar coverage for a 180 degree turn. Figure 8 shows the 180 degree cruise missile turn.

The second flight path was a 270 degree cruise missile turn. This maneuver was also tested by Garton, but the optimization program could not find an acceptable

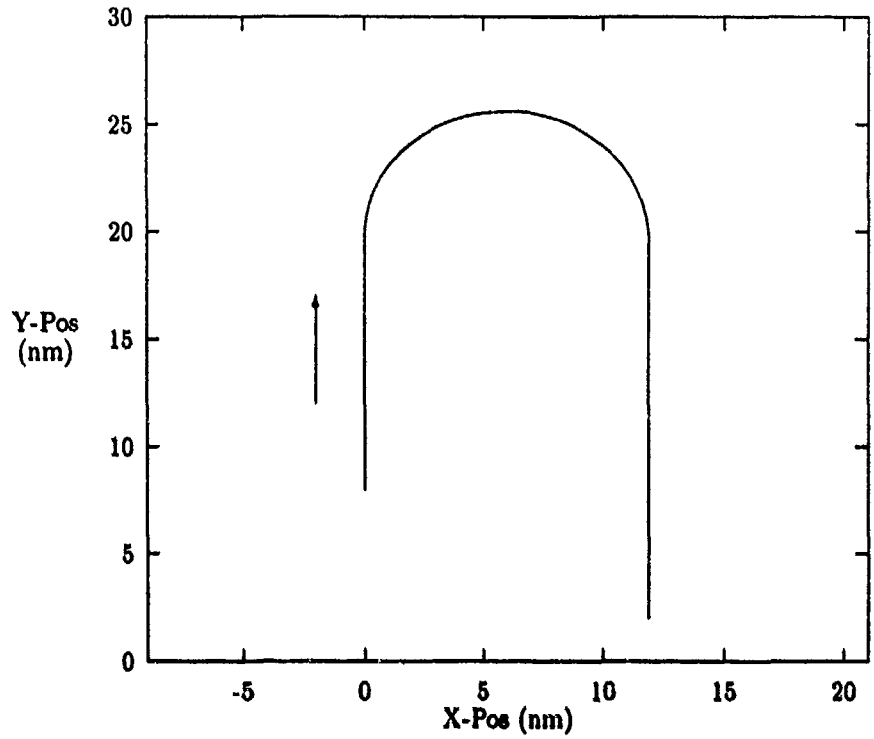

Figure 8. Flight Path One, 180 Degree Cruise Missile Turn

CMMCA flight path for this maneuver. For the 270 degree turn, the program previously achieved approximately 58 percent radar coverage, but the CMMCA exceeded physical limitations over about 10 percent of the flight path. Figure 9 shows the 270 degree cruise missile turn.

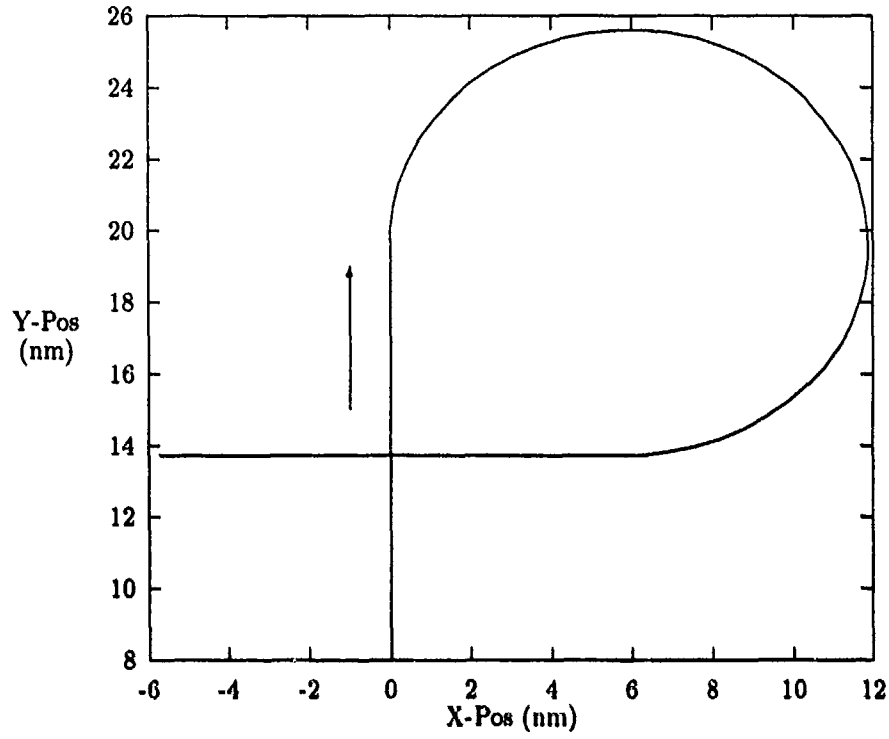

Figure 9. Flight Path Two, 270 Degree Cruise Missile Turn

The third flight path was two 270 degree turns. This flight path was a good test of the program's capability of handling multiple maneuvers at one time. Garton's program had never been tested over this flight path. Figure 10 shows the two 270 degree cruise missile turns.

The final flight path was a section of an actual cruise missile flight path that had previously been flown during cruise missile flight tests. The mission planners were not able to find an ARIA aircraft (EC-135 predecessor to the CMMCA) flight

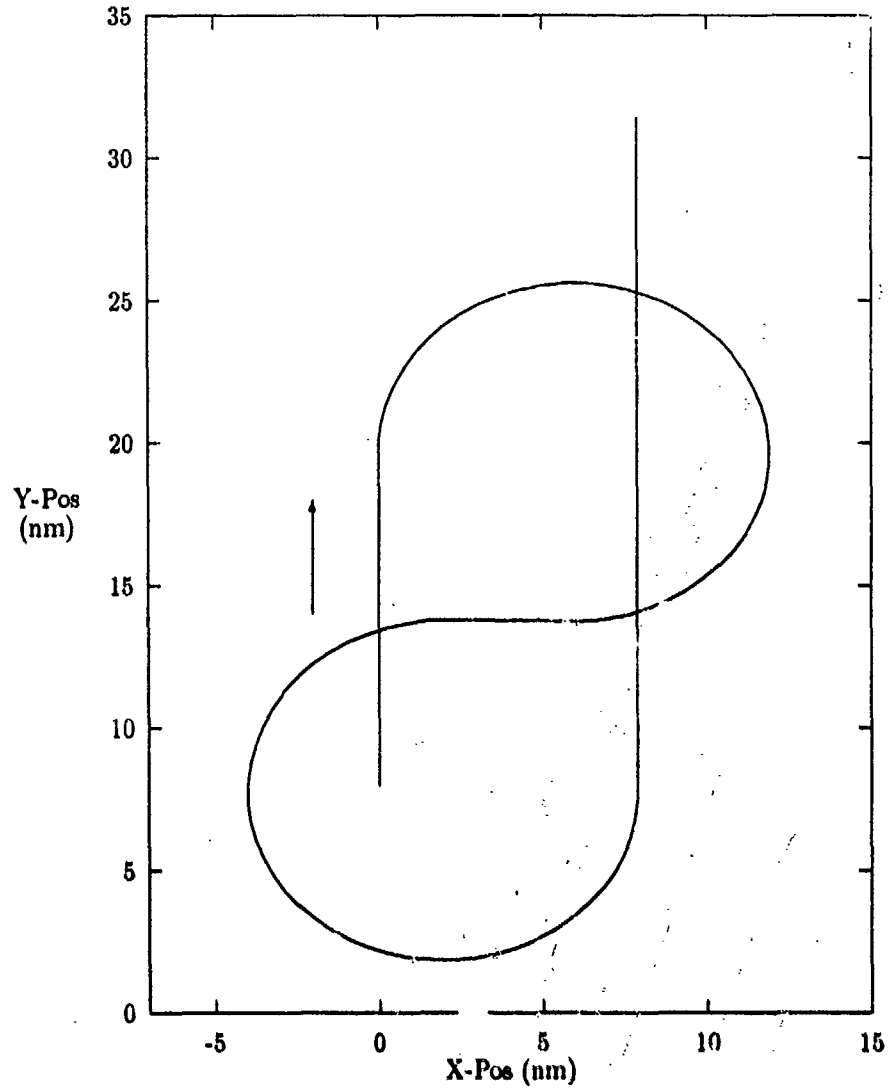

Figure 10. Flight Path Three, Two 270 Degree Cruise Missile Turns

path that would provide 100 percent radar coverage without greatly exceeding the structural and performance limits of the aircraft. Ideally, experimental design would have improved the performance of the optimization algorithm enough to produce a CMMCA flight path that provided 100 percent radar coverage while being within the physical limits for the entire flight path (if possible), but a more realistic goal was to be able to find the maximum radar coverage possible over this flight path. Figure 11 shows the portion of the cruise missile flight test path used for the analysis.

3.5 Initial CMMCA Starting Paths

The optimization program, as part of the input data, requires an initial flight path in order to 'seed' the program with an initial solution. When Garton first constructed the program, the initial CMMCA flight path was a path flying straight North for the entire time duration of the cruise missile maneuver. Although this initial path led to acceptable results for many cruise missile maneuvers, it did not work for some of the longer maneuvers. This could be due to the speculation that the surface represented by the objective functional is not convex, and could possibly have many local optima (1). Therefore, a logical step was to produce an alternate initial CMMCA flight path that was more in line with the expected result.

The alternate initial CMMCA flight path used for this research was the same flight path that the cruise missile follows through the maneuver, except that the CMMCA started the desired nominal distance behind the missile. A FORTRAN program was written that computes the required CMMCA bank angles and airspeeds for following the cruise missile based on the x and y coordinates of the missile at each time point. The program is based on an algorithm derived by Baker (1). The FORTRAN program is contained in Appendix B.

This combination of the two initial flight paths is analogous to the dual simplex method for solving linear programming problems. Using the straight initial flight path can be seen as starting in a feasible position and working to an optimal position,

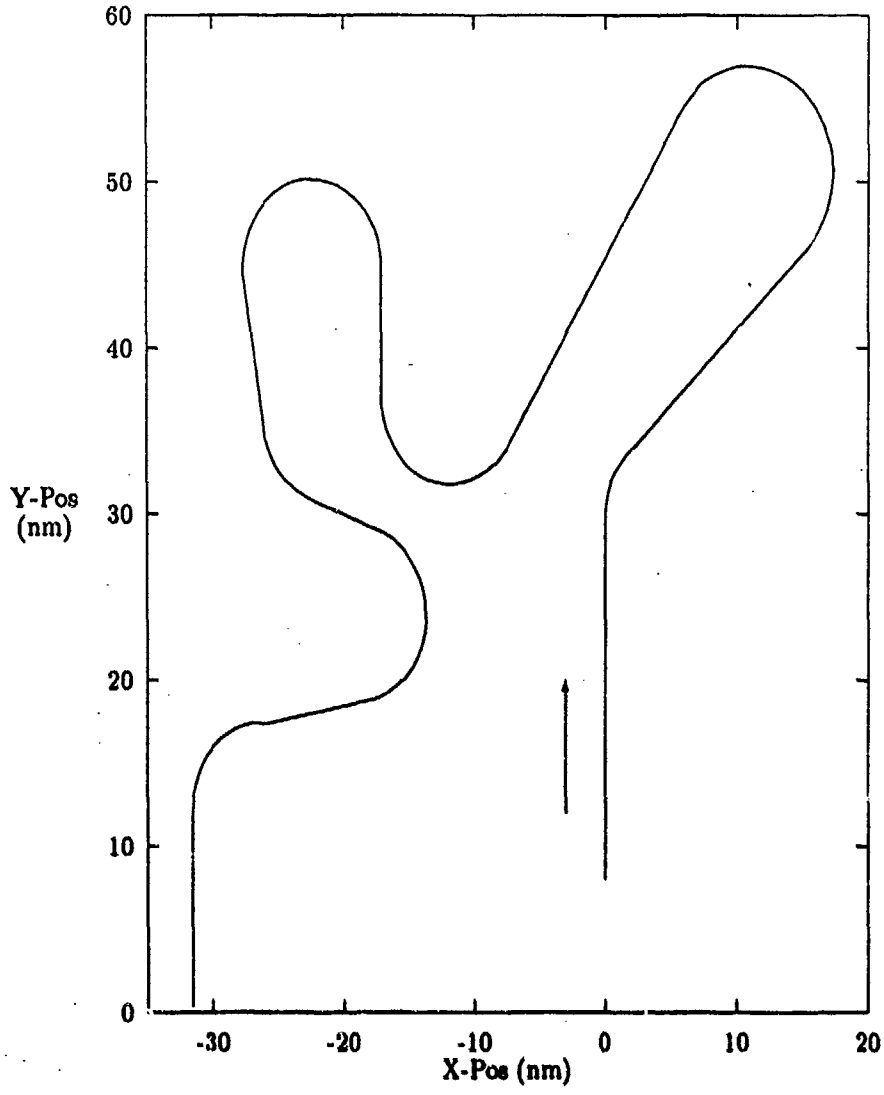

Figure 11. Flight Path Four, Portion of Cruise Missile Flight Test Path

whereas starting with the CMMCA following the cruise missile can be interpreted as the dual solution of starting at an optimal solution and working to a feasible solution(12). Both the straight and missile-following initial flight paths were used as starting conditions for each of the flight paths in order to obtain preliminary results showing the improvements to the algorithm.

3.6 Preliminary Results

With the completion of the code which calculates an initial CMMCA path following the cruise missile, and the construction of the four cruise missile flight paths, the next step was running each of the four flight profiles for both initial CMMCA flight paths. These preliminary results were all done with the scaling factors (which equate the penalties incurred from each component of the objective functional) included in the objective functional and the variable weights W_1, W_2, and W_3 all set at one.

These preliminary results were obtained for two reasons. First, they were done to indicate whether of not adding the scaling factors and starting the optimization program with the CMMCA initially trailing the cruise missile improved upon the results Garton obtained form his research. Second, these runs provided an initial baseline of the program's performance for comparison against the results of further modifications and improvements to the optimization program.

The preliminary results achieved 100 percent coverage and kept the CMMCA within physical limits 100 percent of the time for three of the four flight paths. These results indicated a significant improvement over the results obtained from the optimization program prior to the flight paths from consideration for experimental design, since any changes to the weight parameters or initial CMMCA flight path could only reduce the amount of radar coverage, if it changed at all. Table 5 indicates (with an X) the preliminary runs where 100 percent radar coverage and 100 percent physical restriction was achieved without performing any experimental design.

Table 5. Optimal Covering of Flight Paths for Preliminary Runs

Flight Path	Initial CMMCA Path	Optimality Achieved
1	Straight	X
	Trailing	X
2	Straight	X
	Trailing	X
3	Straight	
	Trailing	X
4	Straight	
	Trailing	X

3.7 Experimental Design

From trial and error initial experimentation with the optimization program, very significant changes in the percent of time the cruise missile was within radar coverage and the percent of time the CMMCA was within physical limits were realized when the objective functional weights and nominal values were altered. Therefore an attempt was made to find the settings for the objective functional weights and nominal range value that produce optimal CMMCA flight paths. This was accomplished by describing the percentage of radar coverage as a function of the objective functional weights and nominal values, and then finding the maximum value of the radar coverage function by adjusting the weights and nominal values. This section describes the experimental design process.

3.7.1 Experiment Variables. When Garton and Baker originally designed the objective functional, they allowed for many of the variables to be altered for the purpose of 'fine-tuning' the algorithm (1). These variables include the weights for the azimuth, airspeed, and bank angle components (W_1, W_2, and W_3), the nominal values for each of the components (r_0, θ_0, U_0, and β_0), and the values affecting the shape of the penalty functions for the airspeed and bank angle (μ, K_3, and K_4).

The individual weight components were included specifically for the purpose of altering the objective functional to improve the performance of the program. Therefore, these variables were altered in an effort to optimize the performance of the program.

The nominal values for the azimuth angle, airspeed, and bank angle components were all left at their current values of 400 KTAS, 0 degrees, and 0 degrees respectively during the experimentation, since these values allow for the greatest variation in the azimuth angle and physical limitations of the CMMCA without exceeding the limits. However, the nominal value for range was experimented with, since a greater nominal range allows for more total azimuth deviation but less range deviation and vice-versa.

The shape of the penalty function for the airspeed and bank angle components can be altered by changing the values of μ, K_3, and K_4, but changing the values of the weights associated with the airspeed and bank angle can have much more of an effect on the overall algorithm. Therefore, the parameters μ, K_3, and K_4 were not altered to improve program performance, since changing the weights W_2 and W_3 associated with the airspeed and bank angle produced significant changes in the performance of the program.

Therefore, the parameters that were altered in order to improve the optimization program are W_1, W_2, W_3, and r_0.

3.7.2 Design Points. The only consideration for how many runs to perform was computer time. There was no cost associated with computer use, but the optimization program did take a considerable amount of time to find a solution for cruise missile maneuvers of considerable length (approximately 1 hour for two 270 degree turns in series, running for 150 program iterations). The design used for the experimental process was a 2^n full factorial design (where n is the number of experimental variables), which means that for each flight path, 2^4 or 16 runs were initially

made. The number of runs made over each flight path was reduced as the variables that proved to be insignificant in improving the performance of the optimization algorithm were eliminated.

The initial experimental design was constructed around the current nominal weight values, which were all initially set to a nominal value of 1. In order to construct an orthogonal design around the current weight parameter settings, the weight parameters W_1, W_2, W_3, were set at 0.5 and 1.5. The nominal distance parameter r_0 was set at 8 and 10 nm. Next, performing a simple linear regression on the results of the initial design indicated the direction of steepest ascent along the function describing the percentage of radar coverage. The steepest ascent direction indicated the changes to the design parameters which would produce the highest percentage of radar coverage attainable given the current radar coverage. At the point of the highest percentage of radar coverage, another experimental design was conducted and another steepest ascent direction was calculated. This process was repeated until the highest possible radar coverage for the flight path was achieved. This method is commonly used to find the optimal values of response surfaces for which the true underlying function is not known. The results of the experiments and the values determined as optimal are presented in Chapter 4.

3.8 Experimentation with Flight Path Four

Flight path four was originally constructed for the purpose of applying the techniques which improved the first three flight profiles to a much longer series of cruise missile maneuvers. It was also constructed to check the performance of the optimization program over a cruise missile flight path for which a CMMCA flight path achieving 100 percent radar coverage of the missile had not been found. Therefore, flight path four was an excellent candidate as an experimental flight path for testing the results of techniques used to increase program performance.

The first technique applied to the fourth flight profile was using the optimal weights found from the flight path three experimental design. This was done to determine if the optimal weighting scheme is independent of the cruise missile maneuver. If the optimal weights are truly independent of the missile's flight path, then the optimal variable settings obtained for flight path three should increase the percentage of radar coverage for flight path four (with respect to the preliminary results). The optimal objective functional variables were applied to flight path four for both initial CMMCA flight path cases.

The second technique used to improve the program's performance over flight path four was increasing the precision of the optimization program. The preliminary results for the flight paths where 100 percent radar coverage was not achieved might have experienced less than optimal coverage due to the precision of the calculations being done by the program. The objective functional optimizing the position of the CMMCA relative to the cruise missile is a function of the airspeed and bank angle at each discrete time point, so for a flight profile of 250 points the objective functional is a function of 500 variables. Every iteration the program finds the gradient of the objective functional with respect to each of the variables, and therefore this may cause some reduction in the precision of the calculations, which may ultimately lead to the program not converging on an optimal CMMCA flight path.

Implementing the precision increase in the program was simply a matter of changing all the real variables and data arrays in the program to double precision real variables and arrays. The increase in precision caused the execution time of the program to more than double, and therefore only two runs were made for the double precision runs of flight path four. Both runs were made using the same weighting scheme as in the preliminary runs, and these weights were applied to flight path four with the CMMCA starting initially flying straight North and also with the CMMCA initially trailing the cruise missile. The results of these runs are presented in Chapter 4.

3.9 Segmentation of Flight Path Four

The final attempt made at increasing the radar coverage over the fourth flight path was segmenting the flight path into two sections of nearly equal length. This was done to test if optimizing the two sections separately and then combining the resulting flight paths provided better and more timely results over the entire flight path than running the entire path at once. The two sections of flight path four are shown in Figure 12 and Figure 13.

These two flight paths were optimized separately using both the preliminary weights and the optimal weights derived from the experimental design, and using both initial CMMCA flight paths. The results of the computer runs, and the combined results showing the performance over the entire flight path, are contained in Chapter 4.

3.10 Program Convergence

Throughout the construction of the objective functional and the optimization program there was concern that the surface described by the objective functional and the particular flight path is not convex and therefore does not have a unique optimal solution (1). Thus, the program may converge to different local optimal solutions for the same cruise missile flight path, based in the initial CMMCA flight path and the direction of approach to the solution (determined by the weights of the components of the objective functional).

Another problem, seen in the output of the preliminary results, was that the algorithm did not always reduce the penalty value after each iteration of the program. This was seen in the output of almost all of the program runs, where the J value essentially oscillated between an upper and lower bound as it gradually decreased, or repeated a cyclic pattern as it slowly converged to a solution. These oscillatory and cyclic trends were observed primarily in the results of the fourth flight profile, and were one of the driving factors for increasing the precision of the program. However,

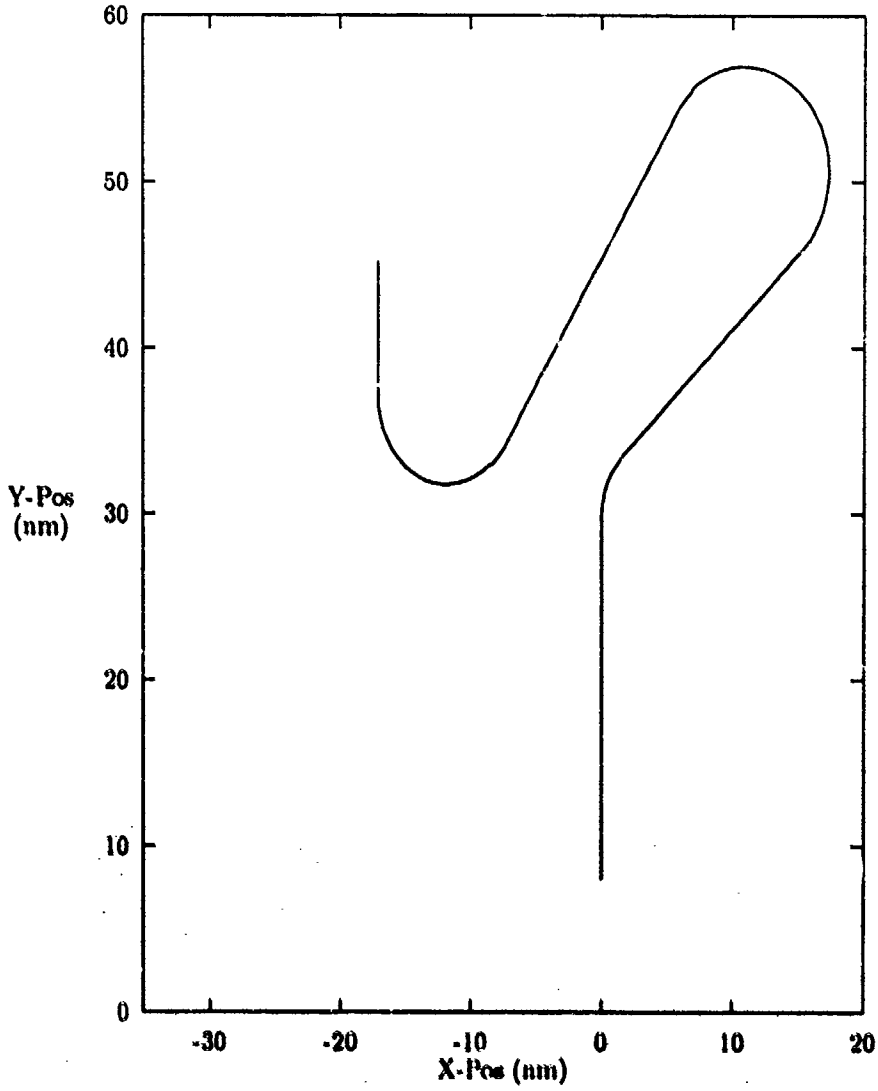

Figure 12. First Segment of Flight Path Four

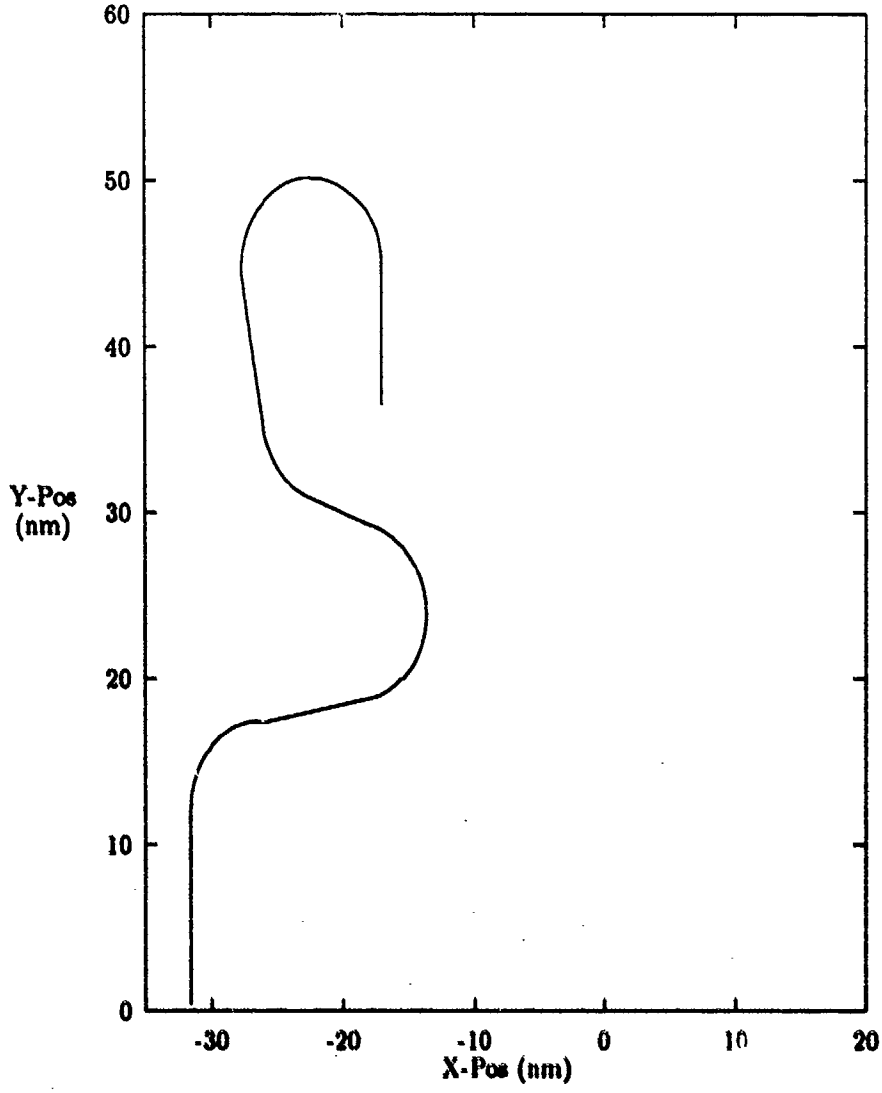

Figure 13. Second Segment of Flight Path Four

as seen in the results of the double precision runs over flight path four (summarized in Chapter 4 and contained in Appendix G), increasing the precision of the program caused no significant change in the performance of the program.

This concern prompted the researcher to include the necessary computer code to record the overall penalty value calculated after each program iteration. The output file JPLOT.OUT contains the iteration number and the penalty value recorded for each iteration. A plot of this data will indicate if the program is converging toward a solution, which will tell if a different gradient seach method is needed for this program. A sample plot of the JPLOT data, using the 90 degree turn example over a span of 150 iterations, is shown in Figure 14.

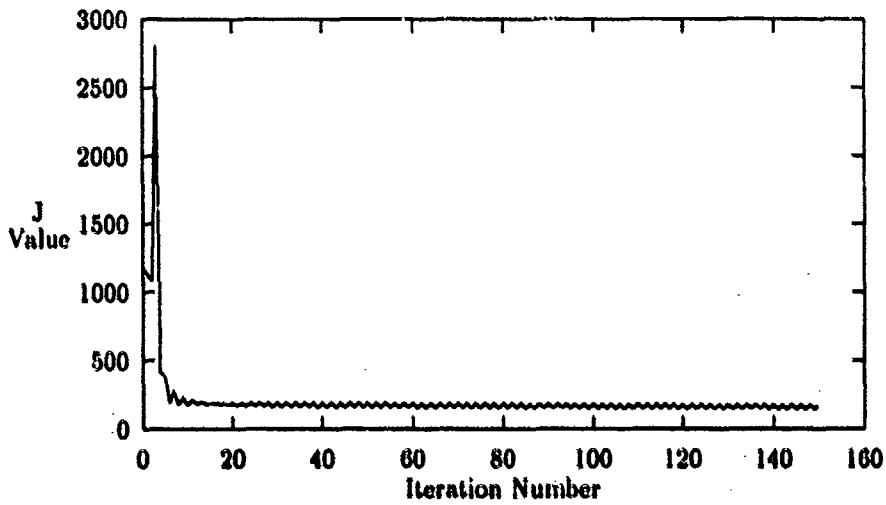

Figure 14. Plot of J Value Versus Iterations, 90 Degree Turn Example

In order to test the convergence of the algorithm the JPLOT.OUT was plotted for each of the flight paths using both the straight initial CMMCA flight path and the alternate initial CMMCA flight path trailing the cruise missile. These plots are inlcuded in Appendix D, as part of the preliminary results of the modified algorithm, and are also included in the output of all runs for which the results were presented.

3.11 Alternate Gradient Search Method

The current gradient search method used by the optimization program produced optimal solutions for all four of the flight paths during the preliminary runs where the CMMCA initially trailed the cruise missile. However, as was mentioned in the previous section, the plots of J value versus iteration number for the preliminary runs (shown in Appendix D) indicated that the algorithm did not always improve the solution after each iteration. In fact, cyclic behavior with the J value oscillating between two values was seen in several of the J value plots.

This discovery led the researcher to explore the possibility of changing the gradient search method so that the J value was always being decreased as the program worked towards an optimal solution. The alternate method used in this research to find the minimum value along the gradient was simply evaluating the objective functional, starting at the current position, at small discrete intervals along the gradient until the minimum was found. Although this is certainly not the most elegant or efficient gradient search method, it does guarantee that the program is always converging towards a solution. This new gradient search procedure was not intended to immediately replace the method Garton used in his work; it was implemented only to explore the possibilities of improving the efficiency of the program.

Figure 15 below illustrates the difference in performance that can possibly occur between the two different gradient search methods. Assuming that the penalty surface is represented by the solid line and the current CMMCA flight profile has the penalty represented by point 1, the parabolic projection method that the program currently uses would calculate the penalty at points 2 and 3, and from the three points would decide the minimum of the penalty surface along the gradient to be at point 4, when the actual corresponding penalty value would be at point 5. This would cause the situation where attempting to minimize along the gradient actually increased the penalty value. In contrast, the alternate gradient search method would calculate the penalty at small increments along the gradient, and would find the

correct minimum along the gradient, shown by point 6. Since the next gradient taken by the alternate search method would start at a lower penalty value, it is obvious that the efficiency would be greatly increased.

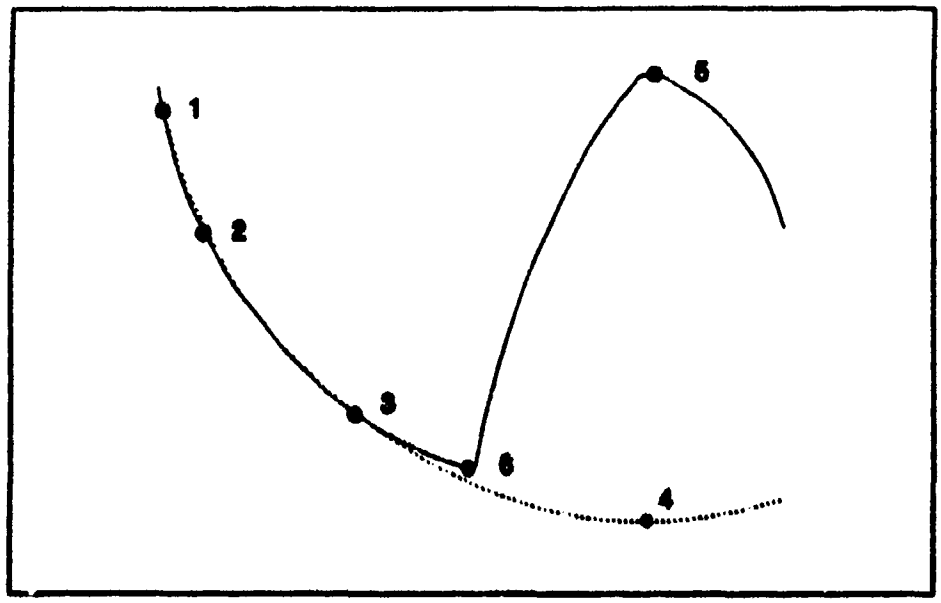

Figure 15. Comparison of Gradient Search Methods

Implementing the new gradient search method was extremely simple. Garton's program already had the code written to perform all of the steps involved in the new search method; some sections of the program needed only minor modifications and a few sections were deleted. The alternate program search method first calculates the penalty associated with the current CMMCA flight path, finds the gradient of the objective functional at that point with respect to the airspeeds and bank angles, and then calculates the penalty value at discrete points along the gradient until the minimum penalty value is found. At that point, the program then calculates the next gradient and increments along that gradient until the minimum is again found.

The program terminates when calculating the gradient and incrementing along the gradient produces no reduction in the penalty value. An example of the performance of the alternate gradient search method is illustrated in Figure 16, which shows the plot of J value versus iteration number for the second flight profile with the CMMCA initially flying straight.

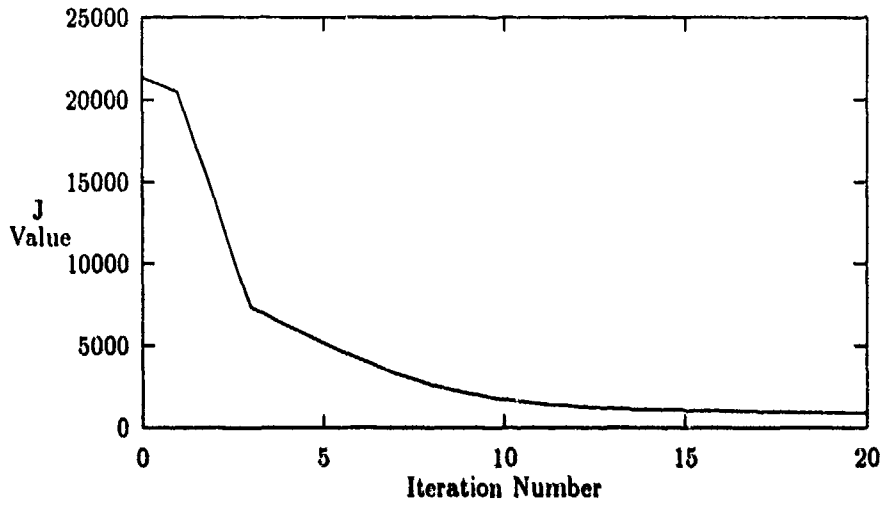

Figure 16. Plot of J Value Versus Iterations, Alternate Gradient Search

The alternate gradient search method was run for each of the four flight profiles using both initial CMMCA flight paths. The results of these runs are presented in Chapter 4. The FORTRAN code for the program with the new gradient search method is presented in Appendix C.

3.12 Alternate Solution Techniques

As part of the research into solving the cruise missile traking problem, proportional navigation was investigated as a possible alternate solution technique for solving the problem. This would have been a likely solution technique had the current method not been improved significantly by this research. However, significant im-

provement was seen in the current method combining simulation and control theory, and therefore the possibility of solving the problem using a proportional navigation solution was not investigated.

3.13 Summary

This chapter presented the changes made to Garton's optimization program that were made in order to provide a better analysis of what the program was really doing. Following that, the chapter described the experimental design techniqes to be used to attempt to fine tune the workings of the program. This included adjusting the weights and the nominal distance and also starting with an alternate initial CMMCA flight path in order to converge to a solution closer to the expected solution. The results obtained through this methodology are presented in the next chapter.

IV. Results

4.1 Introduction

This chapter presents and analyzes the results obtained from the modification of Garton's optimization program and all steps taken towards finding a solution to the cruise missile tracking problem. The first section presents the preliminary results obtained from running all four cruise missile flight paths, and the improvements realized from adding the scaling factors and introducing an alternate initial CMMCA flight path. The second section covers the results obtained from the experimental design performed to improve the percentage of radar coverage by adjusting the variables of the objective functional. The next sections outline the results achieved from applying different weighting schemes and changing the precision of the program calculations for the fourth flight path, and also the results obtained from segmenting flight path four and applying different weighting schemes. The final section of the chapter presents the results achieved from changing the gradient search method.

4.2 Preliminary Results

The preliminary results were obtained for all four of the cruise missile flight paths, with both the straight and trailing initial CMMCA flight paths. The weights W_1, W_2, and W_3 were all set at 1 and the nominal distance r_0 was fixed at 8 nm for these preliminary runs. For all flight paths the program was run for 150 iterations. The results of these computer runs indicate the considerable improvement over Garton's results obtained by adding the scaling factors to equate the objective functional components, and from starting the iterative optimization process with the CMMCA trailing the cruise missile. This set of preliminary results also provided a baseline for beginning the experimental design process to maximize the percentage of radar coverage and the percentage of the flight path the CMMCA is within the physical constraints. This maximization was accomplished by adjusting the objec-

tive functional weights W_1, W_2, and W_3 and also the nominal desired distance from the CMMCA to the cruise missile r_0. The preliminary results obtained from the program are outlined in Table 6, and the rest of the computer output is contained in Appendix C.

Table 6. Preliminary Results of Optimization Program

Flight Path	Init Path	JSTOP	Radar	Physical
1	Straight	447.30	100	100
	Trailing	455.93	100	100
2	Straight	249.84	100	100
	Trailing	250.39	100	100
3	Straight	1217.04	74.15	94.56
	Trailing	926.90	100	100
4	Straight	76391.24	37.41	100
	Trailing	124108.0	64.68	97.90

During the analysis of the output data from the preliminary runs, a significant problem was seen in the files RESULTS.OUT obtained for the preliminary runs over the fourth flight path. The output data for both of these runs is contained in Appendix D. Specifically, the variable θ_i describing the azimuth angle from the nose of the aircraft to the cruise missile must be a value between -180 and 180 degrees for the program to properly minimize the penalty value. However, values for θ_i of over 270 degrees were seen for both runs over flight path four. This problem not only caused the program to calculate the wrong gradient for the minimization process, but also allowed for potentially miscalculating the amount of radar coverage over the flight profile.

In order to correct this problem, a section of FORTRAN code was added to the program to ensure the azimuth angle between the CMMCA and the missile is never less than -180 degrees and never more than 180 degrees. After the code was added, the program was again run for all eight preliminary runs. No change in any

of the preliminary results was seen for the first three flight paths, but a remarkable increase in the radar coverage was seen for the fourth flight path. For the fourth flight path with the CMMCA initially flying straight, the radar coverage increased from 37.41 percent to 46.15 percent, and with the CMMCA initially trailing the missile the coverage increased from 64.68 percent to 100 percent. The preliminary results for the fourth flight path using the corrected algorithm are shown in Table 7.

Table 7. Corrected Flight Path Four Preliminary Results

Init Path	JSTOP	Radar	Physical
Straight	25975.84	46.15	100
Trailing	6112.03	100	97.03

Prior to this research effort, the optimization program achieved only 34.3 percent radar coverage for the 180 degree turn and 58.7 percent radar coverage for the 270 degree turn. The preliminary runs achieved 100 percent radar coverage for both of these cruise missile maneuvers, and kept the CMMCA within the physical limitations 100 percent of the time for both flight paths. 100 percent coverage was also achieved for the 2-270 degree cruise missile turns when the initial CMMCA flight path was trailing the missile. Therefore, significant improvements in the algorithm were seen from the addition of the scaling factors to the objective functional, and even further improvement was seen when the initial CMMCA flight path was changed from a straight flight path to a flight path trailing the missile.

4.3 Optimization of Objective Functional Variables

As was mentioned previously, an experimental design was performed on the optimization program in an attempt to maximize the percentage of radar coverage by adjusting the variables r_0, W_1, W_2, and W_3. The flight path used for this set of experiments was flight path number three (double 270 degree turn), with the CMMCA initially flying a straight path. This was the only flight profile used for the

experimental design. 100 percent radar coverage was already achieved for flight paths one and two from the preliminary runs, so no improvement could be gained from experimentation with these flight profiles. Flight path four was not used due to its extreme length and the amount of computer time required to generate each solution (approximately three VAX model 6420 CPU hours for 150 program iterations), but the optimal weighting scheme derived from the experimental design was applied to flight path four in an attempt to determine if the optimal weights are independent of the cruise missile maneuver and the initial CMMCA flight path.

The first stage of the weight optimization process was building a set of experimental design points around the current weight values and the two nominal distances that were initially used for running the program. Table 8 shows the first set of design points and the final J value, percentage of radar coverage, and the physical limit percentage obtained from each of the design points.

Table 8. First Set of Experimental Design Points

r_0	W_1	W_2	W_3	JSTOP	RADAR	STRUCT
8	.5	.5	.5	1280.67	65.31	100
8	.5	.5	1.5	1275.58	65.31	100
8	.5	1.5	.5	1280.57	65.31	100
8	.5	1.5	1.5	1275.56	65.31	100
8	1.5	.5	.5	2293.87	66.67	100
8	1.5	.5	1.5	2152.60	65.99	100
8	1.5	1.5	.5	2293.73	66.67	100
8	1.5	1.5	1.5	2152.46	65.99	100
10	.5	.5	.5	1374.51	63.26	100
10	.5	.5	1.5	1171.81	65.31	100
10	.5	1.5	.5	1374.38	63.26	100
10	.5	1.5	1.5	1171.91	65.31	100
10	1.5	.5	.5	1510.69	66.67	100
10	1.5	.5	1.5	1358.03	66.67	100
10	1.5	1.5	.5	1510.50	66.67	100
10	1.5	1.5	1.5	1357.74	66.67	100

A significant observation here is that the radar coverage achieved for each of the design points was about 10 percent lower than the radar coverage achieved over the same flight profile during the preliminary runs. This is due to the fact that the preliminary runs were stopped after 150 program iterations, and the exprimental design points were run for only 50 iterations.

The decision was made to run the experimental design points for only 50 iterations, because the plot of overall J value versus iteration number for the preliminary run of flight path three indicated that over 99 percent of the J value reduction occurred within the first 50 iterations. The slight decrease in the overall J value over the last 100 iterations for the preliminary run over flight path three produced a slight improvement in the precentage of radar coverage, but this increase was accompanied by a reduction in the percentage of time the CMMCA was within its physical constraints.

The results of the first set of experimental runs indicated that some improvement in the percentage of coverage was possible when the parameter values were altered. A simple linear regression was performed on the data from the first set of experimental runs, and the following equation describing the percentage of radar coverage with respect to the design variables was derived:

$$RADAR = 65.145 - 0.171 * r_0 + 1.703 * W_1 + 0.343 * W_3 \qquad (16)$$

This equation indicates that the variable W_2 had absolutely no effect on the percentage of radar coverage, while an increase in radar coverage can be achieved by a decrease in nominal distance and an increase in the variables W_1 and W_3.

The next step in the experiment process was to find the gradient of the regression equation, which is simply the coefficient of each of the variables in the equation. The gradient indicates the direction of greatest increase in the percentage of radar coverage. Table 9 shows the design points taken along the path of the gradient. The

value for W_1 was incremented in steps of one, and r_0 and W_3 were incremented in steps of -0.1 and 0.201 respectively.

Table 9. First Gradient Search Points

r_0	W_1	W_2	W_3	JSTOP	RADAR	STRUCT
8.9	2	1	1.201	2433.19	65.31	100
8.8	3	1	1.402	3516.14	67.35	100
8.7	4	1	1.603	4551.97	68.03	100
8.6	5	1	1.804	5640.45	67.35	100

The maximum radar coverage attained in the first gradient search was 68.03 percent. Therefore, the next experimental design was constructed around the point at which the maximum coverage occurred. The second set of design points, and the results obtained at those points, are found in Table 10.

Table 10. Second Set of Experimental Design Points

r_0	W_1	W_2	W_3	JSTOP	RADAR	STRUCT
7.7	3.5	1	1.103	4679.75	67.35	100
7.7	3.5	1	2.103	4362.33	68.03	100
7.7	4.5	1	1.103	5819.03	68.03	100
7.7	4.5	1	2.103	5510.46	67.35	100
9.7	3.5	1	1.103	3739.36	66.67	100
9.7	3.5	1	2.103	3480.42	66.67	100
9.7	4.5	1	1.103	4784.24	67.35	100
9.7	4.5	1	2.103	4429.50	66.67	100

Again, this second set of design points indicated some variation in the percentage of radar coverage, but no coverage over 68.03 percent was seen. A simple linear regression was performed on the data from the second set of experimental design runs, and the following equation was derived.

$$RADAR = 70.555 - 0.425 * r_0 + 0.170 * W_1 - 0.170 * W_3 \qquad (17)$$

Table 11 shows the design points that were run along the second gradient. The value for r_0 was incremented in steps of -0.5 and W_1 and W_3 were incremented in steps of 0.2 and -0.2 respectively.

Table 11. Second Gradient Search Points

r_0	W_1	W_2	W_3	JSTOP	RADAR	STRUCT
8.2	4.2	1	1.403	5097.73	67.35	100
7.7	4.4	1	1.203	5365.18	67.35	100
7.2	4.6	1	1.003	5839.38	67.35	100
6.7	4.8	1	0.803	6214.75	68.03	100
6.2	5.0	1	0.603	7584.15	67.35	100

No percentage of radar coverage over 68.03 percent was seen in the final gradient search. In fact, no improvement in the percentage of radar coverage was gained over the center point of the second set of experimental design points. Also, the variation from the lowest to the highest percentage of radar coverage over all 33 experimental runs was less than five percentage points. This information tends to indicate that, while scaling the weight parameters provided significant improvement in the performance of the program, any further experimentation with the parameters provided only modest gains in the performance.

Also, the set of weight parameters proving the highest precentage of radar coverage was not unique. Several different weighting schemes achieved the maximum observed coverage of 68.03 percent. Therefore, the set of parameters referred to as the optimal parameters for flight path three are the first parameters to achieve the highest observed radar coverage, which are $r_0 = 8.7$, $W_1 = 4$, $W_2 = 1$, and $W_3 = 1.603$.

4.4 *Experimentation with Flight Path Four*

The preliminary results obtained for the fourth experimental flight profile indicated much improvement in the percentage of radar coverage was possible for this flight path when the CMMCA initial flight path was straight. The preliminary run with the CMMCA initially flying a straight path achieved only 46.15 percent radar coverage. Therefore, three different methods for improving the program's performance over flight path four were attempted. The methods were also applied to flight path four with the CMMCA initially trailing the missile to ensure that the methods did not increase the coverage using one initial CMMCA flight path and decrease the coverage for the other initial CMMCA flight path.

4.4.1 Applying Optimum Weights. The first attempt at increasing the radar coverage for this flight path was applying to this flight profile the 'optimum' weights and nominal distance obtained from the experimental design for flight path three. This was done to provide information on whether the optimum objective functional weights and other parameters are the same for each flight profile and CMMCA initial condition, or if the optimum weights are dependent on the particular flight profile. Table 12 shows the results of applying the optimum weights to flight path four.

Table 12. Flight Path Four Results with Optimum Weights

Init Path	JSTOP	RADAR	STRUCT
Straight	16538.15	53.85	100
Trailing	62032.16	100	97.90

The results from applying the optimum weights to flight path four caused a fairly substantial increase in the percentage of radar coverage with respect to the preliminary results for the straight initial CMMCA flight path, and caused no reduction in the coverage for the trailing initial CMMCA flight path. These results tend to confirm the hypothesis that the optimum weight variables and nominal distance are

most likely independent of the cruise missile flight path and initial CMMCA starting position, but much more experimentation over several different flight profiles using both initial CMMCA flight paths is required to truly test this hypothesis.

4.4.2 Double Precision Calculations. The next attempt at improving the performance over flight path four was increasing the precision of the calculations involved in the optimization process. This was accomplished by changing all the real variables in the FORTRAN program code to double precision variables and changing all the single precision functions to double precision functions. Due to the extreme amount of computer time required to run flight path four using double precision calculations (approximately 7 hours of VAX model 6420 CPU time was used for each run of 150 program iterations), flight path four was run only for the preliminary weights with the CMMCA starting both straight and trailing the missile. The results of changing the variables form real to double precision are presented in Table 13.

Table 13. Flight Path Four Results with Double Precision Variables

	Double Precision			Single Precision		
Init Path	JSTOP	RADAR	STRUCT	JSTOP	RADAR	STRUCT
Straight	25884.2	46.15	100	25975.8	46.15	100
Trailing	5244.6	100	98.25	6112.0	100	97.30

The results from running the program using double precision variables indicated no change in the percent of radar coverage with respect to the single precision calculations. For both initial CMMCA cases there was no significant change in the percentage of the flight path that the CMMCA was within its physical constraints from the standard single precision calculation runs. This indicates that the convergence problem discussed in Chapter 3 is most likely not due to the precision of the program's calculations, but due to the method with which the program searches for an optimum solution.

4.5 Segmenting Flight Path Four

The third, and most successful, attempt at increasing the percentage of radar coverage over flight path four was segmenting the flight path into the two sections shown in Chapter 3, and the running the program over each of these sections separately. Each of the two sections of flight path four was run using the preliminary weights and the optimum weights obtained for flight path three, and with both the straight and trailing intial CMMCA flight paths. The results of these runs are presented in Table 14.

Table 14. Results From Segmentation of Flight Path Four

Path	Init Path	Weights	JSTOP	RADAR	STRUCT
4A	Straight	Prelim	5741.87	92.17	100
4A	Straight	Optimum	6857.87	95.78	100
4A	Trailing	Prelim	3026.58	100	98.19
4A	Trailing	Optimum	8264.82	100	98.19
4B	Straight	Prelim	2529.67	96.18	100
4B	Straight	Optimum	6655.61	100	100
4B	Trailing	Prelim	1654.60	100	96.95
4B	Trailing	Optimum	7064.66	100	96.95

The results from the two sections must be combined in order to calculate the true coverage over the entire flight profile. Flight path four consisted of 286 discrete points, whereas the first section had 166 and the second section had 131, for a total of 297. The overlap of 11 points is due to the fact that the program requires the missile and the CMMCA flying straight North for at least the length of the offset between the two. Since 100 percent coverage was always achieved for the first 11 points of the second section, these points were discounted from the results of the second section.

After calculating the percentages of the overall length of flight path four that are contained by each section, and recalculating the percentages of radar coverage

and physical limitation achieved over the second section, the results presented in Table 15 were obtained for flight path four, as the overall results of the combined sections.

Table 15. Results From Segmentation of Flight Path Four

Init Path	Weights	RADAR	STRUCT
Straight	Prelim	93.71	100
Straight	Optimum	97.55	100
Trailing	Prelim	100	97.67
Trailing	Optimum	100	97.67

The results of segmenting the fourth flight path into two sections and then obtaining an overall performance gave extremely encouraging results. No significant changes were seen for the two runs made with the CMMCA initially trailing the missile, but great improvements were made in the results with the CMMCA initially flying straight. Once again, the results with the CMMCA initially flying straight using the optimum weights provided better radar coverage than using the preliminary weights. This lends more evidence that the optimal weights may be independent of the flight profile, but much more experimentation is required in order to prove independence. Also, running both sections of the flight path for 150 iterations took a total of approximately 50 minutes of CPU time, compared to three hours to run 150 iterations over the entire flight profile.

The results of running the two sections separately indicate that there should probably be a restriction on the length of the flight path being run, due to both the improvement in the results when the two sections of the CMMCA flight path were optimized separately and the decrease in the time required to optimize the two segments separately.

4.6 Program Convergence Results

This section discusses the penalty value convergence observed for each section of the program analysis and modification. The plots of the J value versus iteration number are contained in the appendices of the results for each section.

4.6.1 Preliminary Runs. The preliminary results for the first three flight paths show that the optimization program always converged towards a minimum J value, regardless of the initial CMMCA flight path. However, in every case the plot of the J value versus the iteration number indicates an oscillation in the J value as it decreases. It appears that the program is missing the minimum value along the gradient, and is tending to skip back and forth about the true optimum value.

The solutions for the two preliminary runs for flight path three both converged, but to different optimal solutions. This confirmed the hypothesis that the optimal CMMCA flight path found by the algorithm depends on both the particular cruise missile maneuver and the initial CMMCA flight path. This is most likely due to the fact that the surface described by the objective functional and the cruise missile flight path is not convex, and therefore has many local minima(1). Thus, the optimal solution chosen by the algorithm for most cruise missile maneuvers will depend on the starting flight path of the CMMCA.

The fourth flight path with the CMMCA initially flying straight showed convergence towards a solution, but the percentage of radar coverage that was ultimately achieved by this run was far below the percentages achieved over the other three flight profiles. The fourth flight path with the CMMCA initially trailing the missile started at a much lower J value, but the plot of the penaly versus iteration number indicated the cyclic behavior discussed earlier. This indicates that the program was converging towards a solution, but not in an efficient manner. The program did ultimately achieve 100 precent radar coverage for this flight path, but regardless of the 100 percent coverage the penalty value could still have been reduced substantially.

4.6.2 Experimental Design. Over all of the design points of flight path three that were run for the purpose of optimizing the weight values, the same pattern in the plot of J value versus iteration number was observed. All these experimental runs were converging to basically the same flight path with only small differences between them, and thus the plots of J value versus iteration number were just shifted by a factor dependent on the values of the objective functional weights and the nominal distance. For every design point that was run, the J value exhibited a decreasing trend, indicating convergence toward an optimal solution.

4.6.3 Flight Path Four Results. The experimentation with flight path four caused no improvement when the optimal weights for flight path three were used and when the program was changed to double precision. No significant difference was seen in the sequential plots of the J value either. These plots appear to display the same cyclic behavior as the plots for the preliminary runs. Therefore, applying the optimal flight path three weights and changing the precision of the program had no effect on reducing the J value or causing the program to converge.

For the first section of the fourth flight path, the J value for each of the runs displayed some convergence toward an optimal solution, but the J value versus iteration displayed some cyclical effects. For the second section of the fourth flight path, the results of the J value versus iteration were generally not as promising. Running the second section using the preliminary weights and the straight initital CMMCA flight path was the only case where the J value did not exhibit extremely large deviations from a converging pattern.

4.6.4 Segmenting Flight Path Four. As was seen earlier, segmenting the fourth flight path and then combining the results gave solutions with much better radar coverage of the missile. The plots of J value versus iteration indicated some improvement in the convergence of the algorithm for the separate sections of

the fourth flight profile, but some of the results still displayed the random noise that was seen for the preliminary results.

4.7 Alternate Gradient Search Results

As was mentioned in Chapter 3, the preliminary weights were run over the eight different flight path conditions (four cruise missile flight paths and two initial CMMCA flight paths) using the alternate gradient search method. The goal was to attain comparable results to the first set of preliminary runs while achieving these results more efficiently. The results of these alternate preliminary runs using the alternate gradient search method are presented in Table 16.

Table 16. Preliminary Results, Alternate Gradient Search

Path	Init Path	JSTOP	Radar	Physical	Iter
1	Straight	617.12	100	100	7
	Trailing	479.67	100	100	15
2	Straight	919.86	100	100	7
	Trailing	349.57	100	100	15
3	Straight	2042.55	63.94	100	20
	Trailing	949.22	100	100	10
4	Straight	34766.05	19.58	100	20
	Trailing	10356.30	100	97.90	10

The alternate gradient search method was able to replicate the results of the runs where the original gradient search method achieved 100 percent radar coverage, and the 63.94 percent coverage for flight path three with the CMMCA initially flying straight came close to the 74.15 percent originally achieved. The only real failing was flight path four, where only 19.58 percent coverage was achieved with the CMMCA initially flying straight, but the percentage of coverage over this flight path could most likely have been improved by increasing the number of iterations performed.

The most significant difference between the alternate gradient search method and the original method was the time involved in calculating the solutions. The time savings was most apparent for runs using the third and fourth flight profile. The runs over flight path three took approximately 10 CPU minutes for the straight initial CMMCA flight path and 5 CPU minutes for the trailing initial CMMCA flight path. The runs over flight path four took 45 minutes for the straight initial CMMCA flight path and 22 minutes for the trailing initial CMMCA flight path. These performances are significantly better than the original gradient search method, where 150 program iterations consumed 1 hour of CPU time for flight path three and 3 hours of CPU time for flight path four.

The factor that drives the time involved in finding a solution is the number of gradients that the program calculates on the way to finding the solution. Evaluating the penalty and the associated CMMCA flight path at a given point on the gradient takes approximately one percent of the time required to calculate the gradient. By minimizing the penalty value along each gradient before calculating the next direction for minimization, the program requires much fewer gradient calculations in order to converge to the same solution.

The alternate gradient search method was developed to explore the possibility of improving the efficiency of the program by changing the way the program searches for the minimum penalty value. The alternate gradient search method simply shows that the program is capable of running much more efficiently than it currently does, without sacrificing any accuracy.

4.8 Summary of Results

The results of the runs over all of the flight paths for several weighting schemes provide much information on the current capabilities and limitations of the optimization program. The insight gained from the research done and some questions and directions for further research are discussed in the next chapter.

V. Conclusions and Recommendations

5.1 Introduction

This chapter discusses the conclusions of the research and addresses any recommendations for future research and improvements to the optimization program.

5.2 Conclusions

The concept of minimizing the penalty for position error relative to the cruise missile definitely shows promise as a method for solving the cruise missile tracking problem, but the results initially achieved by Garton in his research indicated much room for improvement. Adding the scaling factors to equate the weights of the objective functional caused significant improvement in the performance of the program. Changing the initial CMMCA flight path, so that the CMMCA starts the optimization process trailing the missile, also increased the performance of the program and reduced the number of iterations required to converge upon a solution.

The analysis performed on the program after the initial changes shows evidence that there could possibly be optimum objective functional weights which are independent of the cruise missile flight profile, but much more experimentation needs to be done over a wide range of cruise missile flight paths of various length and complexity, and possibly more of the objective functional parameters need to be included as experiment variables.

The analysis of the segmented fourth flight profile results indicates that the length of the flight profile has some effect on the performance of the algorithm, due to the increase in coverage when flight path four was broken into two sections. The increased performance and decreased solution time for the segmented flight path show that there could possibly be a maximum practical missile flight path length, but again further research into this area is required.

However, the in-depth analysis of the functioning and performance of the program done in this research effort indicates that a significant problem still exists in the optimization program. This problem, which was evident in the results obtained from all of the flight paths, is that the J value, which is expected to exhibit a decreasing trend as the program steps through its iterations, often has large, unfavorable deviations from a convergent path. Also, some of the J value versus iteration plots indicated an oscillatory behavior, especially evident in the preliminary results. This leads to the conclusion that the gradient search method used by the program is not finding the true minimum penalty value along the gradient, and quite often finds a value worse than the previous penalty value. The next section discusses changes that can be made to the program to eliminate this problem.

5.3 Recommendations

5.3.1 Gradient Search Method. As shown by the results obtained from the alternate gradient search method, a promising area of investigation towards solving the convergence problem is improving the gradient search method. Several gradient search methods exist that could improve the results, and guarantee that the J value is decreasing for every gradient that is taken.

The process of finding the gradient consumes most of the computer time used by the system, whereas evaluating the value of the penalty function at points along the gradient is relatively quick by comparison. Therefore, a process that finds the gradient and then guarantees finding the minimum value along that gradient before finding the next direction for minimization would certainly prove to be quicker than the current gradient search method used by the program.

5.3.2 Program Input/Output. Another issue of concern is the input and output files of the program and the ease of use. The program requires an input file of cruise missile x and y coordinate positions (relative to the first CMMCA point)

for every 0.10 minute along the flight profile being optimized. This is not easily obtained from a plot of the ground track of the cruise missile. Although this is a minor problem, a complete program which could be used by the flight crews to aid in flight planning should allow for better data input methods.

5.3.3 Program PATH.FOR. The program PATH.FOR, which computes the initial CMMCA speed and bank angle for a CMMCA path trailing the cruise missile assumes that the missile's ground speed over the entire maneuver is a constant 400 KTAS. This worked well for all of the test profiles, because the cruise missile speed has been fixed at 400 KTAS for all of the flight profiles. This will probably not work for actual cruise missile flight paths if the missile's speed varies much from the assumed constant airspeed for much of the flight profile.

This problem can be fixed by finding the average speed of the missile over the entire maneuver and then assuming that the CMMCA flies the average speed. This will not provide the best initial CMMCA guess, but will put the CMMCA flight path closer to the missile's actual flight path than flying straight North for the entire time of the missile's flight. Another fix would be to rewrite the computer code to allow for the speed to vary from point to point. Although this would complicate the problem, the formulation should still be possible.

Appendix A. *Modified Optimization Program*

```
C*****************************************************************
C*                                                               *
C*    TITLE:  CMMCA Program To Track Cruise Missile Maneuvers    *
C*                                                               *
C*    WRITTEN BY:          Capt Tony M. Garton                   *
C*    DATE:                11 Feb 1990                           *
C*                                                               *
C*    MODIFIED BY:         Capt Andrew C. Hachman                *
C*    DATE LAST MODIFIED:  25 Feb 1992                           *
C*                                                               *
C*    DESCRIPTION:  This program implements an algorithm to track *
C*                  a cruise missile during a turning maneuver.  *
C*                  The program is not user friendly but can easily *
C*                  be learned and used on any VAX/VMS machine or *
C*                  IBM PC with a FORTRAN compiler.              *
C*                                                               *
C*    OPERATING SYSTEM:  This program was most recently modified *
C*                       on a VAX using VMS version 5.4.  This   *
C*                       program should be compatible with any PC *
C*                       version of FORTRAN.                     *
C*                                                               *
C*****************************************************************

      PROGRAM CMMCA

      INTEGER I,LIN,ALL,ITER,K3,K4
      PARAMETER (LIN=78,ALL=156)
      REAL DELTJ(1:ALL),GLAMB(0:1),VLAMB(1:ALL,0:1),
     &  BANK(0:LIN),SPEED(0:LIN),XCN(0:LIN),YCN(0:LIN),
     &  XPLANE(0:LIN),YPLANE(0:LIN),RANGE(1:LIN),THETA(1:LIN),
     &  HDG(0:LIN),WIND(1:2),LAMBDA(0:1),VECTOR(1:ALL),NEWV(1:ALL),
     &  QUADW(0:LIN),W(0:3),WK(0:LIN,1:LIN)
      REAL LAMBOP,JSTOP,DT,RO,THETAO,MU,UO,BO
      COMMON BANK,SPEED,XCN,YCN,XPLANE,YPLANE,RANGE,THETA,HDG
      COMMON /WEIGHT/ QUADW,W,WK,K3,K4
      COMMON /PRELIM/ RO,THETAO,MU,UO,BO

C     Discrete time interval (in minutes) used by the algorithm
```

```
      DT=.1

      OPEN(20,FILE='JPLOT.OUT',STATUS='NEW')

      CALL INPUT(VECTOR,LAMBDA,WIND,DT)
      CALL DELTAJ(DELTJ,JSTOP,WIND,DT)
10    CALL VLAMDA(VECTOR,LAMBDA,VLAMB,DELTJ)
      CALL GLAMDA(VLAMB,GLAMB,WIND,DT)
      CALL OPT(LAMBDA,GLAMB,LAMBOP,JSTOP)
      CALL NEWPOS(VECTOR,LAMBOP,DELTJ,NEWV)
      CALL DECOMP(NEWV)
      CALL DELTAJ(DELTJ,JSTOP,WIND,DT)
      CALL CHECK(LAMBOP,JSTOP,NEWV,VECTOR,ITER)
      GOTO 10
      END



C*********************************************************************
C*                                                                   *
C*    SUBROUTINE:   INPUT                                            *
C*                                                                   *
C*    DESCRIPTION:  Used to input the necessary data for running     *
C*                  the algorithm.                                   *
C*                                                                   *
C*********************************************************************

      SUBROUTINE INPUT(VECTOR,LAMBDA,WIND,DT)
      INTEGER I,J,LIM,ALL,K3,K4
      PARAMETER (LIM=78,ALL=156)
      REAL DT,RO,THETAO,MU,UO,BO
      REAL VECTOR(1:ALL),LAMBDA(0:1),WIND(1:2),BANK(0:LIM),
     &  SPEED(0:LIM),XCM(0:LIM),YCM(0:LIM),XPLANE(0:LIM),
     &  YPLANE(0:LIM),RANGE(1:LIM),THETA(1:LIM),HDG(0:LIM),
     &  QUADW(0:LIM),W(0:3),WK(0:LIM,1:LIM)
      COMMON BANK,SPEED,XCM,YCM,XPLANE,YPLANE,RANGE,THETA,HDG

      COMMON /WEIGHT/ QUADW,W,WK,K3,K4
      COMMON /PRELIM/ RO,THETAO,MU,UO,BO

C     All speeds are in nm/min and all angles are in radians.
C     Initial heading and x-y position for the CMMCA.

      HDG(0)=0
      XPLANE(0)=0.0
```

```
      YPLANE(0)=0

C     Read in a vector containing the initial guess of bank and speed
C     CMMCA should be in during the maneuver.  Also read in x-y
C     position for the cruise missile for each time increment of the
C     maneuver.

      OPEN(10,FILE='INPUT.DAT',STATUS='OLD')
      DO 10 I=0,LIM
        READ(10,*) BANK(I),SPEED(I),XCM(I),YCM(I)
 10   CONTINUE
      CLOSE(10)

C     Contains the step size for the gradient search.

      OPEN(11,FILE='LAMBDA.DAT',STATUS='OLD')
      READ(11,*) (LAMBDA(I), I=0,1)
      CLOSE(11)

C     Contains nominal values of range, azimuth, allowable speed
C     variance, speed, and bank angle variance.

      OPEN(12,FILE='NOMINAL.DAT',STATUS='OLD')
      READ(12,*) R0,THETA0,MU,U0,B0
      CLOSE(12)

C     Wind vector in its two x-y components.

      OPEN(13,FILE='WIND.DAT',STATUS='OLD')
      READ(13,*) (WIND(I), I=1,2)
      CLOSE(13)

C     Adjustable objective function weights.

      OPEN(14,FILE='WEIGHT.DAT',STATUS='OLD')
      READ(14,*) (W(I), I=0,3)
      CLOSE(14)


C     At this point, the different components of the objective
C     function are scaled by multiplying the variable weights
C     by the previously calculated scaling constants.

      W(0) = 1.0*W(0)
      W(1) = 22.797*W(1)
```

```
      W(2) = 19.312*W(2)
      W(3) = 25.000*W(3)

C     Adjustable parabola weights.

      OPEN(15,FILE='K.DAT',STATUS='OLD')
      READ(15,*) K3,K4
      CLOSE(15)

C     Initialize integration weight matrix.

      DO 30 I=0,LIM
         DO 20 J=1,LIM
            WK(I,J)=0
 20      CONTINUE
 30   CONTINUE

C     Read in starter integration weight matrix.  Trapezoidal rule
C     was used.

      OPEN(16,FILE='WK.DAT',STATUS='OLD')
      DO 40 I=0,3
         READ(16,*) (WK(I,J), J=1,3)
 40   CONTINUE
      CLOSE(16)

      DO 60 I=0,3
         DO 50 J=1,3
         WK(I,J)=WK(I,J)*DT
 50      CONTINUE
 60   CONTINUE

C     Generate the full integration weight matrix for the entire
C     maneuver.

      CALL GEN(WK)

C     Take the last column of the integration weight matrix and use
C     it for the quadrature objective function weights.

      DO 70 I=0,LIM
         QUADW(I)=WK(I,LIM)/DT
 70   CONTINUE

C     Combine inputted speed and bank into single vector for later use
```

```
C     in the optimization routine.

      DO 80 I=1,LIM
         VECTOR(I)=SPEED(I)
         VECTOR(LIM+I)=BANK(I)
 80   CONTINUE
      END



C*********************************************************************
C*                                                                   *
C*    SUBROUTINE:   GEN                                              *
C*                                                                   *
C*    DESCRIPTION:  Generates the full integration weight matrix     *
C*                  from the inputted starter matrix.  The size of   *
C*                  the generated matrix is dependent on the         *
C*                  maneuver length.                                 *
C*                                                                   *
C*********************************************************************

      SUBROUTINE GEN(WK)

      INTEGER LIM,ROW,COL,X,Y,I,COUNT
      PARAMETER (LIM=78)
      REAL WK(0:LIM,1:LIM)
      X=2
      Y=2
      COUNT=0

      DO 20 COL=4,LIM
         I=1
         DO 10 ROW=0,LIM
            IF (ROW .LT. X) THEN
               WK(ROW,COL)=WK(ROW,X)
            ENDIF
            IF (ROW .EQ. X) THEN
               WK(ROW,COL)=WK(ROW,X) + WK(0,Y)
            ENDIF
            IF (ROW .GT. X) THEN
               WK(ROW,COL)=WK(I,Y)
               I=I+1
            ENDIF
 10      CONTINUE
         COUNT = COUNT + 1
```

```
         IF (Y .EQ. 2) THEN
            Y=3
            ELSE
            Y=2
         ENDIF
         IF (COUNT .EQ. 2)THEN
            X=X + 2
            COUNT=0
         ENDIF
 20   CONTINUE
      END


C*********************************************************************
C*                                                                   *
C*    SUBROUTINE:   DECOMP                                           *
C*                                                                   *
C*    DESCRIPTION:  Decomposes the maneuver vector back into its     *
C*                  original bank and speed vectors.                 *
C*                                                                   *
C*********************************************************************

      SUBROUTINE DECOMP(V)

      INTEGER I,LIM,ALL
      PARAMETER (LIM=78,ALL=156)
      REAL V(1:ALL),BANK(0:LIM),SPEED(0:LIM)
      COMMON BANK,SPEED,XCM,YCM,XPLANE,YPLANE,RANGE,THETA,HDG

      DO 10 I=1,LIM
         SPEED(I)=V(I)
         BANK(I)=V(LIM+I)
 10   CONTINUE
      END
```

```
C*********************************************************************
C*                                                                   *
C*    SUBROUTINE:   COMP                                             *
C*                                                                   *
C*    DESCRIPTION:  Computes CMMCA position and heading given the    *
C*                  bank and speed vectors for the maneuver.         *
C*                  Also computes range and azimuth from the CMMCA   *
C*                  to the cruise missile given the x-y position     *
C*                  for the missile for the entire maneuver.         *
C*                                                                   *
C*********************************************************************

      SUBROUTINE COMP(WIND,DT)

      INTEGER I,LIM,S,K3,K4
      REAL DT,SUM1,SUM2,SUM3,TWOPI,ALPHA
      PARAMETER (LIM=78)
      REAL WIND(1:2),BANK(0:LIM),SPEED(0:LIM),XCM(0:LIM),YCM(0:LIM),
     &  XPLANE(0:LIM),YPLANE(0:LIM),RANGE(1:LIM),THETA(1:LIM),
     &  HDG(0:LIM),QUADW(0:LIM),W(0:3),WK(0:LIM,1:LIM)
      COMMON BANK,SPEED,XCM,YCM,XPLANE,YPLANE,RANGE,THETA,HDG
      COMMON /WEIGHT/ QUADW,W,WK,K3,K4

      TWOPI=2*(ACOS(-1.))
      SUM1=0
      SUM2=0
      SUM3=0
      DO 40 I=1,LIM
         DO 10 S=0,I
            SUM1=SUM1 + WK(S,I)*19.05*TAN(BANK(S))/SPEED(S)
 10      CONTINUE
         HDG(I)=HDG(0) + SUM1

C     Ensure heading lies between 0 and 2 pi.

 20      IF (HDG(I) .GT. TWOPI)THEN
            HDG(I)=HDG(I)-TWOPI
            GOTO 20
         ENDIF
 30      IF (HDG(I) .LT. -TWOPI)THEN
            HDG(I)=HDG(I)+TWOPI
            GOTO 30
         ENDIF
```

```
         SUM1=0
 40    CONTINUE
       DO 60 I=1,LIM
          DO 50 S=0,I
             SUM2=SUM2 + SPEED(S)*SIN(HDG(S))*WK(S,I)
             SUM3=SUM3 + SPEED(S)*COS(HDG(S))*WK(S,I)
 50       CONTINUE
          XPLANE(I)=XPLANE(0) + SUM2 +  WIND(1)*DT*I
          YPLANE(I)=YPLANE(0) + SUM3 +  WIND(2)*DT*I
          SUM2=0
          SUM3=0
 60    CONTINUE
       DO 70 I=1,LIM
          RANGE(I)=SQRT((XCM(I)-XPLANE(I))**2 +
     &    (YCM(I)-YPLANE(I))**2)

C     The angle ALPHA is measured from the North (or y) axis to the
C     cruise missile.  Counterclockwise from the y axis is a negative
C     ALPHA, clockwise is a positive ALPHA.  Because of the TAN2
C     function ALPHA ranges only from pi to -pi.

          ALPHA= ATAN2(XCM(I)-XPLANE(I),YCM(I)-YPLANE(I))
          THETA(I)= ALPHA - HDG(I)

C     Ensure theta remains between -pi and pi.

          IF (THETA(I) .LT. -TWOPI/2) THETA(I)=THETA(I) + TWOPI
          IF (THETA(I) .GT.  TWOPI/2) THETA(I)=THETA(I) - TWOPI

 70    CONTINUE
       END



C*********************************************************************
C*                                                                   *
C*    SUBROUTINE:   DELTAJ                                           *
C*                                                                   *
C*    DESCRIPTION:  Computes the gradient of J with respect to       *
C*                  velocity and bank angle.                         *
C*                                                                   *
C*********************************************************************

       SUBROUTINE DELTAJ(DELTJ,JSTOP,WIND,DT)
```

```
      INTEGER I,K,K3,K4,KPL,COUNT
      PARAMETER (LIM=78,ALL=156)
      REAL BANK(0:LIM),SPEED(0:LIM),XCM(0:LIM),YCM(0:LIM),
     &  XPLANE(0:LIM),YPLANE(0:LIM),RANGE(1:LIM),THETA(1:LIM),
     &  HDG(0:LIM),WIND(1:2),DELTJ(1:ALL),QUADW(0:LIM),
     &  W(0:3),WK(0:LIM,1:LIM),OLD(1:ALL)
      REAL JSTOP,RO,THETAO,MU,UO,BO,DT,TEMP,A,B,C,L,M,ANGLE,
     &  N,O,P,Q,R,S,T,X,Y,Z,SUM,SUM1,SUM2,SUM3,SUM4,SUM5
      COMMON BANK,SPEED,XCM,YCM,XPLANE,YPLANE,RANGE,THETA,HDG

      COMMON /PRELIM/ RO,THETAO,MU,UO,BO
      COMMON /WEIGHT/ QUADW,W,WK,K3,K4

      SUM=0
      SUM1=0
      SUM2=0
      SUM3=0
      SUM4=0
      CALL COMP(WIND,DT)

C     Initialize the gradient vector to zero.

      DO 10 I=1,ALL
         OLD(I)=DELTJ(I)
         DELTJ(I)=0
 10   CONTINUE
      DO 40 K=1,LIM
         KPL=K+LIM
         DO 30 I=1,LIM
            M=(RANGE(I)-RO)
            N=(THETA(I)-THETAO)
            S=(XCM(I)-XPLANE(I))
            T=(YCM(I)-YPLANE(I))

         IF (K .LE. I)THEN

         IF (I .EQ. K)THEN
            SUM1=(W(2)*2*K3/MU)*(((SPEED(I)-UO)/MU)**(2*K3-1))
            SUM2=(W(3)*2*K4/BO)*((BANK(I)/BO)**(2*K4-1))
         ENDIF
            X=-SIN(HDG(K))*WK(K,I)
            Y=-19.05*TAN(BANK(K))/(SPEED(K)**(2))
            Z=-COS(HDG(K))*WK(K,I)
            A=-19.05*((1/COS(BANK(K)))**2)/SPEED(K)
            DO 20 L=K,I
```

```
                Q=SPEED(L)*COS(HDG(L))*WK(L,I)*WK(K,L)
                R=SPEED(L)*SIN(HDG(L))*WK(L,I)*WK(K,L)
                SUM3= SUM3 + Q
                SUM4= SUM4 + R
 20           CONTINUE
              O=(S*(X-(Y*SUM3)))+(T*(Z+(Y*SUM4)))
              P=(((-S*(Z+(Y*SUM4)))+(T*(X-(Y*SUM3))))/(S**2+T**2))-(Y
     &        *WK(K,I))
              SUM1=SUM1 + (2*M*O/(W(O)*RANGE(I))) + (2*W(1)*P)

              B=(S*(A*SUM3))+(T*(-A)*SUM4)
              C=(((-S*((-A)*SUM4))+(T*A*SUM3))/(S**2+T**2))+(A*WK(K,I))
              SUM2=SUM2 + (2*M*B/(W(O)*RANGE(I))) + (2*W(1)*N*C)
           ENDIF

C          Sum the gradient vector for velocity.

           DELTJ(K)=DELTJ(K) + QUADW(I)*SUM1

C          Sum the gradient vector for bank angle.

           DELTJ(KPL)=DELTJ(KPL) + QUADW(I)*SUM2
           SUM1=0
           SUM2=0
           SUM3=0
           SUM4=0
 30     CONTINUE
 40     CONTINUE

C       Compute the slope of the gradient for each time unit.
       DO 50 I=1,ALL
          TEMP=DELTJ(I)**2
          SUM= SUM + TEMP
 50    CONTINUE
       JSTOP=SQRT(SUM)

C       Compute the normalized gradient of J.
       DO 60 I=1,ALL
          DELTJ(I)=DELTJ(I)/JSTOP
 60    CONTINUE
       IF (COUNT .EQ. 1) THEN
          DO 70 I=1,ALL
             SUM5=OLD(I)*DELTJ(I)
             ANGLE=ANGLE + SUM5
 70       CONTINUE
```

```
      ENDIF
      COUNT=1
C      ANGLE=(ACOS(ANGLE))*180/3.14159
C      PRINT *, 'ANGLE = ',ANGLE
C      ANGLE=0
      END



C*********************************************************************
C*                                                                   *
C*    SUBROUTINE:   VLAMBDA                                          *
C*                                                                   *
C*    DESCRIPTION:  Computes a new column of the maneuver vector     *
C*                  for each of the two lambda step sizes.           *
C*                                                                   *
C*********************************************************************

      SUBROUTINE VLAMDA(VECTOR,LAMBDA,VLAMB,DELTJ)

      INTEGER I,Q,ALL
      PARAMETER (ALL=156)
      REAL DELTJ(1:ALL),VLAMB(1:ALL,0:1),VECTOR(1:ALL),LAMBDA(0:1)
      DO 20 Q=0,1
         DO 10 I=1,ALL
            VLAMB(I,Q)=VECTOR(I)-LAMBDA(Q)*DELTJ(I)
 10      CONTINUE
 20   CONTINUE
      END


C*********************************************************************
C*                                                                   *
C*    SUBROUTINE:   JCOMP                                            *
C*                                                                   *
C*    DESCRIPTION:  Computes a new objective function value given    *
C*                  the appropriate inputs.                          *
C*                                                                   *
C*********************************************************************

      SUBROUTINE JCOMP(J)

      INTEGER I,LIM,K3,K4
      PARAMETER (LIM=78)
      REAL SUM,RO,THETAO,UO,MU,BO,J
```

```
      REAL QUADW(0:LIM),W(0:3),WK(0:LIM,1:LIM),BANK(0:LIM),
     &  SPEED(0:LIM),XCM(0:LIM),YCM(0:LIM),XPLANE(0:LIM),
     &  YPLANE(0:LIM),RANGE(1:LIM),THETA(1:LIM),HDG(0:LIM)
      COMMON BANK,SPEED,XCM,YCM,XPLANE,YPLANE,RANGE,THETA,HDG
      COMMON /PRELIM/ RO,THETAO,MU,UO,BO
      COMMON /WEIGHT/ QUADW,W,WK,K3,K4

      J=0
      DO 10 I=1,LIM
         SUM=W(0)*(RANGE(I)-RO)**2 + W(1)*(THETA(I)-THETAO)**2
     &   + W(2)*(((SPEED(I)-UO)/MU)**(2*K3))
     &   + W(3)*((BANK(I)/BO)**(2*K4))
         J= J + QUADW(I)*SUM
 10   CONTINUE
      END


C*********************************************************************
C*                                                                   *
C*    SUBROUTINE:   GLAMBDA                                          *
C*                                                                   *
C*    DESCRIPTION:  Computes two new objective function values for   *
C*                  each new vector generated in the subroutine      *
C*                  VLAMBDA.  These two values are evaluated in      *
C*                  the subroutine OPT.                              *
C*                                                                   *
C*********************************************************************

      SUBROUTINE GLAMDA(VLAMB,GLAMB,WIND,DT)

      INTEGER I,ALL,LIM,Q,K3,K4
      PARAMETER (LIM=78,ALL=156)
      REAL WIND(1:2),V(1:ALL),BANK(0:LIM),SPEED(0:LIM),
     &  XCM(0:LIM),YCM(0:LIM),XPLANE(0:LIM),YPLANE(0:LIM),
     &  RANGE(1:LIM),THETA(1:LIM),HDG(0:LIM),QUADW(0:LIM),
     &  W(0:3),WK(0:LIM,1:LIM),GLAMB(0:1),VLAMB(1:ALL,0:1)
      REAL J,DT,RO,THETAO,MU,UO,BO
      COMMON BANK,SPEED,XCM,YCM,XPLANE,YPLANE,RANGE,THETA,HDG
      COMMON /PRELIM/ RO,THETAO,MU,UO,BO
      COMMON /WEIGHT/ QUADW,W,WK,K3,K4

      DO 20 Q=0,1
         DO 10 I=1,ALL
            V(I)=VLAMB(I,Q)
 10      CONTINUE
```

```
         CALL DECOMP(V)
         CALL COMP(WIND,DT)
         CALL JCOMP(J)
         GLAMB(Q)=J
 20    CONTINUE
       END


C*************************************************************************
C*                                                                       *
C*    SUBROUTINE:   OPT                                                  *
C*                                                                       *
C*    DESCRIPTION:  Compares the two glambda values and computes         *
C*                  the best step size to take to a new and              *
C*                  better maneuver.                                     *
C*                                                                       *
C*************************************************************************

       SUBROUTINE OPT(LAMBDA,GLAMB,LAMBOP,JSTOP)

       INTEGER LIM,ALL
       PARAMETER (LIM=78,ALL=156)
       REAL GLAMB(0:1),VLAMB(1:ALL,0:1),LAMBDA(0:1)
       REAL JSTOP,LAMBOP,Y

       Y=GLAMB(0) - JSTOP*LAMBDA(1)
       IF (GLAMB(1) .LE. Y) THEN
          LAMBOP=LAMBDA(1)
       ELSE
          LAMBOP=.5*(LAMBDA(1) + ((GLAMB(1)-GLAMB(0))/(-JSTOP*
      &   ((GLAMB(0)-GLAMB(1))/LAMBDA(1)))))
       ENDIF
       IF (LAMBOP .GT. 1) LAMBOP=LAMBDA(1)
       END


C*************************************************************************
C*                                                                       *
C*    SUBROUTINE:   NEWPOS                                               *
C*                                                                       *
C*    DESCRIPTION:  Computes the new maneuver vector given the           *
C*                  best step size determined in the subroutine          *
C*                  OPT.                                                 *
C*                                                                       *
C*************************************************************************
```

```
      SUBROUTINE NEWPOS(VECTOR,LAMBOP,DELTJ,NEWV)

      INTEGER I,ALL
      PARAMETER (ALL=156)
      REAL DELTJ(1:ALL),VECTOR(1:ALL),NEWV(1:ALL)
      REAL LAMBOP
      DO 10 I=1,ALL
         NEWV(I)= VECTOR(I)-LAMBOP*DELTJ(I)
 10   CONTINUE
      END



C*********************************************************************
C*                                                                   *
C*    SUBROUTINE:   CHECK                                            *
C*                                                                   *
C*    DESCRIPTION:  Checks to see if the stopping criteria have      *
C*                  been met.  Output is generated if they have.     *
C*                                                                   *
C*********************************************************************

      SUBROUTINE CHECK(LAMBOP,JSTOP,NEWV,VECTOR,ITER)

      INTEGER ITER,ALL,LIM,I,K3,K4
      PARAMETER (LIM=78,ALL=156)
      REAL JSTOP,LAMBOP,RO,THETAO,UO,MU,BO
      REAL NEWV(1:ALL),VECTOR(1:ALL),BANK(0:LIM),SPEED(0:LIM),
     &  XCM(0:LIM),YCM(0:LIM),XPLANE(0:LIM),YPLANE(0:LIM),
     &  RANGE(1:LIM),THETA(1:LIM),HDG(0:LIM),QUADW(0:LIM),
     &  W(0:3),WK(0:LIM,1:LIM)
      COMMON BANK,SPEED,XCM,YCM,XPLANE,YPLANE,RANGE,THETA,HDG
      COMMON /PRELIM/ RO,THETAO,MU,UO,BO
      COMMON /WEIGHT/ QUADW,W,WK,K3,K4

      PRINT *, ITER, JSTOP
      WRITE(20,*) ITER,JSTOP

      IF ((ABS(LAMBOP) .LT. .1).AND.(JSTOP .LT. .1)) THEN
         ITER=ITER + 1
         CALL OUTPUT(ITER,JSTOP)
      ELSE
      IF (ITER .EQ. 50) THEN
         CALL OUTPUT(ITER,JSTOP)
```

```
      ENDIF
      ITER=ITER + 1

C     Update the old maneuver vector to the new maneuver vector.

      DO 10 I=1,ALL
         VECTOR(I)=NEWV(I)
 10   CONTINUE
      ENDIF
      END



C*********************************************************************
C*                                                                   *
C*    SUBROUTINE:   OUTPUT                                           *
C*                                                                   *
C*    DESCRIPTION:  Changes values of radians and nm/min back to     *
C*                  degrees and knots.  Outputs the final bank and   *
C*                  speed vectors the program determined as being    *
C*                  optimal.  Another file is generated to look at   *
C*                  the results graphically.                         *
C*                                                                   *
C*********************************************************************

      SUBROUTINE OUTPUT(ITER,JSTOP)

      INTEGER I,ITER,LIM,K3,K4
      PARAMETER (LIM=78)
      INTEGER E(1:LIM),F(1:LIM)
      REAL RO,THETAO,UO,MU,BO
      REAL JRANGE,JTHETA,JSPEED,JBANK
      REAL BANK(0:LIM),SPEED(0:LIM),XCM(0:LIM),YCM(0:LIM),
     &  XPLANE(0:LIM),YPLANE(0:LIM),RANGE(1:LIM),THETA(1:LIM),
     &  HDG(0:LIM),QUADW(0:LIM),W(0:3),WK(0:LIM,1:LIM)
      REAL A,B,C,D,PI,LIMIT,JSTOP
      REAL RADSUM,RADPER,STRUCSUM,STRUCPER
      COMMON BANK,SPEED,XCM,YCM,XPLANE,YPLANE,RANGE,THETA,HDG
      COMMON /PRELIM/ RO,THETAO,MU,UO,BO
      COMMON /WEIGHT/ QUADW,W,WK,K3,K4

      PI=ACOS(-1.)
      RADSUM=0.0
      STRUCSUM=0.0
      LIMIT=REAL(LIM)
```

```
      JRANGE=0.0
      JTHETA=0.0
      JSPEED=0.0
      JBANK=0.0

      OPEN(21,FILE='RESULTS.OUT',STATUS='NEW')
      OPEN(22,FILE='PLOT.OUT',STATUS='NEW')
      OPEN(23,FILE='JCALC.OUT',STATUS='NEW')
      WRITE(21,*) 'JSTOP = ',JSTOP
      WRITE(21,10) ITER
 10   FORMAT(1X,'# ITERATIONS = ',I3 //)
      WRITE(21,*)' T      BANK    SPEED     RANGE   ',
     &'THETA    RADAR  STRUCT'
      WRITE(21,*) ' '
      WRITE(23,*) '    JRANGE     JTHETA     JSPEED     JBANK',
     &'     RADAR  STRUCT'

      DO 60 I=1,LIM
         E(I)=1
         F(I)=1
         A=I*.1
         B=BANK(I)*180/PI
         C=SPEED(I)*60
         D=THETA(I)*180/PI

C     Check to see if missile is within radar detection limits.
C     Write a 1 if it is, write a 0 if it is not.

      IF ((RANGE(I) .LT. 5.0) .OR. (RANGE(I) .GT. 15.0)) THEN
         GOTO 20
      ENDIF
      IF ((D .LT. -60) .OR. (D .GT. 60)) THEN
         GOTO 20
      ELSE
         GOTO 30
      ENDIF

 20   E(I)=0
      RADSUM=RADSUM+1.0

C     Check to see if CHNCA is within structural limits.
C     Write a 1 if it is, write a 0 if it is not.

 30   IF ((B .LT. -30.0) .OR. (B .GT. 30.0)) THEN
         GOTO 40
```

```
      ENDIF
      IF ((C .LT. 320) .OR. (C .GT. 480)) THEN
         GOTO 40
      ELSE
         GOTO 50
      ENDIF

 40   F(I)=0
      STRUCSUM=STRUCSUM+1

 50   WRITE(21,70) A,B,C,RANGE(I),D,E(I),F(I)

 60   CONTINUE
 70   FORMAT(F4.1,4(2X,F7.1),6X,I1,6X,I1)

      RADPER=100*(1-(RADSUM/LIMIT))
      WRITE(21,*)' '
      WRITE(21,*)'CM IN RADAR CONE ',RADPER,' PERCENT'

      STRUCPER=100*(1-(STRUCSUM/LIMIT))
      WRITE(21,*)'CMMCA W/IN STRUCTURAL LIMITS ',STRUCPER,' PERCENT'

C     Write the file used to graphically display optimal flight
C     path for the CMMCA and the cruise missile flight path.

      DO 80 I=0,LIM
         WRITE(22,90) XPLANE(I),YPLANE(I),XCM(I),YCM(I)
 80   CONTINUE
 90   FORMAT(4(3X,F8.2))

C     Write the file used to graphically display the objective
C     function components for the optimal flight path.

      DO 100 I=1,LIM
         JRANGE = QUADW(I)*W(0)*((RANGE(I)-RO)**2)
         JTHETA = QUADW(I)*W(1)*((THETA(I)-THETAO)**2)
         JSPEED = QUADW(I)*W(2)*(((SPEED(I)-UO)/MU)**(2*K3))
         JBANK  = QUADW(I)*W(3)*((BANK(I)/BO)**(2*K4))
         WRITE(23,110) JRANGE,JTHETA,JSPEED,JBANK,E(I),F(I)
 100  CONTINUE
 110  FORMAT(4(1X,F10.4),6X,I1,7X,I1)

      STOP
      END
```

Appendix B. *Program to Generate Initial CMMCA Flight Path*

```
C*********************************************************************
C*                                                                   *
C*    TITLE:  Program To Generate Initial CMMCA Flight Path          *
C*                                                                   *
C*    WRITTEN BY:          Capt Andrew C. Hachman                    *
C*    DATE:                22 Jan 1992                               *
C*    DATE LAST MODIFIED:  29 Jan 1992                               *
C*                                                                   *
C*    DESCRIPTION:  This program inputs a cruise missile flight      *
C*                  path and generates the same flight path X nm     *
C*                  behind the missile as an initial guess for       *
C*                  the CMMCA flight path.                           *
C*                                                                   *
C*********************************************************************

      PROGRAM PATH

      INTEGER I,LIM,ALL
      PARAMETER (LIM=79)
      REAL
     &  BANK(0:LIM),SPEED(0:LIM),XCM(0:LIM),YCM(0:LIM),
     &  XPLANE(0:LIM),YPLANE(0:LIM),RANGE(1:LIM),THETA(1:LIM),
     &  HDG(0:LIM),HEAD(0:LIM),ANGLE(0.LIM),ALPHA(0:LIM)
      REAL DT, INIT_DIS, NUMPOINTS, VEL, PI, DELTAX, DELTAY,
     &  DELX, DELY

C     Initialize time interval (in minutes) used by the algorithm,
C     the velocity, and initial CMMCA heading and position

      DT=.1
      VEL = 20.0/3.0
      HDG(0)=0.0
      XPLANE(0)=0.0
      YPLANE(0)=0.0
      PIE = ACOS(-1.0)

C     Read in x-y position for the cruise missile for each time
C     increment of the maneuver and the nominal starting distance.

      OPEN(10,FILE='INPUT.DAT',STATUS='OLD')
```

```
      DO 10 I=0,LIM
        READ(10,*) BANK(I),SPEED(I),XCM(I),YCM(I)
 10   CONTINUE
      CLOSE(10)
      OPEN(11,FILE='NOMINAL.DAT',STATUS='OLD')
      READ(11,*) INIT_DIS
      CLOSE(11)

C     Compute the number of initial points in the path required
C     to account for the nominal CMMCA distance offset.

      NUMPOINTS = INIT_DIS*(1/VEL)*(1/DT)

C     Calculate the CMMCA X and Y position for each point in
C     the initial flight path.

      DO 20 I=1,LIM
        IF (I .LT. NUMPOINTS) THEN
           XPLANE(I) = 0.0
           YPLANE(I) = YPLANE(I-1) + 2.0/3.0
        ELSE
           XPLANE(I) = XCM(I-NUMPOINTS+1)
           YPLANE(I) = YCM(I-NUMPOINTS+1)
        ENDIF
 20   CONTINUE

C     Give the CMMCA an initial path flying due north for the
C     distance of the offset, and calculate the rest of the
C     CMMCA flight path

      DO 50, I=1,LIM

      DELTAX = XPLANE(I) - XPLANE(I-1)
      DELTAY = YPLANE(I) - YPLANE(I-1)
      IF (DELTAY .EQ. 0.0) THEN
         IF (DELTAX .GT. 0.0) THEN
            HDG(I) =  PIE/2.0
         ELSE
            HDG(I) = 3.0*PIE/2.0
         ENDIF
      ELSE
         HDG(I) = ATAN(DELTAX/DELTAY)
      ENDIF
      IF (DELTAY .LT. 0.0) THEN
         HDG(I) = HDG(I) + PIE
```

```
      ENDIF

      DELX = XPLANE(I+1) - XPLANE(I)
      DELY = YPLANE(I+1) - YPLANE(I)
      IF (DELY .EQ. 0.0) THEN
         IF (DELX .GT. 0.0) THEN
            HEAD(I) =  PIE/2.0
         ELSE
            HEAD(I) = 3.0*PIE/2.0
         ENDIF
      ELSE
         HEAD(I) = ATAN(DELX/DELY)
      ENDIF
      IF (DELY .LT. 0.0) THEN
         HEAD(I) = HEAD(I) + PIE
      ENDIF
      ANGLE(I) = HEAD(I) - HDG(I)

      IF (ANGLE(I) .LT. -PIE) THEN
         ANGLE(I) = ANGLE(I) + 2*PIE
      ENDIF
      IF (ANGLE(I) .GT. PIE) THEN
         ANGLE(I) = ANGLE(I) - 2*PIE
      ENDIF

      ALPHA(I) = ATAN(2*VEL/(DT*37.8)*ANGLE(I))

 50   CONTINUE

C     Print out the alternate initial CMMCA flight path
C     into the file INPUT.OUT

      OPEN(21,FILE='INPUT.OUT',STATUS='NEW')
      DO 100 I=0,LIM-1
         WRITE(21,130) ALPHA(I), SPEED(I), XCM(I), YCM(I)
 100  CONTINUE
 130  FORMAT(4(4X,F8.4))

      STOP
      END
```

Appendix C. *Optimization Program, Alternate Gradient Search Method*

```
C*****************************************************************
C*                                                               *
C*    TITLE:  Alternate CMMCA Program For Cruise Missile Tracking *
C*                                                               *
C*    WRITTEN BY:          Capt Tony M. Garton                   *
C*    DATE:                11 Feb 1990                           *
C*                                                               *
C*    MODIFIED BY:         Capt Andrew C. Hachman                *
C*    DATE LAST MODIFIED:  25 Feb 1992                           *
C*                                                               *
C*    DESCRIPTION:  This program implements an algorithm to track *
C*                  a cruise missile during a turning maneuver.  *
C*                  The program is not user friendly but can easily *
C*                  be learned and used on any VAX/VMS machine or *
C*                  IBM PC with a FORTRAN compiler.              *
C*                                                               *
C*    OPERATING SYSTEM:  This program was most recently modified *
C*                       on a VAX using VMS version 5.4.  This   *
C*                       program should be compatible with any PC *
C*                       version of FORTRAN.                     *
C*                                                               *
C*****************************************************************

      PROGRAM ALTERNATE

      INTEGER I,LIM,ALL,ITER,K3,K4
      PARAMETER (LIM=78,ALL=156)
      REAL DELTJ(1:ALL),GLAMB,VLAMB(1:ALL),
     &  BANK(0:LIM),SPEED(0:LIM),XCM(0:LIM),YCM(0:LIM),
     &  XPLANE(0:LIM),YPLANE(0:LIM),RANGE(1:LIM),THETA(1:LIM),
     &  HDG(0:LIM),WIND(1:2),VECTOR(1:ALL),NEWV(1:ALL),
     &  QUADW(0:LIM),W(0:3),WK(0:LIM,1:LIM)
      REAL LAMBCP,JSTOP,DT,RO,THETAO,MU,UO,BO
      COMMON BANK,SPEED,XCM,YCM,XPLANE,YPLANE,RANGE,THETA,HDG
      COMMON /WEIGHT/ QUADW,W,WK,K3,K4
      COMMON /PRELIM/ RO,THETAO,MU,UO,BO
```

```
C     Discrete time interval (in minutes) used by the algorithm

      DT=.1

      OPEN(20,FILE='JPLOT.OUT',STATUS='NEW')

      CALL INPUT(VECTOR,WIND,DT)
      CALL DELTAJ(DELTJ,JSTOP,WIND,DT)
 10   CALL VLAMDA(VECTOR,VLAMB,WIND,DT,DELTJ,ITER)
      CALL DELTAJ(DELTJ,JSTOP,WIND,DT)
      CALL CHECK(LAMBOP,JSTOP,VECTOR,ITER)
      GOTO 10
      END



C*********************************************************************
C*                                                                   *
C*    SUBROUTINE:   INPUT                                            *
C*                                                                   *
C*    DESCRIPTION:  Used to input the necessary data for running     *
C*                  the algorithm.                                   *
C*                                                                   *
C*********************************************************************

      SUBROUTINE INPUT(VECTOR,WIND,DT)
      INTEGER I,J,LIM,ALL,K3,K4
      PARAMETER (LIM=78,ALL=156)
      REAL DT,RO,THETAO,MU,UO,BO
      REAL VECTOR(1:ALL),WIND(1:2),BANK(0:LIM),
     &  SPEED(0:LIM),XCM(0:LIM),YCM(0:LIM),XPLANE(0:LIM),
     &  YPLANE(0:LIM),RANGE(1:LIM),THETA(1:LIM),HDG(0:LIM),
     &  QUADW(0:LIM),W(0:3),WK(0:LIM,1:LIM)
      COMMON BANK,SPEED,XCM,YCM,XPLANE,YPLANE,RANGE,THETA,HDG

      COMMON /WEIGHT/ QUADW,W,WK,K3,K4
      COMMON /PRELIM/ RO,THETAO,MU,UO,BO

C     All speeds are in nm/min and all angles are in radians.
C     Initial heading and x-y position for the CMMCA.

      HDG(0)=0
      XPLANE(0)=0.0
      YPLANE(0)=0
```

```
C     Read in a vector containing the initial guess of bank and speed
C     CMMCA should be in during the maneuver.  Also read in x-y
C     position for the cruise missile for each time increment of the
C     maneuver.

      OPEN(10,FILE='INPUT.DAT',STATUS='OLD')
      DO 10 I=0,LIM
        READ(10,*) BANK(I),SPEED(I),XCM(I),YCM(I)
 10   CONTINUE
      CLOSE(10)

C     Contains nominal values of range, azimuth, allowable speed
C     variance, speed, and bank angle variance.

      OPEN(12,FILE='NOMINAL.DAT',STATUS='OLD')
      READ(12,*) RO,THETAO,MU,UO,BO
      CLOSE(12)

C     Wind vector in its two x-y components.

      OPEN(13,FILE='WIND.DAT',STATUS='OLD')
      READ(13,*) (WIND(I), I=1,2)
      CLOSE(13)

C     Adjustable objective function weights.

      OPEN(14,FILE='WEIGHT.DAT',STATUS='OLD')
      READ(14,*) (W(I), I=0,3)
      CLOSE(14)


C     At this point, the different components of the objective
C     function are normalized by multiplying the variable weights
C     by the previously calculated normalizing constants.

       W(0) = 1.0*W(0)
       W(1) = 22.797*W(1)
       W(2) = 19.312*W(2)
       W(3) = 25.000*W(3)

C     Adjustable parabola weights.

      OPEN(15,FILE='K.DAT',STATUS='OLD')
      READ(15,*) K3,K4
      CLOSE(15)
```

```
C     Initialize integration weight matrix.

      DO 30 I=0,LIM
         DO 20 J=1,LIM
            WK(I,J)=0
 20      CONTINUE
 30   CONTINUE

C     Read in starter integration weight matrix.  Trapezoidal rule
C     was used.

      OPEN(16,FILE='WK.DAT',STATUS='OLD')
      DO 40 I=0,3
         READ(16,*) (WK(I,J), J=1,3)
 40   CONTINUE
      CLOSE(16)

      DO 60 I=0,3
         DO 50 J=1,3
         WK(I,J)=WK(I,J)*DT
 50      CONTINUE
 60   CONTINUE

C     Generate the full integration weight matrix for the entire
C     maneuver.

      CALL GEN(WK)

C     Take the last column of the integration weight matrix and use
C     it for the quadrature objective function weights.

      DO 70 I=0,LIM
         QUADW(I)=WK(I,LIM)/DT
 70   CONTINUE

C     Combine inputted speed and bank into single vector for later use
C     in the optimization routine.

      DO 80 I=1,LIM
         VECTOR(I)=SPEED(I)
         VECTOR(LIM+I)=BANK(I)
 80   CONTINUE
      END
```

```
C*********************************************************************
C*                                                                   *
C*    SUBROUTINE:   GEN                                              *
C*                                                                   *
C*    DESCRIPTION:  Generates the full integration weight matrix     *
C*                  from the inputted starter matrix.  The size of   *
C*                  the generated matrix is dependent on the         *
C*                  maneuver length.                                 *
C*                                                                   *
C*********************************************************************

      SUBROUTINE GEN(WK)

      INTEGER LIM,ROW,COL,X,Y,I,COUNT
      PARAMETER (LIM=78)
      REAL WK(0:LIM,1:LIM)
      X=2
      Y=2
      COUNT=0

      DO 20 COL=4,LIM
         I=1
         DO 10 ROW=0,LIM
            IF (ROW .LT. X) THEN
               WK(ROW,COL)=WK(ROW,X)
            ENDIF
            IF (ROW .EQ. X) THEN
               WK(ROW,COL)=WK(ROW,X) + WK(0,Y)
            ENDIF
            IF (ROW .GT. X) THEN
               WK(ROW,COL)=WK(I,Y)
               I=I+1
            ENDIF
 10      CONTINUE
         COUNT = COUNT + 1
         IF (Y .EQ. 2) THEN
            Y=3
            ELSE
            Y=2
         ENDIF
         IF (COUNT .EQ. 2)THEN
            X=X + 2
```

```
            COUNT=0
          ENDIF
 20     CONTINUE
        END



C*************************************************************************
C*                                                                       *
C*     SUBROUTINE:    DECOMP                                             *
C*                                                                       *
C*     DESCRIPTION:   Decomposes the maneuver vector back into its       *
C*                    original bank and speed vectors.                   *
C*                                                                       *
C*************************************************************************

      SUBROUTINE DECOMP(V)

      INTEGER I,LIM,ALL
      PARAMETER (LIM=78,ALL=156)
      REAL V(1:ALL),BANK(0:LIM),SPEED(0:LIM)
      COMMON BANK,SPEED,XCM,YCM,XPLANE,YPLANE,RANGE,THETA,HDG

      DO 10 I=1,LIM
         SPEED(I)=V(I)
         BANK(I)=V(LIM+I)
 10   CONTINUE
      END



C*************************************************************************
C*                                                                       *
C*     SUBROUTINE:    COMP                                               *
C*                                                                       *
C*     DESCRIPTION:   Computes CNMCA position and heading given the      *
C*                    bank and speed vectors for the maneuver.           *
C*                    Also computes range and azimuth from the CNMCA     *
C*                    to the cruise missile given the x-y position       *
C*                    for the missile for the entire maneuver.           *
C*                                                                       *
C*************************************************************************

      SUBROUTINE COMP(WIND,DT)
```

```
      INTEGER I,LIM,S,K3,K4
      REAL DT,SUM1,SUM2,SUM3,TWOPI,ALPHA
      PARAMETER (LIM=78)
      REAL WIND(1:2),BANK(0:LIM),SPEED(0:LIM),XCM(0:LIM),YCM(0:LIM),
     &  XPLANE(0:LIM),YPLANE(0:LIM),RANGE(1:LIM),THETA(1:LIM),
     &  HDG(0:LIM),QUADW(0:LIM),W(0:3),WK(0:LIM,1:LIM)
      COMMON BANK,SPEED,XCM,YCM,XPLANE,YPLANE,RANGE,THETA,HDG
      COMMON /WEIGHT/ QUADW,W,WK,K3,K4

      TWOPI=2*(ACOS(-1.))
      SUM1=0
      SUM2=0
      SUM3=0
      DO 40 I=1,LIM
         DO 10 S=0,I
            SUM1=SUM1 + WK(S,I)*19.05*TAN(BANK(S))/SPEED(S)
10       CONTINUE
         HDG(I)=HDG(0) + SUM1

C     Ensure heading lies between 0 and 2 pi.

20       IF (HDG(I) .GT. TWOPI)THEN
            HDG(I)=HDG(I)-TWOPI
            GOTO 20
         ENDIF
30       IF (HDG(I) .LT. -TWOPI)THEN
            HDG(I)=HDG(I)+TWOPI
            GOTO 30
         ENDIF
         SUM1=0
40    CONTINUE
      DO 60 I=1,LIM
         DO 50 S=0,I
            SUM2=SUM2 + SPEED(S)*SIN(HDG(S))*WK(S,I)
            SUM3=SUM3 + SPEED(S)*COS(HDG(S))*WK(S,I)
50       CONTINUE
         XPLANE(I)=XPLANE(0) + SUM2 +  WIND(1)*DT*I
         YPLANE(I)=YPLANE(0) + SUM3 +  WIND(2)*DT*I
         SUM2=0
         SUM3=0
60    CONTINUE
      DO 70 I=1,LIM
         RANGE(I)=SQRT((XCM(I)-XPLANE(I))**2 +
     &   (YCM(I)-YPLANE(I))**2)
```

```
C     The angle ALPHA is measured from the North (or y) axis to the
C     cruise missile.  Counterclockwise from the y axis is a negative
C     ALPHA, clockwise is a positive ALPHA.  Because of the TAN2
C     function ALPHA ranges only from pi to -pi.

         ALPHA= ATAN2(XCM(I)-XPLANE(I),YCM(I)-YPLANE(I))
         THETA(I)= ALPHA - HDG(I)

C     Ensure theta remains between -pi and pi.

         IF (THETA(I) .LT. -TWOPI/2) THETA(I)=THETA(I) + TWOPI
         IF (THETA(I) .GT.  TWOPI/2) THETA(I)=THETA(I) - TWOPI

 70   CONTINUE
      END



C*********************************************************************
C*                                                                   *
C*    SUBROUTINE:   DELTAJ                                           *
C*                                                                   *
C*    DESCRIPTION:  Computes the gradient of J with respect to       *
C*                  velocity and bank angle.                         *
C*                                                                   *
C*********************************************************************

      SUBROUTINE DELTAJ(DELTJ,JSTOP,WIND,DT)

      INTEGER I,K,K3,K4,KPL,COUNT
      PARAMETER (LIM=70,ALL=156)
      REAL BANK(0:LIM),SPEED(0:LIM),XCM(0:LIM),YCM(0:LIM),
     &  XPLANE(0:LIM),YPLANE(0:LIM),RANGE(1:LIM),THETA(1:LIM),
     &  HDG(0:LIM),WIND(1:2),DELTJ(1:ALL),QUADW(0:LIM),
     &  W(0:3),WK(0:LIM,1:LIM),OLD(1:ALL)
      REAL JSTOP,RO,THETAO,MU,UO,BO,DT,TEMP,A,B,C,L,M,ANGLE,
     &N,O,P,Q,R,S,T,X,Y,Z,SUM,SUM1,SUM2,SUM3,SUM4,SUM5
      COMMON BANK,SPEED,XCM,YCM,XPLANE,YPLANE,RANGE,THETA,HDG

      COMMON /PRELIM/ RO,THETAO,MU,UO,BO
      COMMON /WEIGHT/ QUADW,W,WK,K3,K4

      SUM=0
      SUM1=0
      SUM2=0
```

```
      SUM3=0
      SUM4=0
      CALL COMP(WIND,DT)

C     Initialize the gradient vector to zero.

      DO 10 I=1,ALL
         OLD(I)=DELTJ(I)
         DELTJ(I)=0
 10   CONTINUE
      DO 40 K=1,LIM
         KPL=K+LIM
         DO 30 I=1,LIM
            M=(RANGE(I)-R0)
            N=(THETA(I)-THETA0)
            S=(XCM(I)-XPLANE(I))
            T=(YCM(I)-YPLANE(I))

         IF (K .LE. I)THEN

         IF (I .EQ. K)THEN
            SUM1=(W(2)*2*K3/MU)*(((SPEED(I)-U0)/MU)**(2*K3-1))
            SUM2=(W(3)*2*K4/B0)*((BANK(I)/B0)**(2*K4-1))
         ENDIF
            X=-SIN(HDG(K))*WK(K,I)
            Y=-19.05*TAN(BANK(K))/(SPEED(K)**(2))
            Z=-COS(HDG(K))*WK(K,I)
            A=-19.05*((1/COS(BANK(K)))**2)/SPEED(K)
            DO 20 L=K,I
               Q=SPEED(L)*COS(HDG(L))*WK(L,I)*WK(K,L)
               R=SPEED(L)*SIN(HDG(L))*WK(L,I)*WK(K,L)
               SUM3= SUM3 + Q
               SUM4= SUM4 + R
 20         CONTINUE
            O=(S*(X-(Y*SUM3)))+(T*(Z+(Y*SUM4)))
            P=(((-S*(Z+(Y*SUM4)))+(T*(X-(Y*SUM3))))/(S**2+T**2))-(Y
     &      *WK(K,I))
            SUM1=SUM1 + (2*M*O/(W(0)*RANGE(I))) + (2*W(1)*P)

            B=(S*(A*SUM3))+(T*(-A)*SUM4)
            C=(((-S*((-A)*SUM4))+(T*A*SUM3))/(S**2+T**2))+(A*WK(K,I))
            SUM2=SUM2 + (2*M*B/(W(0)*RANGE(I))) + (2*W(1)*N*C)
         ENDIF

C        Sum the gradient vector for velocity.
```

```
         DELTJ(K)=DELTJ(K) + QUADW(I)*SUM1

C        Sum the gradient vector for bank angle.

         DELTJ(KPL)=DELTJ(KPL) + QUADW(I)*SUM2
         SUM1=0
         SUM2=0
         SUM3=0
         SUM4=0
 30   CONTINUE
 40   CONTINUE

C     Compute the slope of the gradient for each time unit.

      DO 50 I=1,ALL
         TEMP=DELTJ(I)**2
         SUM= SUM + TEMP
 50   CONTINUE
      JSTOP=SQRT(SUM)

C     Compute the normalized gradient of J.

      DO 60 I=1,ALL
         DELTJ(I)=DELTJ(I)/JSTOP
 60   CONTINUE
      IF (COUNT .EQ. 1) THEN
         DO 70 I=1,ALL
            SUM5=OLD(I)*DELTJ(I)
            ANGLE=ANGLE + SUM5
 70      CONTINUE
      ENDIF
      COUNT=1
C     ANGLE=(ACOS(ANGLE))*180/ACOS(-1.)
C     WRITE(20,*) 'ANGLE = ',ANGLE
C     ANGLE=0
      END
```

```
C*********************************************************************
C*                                                                   *
C*    SUBROUTINE:   VLAMBDA                                          *
C*                                                                   *
C*    DESCRIPTION:  Computes a new column of the maneuver vector     *
C*                  for each increment along the gradient.           *
C*                                                                   *
C*********************************************************************

      SUBROUTINE VLAMDA(VECTOR,VLAMB,WIND,DT,DELTJ,ITER)

      INTEGER I,ALL,LIM,Q,K3,K4,ITER
      PARAMETER (LIM=78,ALL=156)
      REAL WIND(1:2),V(1:ALL),BANK(0:LIM),SPEED(0:LIM),
     &  XCM(0:LIM),YCM(0:LIM),XPLANE(0:LIM),YPLANE(0:LIM),
     &  RANGE(1:LIM),THETA(1:LIM),HDG(0:LIM),QUADW(0:LIM),
     &  W(0:3),WK(0:LIM,1:LIM),GLAMB,VLAMB(1:ALL)
      REAL VECTOR(1:ALL),DELTJ(1:ALL)
      REAL J,DT,RO,THETAO,MU,UO,BO,STEP
      COMMON BANK,SPEED,XCM,YCM,XPLANE,YPLANE,RANGE,THETA,HDG
      COMMON /PRELIM/ RO,THETAO,MU,UO,BO
      COMMON /WEIGHT/ QUADW,W,WK,K3,K4

      CALL GLAMDA(VECTOR,J,WIND,DT)
      WRITE(20,*) ITER,J
      PRINT *,ITER,J

      STEP=1./(1000.)
      PRINT *,'STEP = ',STEP

 5    DO 10 I=1,ALL
         VLAMB(I)=VECTOR(I)-STEP*DELTJ(I)
 10   CONTINUE

      CALL GLAMDA(VLAMB,GLAMB,WIND,DT)
      PRINT *,GLAMB
C     WRITE(20,*) '    ',GLAMB
      IF (GLAMB .GT. J) THEN
         GOTO 100
      ENDIF

      J = GLAMB
      DO 50, I=1,ALL
         VECTOR(I) = VLAMB(I)
 50   CONTINUE
```

```
      GOTO 5

 100  RETURN
      END
```

```
C*********************************************************************
C*                                                                   *
C*    SUBROUTINE:   JCOMP                                            *
C*                                                                   *
C*    DESCRIPTION:  Computes a new objective function value given    *
C*                  the appropriate inputs.                          *
C*                                                                   *
C*********************************************************************

      SUBROUTINE JCOMP(J)

      INTEGER I,LIM,K3,K4
      PARAMETER (LIM=78)
      REAL SUM,RO,THETAO,UO,MU,BO,J
      REAL QUADW(0:LIM),W(0:3),WK(0:LIM,1:LIM),BANK(0:LIM),
     &SPEED(0:LIM),XCM(0:LIM),YCM(0:LIM),XPLANE(0:LIM),
     &YPLANE(0:LIM),RANGE(1:LIM),THETA(1:LIM),HDG(0:LIM)
      COMMON BANK,SPEED,XCM,YCM,XPLANE,YPLANE,RANGE,THETA,HDG
      COMMON /PRELIM/ RO,THETAO,MU,UO,BO
      COMMON /WEIGHT/ QUADW,W,WK,K3,K4

      J=0
      DO 10 I=1,LIM
         SUM=W(0)*(RANGE(I)-RO)**2 + W(1)*(THETA(I)-THETAO)**2
     &   + W(2)*(((SPEED(I)-UO)/MU)**(2*K3))
     &   + W(3)*((BANK(I)/BO)**(2*K4))
         J= J + QUADW(I)*SUM
 10   CONTINUE
      END
```

```
C*********************************************************************
C*                                                                   *
C*    SUBROUTINE:   GLAMBDA                                          *
C*                                                                   *
C*    DESCRIPTION:  Computes the new objective function value for    *
C*                  each new vector generated in the subroutine      *
C*                  VLAMBDA.  These values are evaluated back in     *
C*                  the subroutine VLAMBDA.                          *
C*                                                                   *
C*********************************************************************

      SUBROUTINE GLAMDA(VLAMB,GLAMB,WIND,DT)

      INTEGER I,ALL,LIM,Q,K3,K4
      PARAMETER (LIM=78,ALL=156)
      REAL WIND(1:2),V(1:ALL),BANK(0:LIM),SPEED(0:LIM),
     &XCM(0:LIM),YCM(0:LIM),XPLANE(0:LIM),YPLANE(0:LIM),
     &RANGE(1:LIM),THETA(1:LIM),HDG(0:LIM),QUADW(0:LIM),
     &W(0:3),WK(0:LIM,1:LIM),GLAMB,VLAMB(1:ALL)
      REAL J,DT,RO,THETAO,MU,UO,BO
      COMMON BANK,SPEED,XCM,YCM,XPLANE,YPLANE,RANGE,THETA,HDG
      COMMON /PRELIM/ RO,THETAO,MU,UO,BO
      COMMON /WEIGHT/ QUADW,W,WK,K3,K4

      CALL DECOMP(VLAMB)
      CALL COMP(WIND,DT)
      CALL JCOMP(J)
      GLAMB = J
 20   CONTINUE
      RETURN
      END



C*********************************************************************
C*                                                                   *
C*    SUBROUTINE:   CHECK                                            *
C*                                                                   *
C*    DESCRIPTION:  Checks to see if the stopping criteria have      *
C*                  been met.  Output is generated if they have.     *
C*                                                                   *
C*********************************************************************
```

```
      SUBROUTINE CHECK(LAMBOP,JSTOP,VECTOR,ITER)

      INTEGER ITER,ALL,LIM,I,K3,K4
      PARAMETER (LIM=78,ALL=156)
      REAL JSTOP,LAMBOP,RO,THETAO,UO,MU,BO
      REAL NEWV(1:ALL),VECTOR(1:ALL),BANK(0:LIM),SPEED(0:LIM),
     &XCM(0:LIM),YCM(0:LIM),XPLANE(0:LIM),YPLANE(0:LIM),
     &RANGE(1:LIM),THETA(1:LIM),HDG(0:LIM),QUADW(0:LIM),
     &W(0:3),WK(0:LIM,1:LIM)
      COMMON BANK,SPEED,XCM,YCM,XPLANE,YPLANE,RANGE,THETA,HDG
      COMMON /PRELIM/ RO,THETAO,MU,UO,BO
      COMMON /WEIGHT/ QUADW,W,WK,K3,K4

      PRINT *, ITER, JSTOP
      WRITE(20,*) ITER,JSTOP
      LAMBOP = 10

      IF ((ABS(LAMBOP) .LT. .1).AND.(JSTOP .LT. .1)) THEN
         ITER=ITER + 1
         CALL OUTPUT(ITER,JSTOP)
      ELSE
      IF (ITER .EQ. 20) THEN
         CALL OUTPUT(ITER,JSTOP)
      ENDIF
      ENDIF

      ITER=ITER + 1
      END



C*********************************************************************
C*                                                                   *
C*    SUBROUTINE:   OUTPUT                                           *
C*                                                                   *
C*    DESCRIPTION:  Changes values of radians and nm/min back to     *
C*                  degrees and knots.  Outputs the final bank and   *
C*                  speed vectors the program determined as being    *
C*                  optimal.  Another file is generated to look at   *
C*                  the results graphically.                         *
C*                                                                   *
C*********************************************************************

      SUBROUTINE OUTPUT(ITER,JSTOP)
```

```
      INTEGER I,ITER,LIM,K3,K4
      PARAMETER (LIM=78)
      INTEGER E(1:LIM),F(1:LIM)
      REAL RO,THETAO,UO,MU,BO
      REAL JRANGE,JTHETA,JSPEED,JBANK
      REAL BANK(0:LIM),SPEED(0:LIM),XCM(0:LIM),YCM(0:LIM),
     &XPLANE(0:LIM),YPLANE(0:LIM),RANGE(1:LIM),THETA(1:LIM),
     &HDG(0:LIM),QUADW(0:LIM),W(0:3),WK(0:LIM,1:LIM)
      REAL A,B,C,D,PI,LIMIT,JSTOP
      REAL RADSUM,RADPER,STRUCSUM,STRUCPER
      COMMON BANK,SPEED,XCM,YCM,XPLANE,YPLANE,RANGE,THETA,HDG
      COMMON /PRELIM/ RO,THETAO,MU,UO,BO
      COMMON /WEIGHT/ QUADW,W,WK,K3,K4

      PI=ACOS(-1.)
      RADSUM=0.0
      STRUCSUM=0.0
      LIMIT=REAL(LIM)
      JRANGE=0.0
      JTHETA=0.0
      JSPEED=0.0
      JBANK=0.0

      OPEN(21,FILE='RESULTS.OUT',STATUS='NEW')
      OPEN(22,FILE='PLOT.OUT',STATUS='NEW')
      OPEN(23,FILE='JCALC.OUT',STATUS='NEW')
      WRITE(21,*) 'JSTOP = ',JSTOP
      WRITE(21,10) ITER
10    FORMAT(1X,'# ITERATIONS = ',I3 //)
      WRITE(21,*)' T      BANK    SPEED     RANGE    ',
     &'THETA    RADAR  STRUCT'
      WRITE(21,*) ' '
      WRITE(23,*) '    JRANGE     JTHETA     JSPEED     JBANK',
     &'     RADAR  STRUCT'

      DO 60 I=1,LIM
         E(I)=1
         F(I)=1
         A=I*.1
         B=BANK(I)*180/3.14159
         C=SPEED(I)*60
         D=THETA(I)*180/3.14159

C      Check to see if missile is within radar detection limits.
C      Write a 1 if it is, write a 0 if it is not.
```

```
      IF ((RANGE(I) .LT. 5.0) .OR. (RANGE(I) .GT. 15.0)) THEN
         GOTO 20
      ENDIF
      IF ((D .LT. -60) .OR. (D .GT. 60)) THEN
         GOTO 20
      ELSE
         GOTO 30
      ENDIF

 20   E(I)=0
      RADSUM=RADSUM+1.0

C     Check to see if CMMCA is within structural limits.
C     Write a 1 if it is, write a 0 if it is not.
C
 30   IF ((B .LT. -30.0) .OR. (B .GT. 30.0)) THEN
         GOTO 40
      ENDIF
      IF ((C .LT. 320) .OR. (C .GT. 480)) THEN
         GOTO 40
      ELSE
         GOTO 50
      ENDIF

 40   F(I)=0
      STRUCSUM=STRUCSUM+1

 50   WRITE(21,70) A,B,C,RANGE(I),D,E(I),F(I)

 60   CONTINUE
 70   FORMAT(F4.1,4(2X,F7.1),6X,I1,6X,I1)

      RADPER=100*(1-(RADSUM/LIMIT))
      WRITE(21,*)' '
      WRITE(21,*)'CM IN RADAR CONE ',RADPER,' PERCENT'

      STRUCPER=100*(1-(STRUCSUM/LIMIT))
      WRITE(21,*)'CMMCA W/IN STRUCTURAL LIMITS ',STRUCPER,' PERCENT'

C     Write the file used to graphically display optimal flight
C     path for the CMMCA and the cruise missile flight path.

      DO 80 I=0,LIM
         WRITE(22,90) XPLANE(I),YPLANE(I),XCM(I),YCM(I)
```

```
 80   CONTINUE
 90   FORMAT(4(3X,F8.2))

C     Write the file used to graphically display the objective
C     function components for the optimal flight path.

      DO 100 I=1,LIM
         JRANGE = QUADW(I)*W(0)*((RANGE(I)-R0)**2)
         JTHETA = QUADW(I)*W(1)*((THETA(I)-THETA0)**2)
         JSPEED = QUADW(I)*W(2)*(((SPEED(I)-U0)/MU)**(2*K3))
         JBANK  = QUADW(I)*W(3)*((BANK(I)/B0)**(2*K4))
         WRITE(23,110) JRANGE,JTHETA,JSPEED,JBANK,E(I),F(I)
 100  CONTINUE
 110  FORMAT(4(1X,F10.4),6X,I1,7X,I1)

      STOP
      END
```

Appendix D. *Graphical Output of Preliminary Results*

This appendix contains all graphical output from the preliminary runs. The preliminary runs were done using weights of one for all the objective functional components and a nominal distance of eight nautical miles. This appendix has the results for each of the four flight paths, which were all run using both the straight and trailing initial CMMCA flight path. For every run, there is a plot of the CMMCA flight path relative to the cruise missile flight path, and the plot of the overall J value at each iteration of the program.

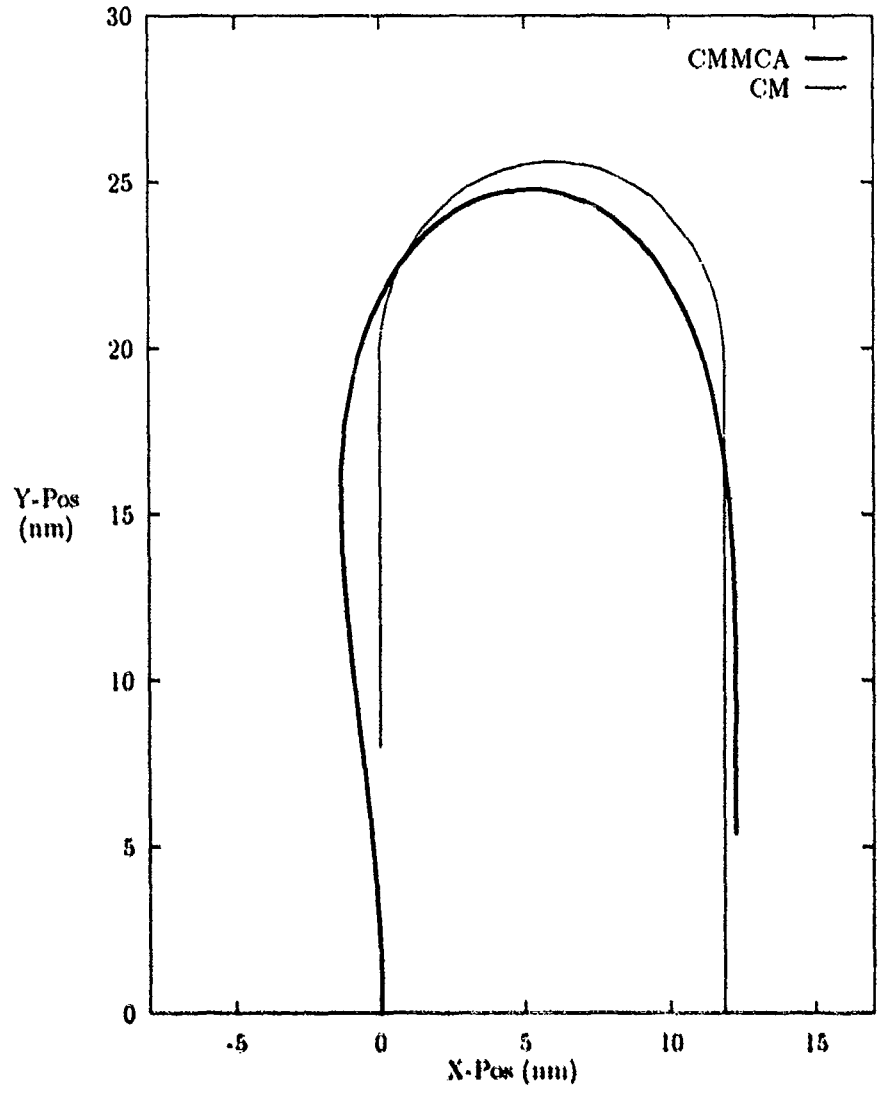

Figure 17. Path 1 CMMCA and CM Paths, CMMCA Starting Straight

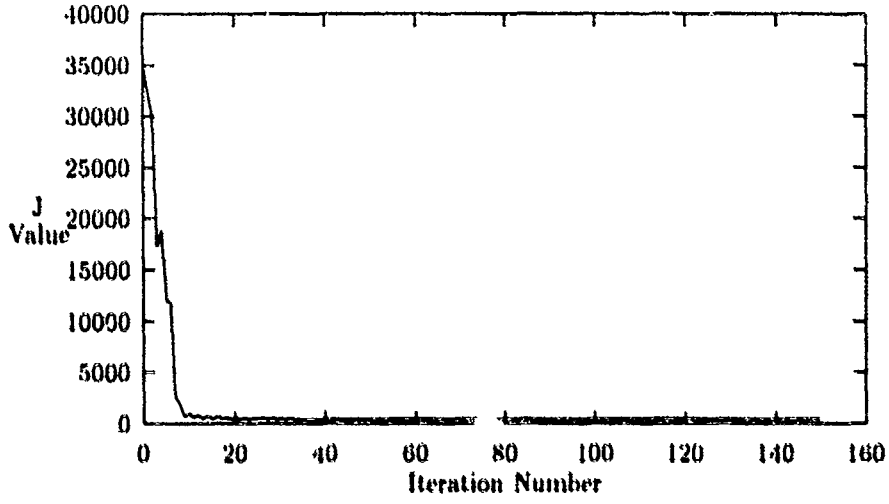

Figure 18. Plot of J Value versus Iteration Number

JSTOP = 447.3045
# ITERATIONS = 150

T	BANK	SPEED	RANGE	THETA	RADAR	STRUCT
0.1	-4.6	399.7	8.0	0.7	1	1
0.2	-4.1	399.6	8.0	2.0	1	1
0.3	-3.5	399.4	8.0	3.3	1	1
0.4	-3.1	399.3	8.0	4.6	1	1
0.5	-2.6	399.2	8.0	5.7	1	1
0.6	-2.2	399.1	8.0	6.9	1	1
0.7	-1.9	399.0	8.0	7.9	1	1
0.8	-1.6	398.9	8.0	8.9	1	1
0.9	-1.2	398.8	8.0	9.9	1	1
1.0	-0.9	398.7	8.1	10.8	1	1
1.1	-0.6	398.6	8.1	11.6	1	1
1.2	-0.3	398.5	8.1	12.4	1	1
1.3	0.0	398.3	8.1	13.0	1	1
1.4	0.4	398.1	8.1	13.6	1	1
1.5	0.8	397.9	8.1	14.0	1	1
1.6	1.2	397.7	8.2	14.3	1	1
1.7	1.7	397.4	8.2	14.5	1	1
1.8	2.2	397.1	8.2	14.4	1	1
1.9	2.8	396.7	8.2	14.6	1	1
2.0	3.5	396.3	8.2	15.2	1	1
2.1	4.2	395.8	8.3	15.9	1	1
2.2	4.9	395.3	8.3	16.8	1	1
2.3	5.7	394.7	8.3	17.9	1	1
2.4	6.5	394.0	8.3	19.1	1	1
2.5	7.3	393.3	8.3	20.4	1	1
2.6	8.2	392.5	8.3	21.8	1	1
2.7	9.1	391.7	8.3	23.2	1	1
2.8	10.0	390.8	8.2	24.6	1	1
2.9	10.9	389.8	8.2	26.0	1	1
3.0	11.9	388.8	8.2	27.3	1	1
3.1	12.8	387.7	8.2	28.5	1	1
3.2	13.8	386.6	8.1	29.6	1	1
3.3	14.8	385.5	8.1	30.5	1	1
3.4	15.8	384.3	8.0	31.3	1	1
3.5	16.7	383.2	8.0	31.8	1	1
3.6	17.7	382.1	7.9	32.2	1	1
3.7	18.6	381.0	7.9	32.3	1	1
3.8	19.4	380.1	7.8	32.2	1	1
3.9	20.1	379.3	7.8	31.8	1	1
4.0	20.8	378.6	7.7	31.3	1	1

4.1	21.3	378.2	7.7	30.6	1	1
4.2	21.7	378.0	7.6	29.7	1	1
4.3	21.9	378.0	7.5	28.8	1	1
4.4	21.9	378.3	7.4	28.0	1	1
4.5	21.6	378.8	7.3	27.0	1	1
4.6	21.2	379.6	7.2	26.3	1	1
4.7	20.6	380.6	7.1	25.5	1	1
4.8	19.8	381.8	6.6	21.6	1	1
4.9	18.8	383.1	7.1	23.3	1	1
5.0	17.7	384.5	7.1	22.1	1	1
5.1	16.5	386.0	7.1	20.8	1	1
5.2	15.3	387.4	7.1	19.4	1	1
5.3	14.0	388.7	7.2	18.1	1	1
5.4	12.9	390.0	7.2	16.7	1	1
5.5	11.7	391.2	7.2	15.4	1	1
5.6	10.6	392.2	7.3	14.1	1	1
5.7	9.5	393.2	7.3	12.8	1	1
5.8	8.5	394.1	7.3	11.7	1	1
5.9	7.6	394.9	7.3	10.5	1	1
6.0	6.7	395.7	7.3	9.5	1	1
6.1	5.9	396.3	7.4	8.6	1	1
6.2	5.1	396.9	7.4	7.7	1	1
6.3	4.4	397.3	7.4	6.9	1	1
6.4	3.8	397.8	7.4	6.1	1	1
6.5	3.2	398.1	7.4	5.5	1	1
6.6	2.7	398.4	7.4	4.9	1	1
6.7	2.3	398.7	7.4	4.4	1	1
6.8	1.9	398.9	7.4	3.9	1	1
6.9	1.5	399.1	7.4	3.6	1	1
7.0	1.2	399.3	7.4	3.2	1	1
7.1	0.9	399.4	7.4	3.0	1	1
7.2	0.7	399.5	7.4	2.7	1	1
7.3	0.5	399.6	7.4	2.6	1	1
7.4	0.3	399.7	7.4	2.4	1	1
7.5	0.2	399.8	7.4	2.3	1	1
7.6	0.1	399.9	7.4	2.2	1	1
7.7	0.0	399.9	7.4	2.1	1	1
7.8	0.0	400.0	7.4	2.1	1	1

CN IN RADAR CONE 100.0000 PERCENT
CNNCA W/IN STRUCTURAL LIMITS 100.0000 PERCENT

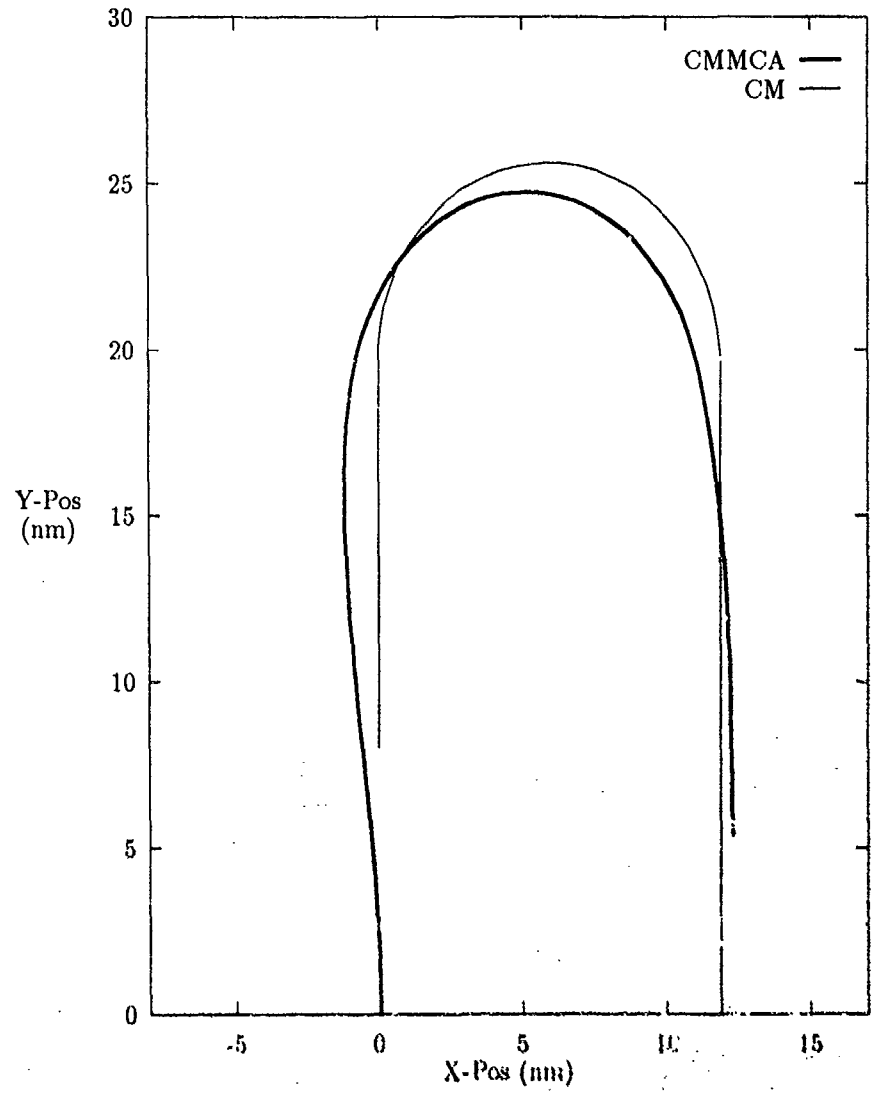

Figure 19. Path 1 CMMCA and CM Paths, CMMCA Starting Trailing

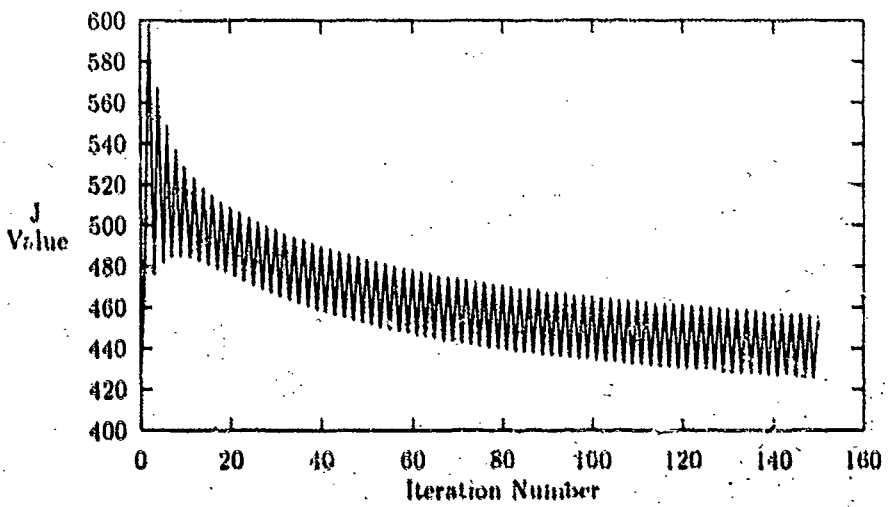

Figure 20. Plot of J Value versus Iteration Number

JSTOP = 455.9345
# ITERATIONS = 150

T	BANK	SPEED	RANGE	THETA	RADAR	STRUCT
0.1	-3.9	398.6	8.0	0.6	1	1
0.2	-3.5	398.6	8.0	1.8	1	1
0.3	-3.1	398.5	8.0	2.9	1	1
0.4	-2.7	398.4	8.0	4.0	1	1
0.5	-2.4	398.4	8.0	5.0	1	1
0.6	-2.0	398.4	8.0	6.0	1	1
0.7	-1.7	398.3	8.0	6.9	1	1
0.8	-1.4	398.3	8.0	7.8	1	1
0.9	-1.1	398.2	8.0	8.7	1	1
1.0	-0.8	398.2	8.1	9.5	1	1
1.1	-0.5	398.2	8.1	10.2	1	1
1.2	-0.2	398.1	8.1	10.8	1	1
1.3	0.1	398.0	8.1	11.4	1	1
1.4	0.4	398.0	8.1	11.8	1	1
1.5	0.8	397.9	8.1	12.2	1	1
1.6	1.2	397.8	8.1	12.4	1	1
1.7	1.6	397.7	8.2	12.5	1	1
1.8	2.0	397.5	8.2	12.4	1	1
1.9	2.5	397.3	8.2	12.6	1	1
2.0	3.0	397.1	8.2	13.2	1	1
2.1	3.5	396.9	8.2	14.1	1	1
2.2	3.9	396.7	8.2	15.3	1	1
2.3	4.4	396.5	8.2	16.7	1	1
2.4	4.8	396.3	8.2	18.5	1	1
2.5	5.2	396.1	8.2	20.4	1	1
2.6	5.5	395.9	8.2	22.7	1	1
2.7	5.8	395.7	8.2	25.2	1	1
2.8	6.0	395.6	8.2	28.0	1	1
2.9	15.1	385.4	8.1	29.7	1	1
3.0	15.2	384.6	8.1	30.0	1	1
3.1	15.6	383.5	8.1	30.3	1	1
3.2	16.1	382.4	8.1	30.6	1	1
3.3	16.4	381.5	8.1	30.9	1	1
3.4	16.8	380.6	8.0	31.1	1	1
3.5	17.4	379.5	8.0	31.3	1	1
3.6	18.0	378.6	8.0	31.3	1	1
3.7	18.4	377.9	7.9	31.3	1	1
3.8	19.0	377.0	7.9	31.1	1	1
3.9	19.7	376.2	7.8	30.7	1	1
4.0	20.0	375.9	7.7	30.3	1	1

4.1	20.3	375.7	7.7	29.7	1	1
4.2	20.7	375.5	7.6	29.1	1	1
4.3	20.9	375.6	7.5	28.5	1	1
4.4	20.8	376.1	7.4	28.0	1	1
4.5	20.8	376.5	7.3	27.3	1	1
4.6	20.6	377.1	7.2	26.9	1	1
4.7	20.1	378.2	7.1	26.3	1	1
4.8	19.6	379.4	6.6	22.5	1	1
4.9	19.0	380.5	7.1	24.3	1	1
5.0	18.6	381.5	7.1	22.8	1	1
5.1	17.5	383.3	7.1	21.2	1	1
5.2	16.9	384.5	7.2	19.3	1	1
5.3	16.4	385.7	7.2	17.2	1	1
5.4	16.3	386.4	7.2	14.8	1	1
5.5	13.8	389.4	7.3	12.3	1	1
5.6	15.0	389.1	7.3	9.7	1	1
5.7	5.3	397.0	7.3	8.1	1	1
5.8	5.0	397.3	7.3	7.8	1	1
5.9	4.6	397.5	7.3	7.5	1	1
6.0	4.3	397.8	7.3	7.2	1	1
6.1	3.9	398.0	7.3	6.8	1	1
6.2	3.6	398.2	7.3	6.5	1	1
6.3	3.3	398.4	7.4	6.1	1	1
6.4	3.0	398.6	7.4	5.8	1	1
6.5	2.7	398.8	7.4	5.5	1	1
6.6	2.4	398.9	7.4	5.2	1	1
6.7	2.1	399.1	7.4	4.9	1	1
6.8	1.9	399.2	7.4	4.6	1	1
6.9	1.6	399.3	7.4	4.3	1	1
7.0	1.4	399.4	7.4	4.1	1	1
7.1	1.2	399.5	7.4	3.9	1	1
7.2	1.0	399.6	7.4	3.7	1	1
7.3	0.8	399.7	7.4	3.6	1	1
7.4	0.6	399.7	7.4	3.5	1	1
7.5	0.4	399.8	7.4	3.4	1	1
7.6	0.3	399.9	7.4	3.4	1	1
7.7	0.1	399.9	7.4	3.4	1	1
7.8	0.0	400.0	7.4	3.4	1	1

CM IN RADAR CONE 100.0000 PERCENT
CMMCA W/IN STRUCTURAL LIMITS 100.0000 PERCENT

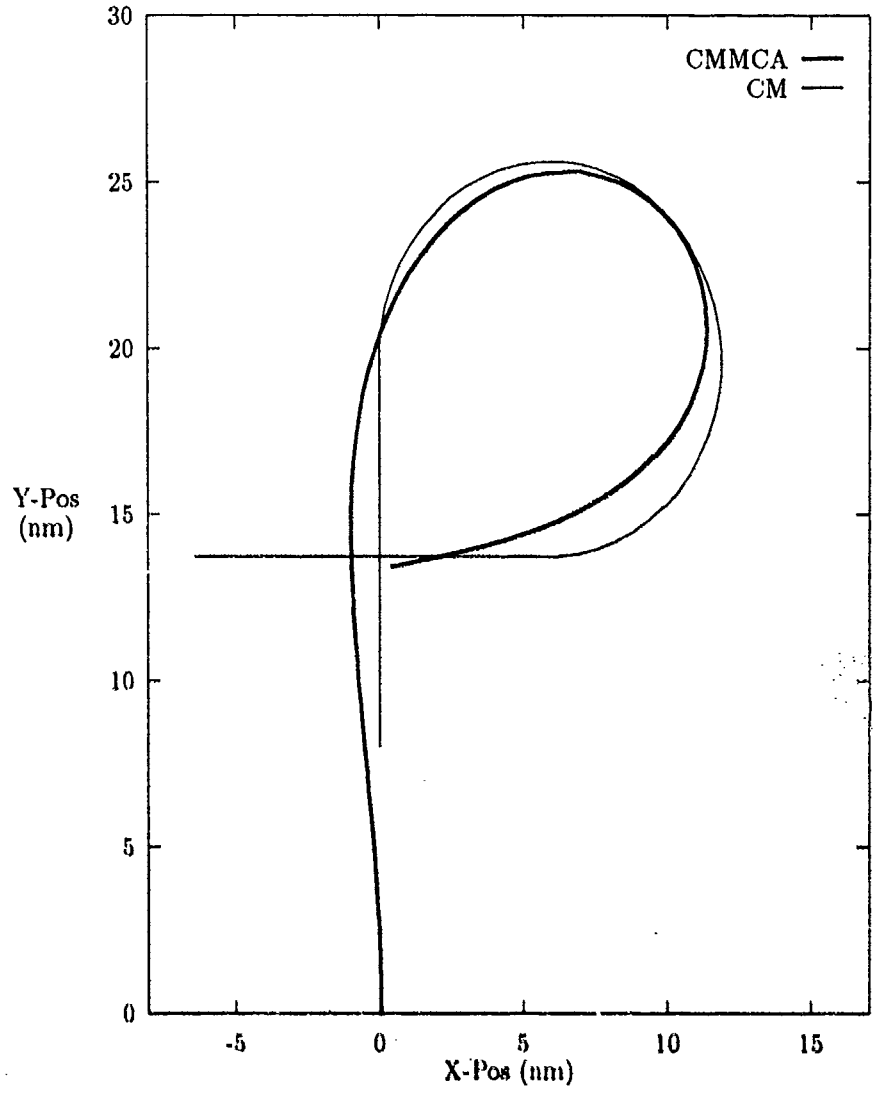

Figure 21. Path 2 CMMCA and CM Paths, CMMCA Starting Straight

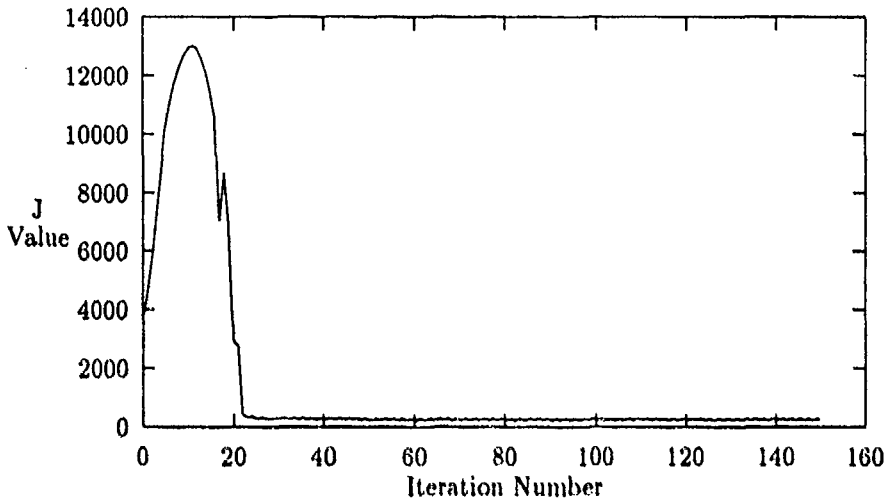

Figure 22. Plot of J Value versus Iteration Number

JSTOP = 249.8399
# ITERATIONS = 150

T	BANK	SPEED	RANGE	THETA	RADAR	STRUCT
0.1	-4.0	404.2	8.0	0.6	1	1
0.2	-3.5	403.6	8.0	1.7	1	1
0.3	-3.0	403.1	8.0	2.8	1	1
0.4	-2.5	402.7	8.0	3.9	1	1
0.5	-2.1	402.3	8.0	4.8	1	1
0.6	-1.8	402.0	8.0	5.7	1	1
0.7	-1.5	401.8	8.0	6.6	1	1
0.8	-1.2	401.6	8.0	7.4	1	1
0.9	-0.9	401.4	8.0	8.2	1	1
1.0	-0.6	401.3	8.0	8.8	1	1
1.1	-0.3	401.1	8.0	9.5	1	1
1.2	0.0	401.0	8.0	10.0	1	1
1.3	0.3	400.9	8.0	10.5	1	1
1.4	0.7	400.8	8.0	10.8	1	1
1.5	1.1	400.7	8.0	11.0	1	1
1.6	1.5	400.6	8.0	11.1	1	1
1.7	2.0	400.5	8.0	11.0	1	1
1.8	2.6	400.4	8.0	10.7	1	1
1.9	3.2	400.3	8.1	10.7	1	1
2.0	3.9	400.1	8.1	11.0	1	1
2.1	4.6	399.9	8.1	11.5	1	1
2.2	5.3	399.7	8.1	12.2	1	1
2.3	6.1	399.5	8.0	13.1	1	1
2.4	6.8	399.3	8.0	14.2	1	1
2.5	7.6	399.0	8.0	15.4	1	1
2.6	8.4	398.8	7.9	16.7	1	1
2.7	9.2	398.4	7.9	18.0	1	1
2.8	10.0	398.1	7.8	19.5	1	1
2.9	10.7	397.7	7.7	21.1	1	1
3.0	11.5	397.2	7.6	22.7	1	1
3.1	12.3	396.7	7.5	24.3	1	1
3.2	13.1	396.1	7.5	26.0	1	1
3.3	13.8	395.4	7.4	27.7	1	1
3.4	14.6	394.7	7.3	29.4	1	1
3.5	15.3	393.9	7.2	31.0	1	1
3.6	16.0	393.0	7.2	32.7	1	1
3.7	16.7	392.0	7.1	34.2	1	1
3.8	17.4	390.9	7.1	35.7	1	1
3.9	18.0	389.7	7.1	37.1	1	1
4.0	18.6	388.5	7.1	38.3	1	1

4.1	19.2	387.1	7.1	39.4	1	1
4.2	19.8	385.8	7.1	40.2	1	1
4.3	20.4	384.4	7.1	40.8	1	1
4.4	20.9	383.0	7.1	41.4	1	1
4.5	21.4	381.6	7.2	41.4	1	1
4.6	21.9	380.2	7.2	41.2	1	1
4.7	22.4	378.9	7.2	40.8	1	1
4.8	22.9	377.8	7.3	40.1	1	1
4.9	23.3	376.7	7.3	39.1	1	1
5.0	23.8	375.9	7.4	37.8	1	1
5.1	24.1	375.3	7.4	36.3	1	1
5.2	24.4	375.0	7.4	34.5	1	1
5.3	24.6	375.0	7.4	32.5	1	1
5.4	24.6	375.3	7.4	30.4	1	1
5.5	24.5	375.9	7.3	28.2	1	1
5.6	24.2	376.8	7.3	26.1	1	1
5.7	23.7	378.0	7.2	24.0	1	1
5.8	23.0	379.4	7.1	22.2	1	1
5.9	22.1	380.9	7.0	20.6	1	1
6.0	21.1	382.7	6.9	19.5	1	1
6.1	19.9	384.5	6.8	18.4	1	1
6.2	18.5	386.3	6.7	17.3	1	1
6.3	17.1	388.0	6.7	16.3	1	1
6.4	15.6	389.6	6.7	15.3	1	1
6.5	14.2	391.1	6.7	14.3	1	1
6.6	12.8	392.5	6.7	13.5	1	1
6.7	11.4	393.7	6.7	12.7	1	1
6.8	10.1	394.8	6.7	12.0	1	1
6.9	8.8	395.7	6.7	11.4	1	1
7.0	7.6	396.5	6.7	10.9	1	1
7.1	6.5	397.2	6.7	10.5	1	1
7.2	5.5	397.7	6.7	10.3	1	1
7.3	4.4	398.3	6.7	10.2	1	1
7.4	3.5	398.7	6.7	10.3	1	1
7.5	2.6	399.1	6.8	10.6	1	1
7.6	1.7	399.4	6.8	11.0	1	1
7.7	0.8	399.7	6.8	11.6	1	1
7.8	0.3	399.9	6.8	12.4	1	1

CM IN RADAR CONE 100.0000 PERCENT
CMMCA W/IN STRUCTURAL LIMITS 100.0000 PERCENT

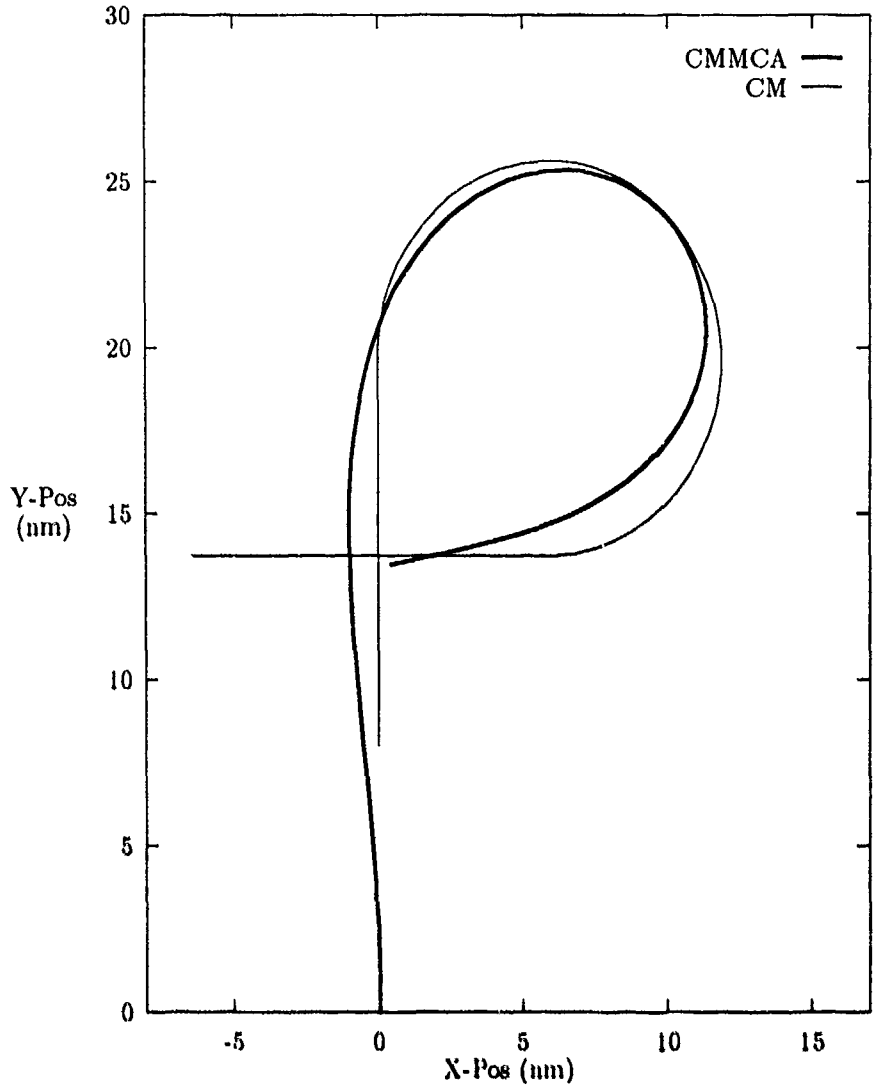

Figure 23. Path 2 CMMCA and CM Paths, CMMCA Starting Trailing

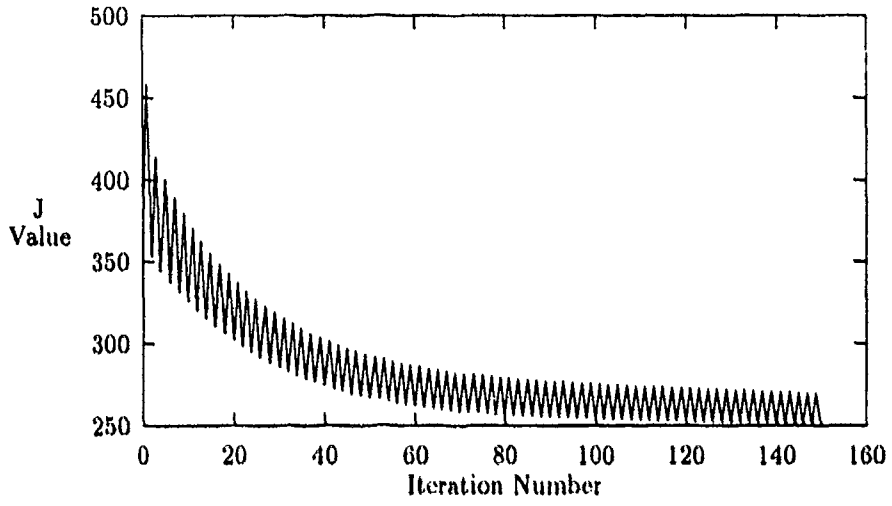

Figure 24. Plot of J Value versus Iteration Number

JSTOP = 250.3886
# ITERATIONS = 150

T	BANK	SPEED	RANGE	THETA	RADAR	STRUCT
0.1	-3.9	404.7	8.0	0.6	1	1
0.2	-3.4	404.2	8.0	1.7	1	1
0.3	-3.0	403.9	8.0	2.8	1	1
0.4	-2.5	403.6	8.0	3.8	1	1
0.5	-2.2	403.3	8.0	4.8	1	1
0.6	-1.8	403.1	8.0	5.7	1	1
0.7	-1.5	402.9	8.0	6.5	1	1
0.8	-1.2	402.8	8.0	7.4	1	1
0.9	-0.9	402.6	8.0	8.1	1	1
1.0	-0.6	402.5	8.0	8.8	1	1
1.1	-0.3	402.4	8.0	9.4	1	1
1.2	0.1	402.4	8.0	9.9	1	1
1.3	0.4	402.3	8.0	10.4	1	1
1.4	0.8	402.2	8.0	10.7	1	1
1.5	1.2	402.2	8.0	10.9	1	1
1.6	1.6	402.1	8.0	10.9	1	1
1.7	2.1	402.1	8.0	10.8	1	1
1.8	2.6	402.0	8.0	10.5	1	1
1.9	3.2	401.9	8.0	10.5	1	1
2.0	3.8	401.9	8.0	10.8	1	1
2.1	4.5	401.8	8.0	11.3	1	1
2.2	5.1	401.7	8.0	12.1	1	1
2.3	5.7	401.6	8.0	13.1	1	1
2.4	6.3	401.6	8.0	14.3	1	1
2.5	6.8	401.5	7.9	15.8	1	1
2.6	7.3	401.5	7.9	17.4	1	1
2.7	7.8	401.5	7.8	19.3	1	1
2.8	8.1	401.5	7.7	21.4	1	1
2.9	13.0	398.1	7.7	23.1	1	1
3.0	13.3	397.8	7.6	24.2	1	1
3.1	13.7	397.3	7.5	25.5	1	1
3.2	14.2	396.7	7.4	26.8	1	1
3.3	14.7	396.1	7.4	28.2	1	1
3.4	15.1	395.4	7.3	29.7	1	1
3.5	15.7	394.5	7.2	31.2	1	1
3.6	16.3	393.5	7.2	32.6	1	1
3.7	16.8	392.6	7.1	34.1	1	1
3.8	17.4	391.4	7.1	35.5	1	1
3.9	18.0	390.1	7.1	36.8	1	1
4.0	18.5	388.8	7.1	37.9	1	1

4.1	19.1	387.5	7.1	39.0	1	1
4.2	19.7	386.0	7.1	39.8	1	1
4.3	20.2	384.6	7.1	40.4	1	1
4.4	20.7	383.2	7.2	41.0	1	1
4.5	21.3	381.7	7.2	40.9	1	1
4.6	21.9	380.1	7.2	40.8	1	1
4.7	22.3	378.9	7.3	40.3	1	1
4.8	22.7	377.8	7.3	39.6	1	1
4.9	23.2	376.7	7.3	38.6	1	1
5.0	23.8	375.5	7.4	37.3	1	1
5.1	23.8	375.2	7.4	35.8	1	1
5.2	24.2	374.6	7.4	34.1	1	1
5.3	24.4	374.3	7.4	32.2	1	1
5.4	24.9	373.7	7.3	30.0	1	1
5.5	23.1	376.5	7.3	28.0	1	1
5.6	24.2	375.4	7.2	26.1	1	1
5.7	23.3	376.9	7.2	24.1	1	1
5.8	22.6	378.3	7.1	22.4	1	1
5.9	21.8	379.7	7.0	21.0	1	1
6.0	20.9	381.2	6.9	20.0	1	1
6.1	19.7	383.0	6.8	19.0	1	1
6.2	18.3	384.9	6.7	18.0	1	1
6.3	17.3	386.4	6.7	17.0	1	1
6.4	15.8	388.2	6.7	15.9	1	1
6.5	14.6	389.8	6.7	14.9	1	1
6.6	13.4	391.1	6.7	13.9	1	1
6.7	12.3	392.4	6.7	12.8	1	1
6.8	11.2	393.7	6.7	11.8	1	1
6.9	10.3	394.7	6.7	10.7	1	1
7.0	9.5	395.7	6.7	9.6	1	1
7.1	4.6	398.3	6.7	9.1	1	1
7.2	3.9	398.6	6.7	9.3	1	1
7.3	3.2	398.9	6.8	9.6	1	1
7.4	2.6	399.2	6.8	10.0	1	1
7.5	1.9	399.4	6.8	10.4	1	1
7.6	1.3	399.6	6.8	11.0	1	1
7.7	0.7	399.8	6.8	11.8	1	1
7.8	0.2	400.0	6.8	12.7	1	1

CM IN RADAR CONE 100.0000 PERCENT
CMMCA W/IN STRUCTURAL LIMITS 100.0000 PERCENT

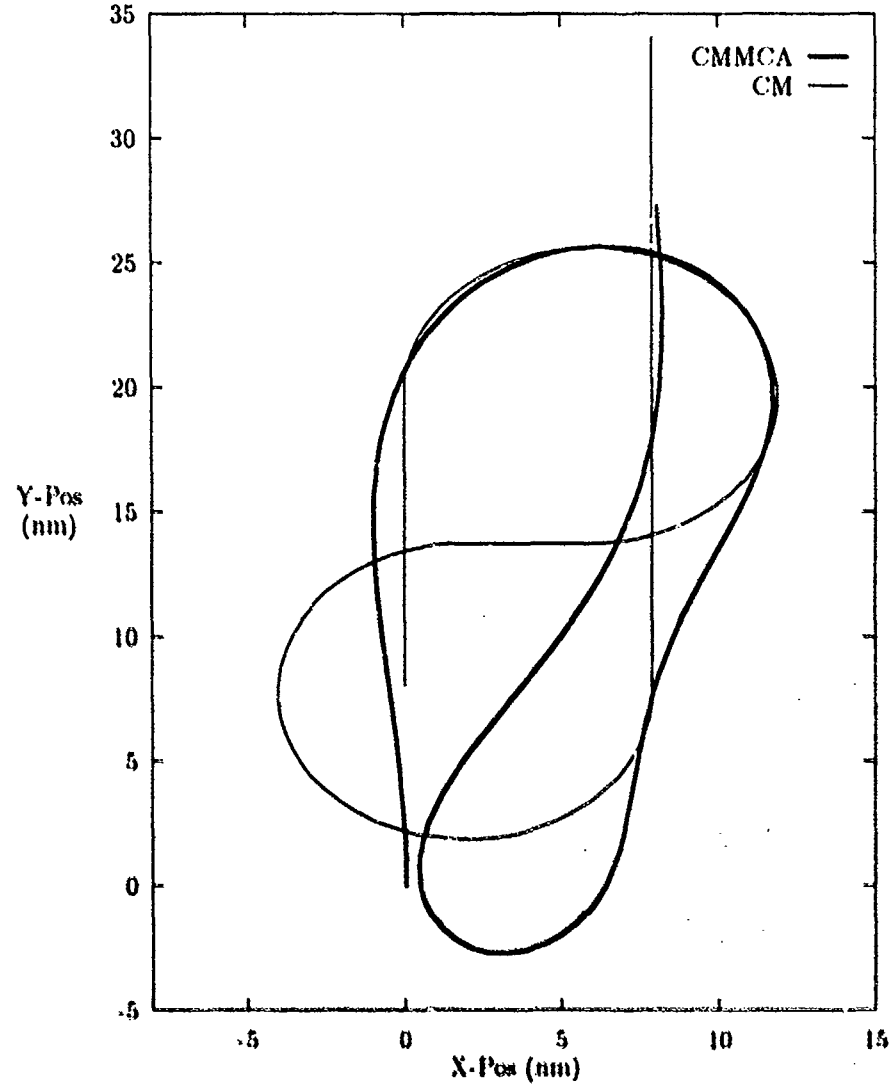

Figure 25. Path 3 CMMCA and CM Paths, CMMCA Starting Straight

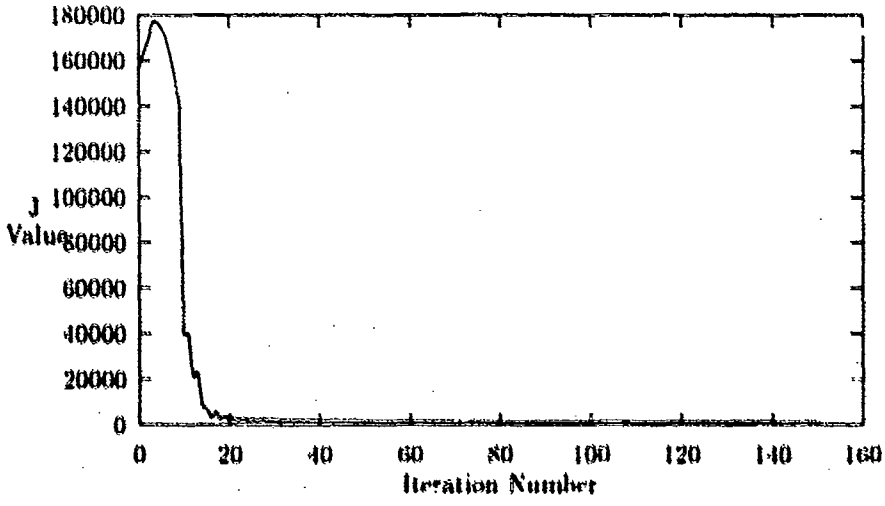

Figure 26. Plot of J Value versus Iteration Number

JSTOP = 1217.040
# ITERATIONS = 150

T	BANK	SPEED	RANGE	THETA	RADAR	STRUCT
0.1	-3.8	402.6	8.0	0.6	1	1
0.2	-3.3	401.9	8.0	1.7	1	1
0.3	-2.8	401.3	8.0	2.7	1	1
0.4	-2.4	400.8	8.0	3.7	1	1
0.5	-2.1	400.3	8.0	4.6	1	1
0.6	-1.7	399.8	8.0	5.5	1	1
0.7	-1.4	399.4	8.0	6.3	1	1
0.8	-1.1	399.0	8.0	7.1	1	1
0.9	-0.8	398.6	8.0	7.8	1	1
1.0	-0.6	398.3	8.0	8.5	1	1
1.1	-0.3	398.0	8.0	9.1	1	1
1.2	0.0	397.7	8.0	9.6	1	1
1.3	0.3	397.4	8.1	10.0	1	1
1.4	0.6	397.2	8.1	10.3	1	1
1.5	1.0	396.9	8.1	10.5	1	1
1.6	1.4	396.6	8.1	10.6	1	1
1.7	1.8	396.4	8.1	10.6	1	1
1.8	2.3	396.1	8.1	10.3	1	1
1.9	2.8	395.9	8.1	10.4	1	1
2.0	3.3	395.6	8.2	10.8	1	1
2.1	3.9	395.4	8.2	11.5	1	1
2.2	4.5	395.2	8.2	12.4	1	1
2.3	5.2	395.0	8.2	13.5	1	1
2.4	5.8	394.8	8.1	14.8	1	1
2.5	6.5	394.6	8.1	16.3	1	1
2.6	7.2	394.4	8.1	18.0	1	1
2.7	8.0	394.3	8.0	19.7	1	1
2.8	8.8	394.2	7.9	21.6	1	1
2.9	9.6	394.1	7.9	23.5	1	1
3.0	10.4	394.0	7.8	25.5	1	1
3.1	11.2	394.0	7.8	27.6	1	1
3.2	12.1	393.9	7.7	29.6	1	1
3.3	13.0	394.0	7.6	31.7	1	1
3.4	13.9	394.0	7.6	33.7	1	1
3.5	14.8	394.1	7.5	35.6	1	1
3.6	15.7	394.2	7.5	37.4	1	1
3.7	16.6	394.3	7.5	39.1	1	1
3.8	17.6	394.5	7.5	40.5	1	1
3.9	18.5	394.7	7.5	41.8	1	1
4.0	19.4	394.9	7.5	42.8	1	1

4.1	20.3	395.1	7.5	43.6	1	1
4.2	21.1	395.3	7.6	44.0	1	1
4.3	21.8	395.5	7.6	44.2	1	1
4.4	22.5	395.7	7.7	44.1	1	1
4.5	23.1	395.9	7.7	43.8	1	1
4.6	23.5	396.1	7.7	43.2	1	1
4.7	23.8	396.2	7.8	42.4	1	1
4.8	23.9	396.4	7.8	41.4	1	1
4.9	23.9	396.5	7.8	40.4	1	1
5.0	23.7	396.6	7.8	39.4	1	1
5.1	23.3	396.6	7.8	38.4	1	1
5.2	22.8	396.6	7.8	37.5	1	1
5.3	22.0	396.7	7.8	36.9	1	1
5.4	21.2	396.7	7.8	36.4	1	1
5.5	20.2	396.7	7.7	36.4	1	1
5.6	19.0	396.7	7.7	36.7	1	1
5.7	17.7	396.8	7.7	37.5	1	1
5.8	16.4	396.8	7.6	38.8	1	1
5.9	14.9	396.9	7.6	40.7	1	1
6.0	13.3	397.0	7.6	43.1	1	1
6.1	11.7	397.2	7.7	45.8	1	1
6.2	10.0	397.4	7.9	48.6	1	1
6.3	8.2	397.6	8.0	51.5	1	1
6.4	6.5	397.8	8.3	54.6	1	1
6.5	4.8	398.0	8.6	57.7	1	1
6.6	3.1	398.3	8.9	60.9	0	1
6.7	1.5	398.6	9.2	63.8	0	1
6.8	0.0	398.8	9.6	66.4	0	1
6.9	-1.4	399.1	10.0	68.8	0	1
7.0	-2.6	399.4	10.3	71.1	0	1
7.1	-3.7	399.6	10.7	73.3	0	1
7.2	-4.5	399.8	11.0	75.4	0	1
7.3	-5.2	400.0	11.2	77.4	0	1
7.4	-5.7	400.2	11.4	79.4	0	1
7.5	-5.9	400.3	11.6	81.3	0	1
7.6	-5.9	400.3	11.7	83.1	0	1
7.7	-5.6	400.2	11.8	84.8	0	1
7.8	-5.1	400.1	11.8	86.3	0	1
7.9	-4.3	399.8	11.7	87.7	0	1
8.0	-3.3	399.4	11.6	88.8	0	1
8.1	-2.1	398.9	11.4	89.7	0	1
8.2	-0.7	398.2	11.2	90.3	0	1
8.3	1.0	397.3	10.9	90.6	0	1
8.4	2.9	396.3	10.5	90.6	0	1
8.5	5.0	395.1	10.1	90.4	0	1

8.6	7.4	393.6	9.6	89.9	0	1
8.7	10.0	391.9	9.0	89.1	0	1
8.8	12.8	390.0	8.4	88.3	0	1
8.9	15.8	387.7	7.7	87.4	0	1
9.0	19.0	385.2	7.0	86.7	0	1
9.1	22.5	382.4	6.3	86.4	0	1
9.2	26.1	379.4	5.7	87.0	0	1
9.3	29.7	376.2	5.1	88.8	0	1
9.4	33.3	372.8	4.7	91.8	0	0
9.5	36.5	369.7	4.6	95.0	0	0
9.6	38.7	367.4	4.8	96.7	0	0
9.7	39.6	366.2	5.2	95.8	0	0
9.8	38.8	366.6	5.7	92.1	0	0
9.9	36.8	368.2	6.3	86.7	0	0
10.0	34.2	370.5	6.9	80.5	0	0
10.1	31.1	373.2	7.5	73.9	0	0
10.2	28.0	376.0	7.9	67.4	0	1
10.3	25.0	378.7	8.3	61.0	0	1
10.4	22.0	381.3	8.5	55.0	1	1
10.5	19.3	383.7	8.7	49.2	1	1
10.6	16.7	385.8	8.7	43.8	1	1
10.7	14.3	387.8	8.6	38.5	1	1
10.8	12.1	389.5	8.5	33.5	1	1
10.9	10.0	391.0	8.3	28.8	1	1
11.0	8.1	392.4	8.2	24.5	1	1
11.1	6.3	393.6	8.0	20.6	1	1
11.2	4.7	394.7	7.8	16.9	1	1
11.3	3.2	395.6	7.6	13.4	1	1
11.4	1.9	396.4	7.5	10.2	1	1
11.5	0.6	397.1	7.3	7.2	1	1
11.6	-0.5	397.7	7.2	4.4	1	1
11.7	-1.5	398.2	7.1	1.9	1	1
11.8	-2.4	398.7	6.9	-0.5	1	1
11.9	-3.2	399.0	6.9	-2.6	1	1
12.0	-3.9	399.3	6.8	-4.5	1	1
12.1	-4.5	399.6	6.7	-6.1	1	1
12.2	-5.0	399.8	6.7	-7.5	1	1
12.3	-5.4	399.9	6.7	-8.7	1	1
12.4	-5.8	400.1	6.6	-9.6	1	1
12.5	-6.0	400.1	6.6	-10.2	1	1
12.6	-6.2	400.2	6.6	-10.7	1	1
12.7	-6.3	400.2	6.6	-10.9	1	1
12.8	-6.3	400.3	6.6	-10.9	1	1
12.9	-6.3	400.3	6.7	-10.8	1	1
13.0	-6.2	400.3	6.7	-10.5	1	1

13.1	-6.1	400.2	6.7	-10.0	1	1
13.2	-5.9	400.2	6.7	-9.4	1	1
13.3	-5.6	400.2	6.7	-8.7	1	1
13.4	-5.3	400.1	6.7	-7.9	1	1
13.5	-5.0	400.1	6.7	-7.1	1	1
13.6	-4.7	400.1	6.7	-6.2	1	1
13.7	-4.3	400.1	6.7	-5.3	1	1
13.8	-4.0	400.0	6.7	-4.3	1	1
13.9	-3.6	400.0	6.7	-3.4	1	1
14.0	-3.2	400.0	6.7	-2.4	1	1
14.1	-2.7	400.0	6.7	-1.5	1	1
14.2	-2.3	400.0	6.7	-0.7	1	1
14.3	-1.9	400.0	6.7	0.1	1	1
14.4	-1.4	400.0	6.7	0.9	1	1
14.5	-0.9	400.0	6.7	1.5	1	1
14.6	-0.5	400.0	6.7	2.0	1	1
14.7	-0.1	400.0	6.7	2.5	1	1

CM IN RADAR CONE 74.14967 PERCENT
CMMCA W/IN STRUCTURAL LIMITS 94.55782 PERCENT

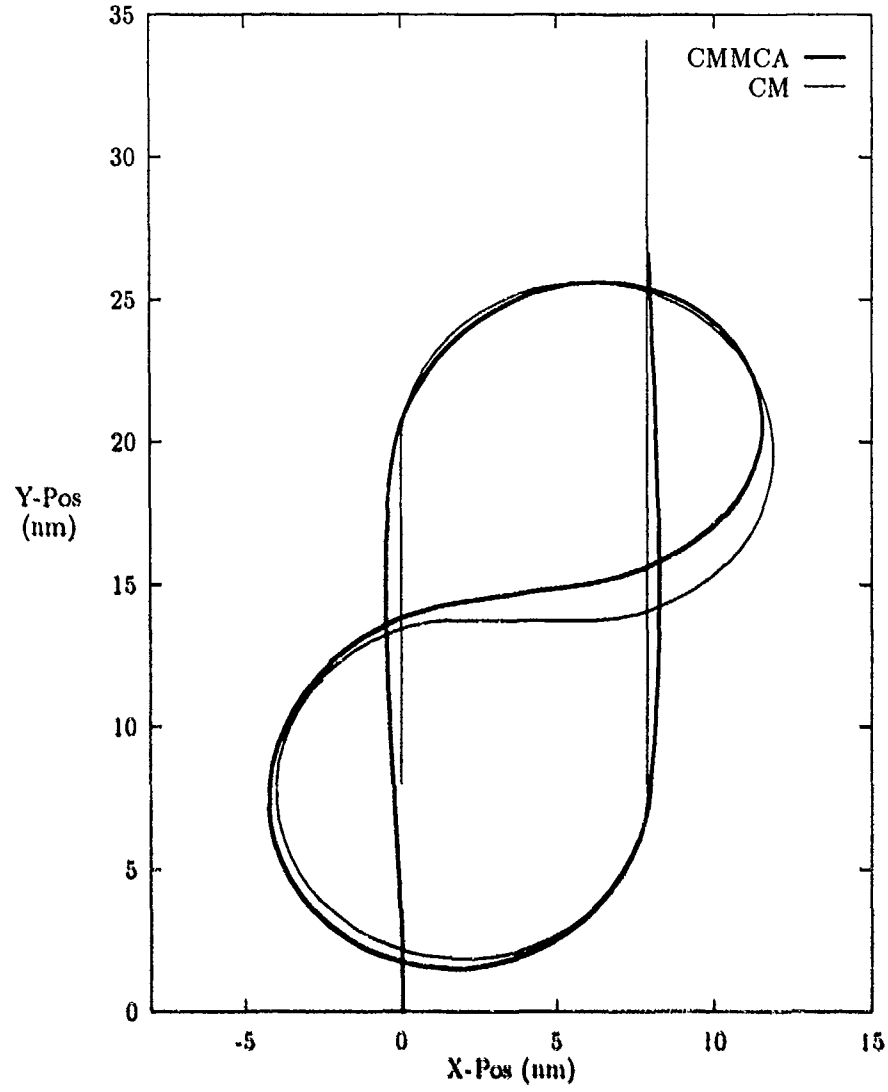

Figure 27. Path 3 CMMCA and CM Paths, CMMCA Starting Trailing

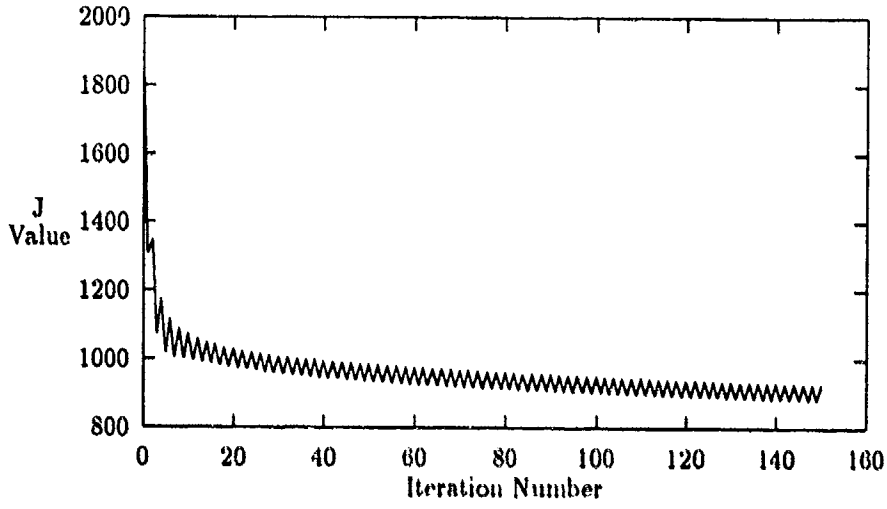

Figure 28. Plot of J Value versus Iteration Number

JSTOP = 926.8980
# ITERATIONS = 150

T	BANK	SPEED	RANGE	THETA	RADAR	STRUCT
0.1	-2.0	399.8	8.0	0.3	1	1
0.2	-1.8	399.7	8.0	0.9	1	1
0.3	-1.6	399.6	8.0	1.5	1	1
0.4	-1.4	399.5	8.0	2.0	1	1
0.5	-1.2	399.4	8.0	2.5	1	1
0.6	-1.0	399.3	8.0	3.0	1	1
0.7	-0.8	399.2	8.0	3.5	1	1
0.8	-0.6	399.1	8.0	3.9	1	1
0.9	-0.4	399.1	8.0	4.3	1	1
1.0	-0.2	399.0	8.0	4.7	1	1
1.1	-0.1	399.0	8.0	5.0	1	1
1.2	0.1	398.9	8.0	5.3	1	1
1.3	0.3	398.8	8.0	5.5	1	1
1.4	0.5	398.8	8.0	5.6	1	1
1.5	0.7	398.8	8.0	5.7	1	1
1.6	0.9	398.7	8.0	5.7	1	1
1.7	1.1	398.7	8.0	5.6	1	1
1.8	1.3	398.6	8.1	5.4	1	1
1.9	1.5	398.6	8.1	5.7	1	1
2.0	1.7	398.6	8.1	6.4	1	1
2.1	1.9	398.5	8.0	7.5	1	1
2.2	2.1	398.5	8.0	9.1	1	1
2.3	2.2	398.5	8.0	11.1	1	1
2.4	2.3	398.6	7.9	13.5	1	1
2.5	2.4	398.6	7.9	16.3	1	1
2.6	2.4	398.6	7.8	19.7	1	1
2.7	2.3	398.7	7.8	23.5	1	1
2.8	2.2	398.8	7.7	27.8	1	1
2.9	16.6	391.4	7.7	30.3	1	1
3.0	16.5	391.7	7.6	30.8	1	1
3.1	16.4	392.0	7.6	31.5	1	1
3.2	16.5	392.2	7.6	32.4	1	1
3.3	16.5	392.5	7.5	33.4	1	1
3.4	16.7	392.7	7.5	34.4	1	1
3.5	16.9	392.9	7.5	35.5	1	1
3.6	17.2	393.0	7.5	36.7	1	1
3.7	17.6	393.2	7.4	37.8	1	1
3.8	18.0	393.3	7.4	39.0	1	1
3.9	18.4	393.4	7.4	40.0	1	1
4.0	18.9	393.5	7.5	41.0	1	1

4.1	19.4	393.6	7.5	41.9	1	1
4.2	20.0	393.6	7.5	42.6	1	1
4.3	20.6	393.6	7.5	43.0	1	1
4.4	21.1	393.6	7.6	43.3	1	1
4.5	21.7	393.6	7.6	43.4	1	1
4.6	22.5	393.4	7.6	43.2	1	1
4.7	22.5	393.6	7.7	42.8	1	1
4.8	23.6	393.2	7.7	42.1	1	1
4.9	23.9	393.2	7.7	41.1	1	1
5.0	24.3	393.0	7.8	39.9	1	1
5.1	24.7	392.8	7.8	38.5	1	1
5.2	24.9	392.7	7.8	36.8	1	1
5.3	25.1	392.5	7.8	35.1	1	1
5.4	25.1	392.3	7.7	33.2	1	1
5.5	25.1	392.1	7.7	31.2	1	1
5.6	24.8	392.0	7.6	29.2	1	1
5.7	24.5	391.9	7.5	27.3	1	1
5.8	24.1	391.7	7.4	25.5	1	1
5.9	23.4	391.7	7.3	23.8	1	1
6.0	22.7	391.6	7.2	22.4	1	1
6.1	21.8	391.6	7.1	20.9	1	1
6.2	21.0	391.6	7.0	19.2	1	1
6.3	19.9	391.7	7.0	17.2	1	1
6.4	19.0	391.7	7.0	15.2	1	1
6.5	18.0	391.8	7.0	12.9	1	1
6.6	16.9	391.9	7.0	10.5	1	1
6.7	16.0	391.9	7.0	7.4	1	1
6.8	15.1	392.0	7.0	3.4	1	1
6.9	14.3	392.1	7.0	-1.3	1	1
7.0	13.7	392.1	7.0	-6.8	1	1
7.1	-1.2	398.6	7.0	-10.8	1	1
7.2	-1.6	398.7	7.0	-13.3	1	1
7.3	-2.0	398.7	7.0	-16.2	1	1
7.4	-2.3	398.8	6.9	-19.6	1	1
7.5	-2.6	398.8	6.9	-23.4	1	1
7.6	-2.8	398.9	6.9	-27.6	1	1
7.7	-17.2	405.4	6.9	-30.1	1	1
7.8	-18.4	406.2	6.9	-30.6	1	1
7.9	-17.5	406.0	6.9	-31.1	1	1
8.0	-18.1	406.5	6.9	-31.8	1	1
8.1	-18.3	406.9	6.9	-32.6	1	1
8.2	-18.5	407.4	6.8	-33.3	1	1
8.3	-18.8	407.9	6.8	-34.1	1	1
8.4	-19.1	408.4	6.8	-34.8	1	1
8.5	-19.4	409.0	6.8	-35.6	1	1

8.6	-19.7	409.6	6.8	-36.3	1	1
8.7	-20.0	410.2	6.9	-37.0	1	1
8.8	-20.4	410.8	6.9	-37.7	1	1
8.9	-20.7	411.4	6.9	-38.2	1	1
9.0	-21.1	412.0	6.9	-38.7	1	1
9.1	-21.4	412.5	6.9	-39.1	1	1
9.2	-21.7	413.1	7.0	-39.4	1	1
9.3	-22.0	413.6	7.0	-39.6	1	1
9.4	-22.4	414.1	7.0	-39.7	1	1
9.5	-22.6	414.5	7.1	-39.6	1	1
9.6	-22.9	414.9	7.1	-39.4	1	1
9.7	-23.1	415.1	7.1	-39.1	1	1
9.8	-23.2	415.3	7.1	-38.7	1	1
9.9	-23.4	415.5	7.2	-38.3	1	1
10.0	-23.5	415.5	7.2	-37.7	1	1
10.1	-23.5	415.5	7.2	-37.1	1	1
10.2	-23.5	415.3	7.2	-36.4	1	1
10.3	-23.4	415.1	7.2	-35.7	1	1
10.4	-23.2	414.8	7.2	-35.0	1	1
10.5	-23.0	414.4	7.2	-34.4	1	1
10.6	-22.8	413.9	7.2	-33.8	1	1
10.7	-22.4	413.3	7.1	-33.3	1	1
10.8	-22.0	412.7	7.1	-32.9	1	1
10.9	-21.5	412.1	7.1	-32.2	1	1
11.0	-21.0	411.4	7.1	-31.1	1	1
11.1	-20.4	410.6	7.2	-29.5	1	1
11.2	-19.9	409.9	7.2	-27.6	1	1
11.3	-19.4	409.2	7.3	-25.3	1	1
11.4	-18.9	408.5	7.3	-22.6	1	1
11.5	-18.5	407.8	7.3	-19.6	1	1
11.6	-18.1	407.1	7.4	-16.2	1	1
11.7	-17.7	406.5	7.4	-12.5	1	1
11.8	-17.5	405.9	7.4	-8.3	1	1
11.9	-2.6	400.2	7.4	-6.0	1	1
12.0	-2.4	400.2	7.4	-5.7	1	1
12.1	-2.3	400.1	7.4	-5.4	1	1
12.2	-2.1	400.1	7.4	-5.1	1	1
12.3	-2.0	400.0	7.4	-4.8	1	1
12.4	-1.8	400.0	7.4	-4.5	1	1
12.5	-1.7	400.0	7.4	-4.1	1	1
12.6	-1.5	400.0	7.4	-3.8	1	1
12.7	-1.4	400.0	7.4	-3.4	1	1
12.8	-1.3	399.9	7.4	-3.1	1	1
12.9	-1.2	399.9	7.4	-2.8	1	1
13.0	-1.1	399.9	7.4	-2.4	1	1

13.1	-0.9	399.9	7.4	-2.1	1	1
13.2	-0.8	399.9	7.4	-1.8	1	1
13.3	-0.8	399.9	7.4	-1.4	1	1
13.4	-0.7	399.9	7.4	-1.1	1	1
13.5	-0.6	399.9	7.4	-0.8	1	1
13.6	-0.5	399.9	7.4	-0.5	1	1
13.7	-0.4	399.9	7.4	-0.2	1	1
13.8	-0.4	399.9	7.4	0.1	1	1
13.9	-0.3	399.9	7.4	0.4	1	1
14.0	-0.3	399.9	7.4	0.6	1	1
14.1	-0.2	399.9	7.4	0.9	1	1
14.2	-0.2	399.9	7.4	1.1	1	1
14.3	-0.1	400.0	7.4	1.4	1	1
14.4	-0.1	400.0	7.4	1.6	1	1
14.5	-0.1	400.0	7.4	1.9	1	1
14.6	0.0	400.0	7.4	2.1	1	1
14.7	0.0	400.0	7.4	2.3	1	1

CM IN RADAR CONE	100.0000	PERCENT
CMMCA W/IN STRUCTURAL LIMITS	100.0000	PERCENT

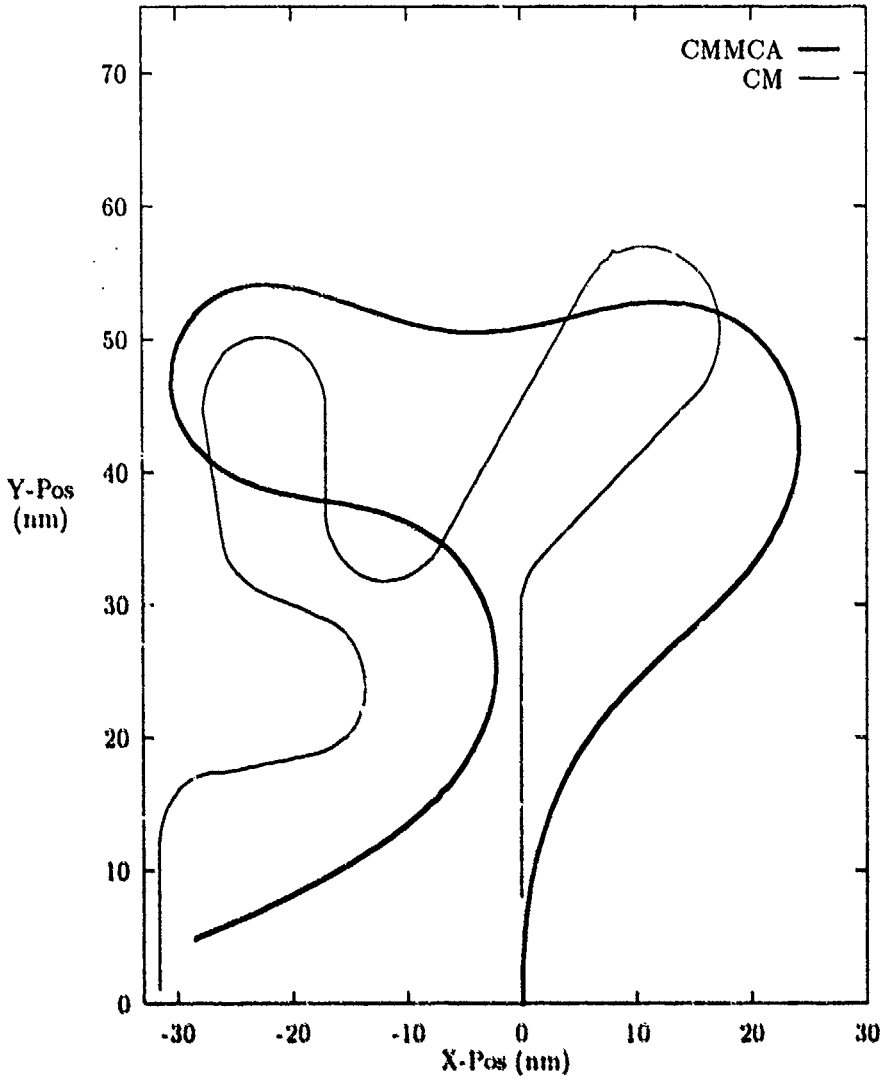

Figure 29. Path 4 CMMCA and CM Paths, CMMCA Starting Straight

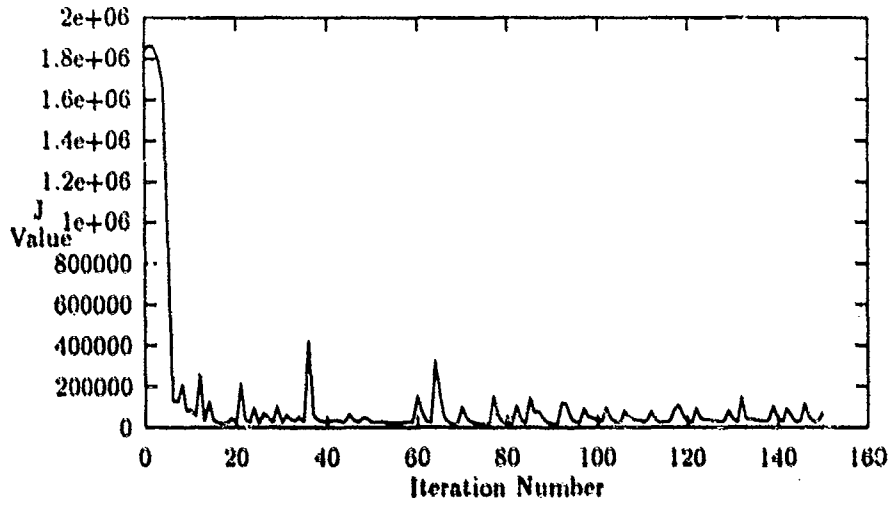

Figure 30. Plot of J Value versus Iteration Number

JSTOP = 76391.24
# ITERATIONS = 150

T	BANK	SPEED	RANGE	THETA	RADAR	STRUCT
0.1	1.4	400.3	8.0	-0.2	1	1
0.2	1.7	400.3	8.0	-0.7	1	1
0.3	2.0	400.3	8.0	-1.3	1	1
0.4	2.3	400.2	8.0	-2.0	1	1
0.5	2.6	400.2	8.0	-2.9	1	1
0.6	2.9	400.2	8.0	-4.0	1	1
0.7	3.2	400.2	8.0	-5.1	1	1
0.8	3.4	400.2	8.0	-6.5	1	1
0.9	3.6	400.2	8.0	-7.9	1	1
1.0	3.9	400.1	8.0	-9.6	1	1
1.1	4.1	400.1	8.0	-11.3	1	1
1.2	4.3	400.1	8.0	-13.3	1	1
1.3	4.4	400.1	8.1	-15.3	1	1
1.4	4.6	400.1	8.1	-17.5	1	1
1.5	4.7	400.1	8.1	-19.9	1	1
1.6	4.9	400.0	8.2	-22.4	1	1
1.7	5.0	400.0	8.2	-25.0	1	1
1.8	5.1	400.0	8.3	-27.8	1	1
1.9	5.2	400.0	8.3	-30.6	1	1
2.0	5.2	400.0	8.4	-33.6	1	1
2.1	5.3	400.0	8.5	-36.6	1	1
2.2	5.3	400.0	8.6	-39.7	1	1
2.3	5.4	399.9	8.8	-42.8	1	1
2.4	5.4	399.9	8.9	-46.0	1	1
2.5	5.4	399.9	9.1	-49.2	1	1
2.6	5.3	399.9	9.3	-52.4	1	1
2.7	5.3	399.9	9.5	-55.6	1	1
2.8	5.2	399.9	9.8	-58.7	1	1
2.9	5.1	399.9	10.0	-61.8	0	1
3.0	5.0	399.9	10.3	-64.9	0	1
3.1	4.9	399.9	10.6	-67.8	0	1
3.2	4.8	399.8	11.0	-70.7	0	1
3.3	4.6	399.8	11.3	-73.4	0	1
3.4	4.5	399.8	11.6	-75.7	0	1
3.5	4.3	399.8	11.9	-77.7	0	1
3.6	4.1	399.8	12.2	-79.3	0	1
3.7	3.8	399.8	12.3	-80.7	0	1
3.8	3.6	399.8	12.4	-81.9	0	1
3.9	3.3	399.8	12.5	-82.9	0	1
4.0	3.0	399.8	12.5	-83.8	0	1

4.1	2.7	399.9	12.5	-84.6	0	1
4.2	2.4	399.9	12.5	-85.4	0	1
4.3	2.1	399.9	12.5	-86.1	0	1
4.4	1.7	399.9	12.5	-86.6	0	1
4.5	1.4	399.9	12.6	-87.0	0	1
4.6	1.0	399.9	12.6	-87.4	0	1
4.7	0.6	399.9	12.7	-87.6	0	1
4.8	0.2	399.9	12.7	-87.8	0	1
4.9	-0.2	399.9	12.7	-87.8	0	1
5.0	-0.7	400.0	12.8	-87.6	0	1
5.1	-1.1	400.0	12.8	-87.4	0	1
5.2	-1.5	400.0	12.9	-87.0	0	1
5.3	-2.0	400.0	12.9	-86.5	0	1
5.4	-2.4	400.0	12.9	-85.9	0	1
5.5	-2.9	400.0	13.0	-85.2	0	1
5.6	-3.4	400.1	13.0	-84.3	0	1
5.7	-3.9	400.1	13.0	-83.2	0	1
5.8	-4.3	400.1	12.9	-82.1	0	1
5.9	-4.8	400.1	12.9	-80.7	0	1
6.0	-5.3	400.1	12.9	-79.3	0	1
6.1	-5.8	400.2	12.8	-77.6	0	1
6.2	-6.3	400.2	12.7	-75.8	0	1
6.3	-6.7	400.2	12.6	-73.9	0	1
6.4	-7.2	400.2	12.5	-71.8	0	1
6.5	-7.7	400.2	12.4	-69.5	0	1
6.6	-8.1	400.3	12.2	-67.0	0	1
6.7	-8.6	400.3	12.0	-64.4	0	1
6.8	-9.0	400.3	11.8	-61.6	0	1
6.9	-9.5	400.3	11.7	-58.6	1	1
7.0	-9.9	400.3	11.7	-55.6	1	1
7.1	-10.3	400.3	11.6	-52.6	1	1
7.2	-10.7	400.4	11.6	-49.5	1	1
7.3	-11.1	400.4	11.6	-46.5	1	1
7.4	-11.4	400.4	11.7	-43.4	1	1
7.5	-11.8	400.4	11.7	-40.4	1	1
7.6	-12.1	400.4	11.8	-37.4	1	1
7.7	-12.3	400.5	11.8	-34.5	1	1
7.8	-12.6	400.5	11.9	-31.6	1	1
7.9	-12.8	400.5	12.0	-28.8	1	1
8.0	-13.0	400.5	12.1	-26.1	1	1
8.1	-13.1	400.5	12.1	-23.5	1	1
8.2	-13.3	400.5	12.2	-20.9	1	1
8.3	-13.3	400.5	12.2	-18.5	1	1
8.4	-13.4	400.6	12.2	-16.1	1	1
8.5	-13.4	400.6	12.2	-13.9	1	1

8.6	-13.4	400.6	12.2	-11.7	1	1
8.7	-13.3	400.6	12.2	-9.7	1	1
8.8	-13.2	400.6	12.1	-7.8	1	1
8.9	-13.0	400.6	12.0	-6.1	1	1
9.0	-12.8	400.6	11.9	-4.5	1	1
9.1	-12.6	400.6	11.7	-3.1	1	1
9.2	-12.3	400.6	11.5	-1.9	1	1
9.3	-12.0	400.7	11.3	-0.9	1	1
9.4	-11.7	400.7	11.2	1.7	1	1
9.5	-11.3	400.7	10.8	0.4	1	1
9.6	-10.9	400.7	10.5	0.6	1	1
9.7	-10.5	400.7	10.2	0.6	1	1
9.8	-10.0	400.7	9.8	0.2	1	1
9.9	-9.5	400.7	9.4	-0.7	1	1
10.0	-9.0	400.7	9.0	-1.9	1	1
10.1	-8.4	400.7	8.7	-3.3	1	1
10.2	-7.9	400.7	8.4	-4.9	1	1
10.3	-7.3	400.7	8.2	-6.9	1	1
10.4	-6.7	400.7	8.0	-9.0	1	1
10.5	-6.1	400.6	7.8	-11.4	1	1
10.6	-5.4	400.6	7.6	-14.0	1	1
10.7	-4.8	400.6	7.5	-16.7	1	1
10.8	-4.2	400.6	7.5	-19.6	1	1
10.9	-3.5	400.6	7.5	-22.7	1	1
11.0	-2.9	400.6	7.5	-25.8	1	1
11.1	-2.2	400.6	7.5	-29.1	1	1
11.2	-1.6	400.5	7.6	-32.4	1	1
11.3	-0.9	400.5	7.7	-35.8	1	1
11.4	-0.3	400.5	7.8	-39.2	1	1
11.5	0.3	400.5	8.0	-42.7	1	1
11.6	0.9	400.5	8.2	-46.2	1	1
11.7	1.5	400.4	8.4	-49.8	1	1
11.8	2.1	400.4	8.6	-53.3	1	1
11.9	2.7	400.4	8.9	-56.9	1	1
12.0	3.3	400.4	9.2	-60.5	0	1
12.1	3.8	400.3	9.5	-64.0	0	1
12.2	4.3	400.3	9.9	-67.6	0	1
12.3	4.7	400.3	10.3	-71.2	0	1
12.4	4.9	400.3	10.7	-74.7	0	1
12.5	5.1	400.2	11.2	-78.1	0	1
12.6	5.3	400.2	11.7	-81.4	0	1
12.7	5.3	400.2	12.2	-84.7	0	1
12.8	5.4	400.2	12.7	-87.8	0	1
12.9	5.4	400.2	13.3	-90.8	0	1
13.0	5.4	400.2	13.9	-93.6	0	1

13.1	5.3	400.1	14.5	263.6	0	1
13.2	5.1	400.1	15.1	261.0	0	1
13.3	4.9	400.1	15.8	258.6	0	1
13.4	4.7	400.1	16.5	256.3	0	1
13.5	4.3	400.1	17.2	254.2	0	1
13.6	4.0	400.1	17.8	252.5	0	1
13.7	3.6	400.1	18.4	251.1	0	1
13.8	3.1	400.1	19.0	250.0	0	1
13.9	2.6	400.1	19.5	249.1	0	1
14.0	2.1	400.0	19.9	248.5	0	1
14.1	1.5	400.0	20.2	248.1	0	1
14.2	0.9	400.0	20.5	247.9	0	1
14.3	0.2	400.0	20.7	247.9	0	1
14.4	-0.5	400.0	20.8	248.0	0	1
14.5	-1.2	400.0	20.8	248.2	0	1
14.6	-2.0	400.0	20.7	248.6	0	1
14.7	-2.7	399.9	20.6	249.1	0	1
14.8	-3.6	399.9	20.4	249.6	0	1
14.9	-4.4	399.9	20.1	250.2	0	1
15.0	-5.3	399.9	19.8	250.8	0	1
15.1	-6.1	399.8	19.4	251.4	0	1
15.2	-7.0	399.8	18.9	251.9	0	1
15.3	-7.9	399.8	18.5	252.4	0	1
15.4	-8.8	399.7	18.0	252.7	0	1
15.5	-9.7	399.7	17.6	252.8	0	1
15.6	-10.6	399.6	17.1	253.0	0	1
15.7	-11.5	399.6	16.7	253.3	0	1
15.8	-12.4	399.5	16.3	253.6	0	1
15.9	-13.2	399.5	15.9	254.0	0	1
16.0	-14.1	399.4	15.5	254.4	0	1
16.1	-14.9	399.4	15.1	254.9	0	1
16.2	-15.6	399.3	14.7	255.3	0	1
16.3	-16.4	399.2	14.4	255.8	0	1
16.4	-17.1	399.2	14.1	256.2	0	1
16.5	-17.7	399.1	13.8	256.6	0	1
16.6	-18.3	399.1	13.6	256.9	0	1
16.7	-18.8	399.0	13.4	257.2	0	1
16.8	-19.2	399.0	13.2	257.6	0	1
16.9	-19.5	399.0	13.0	258.1	0	1
17.0	-19.6	398.9	12.7	258.6	0	1
17.1	-19.7	398.9	12.4	259.0	0	1
17.2	-19.6	398.9	12.1	259.4	0	1
17.3	-19.4	398.8	11.8	259.7	0	1
17.4	-19.2	398.8	11.5	259.9	0	1
17.5	-18.9	398.8	11.1	259.8	0	1

17.6	-18.5	398.8	10.8	259.5	0	1
17.7	-18.0	398.8	10.4	258.9	0	1
17.8	-17.5	398.8	10.1	258.0	0	1
17.9	-16.9	398.8	9.7	256.8	0	1
18.0	-16.3	398.8	9.4	255.2	0	1
18.1	-15.7	398.9	9.0	253.3	0	1
18.2	-15.0	398.9	8.7	251.0	0	1
18.3	-14.3	398.9	8.4	248.3	0	1
18.4	-13.5	398.9	8.2	245.3	0	1
18.5	-12.8	398.9	8.0	241.9	0	1
18.6	-12.0	399.0	7.8	238.2	0	1
18.7	-11.1	399.0	7.6	234.4	0	1
18.8	-10.3	399.0	7.5	230.3	0	1
18.9	-9.5	399.0	7.4	226.2	0	1
19.0	-8.6	399.1	7.4	222.0	0	1
19.1	-7.8	399.1	7.4	217.8	0	1
19.2	-6.9	399.1	7.4	213.8	0	1
19.3	-6.1	399.1	7.4	210.1	0	1
19.4	-5.2	399.1	7.5	206.1	0	1
19.5	-4.4	399.1	7.6	201.9	0	1
19.6	-3.5	399.1	7.8	197.5	0	1
19.7	-2.7	399.2	8.0	193.2	0	1
19.8	-1.9	399.2	8.4	188.9	0	1
19.9	-1.0	399.2	8.7	184.7	0	1
20.0	-0.2	399.2	9.2	180.7	0	1
20.1	0.6	399.2	9.6	176.9	0	1
20.2	1.3	399.1	10.2	173.2	0	1
20.3	2.1	399.1	10.7	169.6	0	1
20.4	2.8	399.1	11.3	166.2	0	1
20.5	3.5	399.1	11.9	162.9	0	1
20.6	4.2	399.1	12.5	159.6	0	1
20.7	4.9	399.1	13.1	156.4	0	1
20.8	5.6	399.1	13.6	153.3	0	1
20.9	6.2	399.1	14.1	150.2	0	1
21.0	6.8	399.0	14.4	147.1	0	1
21.1	7.4	399.0	14.7	144.2	0	1
21.2	8.0	399.0	14.9	141.2	0	1
21.3	8.6	399.0	15.0	138.4	0	1
21.4	9.1	399.0	15.1	135.8	0	1
21.5	9.5	399.0	15.0	133.3	0	1
21.6	10.0	398.9	14.9	130.8	0	1
21.7	10.4	398.9	14.8	128.3	0	1
21.8	10.8	398.9	14.7	125.8	0	1
21.9	11.1	398.9	14.5	123.2	0	1
22.0	11.5	398.9	14.3	120.7	0	1

22.1	11.7	398.9	14.1	118.1	0	1
22.2	12.0	398.9	13.8	115.6	0	1
22.3	12.2	398.9	13.5	113.2	0	1
22.4	12.3	398.9	13.2	110.8	0	1
22.5	12.4	398.9	12.9	108.2	0	1
22.6	12.5	398.9	12.6	105.3	0	1
22.7	12.6	398.9	12.3	102.3	0	1
22.8	12.6	398.9	12.1	99.1	0	1
22.9	12.5	398.9	11.9	95.7	0	1
23.0	12.5	398.9	11.7	92.3	0	1
23.1	12.3	398.9	11.6	88.7	0	1
23.2	12.2	399.0	11.5	85.2	0	1
23.3	12.0	399.0	11.4	81.6	0	1
23.4	11.8	399.0	11.4	78.1	0	1
23.5	11.6	399.0	11.4	74.8	0	1
23.6	11.3	399.1	11.5	71.6	0	1
23.7	11.0	399.1	11.6	68.6	0	1
23.8	10.7	399.1	11.8	65.9	0	1
23.9	10.3	399.2	11.9	63.4	0	1
24.0	10.0	399.2	12.1	61.2	0	1
24.1	9.6	399.2	12.4	59.4	1	1
24.2	9.2	399.2	12.6	57.9	1	1
24.3	8.9	399.3	12.9	56.7	1	1
24.4	8.5	399.3	13.1	55.8	1	1
24.5	8.1	399.3	13.4	55.3	1	1
24.6	7.7	399.4	13.7	54.7	1	1
24.7	7.3	399.4	13.9	54.0	1	1
24.8	6.9	399.4	14.2	53.4	1	1
24.9	6.5	399.5	14.4	52.8	1	1
25.0	6.1	399.5	14.7	52.3	1	1
25.1	5.7	399.5	14.9	51.7	1	1
25.2	5.3	399.5	15.1	51.2	0	1
25.3	5.0	399.6	15.3	50.8	0	1
25.4	4.6	399.6	15.5	50.3	0	1
25.5	4.3	399.6	15.6	49.9	0	1
25.6	4.0	399.6	15.8	49.6	0	1
25.7	3.7	399.6	16.0	49.7	0	1
25.8	3.4	399.7	16.2	49.7	0	1
25.9	3.1	399.7	16.4	49.3	0	1
26.0	2.9	399.7	16.5	48.8	0	1
26.1	2.7	399.7	16.5	48.2	0	1
26.2	2.5	399.7	16.5	47.3	0	1
26.3	2.3	399.7	16.4	46.3	0	1
26.4	2.1	399.7	16.2	45.3	0	1
26.5	2.0	399.7	15.9	44.1	0	1

26.6	1.8	399.8	15.5	42.8	0	1
26.7	1.7	399.8	15.1	41.5	0	1
26.8	1.6	399.8	14.6	40.1	1	1
26.9	1.6	399.8	14.0	38.7	1	1
27.0	1.5	399.8	13.3	37.3	1	1
27.1	1.5	399.8	12.6	35.7	1	1
27.2	1.4	399.8	11.9	34.0	1	1
27.3	1.4	399.8	11.3	32.2	1	1
27.4	1.4	399.9	10.6	30.1	1	1
27.5	1.3	399.9	10.0	27.8	1	1
27.6	1.3	399.9	9.3	25.3	1	1
27.7	1.3	399.9	8.7	22.4	1	1
27.8	1.3	399.9	8.1	19.1	1	1
27.9	1.2	399.9	7.5	15.3	1	1
28.0	1.1	399.9	6.9	10.9	1	1
28.1	1.0	399.9	6.4	5.8	1	1
28.2	0.9	400.0	5.9	-0.1	1	1
28.3	0.7	400.0	5.5	-6.9	1	1
28.4	0.5	400.0	5.2	-14.6	1	1
28.5	0.3	400.0	5.0	-23.0	0	1
28.6	0.1	400.0	4.9	-31.9	0	1

CM IN RADAR CONE 37.41259 PERCENT
CMMCA W/IN STRUCTURAL LIMITS 100.0000 PERCENT

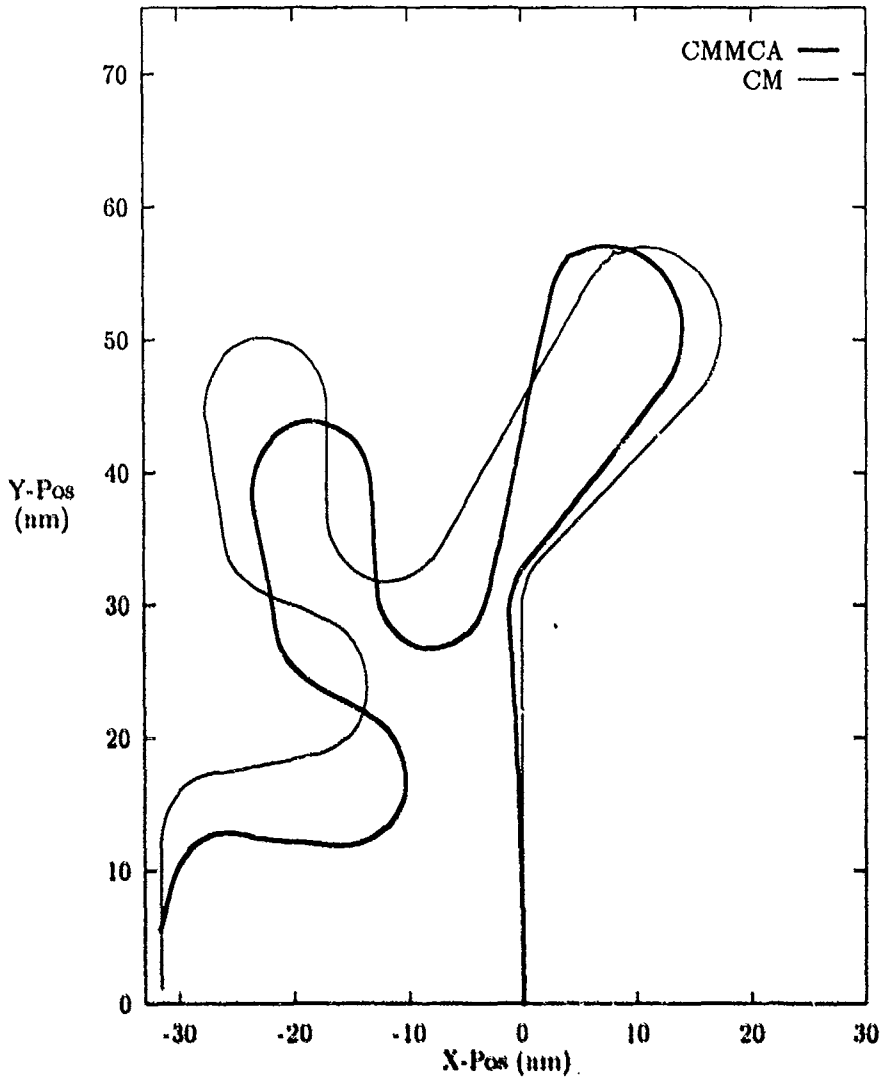

Figure 31. Path 4 CMMCA and CM Paths, CMMCA Starting Trailing

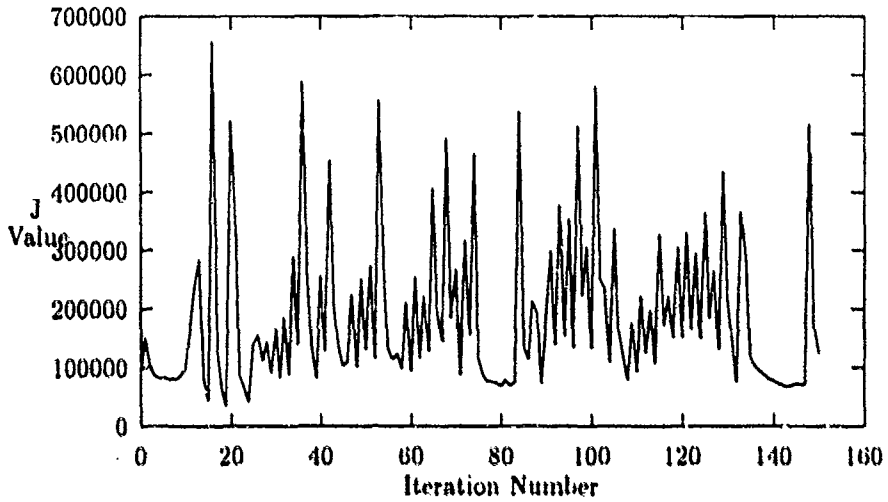

Figure 32. Plot of J Value versus Iteration Number

JSTOP = 124108.0
# ITERATIONS = 150

T	BANK	SPEED	RANGE	THETA	RADAR	STRUCT
0.1	-0.5	400.1	8.0	0.1	1	1
0.2	-0.5	400.1	8.0	0.2	1	1
0.3	-0.5	400.1	8.0	0.4	1	1
0.4	-0.5	400.1	8.0	0.6	1	1
0.5	-0.5	400.1	8.0	0.7	1	1
0.6	-0.5	400.1	8.0	0.9	1	1
0.7	-0.5	400.1	8.0	1.1	1	1
0.8	-0.5	400.1	8.0	1.3	1	1
0.9	-0.4	400.1	8.0	1.6	1	1
1.0	-0.4	400.1	8.0	1.8	1	1
1.1	-0.4	400.1	8.0	2.0	1	1
1.2	-0.4	400.1	8.0	2.3	1	1
1.3	-0.4	400.1	8.0	2.5	1	1
1.4	-0.4	400.1	8.0	2.8	1	1
1.5	-0.4	400.1	8.0	3.1	1	1
1.6	-0.4	400.1	8.0	3.3	1	1
1.7	-0.4	400.1	8.0	3.6	1	1
1.8	-0.4	400.1	8.0	3.9	1	1
1.9	-0.4	400.1	8.0	4.2	1	1
2.0	-0.4	400.1	8.0	4.5	1	1
2.1	-0.4	400.1	8.0	4.9	1	1
2.2	-0.4	400.1	8.0	5.2	1	1
2.3	-0.4	400.1	8.0	5.5	1	1
2.4	-0.4	400.1	8.0	5.8	1	1
2.5	-0.3	400.1	8.0	6.2	1	1
2.6	-0.3	400.1	8.0	6.5	1	1
2.7	-0.3	400.1	8.0	6.9	1	1
2.8	-0.3	400.1	8.0	7.2	1	1
2.9	-0.3	400.1	8.0	7.6	1	1
3.0	-0.3	400.1	8.0	8.0	1	1
3.1	-0.3	400.1	8.0	8.3	1	1
3.2	-0.3	400.1	8.0	8.7	1	1
3.3	-0.3	400.1	8.0	9.1	1	1
3.4	-0.3	400.1	8.1	10.1	1	1
3.5	-0.3	400.1	8.1	11.6	1	1
3.6	-0.3	400.1	8.1	13.8	1	1
3.7	-0.2	400.1	8.1	16.5	1	1
3.8	-0.2	400.1	8.0	19.9	1	1
3.9	-0.2	400.1	8.0	23.7	1	1
4.0	-0.2	400.1	8.0	28.0	1	1

4.1	-0.2	400.1	8.1	32.2	1	1
4.2	-0.2	400.1	8.1	36.3	1	1
4.3	-0.2	400.1	8.3	40.4	1	1
4.4	23.7	399.7	8.4	40.5	1	1
4.5	23.3	399.7	8.6	36.7	1	1
4.6	23.9	399.7	8.7	32.3	1	1
4.7	23.5	399.7	8.8	27.3	1	1
4.8	23.6	399.7	8.8	21.9	1	1
4.9	23.6	399.7	8.9	16.0	1	1
5.0	15.2	399.8	8.9	10.9	1	1
5.1	0.0	400.1	8.9	9.1	1	1
5.2	-0.4	400.1	8.9	9.5	1	1
5.3	2.0	400.0	8.9	9.6	1	1
5.4	-4.5	400.1	8.9	10.3	1	1
5.5	1.8	400.0	8.9	11.0	1	1
5.6	0.0	400.1	8.9	11.2	1	1
5.7	-0.2	400.1	8.9	11.6	1	1
5.8	-0.5	400.1	9.0	12.0	1	1
5.9	-0.2	400.1	9.0	12.5	1	1
6.0	-0.2	400.1	9.0	13.0	1	1
6.1	0.0	400.1	9.0	13.4	1	1
6.2	-0.5	400.1	9.0	13.9	1	1
6.3	-0.3	400.1	9.0	14.4	1	1
6.4	0.0	400.1	9.0	14.8	1	1
6.5	-0.5	400.1	9.0	15.3	1	1
6.6	-0.3	400.1	9.1	15.8	1	1
6.7	0.0	400.1	9.1	16.2	1	1
6.8	-0.5	400.1	9.1	16.3	1	1
6.9	-0.1	400.1	9.0	15.9	1	1
7.0	-0.2	400.1	9.0	15.2	1	1
7.1	-0.5	400.1	8.9	14.0	1	1
7.2	-0.3	400.1	8.8	12.5	1	1
7.3	0.0	400.1	8.6	10.5	1	1
7.4	-0.5	400.1	8.4	8.2	1	1
7.5	-0.2	400.1	8.2	5.4	1	1
7.6	-0.2	400.1	8.0	2.1	1	1
7.7	0.0	400.1	7.7	-1.8	1	1
7.8	-20.7	400.6	7.4	-3.1	1	1
7.9	-20.3	400.6	7.1	-1.6	1	1
8.0	-20.3	400.6	6.8	-0.3	1	1
8.1	-20.6	400.6	6.5	0.8	1	1
8.2	-20.5	400.6	6.1	1.8	1	1
8.3	-20.0	400.6	5.8	2.5	1	1
8.4	-20.6	400.7	5.4	2.8	1	1
8.5	-20.4	400.6	5.1	2.9	1	1

8.6	-20.1	400.6	4.7	2.5	0	1
8.7	-20.2	400.6	4.4	1.5	0	1
8.8	-20.1	400.6	4.1	-0.2	0	1
8.9	-20.5	400.6	3.8	-2.7	0	1
9.0	-19.8	400.6	3.5	-6.1	0	1
9.1	-20.3	400.6	3.2	-10.5	0	1
9.2	-19.8	400.6	3.1	-16.0	0	1
9.3	-20.1	400.6	2.9	-22.4	0	1
9.4	-20.2	400.6	2.9	-21.5	0	1
9.5	-20.0	400.6	2.9	-36.2	0	1
9.6	-20.0	400.5	3.1	-42.6	0	1
9.7	-20.1	400.5	3.2	-48.2	0	1
9.8	-20.3	400.5	3.5	-52.7	0	1
9.9	-20.2	400.5	3.7	-56.6	0	1
10.0	-20.3	400.5	4.1	-58.4	0	1
10.1	-20.1	400.4	4.4	-58.7	0	1
10.2	-20.4	400.4	4.7	-57.7	0	1
10.3	-20.3	400.4	4.9	-55.7	0	1
10.4	60.4	398.0	5.2	-70.9	0	0
10.5	-77.6	404.7	5.5	-51.6	1	0
10.6	43.4	398.9	5.6	-23.3	1	0
10.7	-20.1	400.3	5.6	-27.7	1	1
10.8	-21.0	400.3	5.6	-21.2	1	1
10.9	-27.9	400.4	5.5	-12.6	1	1
11.0	-0.3	399.9	5.4	-6.3	1	1
11.1	-0.2	399.9	5.4	-4.0	1	1
11.2	-0.5	399.9	5.3	-1.6	1	1
11.3	-0.4	399.9	5.3	0.9	1	1
11.4	-0.4	399.9	5.3	3.3	1	1
11.5	-0.4	399.9	5.3	5.8	1	1
11.6	-0.1	399.9	5.3	8.3	1	1
11.7	-0.5	399.9	5.3	10.9	1	1
11.8	-0.5	399.9	5.3	13.5	1	1
11.9	-0.3	399.9	5.3	16.0	1	1
12.0	-0.3	399.9	5.3	18.6	1	1
12.1	-0.3	399.9	5.4	21.1	1	1
12.2	-0.2	399.9	5.4	23.6	1	1
12.3	0.0	399.9	5.5	26.0	1	1
12.4	-0.3	399.9	5.5	28.3	1	1
12.5	-0.1	399.9	5.6	30.6	1	1
12.6	-0.1	399.9	5.7	32.8	1	1
12.7	0.0	399.9	5.8	35.0	1	1
12.8	0.0	399.9	5.9	37.0	1	1
12.9	0.3	399.9	6.0	38.9	1	1
13.0	0.0	399.9	6.1	40.8	1	1

13.1	0.4	399.9	6.2	42.6	1	1
13.2	0.0	399.9	6.4	44.3	1	1
13.3	0.3	399.9	6.5	45.9	1	1
13.4	0.4	399.9	6.6	47.4	1	1
13.5	0.6	399.9	6.8	48.8	1	1
13.6	0.3	399.9	7.0	50.7	1	1
13.7	0.6	399.9	7.2	53.2	1	1
13.8	0.6	399.9	7.4	56.0	1	1
13.9	0.7	399.9	7.7	59.2	1	1
14.0	0.9	399.9	8.1	62.7	0	1
14.1	0.7	399.9	8.5	66.4	0	1
14.2	0.9	399.9	8.9	70.3	0	1
14.3	1.0	399.9	9.3	74.3	0	1
14.4	1.1	399.9	9.8	78.3	0	1
14.5	1.1	399.9	10.4	82.3	0	1
14.6	25.3	399.7	11.0	82.6	0	1
14.7	25.5	399.7	11.5	79.0	0	1
14.8	25.5	399.7	12.0	75.4	0	1
14.9	25.5	399.7	12.4	71.7	0	1
15.0	25.5	399.7	12.8	68.0	0	1
15.1	25.7	399.7	13.1	64.2	0	1
15.2	25.8	399.7	13.4	60.3	0	1
15.3	25.5	399.7	13.6	56.4	1	1
15.4	25.9	399.8	13.7	52.5	1	1
15.5	25.7	399.8	13.8	48.6	1	1
15.6	25.7	399.8	13.9	44.4	1	1
15.7	25.6	399.8	13.9	40.0	1	1
15.8	26.1	399.8	14.0	35.2	1	1
15.9	25.3	399.8	14.0	30.2	1	1
16.0	25.5	399.9	14.0	24.9	1	1
16.1	25.7	399.9	14.0	19.2	1	1
16.2	25.4	399.9	13.9	13.1	1	1
16.3	25.1	399.9	13.9	6.8	1	1
16.4	25.7	399.9	13.9	0.2	1	1
16.5	32.8	399.8	13.9	-8.4	1	0
16.6	1.0	400.0	13.8	-13.5	1	1
16.7	0.9	400.0	13.8	-13.5	1	1
16.8	0.8	400.0	13.8	-13.9	1	1
16.9	0.7	400.0	13.8	-14.6	1	1
17.0	0.6	400.0	13.9	-15.7	1	1
17.1	0.5	400.0	13.9	-17.0	1	1
17.2	0.4	400.0	13.9	-18.7	1	1
17.3	0.3	400.0	13.9	-20.7	1	1
17.4	0.2	400.0	13.9	-23.0	1	1
17.5	0.1	400.0	13.8	-25.6	1	1

17.6	0.0	400.0	13.8	-28.4	1	1
17.7	-0.1	400.0	13.7	-31.5	1	1
17.8	-24.1	400.2	13.7	-31.2	1	1
17.9	-23.8	400.1	13.5	-27.4	1	1
18.0	-24.6	400.1	13.4	-23.4	1	1
18.1	-24.2	400.1	13.1	-19.4	1	1
18.2	-24.3	400.1	12.8	-15.4	1	1
18.3	-24.4	400.1	12.5	-11.4	1	1
18.4	-24.8	400.1	12.1	-7.2	1	1
18.5	-24.1	400.1	11.7	-3.1	1	1
18.6	-24.6	400.1	11.2	1.1	1	1
18.7	-24.5	400.1	10.7	5.3	1	1
18.8	-24.7	400.1	10.1	9.7	1	1
18.9	-24.1	400.1	9.5	14.0	1	1
19.0	-24.4	400.1	8.9	18.4	1	1
19.1	-24.0	400.1	8.2	22.8	1	1
19.2	-24.3	400.1	7.5	27.4	1	1
19.3	-23.9	400.0	6.8	32.2	1	1
19.4	-24.1	400.0	6.0	37.1	1	1
19.5	-23.5	400.0	5.4	42.0	1	1
19.6	-23.6	400.0	4.8	47.0	0	1
19.7	-23.9	400.0	4.3	52.3	0	1
19.8	-22.9	400.0	3.9	57.7	0	1
19.9	-23.6	400.0	3.5	63.4	0	1
20.0	-23.0	400.0	3.2	69.5	0	1
20.1	-23.2	400.0	3.0	75.9	0	1
20.2	-22.8	400.0	2.9	82.7	0	1
20.3	-30.5	400.0	2.8	90.9	0	0
20.4	1.1	400.0	2.8	95.5	0	1
20.5	0.7	400.0	2.9	95.2	0	1
20.6	0.9	400.0	2.9	94.9	0	1
20.7	1.1	400.0	3.0	94.6	0	1
20.8	1.3	400.0	2.9	94.3	0	1
20.9	0.9	400.0	2.8	94.5	0	1
21.0	1.1	400.0	2.6	95.3	0	1
21.1	1.3	400.0	2.3	97.3	0	1
21.2	1.5	400.0	2.0	101.5	0	1
21.3	1.1	400.0	1.6	110.2	0	1
21.4	1.3	400.0	1.3	127.8	0	1
21.5	1.4	400.0	1.2	157.4	0	1
21.6	1.7	400.0	1.4	185.0	0	1
21.7	1.1	400.0	1.9	201.7	0	1
21.8	-21.9	400.0	2.4	214.3	0	1
21.9	-22.0	400.0	3.0	226.0	0	1
22.0	-22.2	400.0	3.5	235.3	0	1

22.1	-22.1	400.0	3.9	243.3	0	1
22.2	-21.7	400.0	4.3	250.5	0	1
22.3	-22.5	400.0	4.6	257.3	0	1
22.4	-22.2	400.0	4.8	264.0	0	1
22.5	-22.1	400.0	4.9	270.6	0	1
22.6	-7.0	400.0	4.9	275.0	0	1
22.7	1.2	400.0	4.7	275.7	0	1
22.8	1.3	400.0	4.4	275.0	0	1
22.9	1.1	400.0	4.0	273.7	0	1
23.0	1.2	400.0	3.6	271.6	0	1
23.1	1.0	400.0	3.2	268.2	0	1
23.2	1.1	400.0	2.7	262.1	0	1
23.3	0.9	400.0	2.2	251.6	0	1
23.4	1.1	400.0	1.8	233.6	0	1
23.5	25.0	399.9	1.8	205.1	0	1
23.6	24.8	399.9	2.1	176.5	0	1
23.7	25.0	399.9	2.7	156.6	0	1
23.8	25.0	399.9	3.4	142.9	0	1
23.9	24.8	399.9	4.1	132.7	0	1
24.0	24.6	399.9	4.9	124.5	0	1
24.1	24.9	399.9	5.6	117.5	0	1
24.2	24.8	399.9	6.4	111.2	0	1
24.3	24.8	399.9	7.1	105.4	0	1
24.4	24.5	399.9	7.8	100.0	0	1
24.5	24.8	399.9	8.5	94.7	0	1
24.6	24.5	399.9	9.0	89.2	0	1
24.7	24.6	399.9	9.6	83.5	0	1
24.8	24.4	399.9	10.0	77.6	0	1
24.9	24.8	399.9	10.3	71.4	0	1
25.0	24.2	399.9	10.6	65.0	0	1
25.1	24.4	399.9	10.8	58.5	1	1
25.2	24.6	399.9	10.9	51.6	1	1
25.3	24.2	400.0	11.0	44.5	1	1
25.4	24.5	400.0	11.0	37.0	1	1
25.5	20.4	400.0	10.9	29.9	1	1
25.6	0.7	400.0	10.9	26.1	1	1
25.7	0.2	400.0	10.8	25.9	1	1
25.8	0.3	400.0	10.8	25.4	1	1
25.9	0.4	400.0	10.7	24.5	1	1
26.0	0.6	400.0	10.5	23.1	1	1
26.1	0.1	400.0	10.3	21.5	1	1
26.2	0.3	400.0	10.1	19.6	1	1
26.3	0.4	400.0	9.7	17.2	1	1
26.4	0.6	400.0	9.3	14.4	1	1
26.5	0.1	400.0	8.9	11.3	1	1

26.6	0.3	400.0	8.4	7.6	1	1
26.7	38.8	400.0	7.8	-3.5	1	0
26.8	-23.7	400.0	7.3	-12.2	1	1
26.9	-23.2	400.0	6.7	-11.6	1	1
27.0	-23.5	400.0	6.1	-11.6	1	1
27.1	-23.4	400.0	5.6	-12.2	1	1
27.2	-23.5	400.0	5.3	-13.1	1	1
27.3	-23.6	400.0	5.0	-14.1	0	1
27.4	-23.2	400.0	4.7	-15.2	0	1
27.5	-23.7	400.0	4.6	-15.8	0	1
27.6	-23.5	400.0	4.5	-15.9	0	1
27.7	-23.4	400.0	4.4	-15.2	0	1
27.8	-23.6	400.0	4.4	-13.6	0	1
27.9	-23.7	400.0	4.4	-11.0	0	1
28.0	-21.1	400.0	4.4	-7.7	0	1
28.1	0.2	400.0	4.4	-7.3	0	1
28.2	0.1	400.0	4.4	-9.9	0	1
28.3	0.1	400.0	4.4	-12.4	0	1
28.4	0.1	400.0	4.4	-14.9	0	1
28.5	0.0	400.0	4.4	342.6	0	1
28.6	0.0	400.0	4.5	340.1	0	1

CM IN RADAR CONE 64.68532 PERCENT
CMMCA W/IN STRUCTURAL LIMITS 97.90209 PERCENT

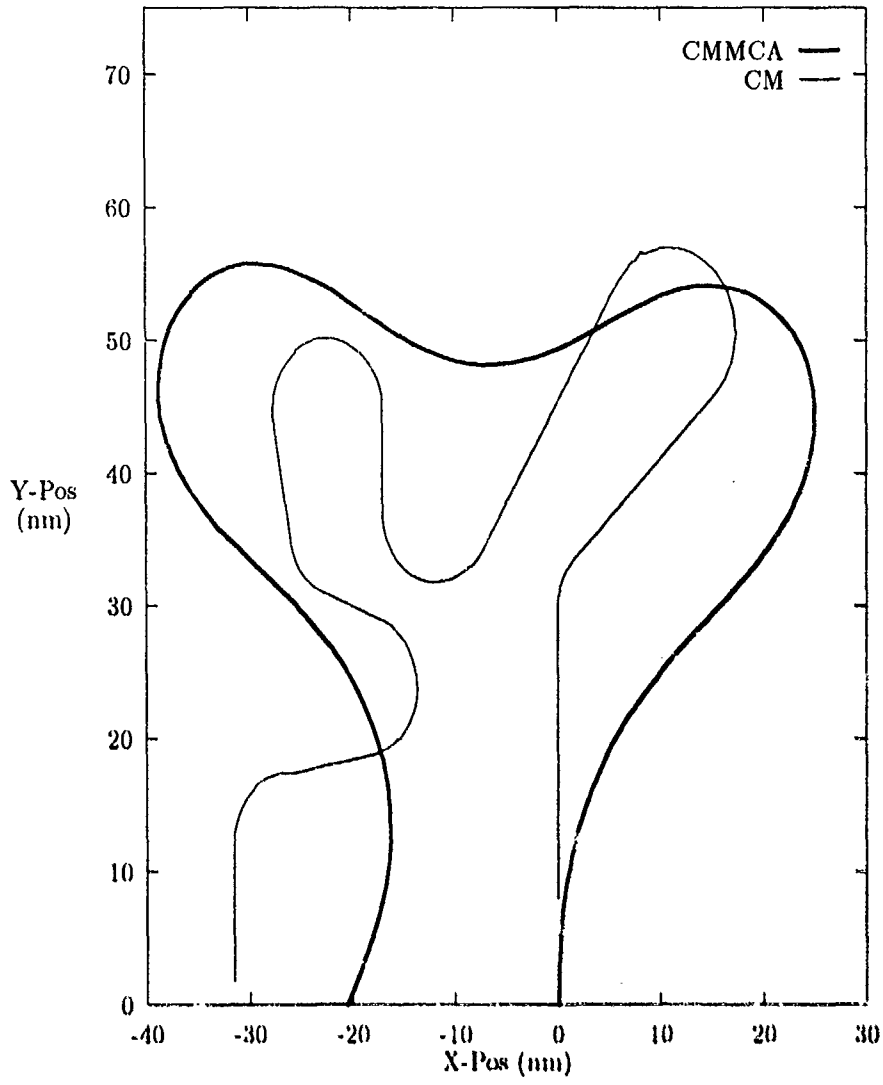

Figure 33. Path 4 Corrected Paths, CMMCA Starting Straight

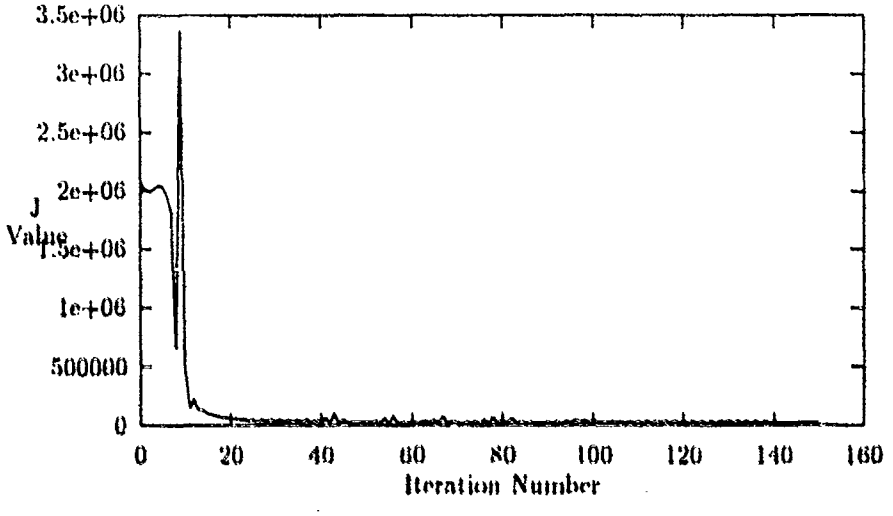

Figure 34. Plot of J Value versus Iteration Number

JSTOP = 25975.84
# ITERATIONS = 150

T	BANK	SPEED	RANGE	THETA	RADAR	STRUCT
0.1	1.9	400.1	8.0	-0.3	1	1
0.2	2.1	400.1	8.0	-0.9	1	1
0.3	2.3	400.1	8.0	-1.6	1	1
0.4	2.5	400.1	8.0	-2.5	1	1
0.5	2.8	400.1	8.0	-3.4	1	1
0.6	3.0	400.1	8.0	-4.5	1	1
0.7	3.1	400.1	8.0	-5.7	1	1
0.8	3.3	400.1	8.0	-7.1	1	1
0.9	3.5	400.1	8.0	-8.6	1	1
1.0	3.7	400.1	8.0	-10.2	1	1
1.1	3.8	400.1	8.0	-11.9	1	1
1.2	3.9	400.1	8.0	-13.8	1	1
1.3	4.1	400.1	8.1	-15.7	1	1
1.4	4.2	400.1	8.1	-17.8	1	1
1.5	4.3	400.1	8.1	-20.1	1	1
1.6	4.4	400.1	8.2	-22.4	1	1
1.7	4.5	400.1	8.2	-24.9	1	1
1.8	4.6	400.1	8.3	-27.4	1	1
1.9	4.6	400.1	8.3	-30.0	1	1
2.0	4.7	400.0	8.4	-32.8	1	1
2.1	4.7	400.0	8.5	-35.6	1	1
2.2	4.7	400.0	8.6	-38.4	1	1
2.3	4.8	400.0	8.8	-41.3	1	1
2.4	4.8	400.0	8.9	-44.3	1	1
2.5	4.8	400.0	9.1	-47.2	1	1
2.6	4.8	400.0	9.2	-50.2	1	1
2.7	4.7	399.9	9.4	-53.2	1	1
2.8	4.7	399.9	9.7	-56.1	1	1
2.9	4.7	399.9	9.9	-59.0	1	1
3.0	4.6	399.9	10.2	-61.9	0	1
3.1	4.5	399.8	10.4	-64.7	0	1
3.2	4.4	399.8	10.7	-67.4	0	1
3.3	4.3	399.8	11.1	-70.0	0	1
3.4	4.2	399.8	11.4	-72.3	0	1
3.5	4.1	399.7	11.6	-74.1	0	1
3.6	3.9	399.7	11.8	-75.7	0	1
3.7	3.8	399.7	11.9	-77.1	0	1
3.8	3.6	399.6	12.0	-78.2	0	1
3.9	3.4	399.6	12.0	-79.2	0	1
4.0	3.2	399.6	12.0	-80.1	0	1

4.1	3.0	399.5	11.9	-81.0	0	1
4.2	2.7	399.5	11.9	-81.8	0	1
4.3	2.5	399.4	11.9	-82.6	0	1
4.4	2.2	399.4	11.9	-83.2	0	1
4.5	2.0	399.3	11.9	-83.8	0	1
4.6	1.7	399.3	11.9	-84.3	0	1
4.7	1.4	399.2	11.9	-84.8	0	1
4.8	1.0	399.2	12.0	-85.1	0	1
4.9	0.7	399.1	12.0	-85.4	0	1
5.0	0.4	399.1	12.0	-85.5	0	1
5.1	0.0	399.0	12.1	-85.6	0	1
5.2	-0.3	399.0	12.1	-85.6	0	1
5.3	-0.7	398.9	12.1	-85.4	0	1
5.4	-1.1	398.8	12.1	-85.2	0	1
5.5	-1.5	398.8	12.2	-84.8	0	1
5.6	-1.9	398.7	12.2	-84.3	0	1
5.7	-2.3	398.6	12.2	-83.7	0	1
5.8	-2.7	398.5	12.2	-83.0	0	1
5.9	-3.1	398.5	12.2	-82.2	0	1
6.0	-3.5	398.4	12.2	-81.2	0	1
6.1	-4.0	398.3	12.1	-80.1	0	1
6.2	-4.4	398.2	12.1	-78.8	0	1
6.3	-4.9	398.2	12.1	-77.5	0	1
6.4	-5.3	398.1	12.0	-75.9	0	1
6.5	-5.8	398.0	11.9	-74.2	0	1
6.6	-6.2	397.9	11.8	-72.4	0	1
6.7	-6.7	397.8	11.7	-70.4	0	1
6.8	-7.1	397.8	11.6	-68.2	0	1
6.9	-7.6	397.7	11.6	-66.0	0	1
7.0	-8.1	397.6	11.6	-63.7	0	1
7.1	-8.5	397.6	11.6	-61.5	0	1
7.2	-9.0	397.5	11.7	-59.2	1	1
7.3	-9.4	397.4	11.8	-56.9	1	1
7.4	-9.8	397.4	11.9	-54.6	1	1
7.5	-10.3	397.3	12.1	-52.4	1	1
7.6	-10.7	397.3	12.2	-50.1	1	1
7.7	-11.1	397.2	12.4	-48.0	1	1
7.8	-11.5	397.2	12.6	-45.8	1	1
7.9	-11.8	397.2	12.7	-43.7	1	1
8.0	-12.2	397.1	12.9	-41.7	1	1
8.1	-12.5	397.1	13.1	-39.6	1	1
8.2	-12.8	397.1	13.2	-37.6	1	1
8.3	-13.1	397.1	13.4	-35.6	1	1
8.4	-13.3	397.1	13.5	-33.7	1	1
8.5	-13.5	397.1	13.6	-31.8	1	1

8.6	-13.7	397.1	13.7	-29.9	1	1
8.7	-13.8	397.2	13.7	-28.0	1	1
8.8	-13.9	397.2	13.7	-26.3	1	1
8.9	-14.0	397.2	13.7	-24.5	1	1
9.0	-14.0	397.3	13.7	-22.9	1	1
9.1	-14.0	397.3	13.7	-21.3	1	1
9.2	-13.9	397.4	13.6	-19.8	1	1
9.3	-13.8	397.5	13.5	-18.5	1	1
9.4	-13.7	397.5	13.5	-15.6	1	1
9.5	-13.5	397.6	13.2	-16.1	1	1
9.6	-13.3	397.7	13.0	-15.2	1	1
9.7	-13.0	397.8	12.8	-14.4	1	1
9.8	-12.7	397.9	12.5	-13.9	1	1
9.9	-12.3	398.0	12.2	-13.7	1	1
10.0	-11.9	398.1	11.9	-13.5	1	1
10.1	-11.5	398.2	11.7	-13.4	1	1
10.2	-11.0	398.3	11.5	-13.5	1	1
10.3	-10.5	398.4	11.3	-13.6	1	1
10.4	-9.9	398.5	11.1	-13.7	1	1
10.5	-9.4	398.6	11.0	-14.0	1	1
10.6	-8.8	398.7	10.9	-14.3	1	1
10.7	-8.2	398.7	10.8	-14.8	1	1
10.8	-7.6	398.8	10.7	-15.3	1	1
10.9	-6.9	398.9	10.6	-15.9	1	1
11.0	-6.3	399.0	10.6	-16.5	1	1
11.1	-5.6	399.1	10.6	-17.3	1	1
11.2	-4.9	399.2	10.6	-18.2	1	1
11.3	-4.2	399.2	10.6	-19.2	1	1
11.4	-3.6	399.3	10.6	-20.3	1	1
11.5	-2.9	399.4	10.6	-21.6	1	1
11.6	-2.2	399.4	10.6	-23.0	1	1
11.7	-1.5	399.5	10.7	-24.5	1	1
11.8	-0.8	399.5	10.7	-26.2	1	1
11.9	-0.2	399.6	10.8	-28.0	1	1
12.0	0.5	399.6	10.9	-30.0	1	1
12.1	1.1	399.6	11.0	-32.2	1	1
12.2	1.7	399.6	11.1	-34.5	1	1
12.3	2.3	399.7	11.2	-36.9	1	1
12.4	2.9	399.7	11.4	-39.6	1	1
12.5	3.5	399.7	11.5	-42.3	1	1
12.6	4.0	399.7	11.7	-45.3	1	1
12.7	4.5	399.7	11.9	-48.3	1	1
12.8	5.0	399.7	12.1	-51.5	1	1
12.9	5.4	399.7	12.4	-54.8	1	1
13.0	5.8	399.7	12.7	-58.2	1	1

13.1	6.2	399.7	13.0	-61.3	0	1
13.2	6.5	399.7	13.3	-65.1	0	1
13.3	6.8	399.7	13.7	-68.7	0	1
13.4	7.1	399.7	14.1	-72.3	0	1
13.5	7.3	399.7	14.5	-75.9	0	1
13.6	7.4	399.7	14.9	-79.2	0	1
13.7	7.5	399.7	15.3	-82.2	0	1
13.8	7.6	399.6	15.7	-85.0	0	1
13.9	7.6	399.6	16.0	-87.6	0	1
14.0	7.6	399.6	16.3	-90.0	0	1
14.1	7.5	399.6	16.6	-92.3	0	1
14.2	7.3	399.6	16.8	-94.5	0	1
14.3	7.1	399.6	16.9	-96.6	0	1
14.4	6.8	399.6	16.9	-98.5	0	1
14.5	6.5	399.5	16.9	-100.5	0	1
14.6	6.2	399.5	16.9	-102.3	0	1
14.7	5.8	399.5	16.8	-104.2	0	1
14.8	5.3	399.5	16.6	-106.0	0	1
14.9	4.8	399.5	16.4	-107.9	0	1
15.0	4.3	399.5	16.1	-109.8	0	1
15.1	3.8	399.5	15.8	-111.8	0	1
15.2	3.2	399.5	15.5	-113.9	0	1
15.3	2.5	399.5	15.1	-116.2	0	1
15.4	1.9	399.5	14.8	-118.6	0	1
15.5	1.2	399.5	14.4	-121.4	0	1
15.6	0.6	399.5	14.1	-124.1	0	1
15.7	-0.1	399.5	13.9	-126.7	0	1
15.8	-0.9	399.5	13.6	-129.2	0	1
15.9	-1.6	399.5	13.4	-131.6	0	1
16.0	-2.3	399.5	13.2	-133.9	0	1
16.1	-3.0	399.5	13.0	-136.0	0	1
16.2	-3.8	399.5	12.9	-138.1	0	1
16.3	-4.5	399.5	12.8	-140.1	0	1
16.4	-5.2	399.5	12.7	-141.9	0	1
16.5	-5.9	399.5	12.7	-143.6	0	1
16.6	-6.6	399.6	12.7	-145.3	0	1
16.7	-7.3	399.6	12.7	-146.8	0	1
16.8	-8.0	399.6	12.7	-147.8	0	1
16.9	-8.7	399.6	12.7	-148.5	0	1
17.0	-9.3	399.6	12.6	-148.7	0	1
17.1	-9.9	399.6	12.6	-148.6	0	1
17.2	-10.5	399.6	12.5	-148.1	0	1
17.3	-11.0	399.6	12.4	-147.2	0	1
17.4	-11.6	399.6	12.3	-145.9	0	1
17.5	-12.1	399.6	12.2	-144.3	0	1

17.6	-12.5	399.7	12.0	-142.4	0	1
17.7	-13.0	399.7	11.9	-140.1	0	1
17.8	-13.3	399.7	11.8	-137.5	0	1
17.9	-13.7	399.7	11.6	-134.5	0	1
18.0	-14.0	399.7	11.5	-131.3	0	1
18.1	-14.2	399.7	11.4	-127.8	0	1
18.2	-14.4	399.7	11.3	-124.1	0	1
18.3	-14.6	399.7	11.2	-120.2	0	1
18.4	-14.7	399.8	11.1	-116.1	0	1
18.5	-14.8	399.8	11.1	-111.9	0	1
18.6	-14.8	399.8	11.1	-107.5	0	1
18.7	-14.8	399.8	11.1	-103.1	0	1
18.8	-14.8	399.8	11.2	-98.8	0	1
18.9	-14.7	399.8	11.3	-94.4	0	1
19.0	-14.5	399.8	11.4	-90.2	0	1
19.1	-14.4	399.8	11.6	-86.1	0	1
19.2	-14.2	399.8	11.8	-82.2	0	1
19.3	-13.9	399.8	12.0	-78.5	0	1
19.4	-13.6	399.8	12.2	-74.9	0	1
19.5	-13.3	399.8	12.4	-71.3	0	1
19.6	-13.0	399.9	12.5	-67.7	0	1
19.7	-12.6	399.9	12.6	-64.2	0	1
19.8	-12.3	399.9	12.6	-60.7	0	1
19.9	-11.9	399.9	12.6	-57.1	1	1
20.0	-11.5	399.9	12.6	-53.7	1	1
20.1	-11.0	399.9	12.5	-50.2	1	1
20.2	-10.6	399.9	12.4	-46.8	1	1
20.3	-10.1	399.9	12.3	-43.3	1	1
20.4	-9.7	399.9	12.1	-39.9	1	1
20.5	-9.2	399.9	12.0	-36.5	1	1
20.6	-8.7	399.9	11.8	-33.1	1	1
20.7	-8.2	399.9	11.6	-29.7	1	1
20.8	-7.7	399.8	11.5	-26.5	1	1
20.9	-7.2	399.8	11.4	-23.7	1	1
21.0	-6.7	399.8	11.4	-21.3	1	1
21.1	-6.1	399.8	11.3	-19.2	1	1
21.2	-5.6	399.8	11.4	-17.7	1	1
21.3	-5.1	399.8	11.4	-16.5	1	1
21.4	-4.6	399.8	11.4	-15.9	1	1
21.5	-4.0	399.8	11.4	-15.8	1	1
21.6	-3.5	399.8	11.4	-15.9	1	1
21.7	-3.0	399.8	11.5	-16.1	1	1
21.8	-2.4	399.8	11.5	-16.4	1	1
21.9	-1.9	399.8	11.5	-16.8	1	1
22.0	-1.4	399.8	11.6	-17.3	1	1

22.1	-0.9	399.7	11.6	-17.9	1	1
22.2	-0.4	399.7	11.6	-18.7	1	1
22.3	0.1	399.7	11.7	-19.6	1	1
22.4	0.6	399.7	11.7	-20.6	1	1
22.5	1.1	399.7	11.7	-21.4	1	1
22.6	1.5	399.7	11.7	-21.9	1	1
22.7	2.0	399.7	11.7	-22.2	1	1
22.8	2.4	399.7	11.7	-22.3	1	1
22.9	2.8	399.7	11.6	-22.2	1	1
23.0	3.2	399.6	11.4	-21.9	1	1
23.1	3.6	399.6	11.2	-21.5	1	1
23.2	3.9	399.6	10.9	-20.9	1	1
23.3	4.2	399.6	10.6	-20.2	1	1
23.4	4.5	399.6	10.3	-19.3	1	1
23.5	4.8	399.6	9.8	-18.2	1	1
23.6	5.1	399.6	9.3	-16.9	1	1
23.7	5.3	399.6	8.8	-15.4	1	1
23.8	5.5	399.6	8.2	-13.6	1	1
23.9	5.7	399.6	7.5	-11.4	1	1
24.0	5.9	399.6	6.9	8.7	1	1
24.1	6.1	399.6	6.1	-5.2	1	1
24.2	6.2	399.5	5.4	-0.8	1	1
24.3	6.4	399.5	4.7	5.3	0	1
24.4	6.5	399.5	3.9	13.8	0	1
24.5	6.6	399.5	3.3	26.1	0	1
24.6	6.7	399.5	3.0	42.6	0	1
24.7	6.8	399.5	3.0	61.1	0	1
24.8	6.9	399.5	3.3	77.3	0	1
24.9	7.0	399.5	3.9	89.2	0	1
25.0	7.1	399.5	4.6	97.1	0	1
25.1	7.2	399.5	5.3	102.3	0	1
25.2	7.2	399.5	6.2	105.5	0	1
25.3	7.3	399.5	7.0	107.6	0	1
25.4	7.4	399.5	7.8	108.8	0	1
25.5	7.4	399.6	8.7	109.4	0	1
25.6	7.4	399.6	9.5	109.6	0	1
25.7	7.4	399.6	10.4	110.2	0	1
25.8	7.4	399.6	11.2	110.0	0	1
25.9	7.3	399.6	12.0	109.2	0	1
26.0	7.2	399.6	12.7	108.1	0	1
26.1	7.0	399.6	13.4	106.7	0	1
26.2	6.9	399.6	14.0	105.1	0	1
26.3	6.6	399.6	14.4	103.3	0	1
26.4	6.4	399.7	14.8	101.5	0	1
26.5	6.1	399.7	15.1	99.8	0	1

26.6	5.8	399.7	15.2	98.0	0	1
26.7	5.4	399.7	15.3	96.4	0	1
26.8	5.1	399.7	15.2	94.9	0	1
26.9	4.8	399.7	15.1	93.6	0	1
27.0	4.4	399.8	14.9	92.5	0	1
27.1	4.1	399.8	14.6	91.5	0	1
27.2	3.8	399.8	14.4	90.6	0	1
27.3	3.5	399.8	14.1	89.8	0	1
27.4	3.1	399.8	13.8	89.1	0	1
27.5	2.8	399.8	13.5	88.4	0	1
27.6	2.5	399.9	13.3	87.9	0	1
27.7	2.2	399.9	12.9	87.5	0	1
27.8	2.0	399.9	12.6	87.2	0	1
27.9	1.7	399.9	12.3	86.9	0	1
28.0	1.4	399.9	12.0	86.8	0	1
28.1	1.2	399.9	11.7	86.7	0	1
28.2	0.9	399.9	11.3	86.8	0	1
28.3	0.7	400.0	11.0	86.9	0	1
28.4	0.4	400.0	10.7	87.1	0	1
28.5	0.2	400.0	10.3	87.4	0	1
28.6	0.1	400.0	10.0	87.8	0	1

CM IN RADAR CONE 46.15384 PERCENT
CMMCA W/IN STRUCTURAL LIMITS 100.0000 PERCENT

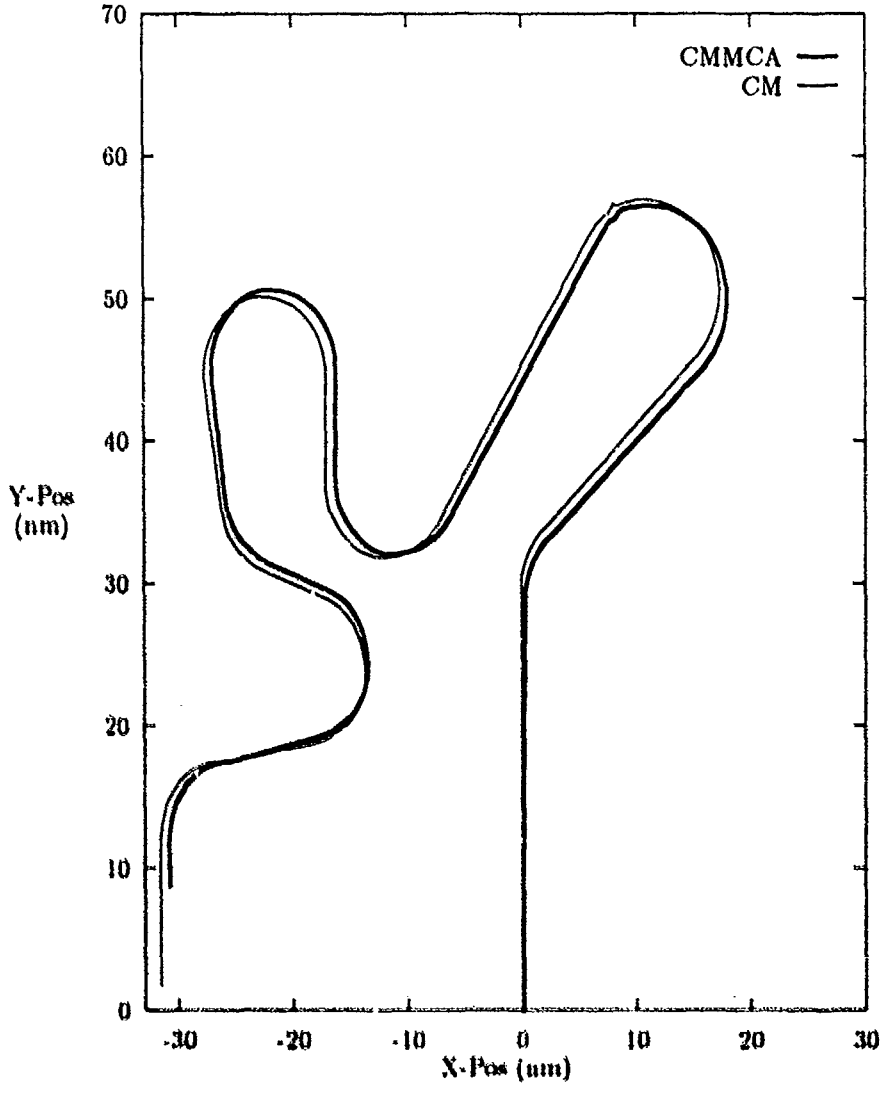

Figure 35. Path 4 Corrected Paths, CMMCA Starting Trailing

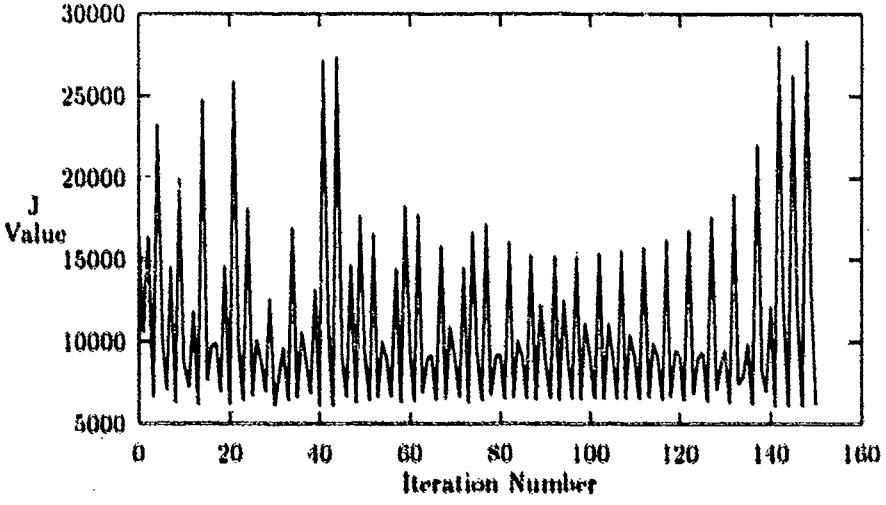

Figure 36. Plot of J Value versus Iteration Number

JSTOP = 6112.035
# ITERATIONS = 150

T	BANK	SPEED	RANGE	THETA	RADAR	STRUCT
0.1	0.1	400.2	8.0	0.0	1	1
0.2	0.1	400.2	8.0	0.0	1	1
0.3	0.1	400.2	8.0	-0.1	1	1
0.4	0.1	400.2	8.0	-0.1	1	1
0.5	0.1	400.2	8.0	-0.1	1	1
0.6	0.1	400.2	8.0	-0.2	1	1
0.7	0.1	400.2	8.0	-0.2	1	1
0.8	0.1	400.2	8.0	-0.2	1	1
0.9	0.1	400.2	8.0	-0.3	1	1
1.0	0.1	400.2	8.0	-0.3	1	1
1.1	0.1	400.2	8.0	-0.3	1	1
1.2	0.1	400.2	8.0	-0.4	1	1
1.3	0.1	400.2	8.0	-0.4	1	1
1.4	0.1	400.2	8.0	-0.5	1	1
1.5	0.1	400.2	8.0	-0.5	1	1
1.6	0.1	400.2	8.0	-0.6	1	1
1.7	0.1	400.2	8.0	-0.6	1	1
1.8	0.1	400.2	8.0	-0.7	1	1
1.9	0.1	400.2	8.0	-0.7	1	1
2.0	0.1	400.2	8.0	-0.8	1	1
2.1	0.1	400.2	8.0	-0.9	1	1
2.2	0.1	400.2	8.0	-0.9	1	1
2.3	0.1	400.2	8.0	-1.0	1	1
2.4	0.1	400.2	8.0	-1.1	1	1
2.5	0.1	400.2	8.0	-1.1	1	1
2.6	0.1	400.2	8.0	-1.2	1	1
2.7	0.1	400.2	8.0	-1.3	1	1
2.8	0.1	400.2	8.0	-1.3	1	1
2.9	0.1	400.2	8.0	-1.4	1	1
3.0	0.1	400.2	8.0	-1.5	1	1
3.1	0.1	400.2	8.0	-1.6	1	1
3.2	0.1	400.2	8.0	-1.7	1	1
3.3	0.1	400.2	8.0	-1.7	1	1
3.4	0.1	400.2	8.0	-1.2	1	1
3.5	0.1	400.2	8.0	-0.1	1	1
3.6	0.1	400.2	7.9	1.6	1	1
3.7	0.1	400.2	7.9	3.8	1	1
3.8	0.1	400.2	7.8	6.7	1	1
3.9	0.1	400.2	7.7	10.2	1	1
4.0	0.0	400.2	7.6	14.1	1	1

4.1	0.0	400.2	7.5	18.1	1	1
4.2	0.0	400.2	7.5	22.1	1	1
4.3	0.0	400.2	7.5	26.2	1	1
4.4	23.7	398.8	7.5	26.5	1	1
4.5	23.2	398.8	7.5	22.8	1	1
4.6	23.8	398.8	7.6	18.5	1	1
4.7	23.4	398.8	7.6	13.5	1	1
4.8	23.4	398.7	7.6	8.0	1	1
4.9	23.5	398.7	7.6	1.8	1	1
5.0	15.2	399.2	7.6	-3.6	1	1
5.1	0.2	400.1	7.6	-5.8	1	1
5.2	-0.3	400.1	7.6	-5.8	1	1
5.3	2.2	399.9	7.6	-6.2	1	1
5.4	-4.2	400.3	7.6	-5.9	1	1
5.5	2.0	399.9	7.6	-5.6	1	1
5.6	0.2	400.0	7.6	-6.0	1	1
5.7	0.1	400.1	7.6	-6.1	1	1
5.8	-0.2	400.1	7.6	-6.1	1	1
5.9	0.0	400.1	7.6	-6.1	1	1
6.0	0.1	400.1	7.6	-6.2	1	1
6.1	0.3	400.0	7.6	-6.3	1	1
6.2	-0.1	400.1	7.6	-6.3	1	1
6.3	0.1	400.1	7.6	-6.4	1	1
6.4	0.3	400.0	7.6	-6.5	1	1
6.5	-0.1	400.1	7.6	-6.6	1	1
6.6	0.1	400.1	7.6	-6.6	1	1
6.7	0.3	400.0	7.6	-6.8	1	1
6.8	-0.1	400.1	7.6	-7.1	1	1
6.9	0.3	400.0	7.6	-8.5	1	1
7.0	0.2	400.1	7.6	-10.2	1	1
7.1	-0.1	400.1	7.6	-12.4	1	1
7.2	0.2	400.1	7.6	-15.1	1	1
7.3	0.4	400.0	7.6	-18.4	1	1
7.4	0.0	400.1	7.6	-22.1	1	1
7.5	0.2	400.0	7.6	-26.3	1	1
7.6	0.2	400.0	7.6	-31.0	1	1
7.7	0.5	400.0	7.6	-36.2	1	1
7.8	-19.9	401.9	7.7	-38.7	1	1
7.9	-19.6	402.0	7.7	-38.4	1	1
8.0	-19.5	402.0	7.8	-38.1	1	1
8.1	-19.9	402.1	7.9	-37.7	1	1
8.2	-19.7	402.1	7.9	-37.2	1	1
8.3	-19.3	402.1	7.9	-36.9	1	1
8.4	-19.9	402.2	8.0	-36.5	1	1
8.5	-19.7	402.3	8.0	-36.0	1	1

8.6	-19.5	402.3	8.0	-35.6	1	1
8.7	-19.7	402.3	8.0	-35.2	1	1
8.8	-19.7	402.3	8.0	-34.8	1	1
8.9	-20.1	402.4	8.0	-34.4	1	1
9.0	-19.4	402.3	8.0	-34.0	1	1
9.1	-20.1	402.4	8.0	-33.6	1	1
9.2	-19.6	402.3	8.0	-33.2	1	1
9.3	-19.9	402.4	7.9	-32.8	1	1
9.4	-20.1	402.4	8.0	-29.6	1	1
9.5	-19.9	402.3	7.9	-32.1	1	1
9.6	-19.9	402.3	7.8	-31.8	1	1
9.7	-20.0	402.3	7.8	-31.5	1	1
9.8	-20.2	402.3	7.7	-31.2	1	1
9.9	-20.1	402.2	7.7	-31.2	1	1
10.0	-20.2	402.2	7.6	-30.7	1	1
10.1	-19.9	402.1	7.6	-29.9	1	1
10.2	-20.2	402.1	7.6	-28.6	1	1
10.3	-20.0	402.0	7.7	-26.8	1	1
10.4	60.2	390.8	7.8	-42.6	1	0
10.5	-76.9	419.6	7.9	-27.7	1	0
10.6	43.2	395.2	7.9	-4.3	1	0
10.7	-19.7	401.8	7.9	-10.5	1	1
10.8	-20.6	401.8	7.9	-5.8	1	1
10.9	-27.3	402.4	7.9	0.8	1	1
11.0	-0.1	399.9	7.9	4.8	1	1
11.1	0.0	399.9	7.9	4.7	1	1
11.2	-0.3	400.0	7.9	4.7	1	1
11.3	-0.1	399.9	7.9	4.7	1	1
11.4	-0.1	399.9	7.9	4.7	1	1
11.5	-0.1	399.9	7.9	4.7	1	1
11.6	0.2	399.9	7.9	4.6	1	1
11.7	-0.2	399.9	7.9	4.6	1	1
11.8	-0.2	400.0	7.9	4.6	1	1
11.9	-0.1	399.9	7.9	4.6	1	1
12.0	0.0	399.9	7.9	4.6	1	1
12.1	0.0	399.9	7.9	4.6	1	1
12.2	0.0	399.9	7.9	4.6	1	1
12.3	0.1	399.9	7.9	4.5	1	1
12.4	-0.2	400.0	7.9	4.5	1	1
12.5	0.0	399.9	7.9	4.5	1	1
12.6	0.0	399.9	7.9	4.5	1	1
12.7	0.0	399.9	7.9	4.4	1	1
12.8	0.0	399.9	7.9	4.4	1	1
12.9	0.2	399.9	7.9	4.3	1	1
13.0	-0.1	400.0	7.9	4.3	1	1

13.1	0.3	399.9	7.9	4.2	1	1
13.2	-0.2	400.0	7.9	4.1	1	1
13.3	0.1	399.9	7.9	4.1	1	1
13.4	0.1	399.9	7.9	4.0	1	1
13.5	0.3	399.9	7.9	3.9	1	1
13.6	0.0	400.0	7.9	4.4	1	1
13.7	0.2	399.9	7.9	5.6	1	1
13.8	0.2	399.9	7.8	7.3	1	1
13.9	0.2	399.9	7.8	9.6	1	1
14.0	0.4	399.9	7.8	12.5	1	1
14.1	0.1	400.0	7.7	15.9	1	1
14.2	0.2	399.9	7.6	20.0	1	1
14.3	0.2	400.0	7.6	24.7	1	1
14.4	0.2	400.0	7.5	30.0	1	1
14.5	0.2	400.0	7.5	35.8	1	1
14.6	23.8	399.0	7.5	38.5	1	1
14.7	23.9	399.0	7.5	37.7	1	1
14.8	23.8	399.1	7.4	36.8	1	1
14.9	23.7	399.1	7.4	36.1	1	1
15.0	23.6	399.2	7.4	35.4	1	1
15.1	23.8	399.2	7.3	34.7	1	1
15.2	23.9	399.3	7.2	34.0	1	1
15.3	23.5	399.3	7.2	33.5	1	1
15.4	23.8	399.3	7.1	33.0	1	1
15.5	23.6	399.4	7.0	32.8	1	1
15.6	23.6	399.4	6.9	32.1	1	1
15.7	23.4	399.4	6.9	31.1	1	1
15.8	23.9	399.4	6.9	29.3	1	1
15.9	23.2	399.4	6.9	27.0	1	1
16.0	23.4	399.4	7.0	24.1	1	1
16.1	23.7	399.4	7.0	20.5	1	1
16.2	23.4	399.4	7.0	16.2	1	1
16.3	23.2	399.4	7.0	11.4	1	1
16.4	23.8	399.3	7.0	5.8	1	1
16.5	30.8	399.0	7.0	-1.9	1	0
16.6	-0.1	400.1	7.0	-6.6	1	1
16.7	-0.1	400.1	7.0	-6.6	1	1
16.8	-0.1	400.1	7.0	-7.3	1	1
16.9	-0.1	400.1	7.0	-8.7	1	1
17.0	-0.1	400.1	7.0	-10.7	1	1
17.1	-0.1	400.1	7.0	-13.5	1	1
17.2	-0.1	400.1	7.0	-16.8	1	1
17.3	0.0	400.1	7.0	-20.9	1	1
17.4	0.0	400.1	6.9	-25.6	1	1
17.5	0.0	400.1	6.9	-30.9	1	1

17.6	0.0	400.1	6.9	-36.9	1	1
17.7	0.1	400.1	7.0	-43.3	1	1
17.8	-23.6	401.1	7.1	-46.6	1	1
17.9	-23.1	401.1	7.2	-46.3	1	1
18.0	-23.7	401.2	7.3	-46.0	1	1
18.1	-23.2	401.2	7.4	-45.6	1	1
18.2	-23.3	401.3	7.4	-45.2	1	1
18.3	-23.3	401.3	7.5	-44.7	1	1
18.4	-23.6	401.3	7.6	-44.2	1	1
18.5	-23.0	401.3	7.6	-43.6	1	1
18.6	-23.4	401.3	7.7	-43.1	1	1
18.7	-23.4	401.3	7.7	-42.5	1	1
18.8	-23.6	401.3	7.7	-41.8	1	1
18.9	-23.1	401.3	7.7	-41.2	1	1
19.0	-23.5	401.3	7.8	-40.5	1	1
19.1	-23.3	401.2	7.7	-39.9	1	1
19.2	-23.7	401.2	7.7	-39.3	1	1
19.3	-23.5	401.2	7.7	-38.8	1	1
19.4	-23.8	401.2	7.7	-37.9	1	1
19.5	-23.4	401.1	7.7	-36.5	1	1
19.6	-23.6	401.1	7.7	-34.6	1	1
19.7	-24.1	401.0	7.8	-31.9	1	1
19.8	-23.3	401.0	7.9	-28.8	1	1
19.9	-24.1	400.9	7.9	-25.0	1	1
20.0	-23.7	400.9	7.9	-20.6	1	1
20.1	-24.0	400.8	8.0	-15.7	1	1
20.2	-23.7	400.8	8.0	-10.1	1	1
20.3	-31.6	401.0	8.0	-2.5	1	0
20.4	0.0	399.9	8.0	2.1	1	1
20.5	-0.5	399.9	8.0	2.0	1	1
20.6	-0.4	399.9	8.0	1.9	1	1
20.7	-0.3	399.9	8.0	1.8	1	1
20.8	-0.1	399.9	8.0	1.1	1	1
20.9	-0.6	399.9	7.9	-0.2	1	1
21.0	-0.4	399.9	7.9	-2.0	1	1
21.1	-0.3	399.9	7.8	-4.4	1	1
21.2	-0.2	399.9	7.7	-7.5	1	1
21.3	-0.7	399.9	7.6	-11.1	1	1
21.4	-0.5	399.9	7.5	-15.3	1	1
21.5	-0.4	399.9	7.3	-20.1	1	1
21.6	-0.1	399.9	7.2	-25.4	1	1
21.7	-0.7	399.9	7.2	-30.6	1	1
21.8	-23.9	400.4	7.2	-32.1	1	1
21.9	-24.0	400.4	7.3	-29.6	1	1
22.0	-24.2	400.3	7.3	-26.4	1	1

22.1	-24.0	400.3	7.4	-22.6	1	1
22.2	-23.6	400.3	7.4	-18.3	1	1
22.3	-24.3	400.3	7.4	-13.2	1	1
22.4	-23.9	400.3	7.4	-7.5	1	1
22.5	-23.7	400.3	7.4	-0.5	1	1
22.6	-8.5	400.0	7.4	5.2	1	1
22.7	-0.3	399.9	7.4	8.3	1	1
22.8	-0.1	399.9	7.4	10.9	1	1
22.9	-0.3	399.9	7.3	14.1	1	1
23.0	0.0	399.9	7.3	17.9	1	1
23.1	-0.2	399.9	7.2	22.4	1	1
23.2	0.0	399.9	7.2	27.5	1	1
23.3	-0.2	399.9	7.2	33.2	1	1
23.4	0.0	399.9	7.2	39.5	1	1
23.5	23.4	399.5	7.2	42.5	1	1
23.6	23.2	399.5	7.3	42.2	1	1
23.7	23.5	399.4	7.3	41.8	1	1
23.8	23.5	399.4	7.3	41.3	1	1
23.9	23.4	399.5	7.3	40.8	1	1
24.0	23.2	399.5	7.4	40.4	1	1
24.1	23.5	399.5	7.4	40.0	1	1
24.2	23.4	399.5	7.4	39.5	1	1
24.3	23.4	399.5	7.4	39.0	1	1
24.4	23.2	399.5	7.3	38.6	1	1
24.5	23.5	399.5	7.3	38.2	1	1
24.6	23.2	399.6	7.4	37.2	1	1
24.7	23.3	399.6	7.4	35.7	1	1
24.8	23.2	399.6	7.5	33.5	1	1
24.9	23.6	399.6	7.5	30.8	1	1
25.0	23.1	399.7	7.6	27.4	1	1
25.1	23.2	399.7	7.7	23.5	1	1
25.2	23.4	399.7	7.7	18.9	1	1
25.3	23.1	399.8	7.7	13.8	1	1
25.4	23.5	399.8	7.7	8.1	1	1
25.5	19.4	399.8	7.7	2.4	1	1
25.6	0.0	400.0	7.7	-0.2	1	1
25.7	-0.5	400.0	7.7	1.2	1	1
25.8	-0.3	400.0	7.7	2.0	1	1
25.9	-0.2	400.0	7.7	2.2	1	1
26.0	0.0	400.0	7.7	1.7	1	1
26.1	-0.5	400.0	7.7	0.7	1	1
26.2	-0.3	400.0	7.6	-1.0	1	1
26.3	-0.2	400.0	7.6	-3.2	1	1
26.4	0.0	400.0	7.5	-6.1	1	1
26.5	-0.5	400.0	7.4	-9.6	1	1

26.6	-0.2	400.0	7.3	-13.7	1	1
26.7	37.5	399.8	7.2	-25.1	1	0
26.8	-24.1	400.2	7.1	-33.9	1	1
26.9	-23.5	400.1	7.0	-33.4	1	1
27.0	-23.8	400.1	7.0	-32.8	1	1
27.1	-23.6	400.1	6.9	-31.8	1	1
27.2	-23.6	400.1	6.9	-30.1	1	1
27.3	-23.7	400.1	7.0	-27.9	1	1
27.4	-23.3	400.1	7.0	-25.0	1	1
27.5	-23.8	400.1	7.0	-21.5	1	1
27.6	-23.5	400.1	7.1	-17.3	1	1
27.7	-23.4	400.1	7.1	-12.5	1	1
27.8	-23.5	400.0	7.1	-7.1	1	1
27.9	-23.7	400.0	7.1	-0.9	1	1
28.0	-21.1	400.0	7.1	5.5	1	1
28.1	0.0	400.0	7.1	8.8	1	1
28.2	0.0	400.0	7.1	9.0	1	1
28.3	0.0	400.0	7.1	9.3	1	1
28.4	0.0	400.0	7.1	9.5	1	1
28.5	0.0	400.0	7.1	9.8	1	1
28.6	0.0	400.0	7.1	10.1	1	1

CM IN RADAR CONE	100.0000	PERCENT
CMMCA W/IN STRUCTURAL LIMITS	97.90209	PERCENT

Appendix E. *Graphical Output of Experimental Results*

This appendix contains the graphical output from the results of the experimental design point which achieved the highest percentage of radar coverage over flight path three. This appendix contains a plot of the CMMCA flight path relative to the cruise missile flight path, the plot of the overall J value at each iteration of the program, and the output file RESULTS.OUT, which contains the CMMCA bank angle, airspeed, and position relative to the cruise missile at every point in the solution.

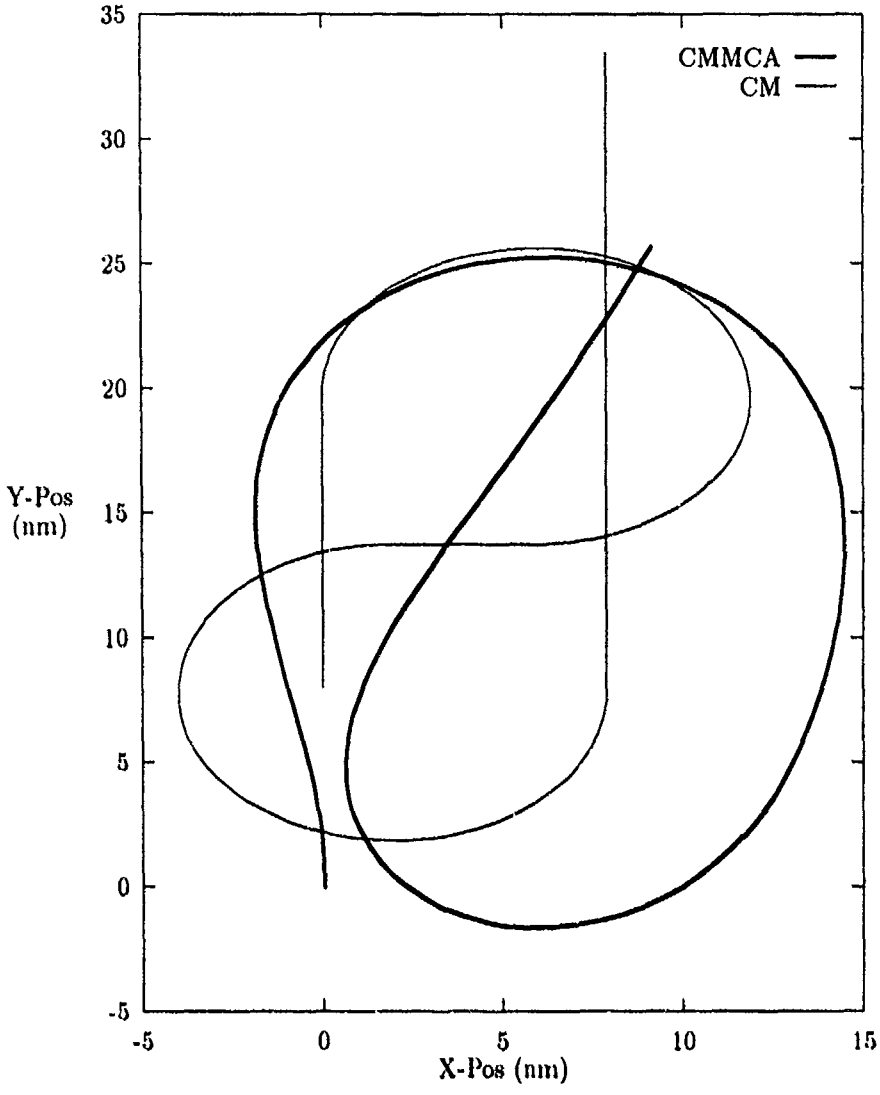

Figure 37. Plot of CMMCA and Cruise Missile Flight Paths

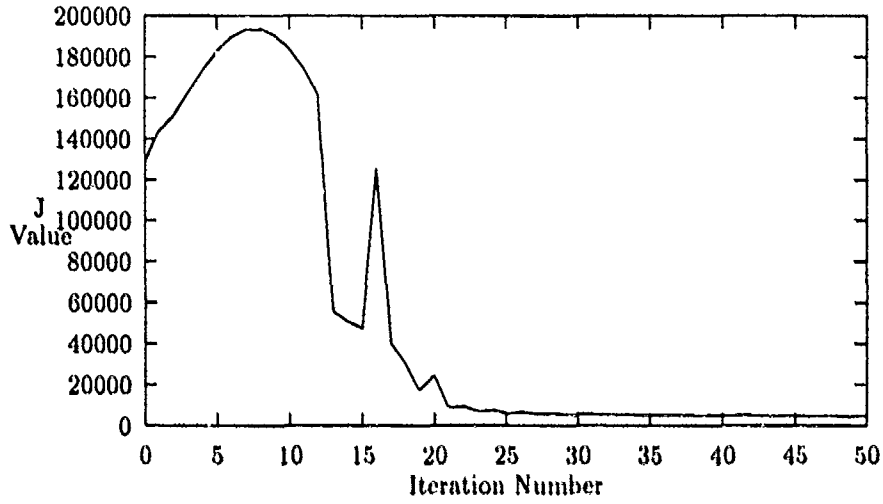

Figure 38. Plot of J Value versus Iteration Number

JSTOP = 4551.968
# ITERATIONS = 50

T	BANK	SPEED	RANGE	THETA	RADAR	STRUCT
0.1	-6.5	400.8	8.0	1.0	1	1
0.2	-5.8	400.5	8.0	2.9	1	1
0.3	-5.2	400.3	8.0	4.7	1	1
0.4	-4.6	400.0	8.0	6.6	1	1
0.5	-4.0	399.8	8.0	8.3	1	1
0.6	-3.4	399.6	8.0	10.0	1	1
0.7	-2.8	399.4	8.0	11.6	1	1
0.8	-2.2	399.2	8.0	13.0	1	1
0.9	-1.7	399.1	8.1	14.4	1	1
1.0	-1.1	398.9	8.1	15.6	1	1
1.1	-0.5	398.8	8.1	16.7	1	1
1.2	0.1	398.6	8.1	17.6	1	1
1.3	0.6	398.5	8.2	18.4	1	1
1.4	1.2	398.4	8.2	18.9	1	1
1.5	1.8	398.3	8.2	19.3	1	1
1.6	2.5	398.2	8.3	19.4	1	1
1.7	3.1	398.1	8.3	19.3	1	1
1.8	3.8	398.0	8.3	19.0	1	1
1.9	4.4	397.9	8.4	18.8	1	1
2.0	5.1	397.9	8.4	18.9	1	1
2.1	5.8	397.8	8.4	19.2	1	1
2.2	6.5	397.8	8.5	19.6	1	1
2.3	7.2	397.7	8.5	20.1	1	1
2.4	8.0	397.7	8.5	20.8	1	1
2.5	8.7	397.6	8.5	21.5	1	1
2.6	9.4	397.6	8.5	22.3	1	1
2.7	10.1	397.6	8.5	23.2	1	1
2.8	10.8	397.6	8.5	24.1	1	1
2.9	11.5	397.6	8.5	25.1	1	1
3.0	12.2	397.6	8.4	26.0	1	1
3.1	12.9	397.7	8.4	27.0	1	1
3.2	13.5	397.7	8.3	28.0	1	1
3.3	14.1	397.8	8.3	29.0	1	1
3.4	14.7	397.8	8.2	30.0	1	1
3.5	15.3	397.9	8.1	31.0	1	1
3.6	15.8	398.0	8.1	32.0	1	1
3.7	16.3	398.0	8.0	33.0	1	1
3.8	16.8	398.1	7.9	34.0	1	1
3.9	17.2	398.2	7.9	35.1	1	1
4.0	17.5	398.3	7.8	36.1	1	1

4.1	17.8	398.3	7.8	37.2	1	1
4.2	18.0	398.4	7.7	38.3	1	1
4.3	18.2	398.5	7.7	39.5	1	1
4.4	18.3	398.6	7.7	40.7	1	1
4.5	18.3	398.7	7.6	42.0	1	1
4.6	18.2	398.7	7.6	43.4	1	1
4.7	18.0	398.8	7.7	44.9	1	1
4.8	17.8	398.8	7.7	46.5	1	1
4.9	17.5	398.9	7.7	48.3	1	1
5.0	17.1	398.9	7.8	50.1	1	1
5.1	16.7	399.0	7.9	52.0	1	1
5.2	16.3	399.0	8.0	54.1	1	1
5.3	15.8	399.0	8.1	56.3	1	1
5.4	15.2	399.0	8.3	58.6	1	1
5.5	14.6	399.0	8.5	61.0	0	1
5.6	14.0	399.1	8.7	63.5	0	1
5.7	13.4	399.1	8.9	66.1	0	1
5.8	12.7	399.1	9.2	68.8	0	1
5.9	12.0	399.1	9.5	71.6	0	1
6.0	11.3	399.1	9.8	74.4	0	1
6.1	10.5	399.1	10.2	77.0	0	1
6.2	9.8	399.1	10.7	79.3	0	1
6.3	9.1	399.1	11.2	81.3	0	1
6.4	8.4	399.1	11.7	83.1	0	1
6.5	7.7	399.1	12.3	84.6	0	1
6.6	7.0	399.1	12.9	86.0	0	1
6.7	6.4	399.1	13.6	87.0	0	1
6.8	5.8	399.1	14.2	87.5	0	1
6.9	5.3	399.1	14.8	87.8	0	1
7.0	4.8	399.1	15.4	87.8	0	1
7.1	4.5	399.1	15.9	87.5	0	1
7.2	4.2	399.1	16.4	87.1	0	1
7.3	4.0	399.1	16.8	86.5	0	1
7.4	3.9	399.0	17.1	85.8	0	1
7.5	3.9	399.0	17.4	84.9	0	1
7.6	4.0	398.9	17.6	83.9	0	1
7.7	4.2	398.8	17.7	82.8	0	1
7.8	4.5	398.7	17.7	81.6	0	1
7.9	4.9	398.6	17.6	80.2	0	1
8.0	5.4	398.5	17.4	78.7	0	1
8.1	6.0	398.4	17.2	77.0	0	1
8.2	6.7	398.2	16.8	75.2	0	1
8.3	7.5	398.0	16.4	73.2	0	1
8.4	8.4	397.8	15.8	71.1	0	1
8.5	9.4	397.6	15.2	68.8	0	1

8.6	10.5	397.4	14.5	66.4	0	1
8.7	11.6	397.1	13.7	63.9	0	1
8.8	12.8	396.8	12.9	61.3	0	1
8.9	14.0	396.5	11.9	58.8	1	1
9.0	15.3	396.2	10.9	56.3	1	1
9.1	16.6	395.9	9.9	54.0	1	1
9.2	18.0	395.6	8.8	52.1	1	1
9.3	19.3	395.3	7.8	51.0	1	1
9.4	20.5	395.0	6.7	51.1	1	1
9.5	21.7	394.7	5.8	53.1	1	1
9.6	22.8	394.4	5.0	57.7	1	1
9.7	23.7	394.2	4.5	65.2	0	1
9.8	24.4	394.0	4.3	74.4	0	1
9.9	24.7	393.9	4.5	82.9	0	1
10.0	24.7	393.9	5.0	88.5	0	1
10.1	24.4	393.9	5.6	91.0	0	1
10.2	23.9	394.0	6.2	90.8	0	1
10.3	23.1	394.2	6.9	88.8	0	1
10.4	22.2	394.4	7.5	85.7	0	1
10.5	21.3	394.6	8.1	81.8	0	1
10.6	20.2	394.8	8.5	77.4	0	1
10.7	19.2	395.1	8.8	72.7	0	1
10.8	18.2	395.4	9.0	67.9	0	1
10.9	17.0	395.7	9.2	63.2	0	1
11.0	15.8	396.0	9.3	58.7	1	1
11.1	14.5	396.3	9.4	54.4	1	1
11.2	13.3	396.6	9.4	50.4	1	1
11.3	12.1	396.9	9.4	46.5	1	1
11.4	10.9	397.2	9.3	42.9	1	1
11.5	9.8	397.5	9.2	39.4	1	1
11.6	8.8	397.8	9.1	36.0	1	1
11.7	7.8	398.0	9.0	32.8	1	1
11.8	6.9	398.2	8.9	29.8	1	1
11.9	6.0	398.4	8.8	26.8	1	1
12.0	5.2	398.6	8.6	23.9	1	1
12.1	4.4	398.8	8.5	21.1	1	1
12.2	3.7	398.9	8.4	18.4	1	1
12.3	3.0	399.1	8.2	15.8	1	1
12.4	2.4	399.2	8.1	13.2	1	1
12.5	1.8	399.3	8.0	10.7	1	1
12.6	1.3	399.4	7.9	8.2	1	1
12.7	0.9	399.5	7.8	5.8	1	1
12.8	0.5	399.6	7.7	3.4	1	1
12.9	0.1	399.7	7.6	1.1	1	1
13.0	-0.2	399.7	7.5	-1.2	1	1

13.1	-0.5	399.8	7.5	-3.5	1	1
13.2	-0.7	399.8	7.4	-5.6	1	1
13.3	-0.9	399.9	7.4	-7.8	1	1
13.4	-1.0	399.9	7.3	-9.9	1	1
13.5	-1.1	400.0	7.3	-11.9	1	1
13.6	-1.2	400.0	7.3	-13.9	1	1
13.7	-1.2	400.0	7.3	-15.9	1	1
13.8	-1.2	400.0	7.4	-17.8	1	1
13.9	-1.2	400.0	7.4	-19.6	1	1
14.0	-1.1	400.0	7.4	-21.5	1	1
14.1	-1.0	400.0	7.5	-23.3	1	1
14.2	-0.9	400.0	7.5	-25.1	1	1
14.3	-0.8	400.0	7.6	-26.8	1	1
14.4	-0.6	400.0	7.7	-28.6	1	1
14.5	-0.4	400.0	7.8	-30.3	1	1
14.6	-0.2	400.0	7.9	-32.1	1	1
14.7	-0.1	400.0	8.0	-33.8	1	1

CM IN RADAR CONE	68.02721	PERCENT
CMMCA W/IN STRUCTURAL LIMITS	100.0000	PERCENT

Appendix F. *Graphical Output of Optimal Weights for Flight Path Four*

This appendix contains the graphical output from the results of the optimal weights found from the experimental design process being applied to the fourth flight profile. For both the straight and trailing initial CMMCA flight paths, this appendix contains a plot of the CMMCA flight path relative to the cruise missile flight path, the plot of the overall J value at each iteration of the program, and the output file RESULTS.OUT, which contains the CMMCA bank angle, airspeed, and position relative to the cruise missile at every point in the solution.

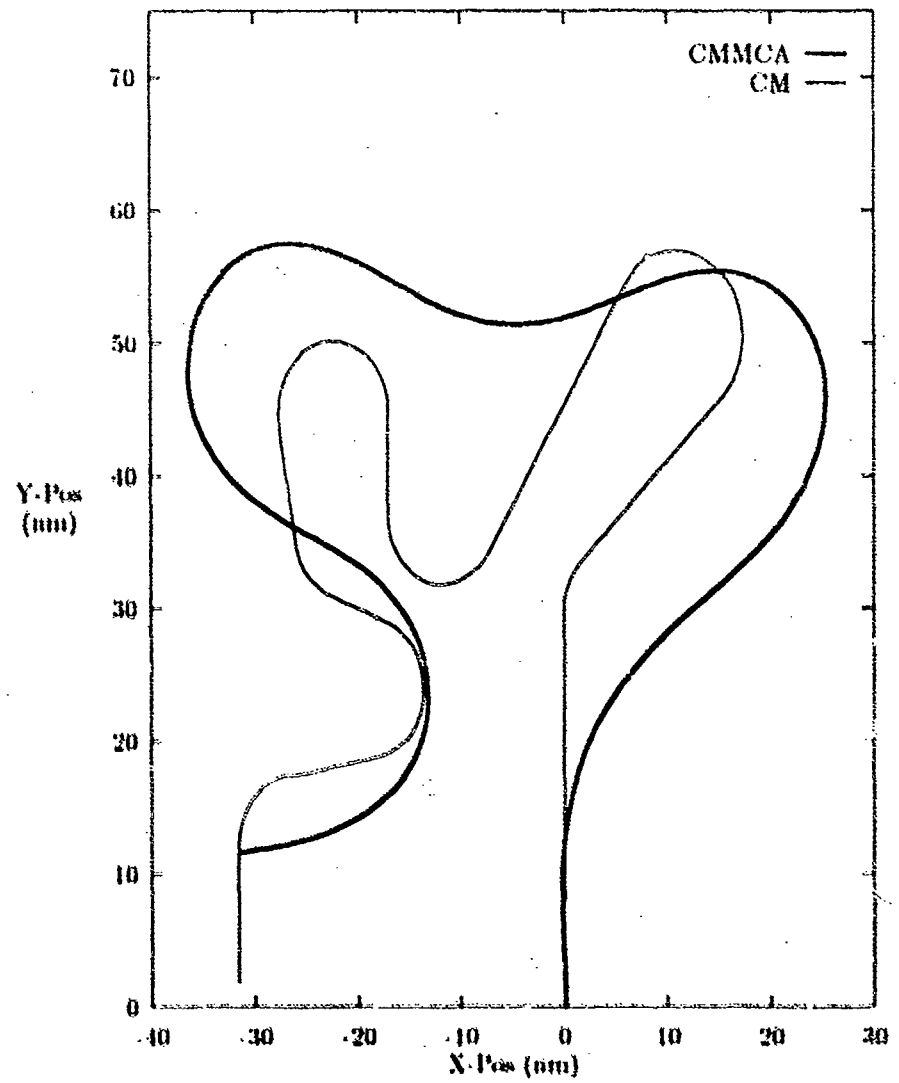

Figure 39. CMMCA and Cruise Missile Paths CMMCA Starting Straight

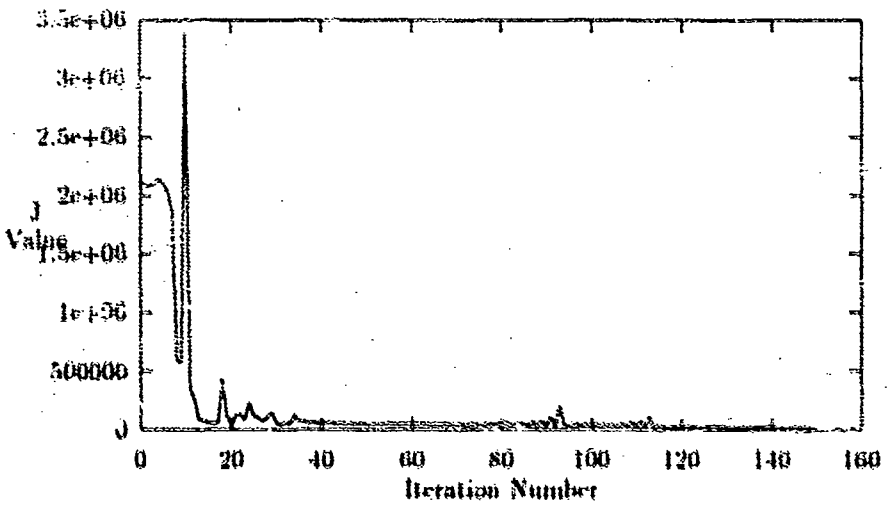

Figure 40. Plot of *J* Value versus Iteration Number

JSTOP = 16538.15
# ITERATIONS = 150

T	BANK	SPEED	RANGE	THETA	RADAR	STRUCT
0.1	-3.7	400.2	8.0	0.5	1	1
0.2	-2.9	400.3	8.0	1.6	1	1
0.3	-2.2	400.4	8.0	2.5	1	1
0.4	-1.5	400.5	8.0	3.2	1	1
0.5	-0.9	400.5	8.0	3.8	1	1
0.6	-0.3	400.6	8.0	4.2	1	1
0.7	0.4	400.6	8.0	4.5	1	1
0.8	0.9	400.6	8.0	4.5	1	1
0.9	1.5	400.7	8.0	4.4	1	1
1.0	2.0	400.7	8.0	4.1	1	1
1.1	2.5	400.7	8.0	3.6	1	1
1.2	3.0	400.7	8.0	2.9	1	1
1.3	3.5	400.7	8.0	2.0	1	1
1.4	3.9	400.7	8.0	0.9	1	1
1.5	4.3	400.7	8.0	-0.4	1	1
1.6	4.6	400.7	8.0	-1.9	1	1
1.7	5.0	400.7	8.0	-3.7	1	1
1.8	5.3	400.6	8.0	-5.6	1	1
1.9	5.5	400.6	8.0	-7.8	1	1
2.0	5.8	400.6	8.0	-10.1	1	1
2.1	6.0	400.5	8.0	-12.7	1	1
2.2	6.1	400.5	8.0	-15.4	1	1
2.3	6.3	400.4	8.1	-18.3	1	1
2.4	6.4	400.4	8.1	-21.4	1	1
2.5	6.5	400.3	8.2	-24.7	1	1
2.6	6.5	400.2	8.2	-28.0	1	1
2.7	6.6	400.2	8.3	-31.5	1	1
2.8	6.6	400.1	8.4	-35.1	1	1
2.9	6.6	400.0	8.5	-38.8	1	1
3.0	6.5	400.0	8.7	-42.5	1	1
3.1	6.4	399.9	8.8	-46.3	1	1
3.2	6.4	399.8	9.0	-50.0	1	1
3.3	6.2	399.7	9.2	-53.7	1	1
3.4	6.1	399.7	9.4	-56.9	1	1
3.5	6.0	399.6	9.6	-59.7	1	1
3.6	5.8	399.5	9.8	-62.0	0	1
3.7	5.6	399.4	9.9	-64.0	0	1
3.8	5.4	399.3	9.9	-65.8	0	1
3.9	5.2	399.3	9.9	-67.3	0	1
4.0	4.9	399.2	9.9	-68.6	0	1

4.1	4.6	399.1	9.9	-69.9	0	1
4.2	4.4	399.0	9.9	-71.2	0	1
4.3	4.1	398.9	9.9	-72.4	0	1
4.4	3.8	398.8	9.9	-73.5	0	1
4.5	3.4	398.8	9.9	-74.6	0	1
4.6	3.1	398.7	10.0	-75.6	0	1
4.7	2.8	398.6	10.0	-76.5	0	1
4.8	2.4	398.5	10.1	-77.3	0	1
4.9	2.1	398.4	10.1	-78.1	0	1
5.0	1.7	398.3	10.2	-78.7	0	1
5.1	1.3	398.2	10.3	-79.2	0	1
5.2	0.9	398.2	10.4	-79.7	0	1
5.3	0.6	398.1	10.5	-80.0	0	1
5.4	0.2	398.0	10.5	-80.2	0	1
5.5	-0.2	397.9	10.6	-80.3	0	1
5.6	-0.6	397.8	10.7	-80.2	0	1
5.7	-1.0	397.7	10.8	-80.1	0	1
5.8	-1.4	397.6	10.9	-79.8	0	1
5.9	-1.9	397.6	11.0	-79.4	0	1
6.0	-2.3	397.5	11.0	-78.9	0	1
6.1	-2.7	397.4	11.1	-78.3	0	1
6.2	-3.1	397.3	11.2	-77.5	0	1
6.3	-3.5	397.3	11.2	-76.6	0	1
6.4	-4.0	397.2	11.2	-75.5	0	1
6.5	-4.4	397.1	11.3	-74.3	0	1
6.6	-4.9	397.1	11.3	-73.0	0	1
6.7	-5.3	397.0	11.3	-71.4	0	1
6.8	-5.8	397.0	11.3	-69.9	0	1
6.9	-6.2	396.9	11.4	-68.3	0	1
7.0	-6.7	396.9	11.5	-66.8	0	1
7.1	-7.2	396.8	11.7	-65.3	0	1
7.2	-7.6	396.8	11.9	-63.8	0	1
7.3	-8.1	396.8	12.1	-62.3	0	1
7.4	-8.5	396.8	12.3	-60.9	0	1
7.5	-9.0	396.8	12.6	-59.5	1	1
7.6	-9.5	396.8	12.9	-58.1	1	1
7.7	-9.9	396.8	13.1	-56.7	1	1
7.8	-10.3	396.8	13.4	-55.4	1	1
7.9	-10.8	396.9	13.7	-54.1	1	1
8.0	-11.2	396.8	13.9	-52.8	1	1
8.1	-11.6	396.9	14.2	-51.5	1	1
8.2	-11.9	397.0	14.5	-50.1	1	1
8.3	-12.3	397.1	14.7	-48.8	1	1
8.4	-12.6	397.2	14.9	-47.5	1	1
8.5	-12.9	397.3	15.1	-46.1	0	1

8.6	-13.2	397.3	15.3	-44.8	0	1
8.7	-13.5	397.5	15.4	-43.4	0	1
8.8	-13.7	397.6	15.6	-42.1	0	1
8.9	-13.9	397.7	15.7	-40.7	0	1
9.0	-14.0	397.8	15.7	-39.4	0	1
9.1	-14.1	397.9	15.8	-38.1	0	1
9.2	-14.2	398.1	15.8	-36.9	0	1
9.3	-14.2	398.2	15.8	-35.7	0	1
9.4	-14.2	398.4	15.8	-33.1	0	1
9.5	-14.1	398.5	15.6	-33.5	0	1
9.6	-14.0	398.6	15.5	-32.5	0	1
9.7	-13.9	398.8	15.4	-31.6	0	1
9.8	-13.7	398.9	15.2	-30.9	0	1
9.9	-13.4	399.1	15.0	-30.4	1	1
10.0	-13.1	399.2	14.8	-29.9	1	1
10.1	-12.7	399.3	14.6	-29.4	1	1
10.2	-12.3	399.5	14.5	-29.0	1	1
10.3	-11.9	399.6	14.4	-28.7	1	1
10.4	-11.4	399.7	14.3	-28.3	1	1
10.5	-10.9	399.8	14.2	-28.1	1	1
10.6	-10.4	399.9	14.2	-27.9	1	1
10.7	-9.8	400.0	14.1	-27.7	1	1
10.8	-9.2	400.1	14.1	-27.6	1	1
10.9	-8.6	400.2	14.1	-27.6	1	1
11.0	-8.0	400.3	14.1	-27.6	1	1
11.1	-7.3	400.3	14.1	-27.7	1	1
11.2	-6.6	400.4	14.2	-28.0	1	1
11.3	-6.0	400.5	14.2	-28.3	1	1
11.4	-5.3	400.5	14.3	-28.8	1	1
11.5	-4.6	400.6	14.3	-29.3	1	1
11.6	-3.9	400.6	14.4	-30.0	1	1
11.7	-3.2	400.6	14.5	-30.9	1	1
11.8	-2.5	400.7	14.6	-31.8	1	1
11.9	-1.9	400.7	14.7	-32.9	1	1
12.0	-1.2	400.7	14.8	-34.2	1	1
12.1	-0.5	400.7	14.9	-35.6	1	1
12.2	0.1	400.7	15.0	-37.2	0	1
12.3	0.7	400.7	15.2	-38.9	0	1
12.4	1.3	400.7	15.3	-40.7	0	1
12.5	1.9	400.7	15.5	-42.7	0	1
12.6	2.5	400.7	15.7	-44.9	0	1
12.7	3.0	400.7	15.9	-47.2	0	1
12.8	3.5	400.7	16.1	-49.6	0	1
12.9	4.0	400.7	16.3	-52.2	0	1
13.0	4.4	400.7	16.6	-54.8	0	1

13.1	4.8	400.7	16.9	-57.6	0	1
13.2	5.2	400.6	17.2	-60.5	0	1
13.3	5.5	400.6	17.5	-63.4	0	1
13.4	5.8	400.6	17.9	-66.4	0	1
13.5	6.0	400.6	18.2	-69.4	0	1
13.6	6.3	400.6	18.6	-72.3	0	1
13.7	6.4	400.6	19.0	-74.9	0	1
13.8	6.5	400.6	19.3	-77.4	0	1
13.9	6.6	400.5	19.6	-79.7	0	1
14.0	6.6	400.5	19.9	-81.9	0	1
14.1	6.5	400.5	20.1	-83.9	0	1
14.2	6.4	400.5	20.3	-85.9	0	1
14.3	6.3	400.5	20.3	-87.8	0	1
14.4	6.1	400.5	20.4	-89.5	0	1
14.5	5.8	400.5	20.3	-91.2	0	1
14.6	5.5	400.5	20.2	-92.9	0	1
14.7	5.2	400.6	20.1	-94.5	0	1
14.8	4.8	400.6	19.9	-96.1	0	1
14.9	4.4	400.6	19.6	-97.7	0	1
15.0	3.9	400.6	19.3	-99.4	0	1
15.1	3.4	400.6	18.9	-101.0	0	1
15.2	2.8	400.7	18.5	-102.8	0	1
15.3	2.2	400.7	18.0	-104.6	0	1
15.4	1.6	400.7	17.6	-106.6	0	1
15.5	1.0	400.8	17.1	-108.8	0	1
15.6	0.3	400.8	16.7	-111.0	0	1
15.7	-0.3	400.9	16.3	-113.0	0	1
15.8	-1.0	400.9	15.9	-115.0	0	1
15.9	-1.7	401.0	15.5	-116.9	0	1
16.0	-2.4	401.0	15.1	-118.8	0	1
16.1	-3.1	401.1	14.8	-120.5	0	1
16.2	-3.8	401.2	14.5	-122.2	0	1
16.3	-4.5	401.2	14.2	-123.8	0	1
16.4	-5.2	401.3	14.0	-125.4	0	1
16.5	-5.9	401.3	13.7	-126.9	0	1
16.6	-6.6	401.4	13.5	-128.4	0	1
16.7	-7.3	401.4	13.3	-129.8	0	1
16.8	-7.9	401.5	13.1	-130.9	0	1
16.9	-8.6	401.6	12.9	-131.6	0	1
17.0	-9.2	401.6	12.7	-131.9	0	1
17.1	-9.8	401.6	12.5	-131.9	0	1
17.2	-10.3	401.7	12.3	-131.5	0	1
17.3	-10.8	401.7	12.1	-130.8	0	1
17.4	-11.3	401.8	11.8	-129.7	0	1
17.5	-11.8	401.8	11.6	-128.3	0	1

17.6	-12.2	401.8	11.4	-126.5	0	1
17.7	-12.6	401.8	11.1	-124.4	0	1
17.8	-13.0	401.8	10.9	-122.0	0	1
17.9	-13.3	401.8	10.7	-119.3	0	1
18.0	-13.6	401.8	10.5	-116.3	0	1
18.1	-13.9	401.8	10.3	-113.0	0	1
18.2	-14.1	401.8	10.2	-109.4	0	1
18.3	-14.3	401.8	10.0	-105.7	0	1
18.4	-14.4	401.8	9.9	-101.7	0	1
18.5	-14.5	401.7	9.9	-97.6	0	1
18.6	-14.6	401.7	9.8	-93.4	0	1
18.7	-14.7	401.6	9.8	-89.2	0	1
18.8	-14.7	401.6	9.8	-84.9	0	1
18.9	-14.7	401.5	9.9	-80.7	0	1
19.0	-14.6	401.5	10.0	-76.6	0	1
19.1	-14.6	401.4	10.1	-72.7	0	1
19.2	-14.5	401.4	10.3	-68.9	0	1
19.3	-14.3	401.3	10.5	-65.4	0	1
19.4	-14.2	401.2	10.6	-61.8	0	1
19.5	-14.0	401.2	10.7	-58.1	1	1
19.6	-13.7	401.1	10.8	-54.4	1	1
19.7	-13.5	401.0	10.8	-50.6	1	1
19.8	-13.2	401.0	10.8	-46.7	1	1
19.9	-12.9	400.9	10.8	-42.8	1	1
20.0	-12.6	400.8	10.7	-38.7	1	1
20.1	-12.2	400.8	10.6	-34.6	1	1
20.2	-11.9	400.7	10.5	-30.4	1	1
20.3	-11.5	400.6	10.4	-26.1	1	1
20.4	-11.1	400.5	10.2	-21.7	1	1
20.5	-10.7	400.5	10.1	-17.1	1	1
20.6	-10.2	400.4	9.9	-12.5	1	1
20.7	-9.8	400.4	9.8	-7.8	1	1
20.8	-9.3	400.3	9.7	-3.3	1	1
20.9	-8.8	400.3	9.6	0.8	1	1
21.0	-8.3	400.2	9.6	4.5	1	1
21.1	-7.8	400.2	9.6	7.6	1	1
21.2	-7.2	400.1	9.6	10.3	1	1
21.3	-6.6	400.1	9.6	12.5	1	1
21.4	-6.1	400.0	9.6	14.1	1	1
21.5	-5.5	400.0	9.6	15.2	1	1
21.6	-4.8	399.9	9.5	16.1	1	1
21.7	-4.2	399.9	9.5	16.9	1	1
21.8	-3.5	399.8	9.5	17.6	1	1
21.9	-2.8	399.8	9.5	18.1	1	1
22.0	-2.1	399.8	9.4	18.5	1	1

22.1	-1.4	399.7	9.4	18.7	1	1
22.2	-0.7	399.7	9.4	18.8	1	1
22.3	0.1	399.7	9.4	18.6	1	1
22.4	0.8	399.6	9.4	18.3	1	1
22.5	1.6	399.6	9.4	18.2	1	1
22.6	2.3	399.6	9.4	18.3	1	1
22.7	3.1	399.5	9.5	18.7	1	1
22.8	3.8	399.5	9.5	19.3	1	1
22.9	4.6	399.5	9.5	20.1	1	1
23.0	5.3	399.4	9.5	21.1	1	1
23.1	6.0	399.4	9.6	22.3	1	1
23.2	6.8	399.4	9.6	23.6	1	1
23.3	7.5	399.3	9.5	25.0	1	1
23.4	8.1	399.3	9.5	26.6	1	1
23.5	8.8	399.3	9.5	28.2	1	1
23.6	9.5	399.2	9.4	30.0	1	1
23.7	10.1	399.2	9.4	31.8	1	1
23.8	10.7	399.2	9.3	33.8	1	1
23.9	11.3	399.2	9.2	35.8	1	1
24.0	11.8	399.2	9.2	37.9	1	1
24.1	12.3	399.2	9.1	40.1	1	1
24.2	12.8	399.1	9.0	42.4	1	1
24.3	13.3	399.1	9.0	44.8	1	1
24.4	13.7	399.1	8.9	47.2	1	1
24.5	14.0	399.1	8.9	49.7	1	1
24.6	14.3	399.1	9.0	51.8	1	1
24.7	14.6	399.1	9.1	53.5	1	1
24.8	14.8	399.2	9.3	54.8	1	1
24.9	14.9	399.2	9.5	55.6	1	1
25.0	14.9	399.2	9.7	56.0	1	1
25.1	14.8	399.2	10.0	56.1	1	1
25.2	14.6	399.3	10.3	55.7	1	1
25.3	14.4	399.3	10.6	55.1	1	1
25.4	14.1	399.3	10.8	54.2	1	1
25.5	13.8	399.4	11.1	53.1	1	1
25.6	13.4	399.4	11.4	51.8	1	1
25.7	13.0	399.4	11.6	51.1	1	1
25.8	12.5	399.5	11.9	49.9	1	1
25.9	12.1	399.5	12.1	48.2	1	1
26.0	11.6	399.5	12.3	46.1	1	1
26.1	11.1	399.6	12.4	43.6	1	1
26.2	10.6	399.6	12.4	40.8	1	1
26.3	10.0	399.6	12.4	37.8	1	1
26.4	9.5	399.6	12.3	34.4	1	1
26.5	9.0	399.7	12.2	30.9	1	1

26.6	8.5	399.7	11.9	27.1	1	1
26.7	7.9	399.7	11.5	23.1	1	1
26.8	7.4	399.7	11.1	18.9	1	1
26.9	6.9	399.8	10.6	14.5	1	1
27.0	6.4	399.8	10.1	9.7	1	1
27.1	5.9	399.8	9.6	4.6	1	1
27.2	5.5	399.8	9.1	-0.9	1	1
27.3	5.0	399.8	8.6	-6.7	1	1
27.4	4.6	399.9	8.3	-13.0	1	1
27.5	4.1	399.9	7.9	-19.7	1	1
27.6	3.7	399.9	7.7	-26.7	1	1
27.7	3.3	399.9	7.6	-34.0	1	1
27.8	2.9	399.9	7.5	-41.4	1	1
27.9	2.5	399.9	7.6	-48.6	1	1
28.0	2.1	399.9	7.8	-55.7	1	1
28.1	1.7	400.0	8.1	-62.2	0	1
28.2	1.3	400.0	8.4	-68.3	0	1
28.3	1.0	400.0	8.8	-73.7	0	1
28.4	0.6	400.0	9.3	-78.5	0	1
28.5	0.3	400.0	9.9	-82.8	0	1
28.6	0.1	400.0	10.5	-86.5	0	1

CM IN RADAR CONE 53.84616 PERCENT
CMMCA W/IN STRUCTURAL LIMITS 100.0000 PERCENT

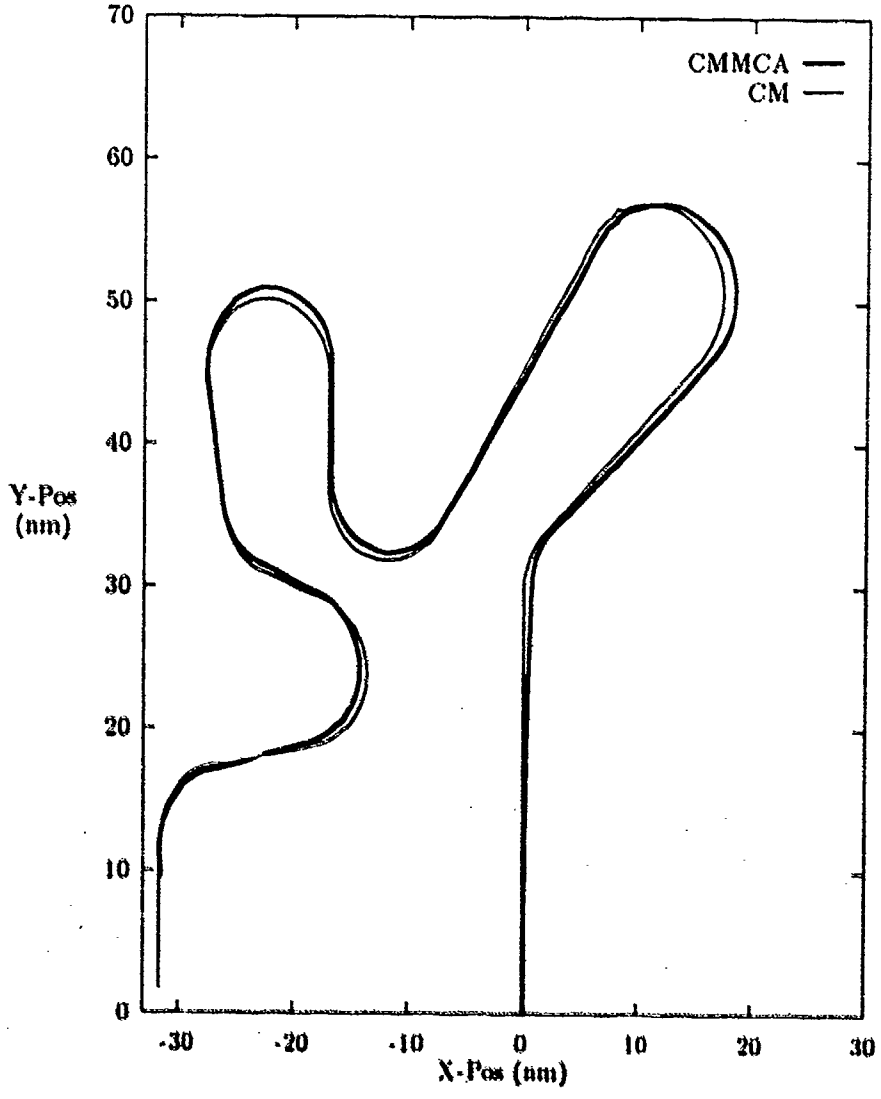

Figure 41. CMMCA and Cruise Missile Paths, CMMCA Starting Trailing

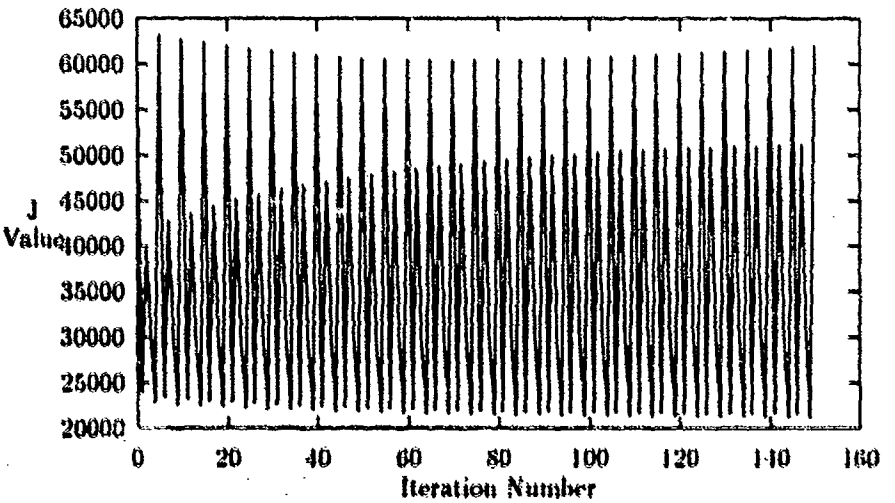

Figure 42. Plot of J Value versus Iteration Number

JSTOP = 62032.16
# ITERATIONS = 150

T	BANK	SPEED	RANGE	THETA	RADAR	STRUCT
0.1	0.1	400.2	8.0	0.0	1	1
0.2	0.1	400.2	8.0	0.0	1	1
0.3	0.1	400.2	8.0	-0.1	1	1
0.4	0.1	400.2	8.0	-0.1	1	1
0.5	0.1	400.2	8.0	-0.2	1	1
0.6	0.1	400.2	8.0	-0.2	1	1
0.7	0.1	400.2	8.0	-0.3	1	1
0.8	0.1	400.2	8.0	-0.3	1	1
0.9	0.1	400.2	8.0	-0.4	1	1
1.0	0.2	400.2	8.0	-0.5	1	1
1.1	0.2	400.2	8.0	-0.5	1	1
1.2	0.2	400.2	8.0	-0.6	1	1
1.3	0.2	400.2	8.0	-0.7	1	1
1.4	0.2	400.2	8.0	-0.8	1	1
1.5	0.2	400.2	8.0	-0.9	1	1
1.6	0.2	400.2	8.0	-1.0	1	1
1.7	0.2	400.2	8.0	-1.1	1	1
1.8	0.2	400.2	8.0	-1.2	1	1
1.9	0.2	400.2	8.0	-1.4	1	1
2.0	0.2	400.2	8.0	-1.5	1	1
2.1	0.2	400.2	8.0	-1.6	1	1
2.2	0.2	400.2	8.0	-1.8	1	1
2.3	0.2	400.2	8.0	-1.9	1	1
2.4	0.3	400.2	8.0	-2.1	1	1
2.5	0.3	400.2	8.0	-2.3	1	1
2.6	0.3	400.2	8.0	-2.5	1	1
2.7	0.3	400.2	8.0	-2.7	1	1
2.8	0.3	400.2	8.0	-2.9	1	1
2.9	0.3	400.2	8.0	-3.1	1	1
3.0	0.3	400.2	8.0	-3.3	1	1
3.1	0.3	400.2	8.0	-3.5	1	1
3.2	0.3	400.2	8.0	-3.7	1	1
3.3	0.3	400.2	8.0	-4.0	1	1
3.4	0.3	400.2	8.0	-3.6	1	1
3.5	0.3	400.2	8.0	-2.7	1	1
3.6	0.3	400.2	7.9	-1.2	1	1
3.7	0.3	400.2	7.8	0.9	1	1
3.8	0.3	400.2	7.7	3.5	1	1
3.9	0.3	400.2	7.6	6.8	1	1
4.0	0.3	400.2	7.5	10.5	1	1

4.1	0.3	400.2	7.4	14.3	1	1
4.2	0.2	400.2	7.4	18.1	1	1
4.3	0.2	400.2	7.3	22.1	1	1
4.4	0.2	400.2	7.3	26.0	1	1
4.5	0.1	400.2	7.4	29.9	1	1
4.6	23.9	398.0	7.5	29.9	1	1
4.7	23.4	398.0	7.5	26.0	1	1
4.8	24.0	397.9	7.6	21.3	1	1
4.9	23.5	397.9	7.6	16.1	1	1
5.0	23.5	397.8	7.7	10.3	1	1
5.1	23.5	397.7	7.7	3.9	1	1
5.2	15.2	398.6	7.7	-1.7	1	1
5.3	0.1	400.0	7.7	-4.1	1	1
5.4	-0.4	400.1	7.7	-4.3	1	1
5.5	2.0	399.8	7.7	-4.8	1	1
5.6	-4.5	400.5	7.7	-4.7	1	1
5.7	1.7	399.9	7.7	-4.5	1	1
5.8	-0.1	400.0	7.7	-5.0	1	1
5.9	-0.3	400.1	7.7	-5.1	1	1
6.0	-0.6	400.1	7.7	-5.2	1	1
6.1	-0.4	400.1	7.7	-5.2	1	1
6.2	-0.4	400.1	7.7	-5.3	1	1
6.3	-0.2	400.0	7.7	-5.4	1	1
6.4	-0.7	400.1	7.7	-5.4	1	1
6.5	-0.5	400.1	7.7	-5.4	1	1
6.6	-0.3	400.1	7.7	-5.4	1	1
6.7	-0.8	400.1	7.7	-5.4	1	1
6.8	-0.6	400.1	7.7	-5.8	1	1
6.9	-0.4	400.1	7.7	-6.8	1	1
7.0	-0.9	400.1	7.7	-8.3	1	1
7.1	-0.5	400.1	7.7	-10.2	1	1
7.2	-0.7	400.1	7.6	-12.7	1	1
7.3	-0.9	400.1	7.6	-15.5	1	1
7.4	-0.7	400.1	7.6	-18.9	1	1
7.5	-0.5	400.1	7.6	-22.8	1	1
7.6	-1.0	400.1	7.5	-27.2	1	1
7.7	-0.8	400.1	7.5	-32.0	1	1
7.8	-0.7	400.1	7.6	-37.2	1	1
7.9	-0.5	400.1	7.6	-42.9	1	1
8.0	-21.1	403.2	7.7	-45.7	1	1
8.1	-20.7	403.2	7.8	-45.6	1	1
8.2	-20.7	403.3	7.9	-45.4	1	1
8.3	-21.1	403.4	8.0	-45.2	1	1
8.4	-20.9	403.5	8.1	-44.8	1	1
8.5	-20.4	403.5	8.2	-44.4	1	1

8.6	-21.0	403.7	8.3	-43.9	1	1
8.7	-20.8	403.7	8.4	-43.3	1	1
8.8	-20.6	403.7	8.4	-42.8	1	1
8.9	-20.7	403.8	8.5	-42.2	1	1
9.0	-20.6	403.8	8.6	-41.6	1	1
9.1	-21.0	403.9	8.6	-40.8	1	1
9.2	-20.3	403.8	8.6	-40.1	1	1
9.3	-20.9	403.9	8.7	-39.4	1	1
9.4	-20.4	403.8	8.8	-36.1	1	1
9.5	-20.6	403.9	8.7	-38.0	1	1
9.6	-20.7	403.9	8.7	-37.2	1	1
9.7	-20.5	403.8	8.7	-36.5	1	1
9.8	-20.4	403.8	8.7	-35.8	1	1
9.9	-20.4	403.7	8.6	-35.3	1	1
10.0	-20.6	403.7	8.6	-34.4	1	1
10.1	-20.4	403.6	8.6	-33.1	1	1
10.2	-20.4	403.6	8.7	-31.4	1	1
10.3	-20.1	403.4	8.7	-29.3	1	1
10.4	-20.3	403.4	8.7	-26.9	1	1
10.5	-20.1	403.3	8.8	-23.9	1	1
10.6	60.5	384.7	8.9	-39.1	1	0
10.7	-75.7	429.9	9.0	-27.2	1	0
10.8	43.5	392.2	9.0	-7.0	1	0
10.9	-19.7	402.9	9.0	-13.1	1	1
11.0	-20.5	402.9	9.0	-8.3	1	1
11.1	-27.2	403.9	9.0	-1.7	1	1
11.2	0.0	399.9	9.0	2.3	1	1
11.3	0.2	399.9	9.0	2.2	1	1
11.4	-0.1	400.0	9.0	2.1	1	1
11.5	0.1	399.9	9.0	2.1	1	1
11.6	0.1	399.9	9.0	2.0	1	1
11.7	0.1	399.9	9.0	2.0	1	1
11.8	0.3	399.9	9.0	1.9	1	1
11.9	0.0	399.9	9.0	1.8	1	1
12.0	-0.1	399.9	9.0	1.7	1	1
12.1	0.1	399.9	9.0	1.7	1	1
12.2	0.1	399.9	9.0	1.6	1	1
12.3	0.1	399.9	9.0	1.5	1	1
12.4	0.2	399.9	9.0	1.4	1	1
12.5	0.3	399.9	9.0	1.2	1	1
12.6	0.0	399.9	9.0	1.1	1	1
12.7	0.2	399.9	9.0	1.0	1	1
12.8	0.2	399.9	9.0	0.9	1	1
12.9	0.2	399.9	9.0	0.7	1	1
13.0	0.2	399.9	9.0	0.6	1	1

13.1	0.4	399.9	9.0	0.4	1	1
13.2	0.1	399.9	9.0	0.2	1	1
13.3	0.5	399.9	9.0	0.0	1	1
13.4	0.0	399.9	9.0	-0.2	1	1
13.5	0.3	399.9	9.0	-0.3	1	1
13.6	0.3	399.9	9.0	0.0	1	1
13.7	0.5	399.9	9.0	0.8	1	1
13.8	0.2	399.9	8.9	2.2	1	1
13.9	0.4	399.9	8.9	4.0	1	1
14.0	0.4	399.9	8.8	6.4	1	1
14.1	0.4	399.9	8.7	9.3	1	1
14.2	0.5	399.9	8.6	12.7	1	1
14.3	0.2	399.9	8.4	16.6	1	1
14.4	0.4	399.9	8.3	21.2	1	1
14.5	0.3	399.9	8.1	26.3	1	1
14.6	0.3	399.9	8.0	32.0	1	1
14.7	0.3	399.9	7.9	38.3	1	1
14.8	23.9	398.4	7.8	41.4	1	1
14.9	24.0	398.5	7.8	41.0	1	1
15.0	23.9	398.6	7.7	40.7	1	1
15.1	23.8	398.6	7.6	40.5	1	1
15.2	23.6	398.7	7.5	40.4	1	1
15.3	23.7	398.8	7.5	40.4	1	1
15.4	23.8	398.8	7.4	40.4	1	1
15.5	23.4	398.9	7.3	40.7	1	1
15.6	23.7	398.9	7.3	40.7	1	1
15.7	23.4	399.0	7.3	40.3	1	1
15.8	23.4	399.0	7.3	39.3	1	1
15.9	23.2	399.0	7.4	37.7	1	1
16.0	23.6	399.0	7.5	35.5	1	1
16.1	22.9	399.1	7.6	32.7	1	1
16.2	23.1	399.1	7.7	29.4	1	1
16.3	23.3	399.0	7.7	25.5	1	1
16.4	23.1	399.0	7.8	20.9	1	1
16.5	22.8	399.0	7.8	15.8	1	1
16.6	23.4	398.9	7.8	10.2	1	1
16.7	30.4	398.4	7.8	2.5	1	0
16.8	-0.6	400.2	7.8	-2.8	1	1
16.9	-0.6	400.2	7.8	-3.9	1	1
17.0	-0.6	400.2	7.8	-5.6	1	1
17.1	-0.6	400.2	7.8	-8.0	1	1
17.2	-0.5	400.2	7.7	-10.9	1	1
17.3	-0.5	400.2	7.6	-14.4	1	1
17.4	-0.5	400.2	7.5	-18.5	1	1
17.5	-0.5	400.2	7.4	-23.2	1	1

17.6	-0.5	400.2	7.4	-28.6	1	1
17.7	-0.4	400.1	7.3	-34.5	1	1
17.8	-0.4	400.1	7.3	-41.1	1	1
17.9	-0.4	400.1	7.3	-48.1	1	1
18.0	-24.2	401.8	7.4	-51.8	1	1
18.1	-23.6	401.8	7.5	-52.1	1	1
18.2	-24.2	401.9	7.6	-52.2	1	1
18.3	-23.7	402.0	7.7	-52.2	1	1
18.4	-23.7	402.0	7.7	-52.2	1	1
18.5	-23.8	402.0	7.8	-52.1	1	1
18.6	-24.0	402.1	7.9	-51.9	1	1
18.7	-23.3	402.1	8.0	-51.7	1	1
18.8	-23.7	402.1	8.1	-51.5	1	1
18.9	-23.7	402.1	8.2	-51.1	1	1
19.0	-23.8	402.1	8.3	-50.7	1	1
19.1	-23.3	402.1	8.3	-50 3	1	1
19.2	-23.6	402.1	8.4	-49.9	1	1
19.3	-23.3	402.0	8.4	-49.6	1	1
19.4	-23.7	402.0	8.5	-48.9	1	1
19.5	-23.4	401.9	8.6	-47.6	1	1
19.6	-23.7	401.9	8.7	-45.8	1	1
19.7	-23.2	401.8	8.9	-43.5	1	1
19.8	-23.4	401.7	9.0	-40.8	1	1
19.9	-23.8	401.7	9.1	-37.4	1	1
20.0	-23.0	401.6	9.2	-33.6	1	1
20.1	-23.8	401.5	9.3	-29.2	1	1
20.2	-23.3	401.4	9.4	-24.4	1	1
20.3	-23.6	401.4	9.4	-19.1	1	1
20.4	-23.4	401.3	9.5	-13.3	1	1
20.5	-31.2	401.7	9.5	-5.5	1	0
20.6	0.3	399.9	9.5	-0.9	1	1
20.7	-0.2	399.9	9.5	-1.1	1	1
20.8	0.0	399.9	9.5	-1.6	1	1
20.9	0.1	399.9	9.4	-2.8	1	1
21.0	0.2	399.9	9.4	-4.4	1	1
21.1	-0.3	399.9	9.3	-6.5	1	1
21.2	-0.1	399.9	9.3	-9.1	1	1
21.3	0.0	399.9	9.2	-12.1	1	1
21.4	0.2	399.9	9.0	-15.8	1	1
21.5	-0.3	399.9	8.9	-19.9	1	1
21.6	-0.1	399.9	8.8	-24.2	1	1
21.7	0.0	399.9	8.8	-28.6	1	1
21.8	0.3	399.9	8.8	-33.1	1	1
21.9	-0.3	399.9	8.8	-37.5	1	1
22.0	-23.5	400.7	8.9	-38.2	1	1

22.1	-23.5	400.7	9.0	-34.9	1	1
22.2	-23.7	400.6	9.1	-31.1	1	1
22.3	-23.5	400.6	9.2	-26.8	1	1
22.4	-23.1	400.5	9.2	-22.1	1	1
22.5	-23.8	400.5	9.2	-16.3	1	1
22.6	-23.5	400.5	9.3	-9.5	1	1
22.7	-23.3	400.5	9.2	-1.7	1	1
22.8	-8.1	400.0	9.2	4.7	1	1
22.9	0.1	399.8	9.1	8.1	1	1
23.0	0.3	399.8	9.0	11.0	1	1
23.1	0.1	399.8	8.9	14.3	1	1
23.2	0.3	399.8	8.8	18.2	1	1
23.3	0.0	399.8	8.7	22.6	1	1
23.4	0.2	399.8	8.6	27.6	1	1
23.5	0.0	399.8	8.4	33.1	1	1
23.6	0.1	399.8	8.3	39.1	1	1
23.7	23.6	399.1	8.3	41.9	1	1
23.8	23.4	399.1	8.2	41.4	1	1
23.9	23.6	399.1	8.1	40.9	1	1
24.0	23.5	399.1	8.1	40.4	1	1
24.1	23.3	399.1	8.0	40.1	1	1
24.2	23.1	399.2	7.9	39.9	1	1
24.3	23.3	399.2	7.8	39.8	1	1
24.4	23.2	399.2	7.7	39.8	1	1
24.5	23.2	399.2	7.6	39.9	1	1
24.6	22.8	399.3	7.6	39.6	1	1
24.7	23.1	399.3	7.6	38.9	1	1
24.8	22.8	399.3	7.6	37.7	1	1
24.9	22.9	399.4	7.7	36.0	1	1
25.0	22.6	399.4	7.8	33.7	1	1
25.1	23.0	399.5	7.8	30.8	1	1
25.2	22.5	399.5	7.9	27.4	1	1
25.3	22.6	399.6	8.0	23.5	1	1
25.4	22.8	399.6	8.0	19.0	1	1
25.5	22.5	399.6	8.0	13.9	1	1
25.6	22.9	399.7	8.1	8.3	1	1
25.7	18.9	399.8	8.0	3.7	1	1
25.8	-0.6	400.1	8.0	1.8	1	1
25.9	-1.1	400.1	8.0	2.1	1	1
26.0	-0.9	400.1	8.0	1.9	1	1
26.1	-0.7	400.1	8.0	1.1	1	1
26.2	-0.5	400.1	8.0	-0.4	1	1
26.3	-1.0	400.1	7.9	-2.4	1	1
26.4	-0.8	400.1	7.8	-4.9	1	1
26.5	-0.6	400.1	7.7	-8.0	1	1

26.6	-0.4	400.1	7.6	-11.8	1	1
26.7	-0.8	400.1	7.4	-16.2	1	1
26.8	-0.6	400.1	7.3	-21.2	1	1
26.9	37.2	399.8	7.2	-33.5	1	0
27.0	-24.5	400.2	7.1	-43.1	1	1
27.1	-23.9	400.2	7.2	-42.7	1	1
27.2	-24.0	400.2	7.2	-41.7	1	1
27.3	-23.8	400.2	7.3	-40.1	1	1
27.4	-23.8	400.2	7.4	-37.8	1	1
27.5	-23.9	400.1	7.6	-34.9	1	1
27 6	-23.5	400.1	7.6	-31.4	1	1
27.7	-23.9	400.1	7.7	-27.4	1	1
27.8	-23.6	400.1	7.8	-22.7	1	1
27.9	-23.5	400.1	7.8	-17.4	1	1
28.0	-23.3	400.1	7.9	-11.6	1	1
28.1	-23.7	400.0	7.9	-5.1	1	1
28.2	-21.1	400.0	7.9	1.5	1	1
28.3	0.1	400.0	7.9	4.9	1	1
28.4	0.0	400.0	7.9	5.4	1	1
28.5	0.0	400.0	7.9	5.8	1	1
28.6	0.0	400.0	7.9	6.2	1	1

CM IN RADAR CONE 100.0000 PERCENT
CMMCA W/IN STRUCTURAL LIMITS 97.90209 PERCENT

Appendix G. *Graphical Output for Double Precision Runs*

This appendix contains the graphical output from the results of running the program using double precision variables over the fourth flight profile. For both initial CMMCA flight paths, this appendix contains a plot of the CMMCA flight path relative to the cruise missile flight path, the plot of the overall J value at each iteration of the program, and the output file RESULTS.OUT, which contains the CMMCA bank angle, airspeed, and position relative to the cruise missile at every point in the solution.

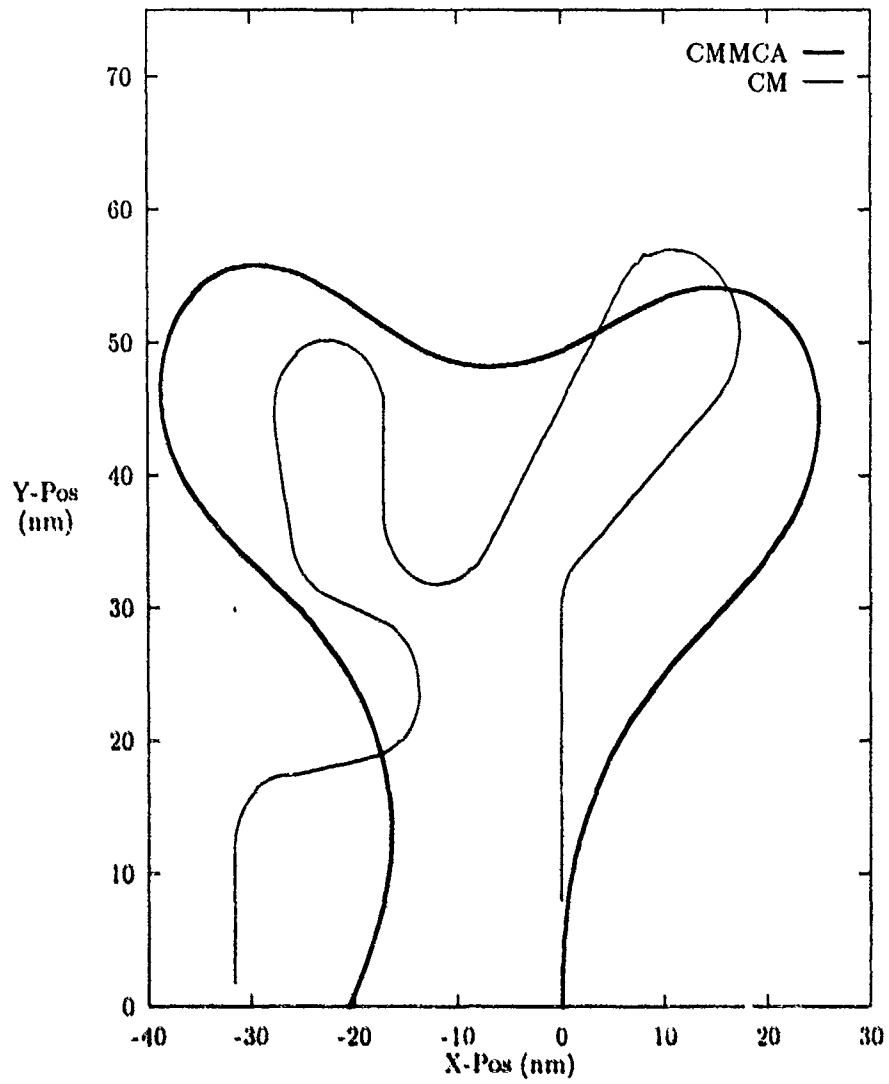

Figure 43. CMMCA and Cruise Missile Paths, CMMCA Starting Straight

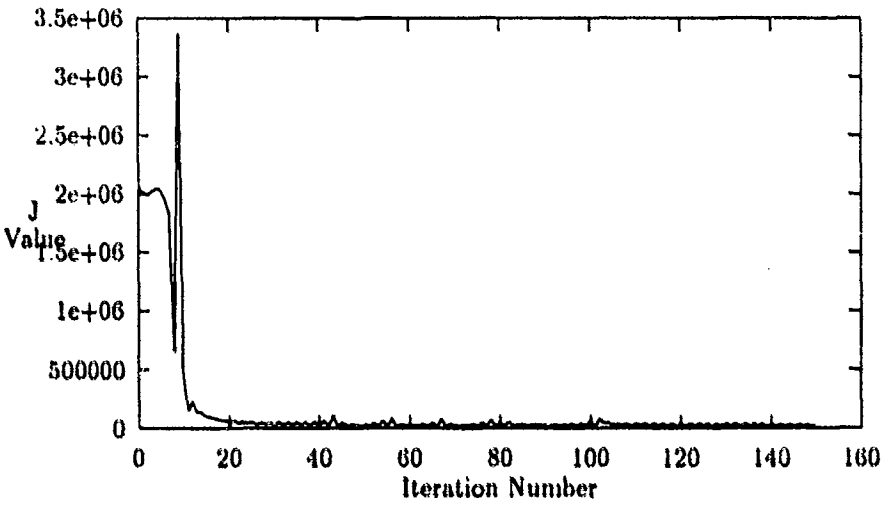

Figure 44. Plot of J Value versus Iteration Number

JSTOP = 25884.17258196169
# ITERATIONS = 150

T	BANK	SPEED	RANGE	THETA	RADAR	STRUCT
0.1	1.9	400.1	8.0	-0.3	1	1
0.2	2.1	400.1	8.0	-0.9	1	1
0.3	2.3	400.1	8.0	-1.6	1	1
0.4	2.5	400.1	8.0	-2.5	1	1
0.5	2.8	400.1	8.0	-3.4	1	1
0.6	3.0	400.1	8.0	-4.5	1	1
0.7	3.1	400.1	8.0	-5.7	1	1
0.8	3.3	400.1	8.0	-7.1	1	1
0.9	3.5	400.1	8.0	-8.6	1	1
1.0	3.7	400.1	8.0	-10.2	1	1
1.1	3.8	400.1	8.0	-11.9	1	1
1.2	3.9	400.1	8.0	-13.8	1	1
1.3	4.1	400.1	8.1	-15.8	1	1
1.4	4.2	400.1	8.1	-17.9	1	1
1.5	4.3	400.1	8.1	-20.1	1	1
1.6	4.4	400.1	8.2	-22.4	1	1
1.7	4.5	400.1	8.2	-24.9	1	1
1.8	4.6	400.1	8.3	-27.4	1	1
1.9	4.6	400.1	8.3	-30.1	1	1
2.0	4.7	400.0	8.4	-32.8	1	1
2.1	4.7	400.0	8.5	-35.6	1	1
2.2	4.7	400.0	8.6	-38.5	1	1
2.3	4.8	400.0	8.8	-41.4	1	1
2.4	4.8	400.0	8.9	-44.3	1	1
2.5	4.8	400.0	9.1	-47.3	1	1
2.6	4.8	400.0	9.2	-50.2	1	1
2.7	4.7	399.9	9.4	-53.2	1	1
2.8	4.7	399.9	9.7	-56.1	1	1
2.9	4.7	399.9	9.9	-59.0	1	1
3.0	4.6	399.9	10.2	-61.9	0	1
3.1	4.5	399.8	10.4	-64.7	0	1
3.2	4.4	399.8	10.7	-67.4	0	1
3.3	4.3	399.8	11.1	-70.1	0	1
3.4	4.2	399.8	11.4	-72.3	0	1
3.5	4.1	399.7	11.5	-74.2	0	1
3.6	3.9	399.7	11.8	-75.7	0	1
3.7	3.8	399.7	11.9	-77.1	0	1
3.8	3.6	399.6	12.0	-78.2	0	1
3.9	3.4	399.6	12.0	-79.2	0	1
4.0	3.2	399.6	12.0	-80.1	0	1

4.1	3.0	399.5	11.9	-81.0	0	1
4.2	2.7	399.5	11.9	-81.8	0	1
4.3	2.5	399.4	11.9	-82.6	0	1
4.4	2.2	399.4	11.9	-83.2	0	1
4.5	2.0	399.3	11.9	-83.8	0	1
4.6	1.7	399.3	11.9	-84.3	0	1
4.7	1.4	399.2	11.9	-84.8	0	1
4.8	1.0	399.2	12.0	-85.1	0	1
4.9	0.7	399.1	12.0	-85.4	0	1
5.0	0.4	399.1	12.0	-85.5	0	1
5.1	0.0	399.0	12.1	-85.6	0	1
5.2	-0.3	399.0	12.1	-85.6	0	1
5.3	-0.7	398.9	12.1	-85.4	0	1
5.4	-1.1	398.8	12.1	-85.2	0	1
5.5	-1.5	398.8	12.2	-84.8	0	1
5.6	-1.9	398.7	12.2	-84.3	0	1
5.7	-2.3	398.6	12.2	-83.8	0	1
5.8	-2.7	398.5	12.2	-83.0	0	1
5.9	-3.1	398.5	12.2	-82.2	0	1
6.0	-3.5	398.4	12.2	-81.2	0	1
6.1	-4.0	398.3	12.2	-80.1	0	1
6.2	-4.4	398.2	12.1	-78.9	0	1
6.3	-4.9	398.2	12.1	-77.5	0	1
6.4	-5.3	398.1	12.0	-75.9	0	1
6.5	-5.8	398.0	11.9	-74.2	0	1
6.6	-6.2	397.9	11.8	-72.4	0	1
6.7	-6.7	397.8	11.7	-70.4	0	1
6.8	-7.1	397.8	11.6	-68.2	0	1
6.9	-7.6	397.7	11.6	-66.0	0	1
7.0	-8.1	397.6	11.6	-63.8	0	1
7.1	-8.5	397.5	11.6	-61.5	0	1
7.2	-9.0	397.5	11.7	-59.2	1	1
7.3	-9.4	397.4	11.8	-56.9	1	1
7.4	-9.8	397.4	11.9	-54.6	1	1
7.5	-10.3	397.3	12.1	-52.4	1	1
7.6	-10.7	397.3	12.2	-50.2	1	1
7.7	-11.1	397.2	12.4	-48.0	1	1
7.8	-11.4	397.2	12.6	-45.9	1	1
7.9	-11.8	397.1	12.8	-43.8	1	1
8.0	-12.2	397.1	12.9	-41.7	1	1
8.1	-12.5	397.1	13.1	-39.7	1	1
8.2	-12.8	397.1	13.2	-37.6	1	1
8.3	-13.0	397.1	13.4	-35.7	1	1
8.4	-13.3	397.1	13.5	-33.7	1	1
8.5	-13.5	397.1	13.6	-31.8	1	1

8.6	-13.7	397.1	13.7	-29.9	1	1
8.7	-13.8	397.1	13.7	-28.1	1	1
8.8	-13.9	397.2	13.8	-26.3	1	1
8.9	-14.0	397.2	13.8	-24.6	1	1
9.0	-14.0	397.3	13.7	-23.0	1	1
9.1	-14.0	397.3	13.7	-21.4	1	1
9.2	-13.9	397.4	13.6	-19.9	1	1
9.3	-13.8	397.4	13.5	-18.5	1	1
9.4	-13.7	397.5	13.5	-15.7	1	1
9.5	-13.5	397.6	13.2	-16.2	1	1
9.6	-13.3	397.7	13.0	-15.3	1	1
9.7	-13.0	397.8	12.8	-14.5	1	1
9.8	-12.7	397.9	12.5	-14.0	1	1
9.9	-12.3	398.0	12.2	-13.7	1	1
10.0	-11.9	398.1	11.9	-13.6	1	1
10.1	-11.5	398.1	11.7	-13.5	1	1
10.2	-11.0	398.2	11.5	-13.5	1	1
10.3	-10.5	398.3	11.3	-13.6	1	1
10.4	-9.9	398.4	11.1	-13.8	1	1
10.5	-9.4	398.5	11.0	-14.1	1	1
10.6	-8.8	398.6	10.9	-14.4	1	1
10.7	-8.2	398.7	10.8	-14.8	1	1
10.8	-7.6	398.8	10.7	-15.3	1	1
10.9	-6.9	398.9	10.7	-15.9	1	1
11.0	-6.3	399.0	10.6	-16.6	1	1
11.1	-5.6	399.1	10.6	-17.4	1	1
11.2	-4.9	399.1	10.6	-18.3	1	1
11.3	-4.2	399.2	10.6	-19.3	1	1
11.4	-3.6	399.3	10.6	-20.4	1	1
11.5	-2.9	399.3	10.6	-21.7	1	1
11.6	-2.2	399.4	10.7	-23.1	1	1
11.7	-1.5	399.5	10.7	-24.6	1	1
11.8	-0.9	399.5	10.8	-26.3	1	1
11.9	-0.2	399.5	10.8	-28.1	1	1
12.0	0.5	399.6	10.9	-30.1	1	1
12.1	1.1	399.6	11.0	-32.2	1	1
12.2	1.7	399.6	11.1	-34.5	1	1
12.3	2.3	399.7	11.3	-37.0	1	1
12.4	2.9	399.7	11.4	-39.6	1	1
12.5	3.5	399.7	11.6	-42.4	1	1
12.6	4.0	399.7	11.7	-45.3	1	1
12.7	4.5	399.7	11.9	-48.4	1	1
12.8	5.0	399.7	12.2	-51.5	1	1
12.9	5.4	399.7	12.4	-54.8	1	1
13.0	5.8	399.7	12.7	-58.2	1	1

13.1	6.2	399.7	13.0	-61.6	0	1
13.2	6.5	399.7	13.3	-65.2	0	1
13.3	6.8	399.7	13.7	-68.7	0	1
13.4	7.1	399.7	14.1	-72.3	0	1
13.5	7.3	399.7	14.5	-75.9	0	1
13.6	7.4	399.7	15.0	-79.2	0	1
13.7	7.5	399.7	15.4	-82.2	0	1
13.8	7.6	399.6	15.7	-85.0	0	1
13.9	7.6	399.6	16.1	-87.6	0	1
14.0	7.5	399.6	16.4	-90.0	0	1
14.1	7.4	399.6	16.6	-92.3	0	1
14.2	7.3	399.6	16.8	-94.5	0	1
14.3	7.1	399.6	16.9	-96.5	0	1
14.4	6.8	399.6	17.0	-98.5	0	1
14.5	6.5	399.5	17.0	-100.4	0	1
14.6	6.2	399.5	16.9	-102.3	0	1
14.7	5.8	399.5	16.8	-104.1	0	1
14.8	5.3	399.5	16.6	-106.0	0	1
14.9	4.8	399.5	16.4	-107.8	0	1
15.0	4.3	399.5	16.1	-109.8	0	1
15.1	3.8	399.5	15.8	-111.7	0	1
15.2	3.2	399.5	15.5	-113.9	0	1
15.3	2.5	399.5	15.2	-116.1	0	1
15.4	1.9	399.5	14.8	-118.6	0	1
15.5	1.2	399.5	14.5	-121.3	0	1
15.6	0.5	399.5	14.2	-124.0	0	1
15.7	-0.2	399.5	13.9	-126.6	0	1
15.8	-0.9	399.5	13.6	-129.1	0	1
15.9	-1.6	399.5	13.4	-131.5	0	1
16.0	-2.3	399.5	13.2	-133.8	0	1
16.1	-3.0	399.5	13.1	-136.0	0	1
16.2	-3.8	399.5	12.9	-138.0	0	1
16.3	-4.5	399.5	12.8	-140.0	0	1
16.4	-5.2	399.5	12.7	-141.8	0	1
16.5	-5.9	399.5	12.7	-143.5	0	1
16.6	-6.6	399.5	12.7	-145.2	0	1
16.7	-7.3	399.6	12.7	-146.7	0	1
16.8	-8.0	399.6	12.7	-147.7	0	1
16.9	-8.7	399.6	12.7	-148.4	0	1
17.0	-9.3	399.6	12.6	-148.6	0	1
17.1	-9.9	399.6	12.6	-148.5	0	1
17.2	-10.5	399.6	12.5	-148.0	0	1
17.3	-11.0	399.6	12.4	-147.1	0	1
17.4	-11.6	399.6	12.3	-145.8	0	1
17.5	-12.1	399.6	12.2	-144.2	0	1

17.6	-12.5	399.6	12.0	-142.3	0	1
17.7	-12.9	399.7	11.9	-140.0	0	1
17.8	-13.3	399.7	11.8	-137.4	0	1
17.9	-13.7	399.7	11.6	-134.4	0	1
18.0	-14.0	399.7	11.5	-131.2	0	1
18.1	-14.2	399.7	11.4	-127.8	0	1
18.2	-14.4	399.7	11.3	-124.0	0	1
18.3	-14.6	399.7	11.2	-120.1	0	1
18.4	-14.7	399.7	11.1	-116.0	0	1
18.5	-14.8	399.7	11.1	-111.8	0	1
18.6	-14.8	399.8	11.1	-107.4	0	1
18.7	-14.8	399.8	11.1	-103.1	0	1
18.8	-14.8	399.8	11.2	-98.7	0	1
18.9	-14.7	399.8	11.3	-94.4	0	1
19.0	-14.5	399.8	11.4	-90.1	0	1
19.1	-14.4	399.8	11.6	-86.0	0	1
19.2	-14.1	399.8	11.8	-82.1	0	1
19.3	-13.9	399.8	12.0	-78.5	0	1
19.4	-13.6	399.8	12.2	-74.9	0	1
19.5	-13.3	399.8	12.4	-71.3	0	1
19.6	-13.0	399.8	12.5	-67.7	0	1
19.7	-12.6	399.8	12.6	-64.2	0	1
19.8	-12.3	399.9	12.6	-60.7	0	1
19.9	-11.9	399.9	12.6	-57.2	1	1
20.0	-11.4	399.9	12.6	-53.7	1	1
20.1	-11.0	399.9	12.5	-50.2	1	1
20.2	-10.6	399.9	12.4	-46.8	1	1
20.3	-10.1	399.9	12.3	-43.4	1	1
20.4	-9.6	399.9	12.2	-40.0	1	1
20.5	-9.2	399.9	12.0	-36.6	1	1
20.6	-8.7	399.9	11.8	-33.2	1	1
20.7	-8.2	399.9	11.6	-29.8	1	1
20.8	-7.7	399.8	11.5	-26.6	1	1
20.9	-7.2	399.8	11.4	-23.8	1	1
21.0	-6.6	399.8	11.4	-21.4	1	1
21.1	-6.1	399.8	11.4	-19.4	1	1
21.2	-5.6	399.8	11.4	-17.8	1	1
21.3	-5.1	399.8	11.4	-16.7	1	1
21.4	-4.5	399.8	11.4	-16.1	1	1
21.5	-4.0	399.8	11.4	-16.0	1	1
21.6	-3.5	399.8	11.5	-16.1	1	1
21.7	-3.0	399.8	11.5	-16.3	1	1
21.8	-2.4	399.8	11.5	-16.6	1	1
21.9	-1.9	399.8	11.6	-17.0	1	1
22.0	-1.4	399.8	11.6	-17.5	1	1

22.1	-0.9	399.8	11.6	-18.1	1	1
22.2	-0.4	399.7	11.7	-18.9	1	1
22.3	0.1	399.7	11.7	-19.8	1	1
22.4	0.6	399.7	11.7	-20.8	1	1
22.5	1.1	399.7	11.8	-21.6	1	1
22.6	1.5	399.7	11.8	-22.1	1	1
22.7	2.0	399.7	11.8	-22.4	1	1
22.8	2.4	399.7	11.7	-22.5	1	1
22.9	2.8	399.7	11.6	-22.4	1	1
23.0	3.2	399.6	11.4	-22.2	1	1
23.1	3.5	399.6	11.2	-21.7	1	1
23.2	3.9	399.6	11.0	-21.1	1	1
23.3	4.2	399.6	10.7	-20.4	1	1
23.4	4.5	399.6	10.3	-19.5	1	1
23.5	4.8	399.6	9.8	-18.4	1	1
23.6	5.0	399.6	9.4	-17.2	1	1
23.7	5.3	399.6	8.8	-15.7	1	1
23.8	5.5	399.6	8.2	-13.9	1	1
23.9	5.7	399.6	7.6	-11.7	1	1
24.0	5.9	399.6	6.9	-9.0	1	1
24.1	6.0	399.6	6.2	-5.6	1	1
24.2	6.2	399.6	5.4	-1.2	1	1
24.3	6.3	399.6	4.7	4.8	0	1
24.4	6.4	399.5	3.9	13.2	0	1
24.5	6.5	399.5	3.3	25.4	0	1
24.6	6.6	399.5	2.9	42.0	0	1
24.7	6.7	399.5	2.9	60.8	0	1
24.8	6.8	399.5	3.2	77.3	0	1
24.9	6.9	399.5	3.8	89.3	0	1
25.0	7.0	399.5	4.5	97.3	0	1
25.1	7.1	399.5	5.3	102.5	0	1
25.2	7.2	399.5	6.1	105.8	0	1
25.3	7.3	399.5	7.0	107.9	0	1
25.4	7.3	399.5	7.8	109.1	0	1
25.5	7.4	399.6	8.6	109.7	0	1
25.6	7.4	399.6	9.5	109.9	0	1
25.7	7.4	399.6	10.4	110.5	0	1
25.8	7.4	399.6	11.2	110.3	0	1
25.9	7.3	399.6	12.0	109.6	0	1
26.0	7.2	399.6	12.7	108.4	0	1
26.1	7.0	399.6	13.4	107.0	0	1
26.2	6.8	399.6	13.9	105.4	0	1
26.3	6.6	399.6	14.4	103.6	0	1
26.4	6.4	399.7	14.8	101.8	0	1
26.5	6.1	399.7	15.1	100.1	0	1

26.6	5.7	399.7	15.2	98.3	0	1
26.7	5.4	399.7	15.3	96.7	0	1
26.8	5.1	399.7	15.2	95.2	0	1
26.9	4.7	399.7	15.1	93.9	0	1
27.0	4.4	399.8	14.9	92.8	0	1
27.1	4.1	399.8	14.7	91.8	0	1
27.2	3.8	399.8	14.4	90.9	0	1
27.3	3.5	399.8	14.1	90.1	0	1
27.4	3.1	399.8	13.9	89.4	0	1
27.5	2.8	399.8	13.6	88.8	0	1
27.6	2.5	399.9	13.3	88.2	0	1
27.7	2.2	399.9	13.0	87.8	0	1
27.8	2.0	399.9	12.7	87.5	0	1
27.9	1.7	399.9	12.4	87.2	0	1
28.0	1.4	399.9	12.0	87.1	0	1
28.1	1.2	399.9	11.7	87.1	0	1
28.2	0.9	399.9	11.4	87.1	0	1
28.3	0.7	400.0	11.1	87.2	0	1
28.4	0.4	400.0	10.7	87.4	0	1
28.5	0.2	400.0	10.4	87.7	0	1
28.6	0.1	400.0	10.1	88.1	0	1

CM IN RADAR CONE 46.15384615384615 PERCENT
CMMCA W/IN STRUCTURAL LIMITS 100.0000000000000 PERCENT

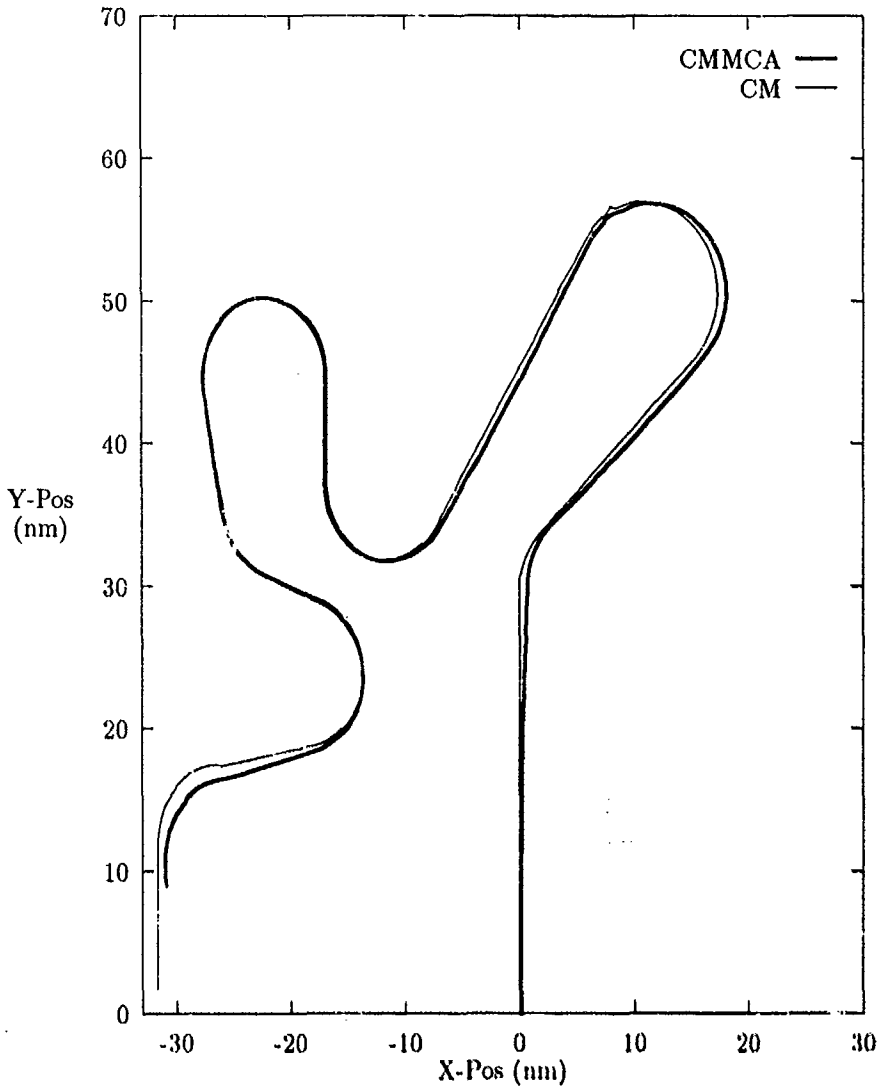

Figure 45. CMMCA and Cruise Missile Paths, CMMCA Starting Trailing

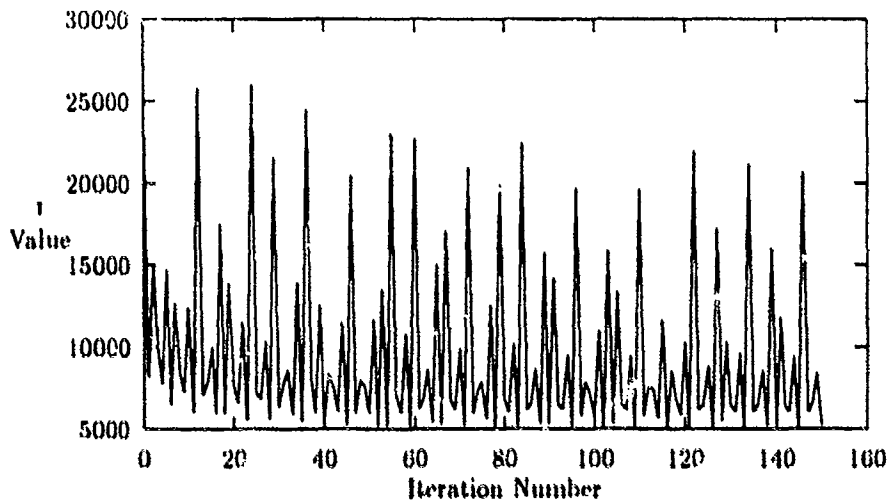

Figure 46. Plot of J Value versus Iteration Number

JSTOP = 5244.641440491642
# ITERATIONS = 150

T	BANK	SPEED	RANGE	THETA	RADAR	STRUCT
0.1	0.0	400.2	8.0	0.0	1	1
0.2	0.0	400.2	8.0	0.0	1	1
0.3	0.1	400.2	8.0	0.0	1	1
0.4	0.1	400.2	8.0	0.0	1	1
0.5	0.1	400.2	8.0	-0.1	1	1
0.6	0.1	400.2	8.0	-0.1	1	1
0.7	0.1	400.2	8.0	-0.1	1	1
0.8	0.1	400.2	8.0	-0.2	1	1
0.9	0.1	400.2	8.0	-0.2	1	1
1.0	0.1	400.2	8.0	-0.3	1	1
1.1	0.1	400.2	8.0	-0.3	1	1
1.2	0.2	400.2	8.0	-0.4	1	1
1.3	0.2	400.2	8.0	-0.5	1	1
1.4	0.2	400.2	8.0	-0.5	1	1
1.5	0.2	400.2	8.0	-0.6	1	1
1.6	0.2	400.2	8.0	-0.7	1	1
1.7	0.2	400.2	8.0	-0.8	1	1
1.8	0.2	400.2	8.0	-0.9	1	1
1.9	0.2	400.2	8.0	-1.0	1	1
2.0	0.2	400.2	8.0	-1.2	1	1
2.1	0.3	400.2	8.0	-1.3	1	1
2.2	0.3	400.2	8.0	-1.4	1	1
2.3	0.3	400.2	8.0	-1.6	1	1
2.4	0.3	400.2	8.0	-1.8	1	1
2.5	0.3	400.2	8.0	-1.9	1	1
2.6	0.3	400.2	8.0	-2.1	1	1
2.7	0.3	400.2	8.0	-2.3	1	1
2.8	0.3	400.2	8.0	-2.5	1	1
2.9	0.3	400.2	8.0	-2.7	1	1
3.0	0.3	400.2	8.0	-2.9	1	1
3.1	0.4	400.2	8.0	-3.2	1	1
3.2	0.4	400.2	8.0	-3.4	1	1
3.3	0.4	400.2	8.0	-3.7	1	1
3.4	0.4	400.2	8.0	-3.4	1	1
3.5	0.4	400.2	8.0	-2.4	1	1
3.6	0.4	400.2	7.9	-1.0	1	1
3.7	0.4	400.2	7.9	1.1	1	1
3.8	0.4	400.2	7.8	3.7	1	1
3.9	0.4	400.2	7.6	6.9	1	1
4.0	0.4	400.2	7.5	10.6	1	1

4.1	0.4	400.2	7.4	14.3	1	1
4.2	0.3	400.2	7.4	18.2	1	1
4.3	0.3	400.2	7.3	22.1	1	1
4.4	0.3	400.2	7.4	25.9	1	1
4.5	0.2	400.2	7.4	29.7	1	1
4.6	23.7	398.1	7.5	29.8	1	1
4.7	23.2	398.1	7.6	25.9	1	1
4.8	23.8	398.0	7.6	21.3	1	1
4.9	23.3	398.0	7.6	16.1	1	1
5.0	23.3	397.9	7.7	10.4	1	1
5.1	23.3	397.8	7.7	4.1	1	1
5.2	15.0	398.6	7.7	-1.5	1	1
5.3	0.1	400.0	7.7	-3.8	1	1
5.4	-0.4	400.0	7.7	-4.0	1	1
5.5	2.0	399.8	7.7	-4.5	1	1
5.6	-4.4	400.4	7.7	-4.4	1	1
5.7	1.6	399.8	7.7	-4.2	1	1
5.8	-0.2	400.0	7.7	-4.6	1	1
5.9	-0.4	400.0	7.7	-4.7	1	1
6.0	-0.7	400.1	7.7	-4.7	1	1
6.1	-0.5	400.0	7.7	-4.8	1	1
6.2	-0.5	400.0	7.7	-4.8	1	1
6.3	-0.4	400.0	7.7	-4.8	1	1
6.4	-0.9	400.1	7.7	-4.7	1	1
6.5	-0.7	400.1	7.7	-4.6	1	1
6.6	-0.5	400.0	7.7	-4.6	1	1
6.7	-1.0	400.1	7.7	-4.4	1	1
6.8	-0.8	400.1	7.7	-4.8	1	1
6.9	-0.7	400.0	7.7	-5.6	1	1
7.0	-1.1	400.1	7.7	-6.9	1	1
7.1	-0.8	400.1	7.7	-8.7	1	1
7.2	-1.0	400.1	7.6	-11.0	1	1
7.3	-1.3	400.1	7.6	-13.7	1	1
7.4	-1.1	400.1	7.6	-16.9	1	1
7.5	-0.9	400.1	7.5	-20.7	1	1
7.6	-1.3	400.1	7.5	-24.9	1	1
7.7	-1.1	400.1	7.5	-29.5	1	1
7.8	-1.2	400.1	7.5	-34.6	1	1
7.9	-0.9	400.1	7.5	-40.1	1	1
8.0	-21.4	403.1	7.6	-42.8	1	1
8.1	-20.9	403.1	7.6	-42.7	1	1
8.2	-21.0	403.2	7.7	-42.5	1	1
8.3	-21.3	403.3	7.8	-42.2	1	1
8.4	-21.2	403.4	7.8	-41.8	1	1
8.5	-20.7	403.4	7.9	-41.4	1	1

8.6	-21.3	403.6	8.0	-41.0	1	1
8.7	-21.1	403.6	8.0	-40.4	1	1
8.8	-20.8	403.6	8.1	-39.9	1	1
8.9	-20.9	403.7	8.1	-39.3	1	1
9.0	-20.9	403.7	8.1	-38.7	1	1
9.1	-21.2	403.8	8.1	-38.1	1	1
9.2	-20.5	403.7	8.2	-37.5	1	1
9.3	-21.0	403.8	8.2	-36.8	1	1
9.4	-20.5	403.8	8.2	-33.5	1	1
9.5	-20.7	403.8	8.2	-35.6	1	1
9.6	-20.8	403.8	8.2	-35.0	1	1
9.7	-20.5	403.7	8.1	-34.4	1	1
9.8	-20.4	403.7	8.1	-33.8	1	1
9.9	-20.4	403.7	8.1	-33.5	1	1
10.0	-20.5	403.6	8.1	-32.8	1	1
10.1	-20.3	403.5	8.1	-31.7	1	1
10.2	-20.3	403.5	8.1	-30.1	1	1
10.3	-20.0	403.4	8.1	-28.1	1	1
10.4	-20.2	403.3	8.2	-25.7	1	1
10.5	-19.9	403.2	8.2	-22.9	1	1
10.6	59.4	385.4	8.3	-37.4	1	0
10.7	-75.2	428.3	8.4	-25.8	1	0
10.8	42.9	392.5	8.4	-6.3	1	0
10.9	-19.4	402.8	8.4	-12.2	1	1
11.0	-20.2	402.8	8.4	-7.4	1	1
11.1	-26.8	403.8	8.4	-0.8	1	1
11.2	0.1	399.9	8.4	3.3	1	1
11.3	0.2	399.9	8.4	3.3	1	1
11.4	-0.1	400.0	8.4	3.4	1	1
11.5	0.1	399.9	8.4	3.5	1	1
11.6	0.1	399.9	8.4	3.6	1	1
11.7	0.2	399.9	8.4	3.7	1	1
11.8	0.4	399.9	8.4	3.7	1	1
11.9	0.1	399.9	8.4	3.7	1	1
12.0	0.1	400.0	8.4	3.7	1	1
12.1	0.2	399.9	8.4	3.8	1	1
12.2	0.3	399.9	8.4	3.8	1	1
12.3	0.3	399.9	8.4	3.8	1	1
12.4	0.3	399.9	8.4	3.8	1	1
12.5	0.5	399.9	8.4	3.7	1	1
12.6	0.2	399.9	8.4	3.7	1	1
12.7	0.4	399.9	8.4	3.6	1	1
12.8	0.4	399.9	8.4	3.6	1	1
12.9	0.4	399.9	8.4	3.5	1	1
13.0	0.5	399.9	8.4	3.4	1	1

13.1	0.6	399.9	8.4	3.2	1	1
13.2	0.3	399.9	8.4	3.1	1	1
13.3	0.8	399.9	8.4	2.9	1	1
13.4	0.3	399.9	8.4	2.7	1	1
13.5	0.6	399.9	8.4	2.5	1	1
13.6	0.6	399.9	8.4	2.9	1	1
13.7	0.8	399.9	8.4	3.8	1	1
13.8	0.5	399.9	8.4	5.2	1	1
13.9	0.7	399.9	8.3	7.2	1	1
14.0	0.7	399.9	8.3	9.7	1	1
14.1	0.7	399.9	8.2	12.7	1	1
14.2	0.9	399.9	8.1	16.3	1	1
14.3	0.5	399.9	8.0	20.5	1	1
14.4	0.7	399.9	7.9	25.2	1	1
14.5	0.7	399.9	7.8	30.6	1	1
14.6	0.7	399.9	7.7	36.4	1	1
14.7	0.7	399.9	7.7	42.8	1	1
14.8	24.1	398.4	7.7	46.0	1	1
14.9	24.2	398.5	7.7	45.6	1	1
15.0	24.1	398.6	7.7	45.3	1	1
15.1	23.9	398.7	7.7	45.0	1	1
15.2	23.8	398.7	7.7	44.7	1	1
15.3	23.8	398.8	7.7	44.4	1	1
15.4	23.9	398.8	7.7	44.1	1	1
15.5	23.5	398.9	7.7	44.1	1	1
15.6	23.7	399.0	7.7	43.7	1	1
15.7	23.4	399.0	7.8	42.7	1	1
15.8	23.4	399.0	7.9	41.3	1	1
15.9	23.1	399.1	8.0	39.3	1	1
16.0	23.5	399.1	8.1	36.7	1	1
16.1	22.7	399.1	8.2	33.6	1	1
16.2	23.9	399.1	8.3	30.1	1	1
16.3	23.1	399.0	8.3	25.9	1	1
16.4	22.8	399.0	8.4	21.2	1	1
16.5	22.5	399.0	8.4	16.1	1	1
16.6	23.1	398.9	8.4	10.4	1	1
16.7	29.9	398.4	8.4	2.8	1	1
16.8	-0.6	400.1	8.4	-2.3	1	1
16.9	-0.6	400.1	8.4	-3.4	1	1
17.0	-0.6	400.1	8.4	-4.9	1	1
17.1	-0.6	400.1	8.3	-7.0	1	1
17.2	-0.7	400.1	8.3	-9.7	1	1
17.3	-0.7	400.1	8.2	-12.8	1	1
17.4	-0.7	400.1	8.1	-16.6	1	1
17.5	-0.7	400.1	8.0	-20.9	1	1

17.6	-0.7	400.1	7.9	-25.7	1	1
17.7	-0.7	400.1	7.8	-31.2	1	1
17.8	-0.7	400.1	7.7	-37.2	1	1
17.9	-0.6	400.1	7.7	-43.8	1	1
18.0	-24.2	401.8	7.7	-47.2	1	1
18.1	-23.7	401.8	7.7	-47.1	1	1
18.2	-24.3	401.9	7.7	-47.0	1	1
18.3	-23.9	401.9	7.7	-46.9	1	1
18.4	-23.9	401.9	7.7	-46.8	1	1
18.5	-23.9	402.0	7.7	-46.7	1	1
18.6	-24.2	402.0	7.7	-46.6	1	1
18.7	-23.5	402.0	7.7	-46.5	1	1
18.8	-24.0	402.1	7.8	-46.4	1	1
18.9	-23.9	402.1	7.8	-46.3	1	1
19.0	-24.0	402.1	7.8	-46.2	1	1
19.1	-23.5	402.0	7.8	-46.1	1	1
19.2	-23.8	402.0	7.8	-46.1	1	1
19.3	-23.5	402.0	7.7	-46.2	1	1
19.4	-23.9	402.0	7.8	-45.9	1	1
19.5	-23.6	401.9	7.8	-45.0	1	1
19.6	-23.8	401.9	7.9	-43.6	1	1
19.7	-23.4	401.8	8.1	-41.7	1	1
19.8	-23.5	401.7	8.2	-39.2	1	1
19.9	-23.9	401.7	8.3	-36.0	1	1
20.0	-23.0	401.6	8.4	-32.3	1	1
20.1	-23.8	401.5	8.5	-28.2	1	1
20.2	-23.3	401.4	8.6	-23.4	1	1
20.3	-23.6	401.4	8.6	-18.1	1	1
20.4	-23.3	401.3	8.6	-12.3	1	1
20.5	-31.1	401.7	8.6	-4.5	1	0
20.6	0.1	399.9	8.6	0.2	1	1
20.7	-0.4	399.9	8.6	0.2	1	1
20.8	-0.2	399.9	8.6	-0.2	1	1
20.9	-0.1	399.9	8.6	-1.2	1	1
21.0	0.1	399.9	8.6	-2.9	1	1
21.1	-0.4	399.9	8.5	-5.0	1	1
21.2	-0.2	399.9	8.4	-7.6	1	1
21.3	-0.1	399.9	8.3	-10.8	1	1
21.4	0.1	399.9	8.2	-14.6	1	1
21.5	-0.4	399.9	8.1	-18.9	1	1
21.6	-0.1	399.9	8.0	-23.5	1	1
21.7	0.0	399.9	7.9	-28.3	1	1
21.8	0.3	399.9	8.0	-33.0	1	1
21.9	-0.3	399.9	8.0	-37.7	1	1
22.0	-23.2	400.7	8.1	-38.7	1	1

22.1	-23.2	400.6	8.2	-35.7	1	1
22.2	-23.4	400.6	8.3	-32.2	1	1
22.3	-23.2	400.6	8.4	-28.1	1	1
22.4	-22.7	400.5	8.5	-23.6	1	1
22.5	-23.4	400.5	8.5	-17.9	1	1
22.6	-23.0	400.5	8.5	-11.1	1	1
22.7	-22.9	400.5	8.5	-3.3	1	1
22.8	-7.9	400.0	8.4	3.1	1	1
22.9	0.2	399.8	8.4	6.8	1	1
23.0	0.4	399.8	8.3	9.9	1	1
23.1	0.2	399.8	8.1	13.6	1	1
23.2	0.4	399.8	8.0	17.9	1	1
23.3	0.2	399.8	7.9	22.8	1	1
23.4	0.4	399.8	7.7	28.2	1	1
23.5	0.2	399.8	7.6	34.3	1	1
23.6	0.4	399.8	7.6	41.0	1	1
23.7	23.6	399.1	7.5	44.5	1	1
23.8	23.4	399.1	7.5	44.6	1	1
23.9	23.6	399.1	7.5	44.8	1	1
24.0	23.6	399.1	7.5	45.0	1	1
24.1	23.4	399.1	7.5	45.2	1	1
24.2	23.2	399.1	7.4	45.5	1	1
24.3	23.4	399.1	7.4	45.8	1	1
24.4	23.2	399.2	7.4	46.2	1	1
24.5	23.2	399.2	7.5	46.5	1	1
24.6	22.9	399.3	7.5	46.3	1	1
24.7	23.1	399.3	7.6	45.6	1	1
24.8	22.8	399.3	7.8	44.3	1	1
24.9	22.8	399.4	7.9	42.4	1	1
25.0	22.6	399.4	8.0	39.9	1	1
25.1	23.0	399.5	8.2	36.9	1	1
25.2	22.4	399.5	8.3	33.3	1	1
25.3	22.6	399.6	8.4	29.3	1	1
25.4	22.7	399.6	8.5	24.7	1	1
25.5	22.4	399.6	8.5	19.6	1	1
25.6	22.8	399.7	8.5	13.9	1	1
25.7	18.8	399.8	8.6	9.4	1	1
25.8	-0.4	400.1	8.6	7.5	1	1
25.9	-0.9	400.1	8.6	7.8	1	1
26.0	-0.7	400.1	8.6	7.6	1	1
26.1	-0.6	400.1	8.5	6.9	1	1
26.2	-0.4	400.1	8.5	5.6	1	1
26.3	-0.9	400.1	8.4	3.8	1	1
26.4	-0.7	400.1	8.2	1.5	1	1
26.5	-0.6	400.1	8.1	-1.3	1	1

26.6	-0.4	400.1	7.9	-4.8	1	1
26.7	-0.8	400.1	7.7	-8.8	1	1
26.8	-0.5	400.1	7.4	-13.5	1	1
26.9	36.7	399.8	7.2	-25.4	1	0
27.0	-24.2	400.2	7.1	-34.7	1	1
27.1	-23.5	400.2	7.0	-34.4	1	1
27.2	-23.7	400.2	7.0	-33.7	1	1
27.3	-23.5	400.2	7.0	-32.5	1	1
27.4	-23.5	400.2	7.0	-30.7	1	1
27.5	-23.6	400.1	7.0	-28.3	1	1
27.6	-23.2	400.1	7.1	-25.2	1	1
27.7	-23.6	400.1	7.1	-21.6	1	1
27.8	-23.3	400.1	7.1	-17.2	1	1
27.9	-23.2	400.1	7.1	-12.3	1	1
28.0	-23.3	400.1	7.2	-6.8	1	1
28.1	-23.4	400.0	7.2	-0.5	1	1
28.2	-20.8	400.0	7.2	6.0	1	1
28.3	0.0	400.0	7.2	9.4	1	1
28.4	0.0	400.0	7.2	9.8	1	1
28.5	0.0	400.0	7.2	10.2	1	1
28.6	0.0	400.0	7.2	10.6	1	1

CM IN RADAR CONE 100.0000000000000 PERCENT
CMMCA W/IN STRUCTURAL LIMITS 98.25174825174825 PERCENT

Appendix H. *Results of Segmenting Flight Path Four*

This appendix contains the graphical output from the results of the segmentation of the fourth flight path. The output from the first section of the fourth flight path is presented first. This covers the cases where the initial CMMCA flight path was straight and the preliminary weighting scheme was used, the initial CMMCA flight path was straight and the optimal weighting scheme was used, the initial CMMCA flight path was trailing and the preliminary weighting scheme was used, and finally the initial CMMCA flight path was trailing and the optimal weighting scheme was used. The same four cases are then presented for the second section of the fourth flight path.

Each section of output contains a plot of the CMMCA flight path relative to the cruise missile flight path, the plot of the overall J value at each iteration of the program, and the output file RESULTS.OUT, which contains the CMMCA bank angle, airspeed, and position relative to the cruise missile at every point in the solution.

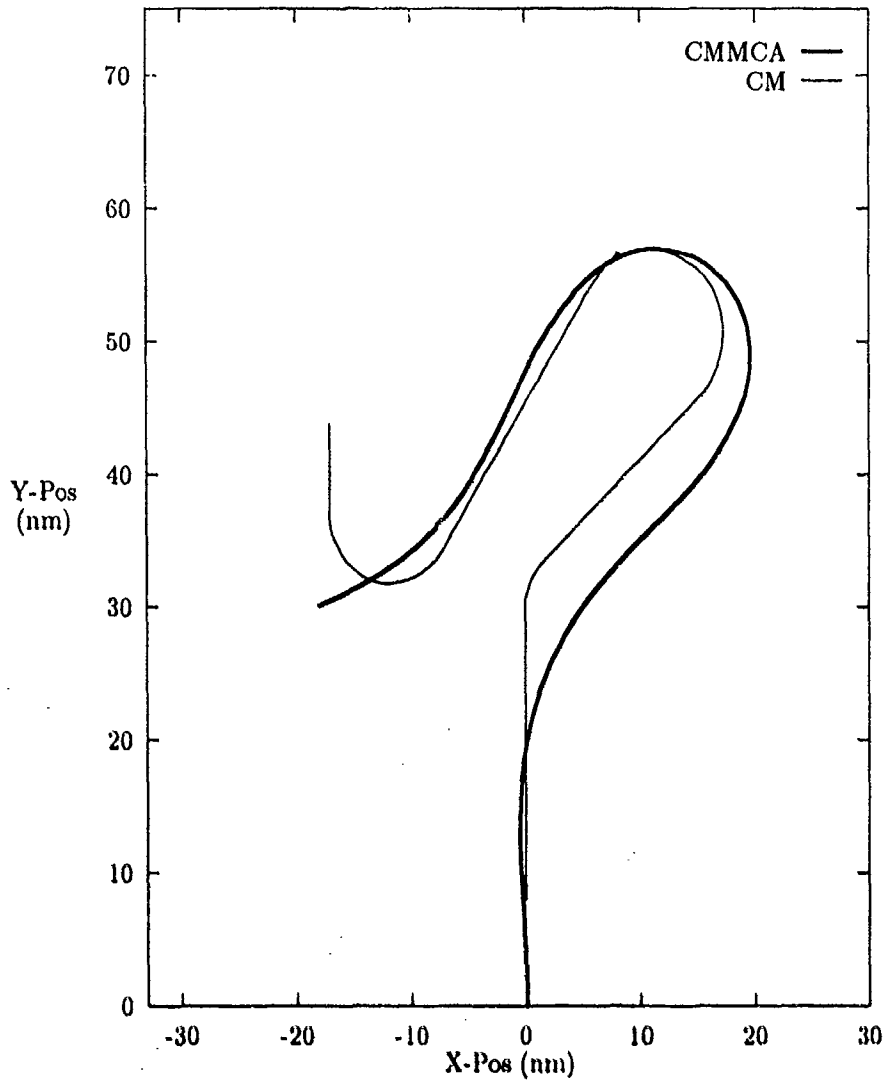

Figure 47. Section 1 CMMCA and CM Paths, CMMCA Starting Straight

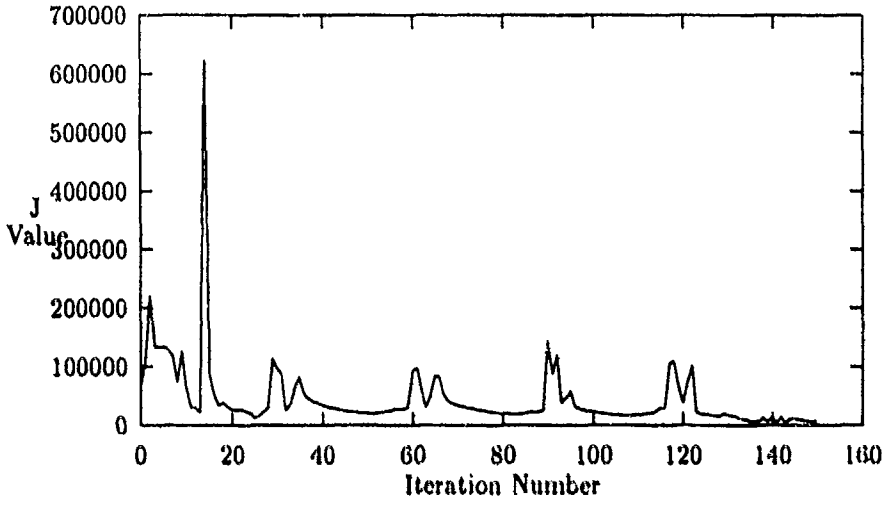

Figure 48. Plot of J Value versus Iteration Number

JSTOP = 5741.868
# ITERATIONS = 150

T	BANK	SPEED	RANGE	THETA	RADAR	STRUCT
0.1	-2.5	400.8	8.0	0.4	1	1
0.2	-2.3	400.8	8.0	1.1	1	1
0.3	-2.0	400.8	8.0	1.9	1	1
0.4	-1.8	400.8	8.0	2.6	1	1
0.5	-1.5	400.8	8.0	3.2	1	1
0.6	-1.2	400.8	8.0	3.9	1	1
0.7	-0.9	400.8	8.0	4.4	1	1
0.8	-0.7	400.8	8.0	5.0	1	1
0.9	-0.4	400.7	8.0	5.4	1	1
1.0	-0.1	400.7	8.0	5.8	1	1
1.1	0.2	400.7	8.0	6.1	1	1
1.2	0.5	400.7	8.0	6.3	1	1
1.3	0.8	400.7	8.0	6.4	1	1
1.4	1.1	400.7	8.0	6.5	1	1
1.5	1.4	400.7	8.0	6.4	1	1
1.6	1.7	400.6	8.0	6.2	1	1
1.7	2.0	400.6	8.0	5.8	1	1
1.8	2.3	400.6	8.0	5.3	1	1
1.9	2.5	400.6	8.0	4.7	1	1
2.0	2.8	400.5	8.0	4.0	1	1
2.1	3.1	400.5	8.0	3.1	1	1
2.2	3.4	400.5	8.0	2.1	1	1
2.3	3.6	400.5	8.0	0.9	1	1
2.4	3.9	400.5	8.0	-0.5	1	1
2.5	4.2	400.4	8.0	-2.0	1	1
2.6	4.4	400.4	8.0	-3.7	1	1
2.7	4.6	400.4	8.0	-5.6	1	1
2.8	4.8	400.4	8.0	-7.6	1	1
2.9	5.0	400.4	8.0	-9.9	1	1
3.0	5.2	400.3	8.0	-12.2	1	1
3.1	5.4	400.3	8.0	-14.8	1	1
3.2	5.5	400.3	8.1	-17.5	1	1
3.3	5.7	400.3	8.1	-20.4	1	1
3.4	5.8	400.3	8.1	-22.9	1	1
3.5	5.9	400.3	8.2	-24.9	1	1
3.6	5.9	400.3	8.2	-26.5	1	1
3.7	6.0	400.2	8.1	-27.8	1	1
3.8	6.0	400.2	8.0	-28.7	1	1
3.9	6.0	400.2	7.9	-29.3	1	1
4.0	5.9	400.2	7.8	-29.6	1	1

4.1	5.8	400.2	7.6	-30.1	1	1
4.2	5.7	400.2	7.5	-30.6	1	1
4.3	5.6	400.2	7.4	-31.2	1	1
4.4	5.4	400.3	7.3	-31.8	1	1
4.5	5.3	400.3	7.2	-32.5	1	1
4.6	5.0	400.3	7.1	-33.2	1	1
4.7	4.8	400.3	7.1	-33.9	1	1
4.8	4.6	400.3	7.0	-34.7	1	1
4.9	4.3	400.3	7.0	-35.5	1	1
5.0	4.0	400.3	6.9	-36.3	1	1
5.1	3.7	400.4	6.9	-37.1	1	1
5.2	3.3	400.4	6.9	-37.9	1	1
5.3	3.0	400.4	6.9	-38.6	1	1
5.4	2.6	400.4	6.9	-39.3	1	1
5.5	2.2	400.5	6.9	-40.0	1	1
5.6	1.7	400.5	6.9	-40.6	1	1
5.7	1.3	400.5	6.9	-41.0	1	1
5.8	0.8	400.6	6.9	-41.4	1	1
5.9	0.4	400.6	6.9	-41.7	1	1
6.0	-0.1	400.7	6.9	-41.8	1	1
6.1	-0.6	400.7	6.9	-41.8	1	1
6.2	-1.2	400.7	6.9	-41.7	1	1
6.3	-1.7	400.8	6.9	-41.3	1	1
6.4	-2.3	400.8	6.9	-40.8	1	1
6.5	-2.9	400.9	6.9	-40.1	1	1
6.6	-3.5	400.9	6.9	-39.1	1	1
6.7	-4.1	400.9	6.9	-37.9	1	1
6.8	-4.7	401.0	6.9	-36.8	1	1
6.9	-5.3	401.0	6.9	-36.0	1	1
7.0	-6.0	401.1	7.0	-35.4	1	1
7.1	-6.6	401.1	7.1	-35.0	1	1
7.2	-7.3	401.2	7.2	-34.7	1	1
7.3	-7.9	401.2	7.3	-34.6	1	1
7.4	-8.6	401.2	7.4	-34.6	1	1
7.5	-9.2	401.3	7.5	-34.7	1	1
7.6	-9.9	401.3	7.6	-34.8	1	1
7.7	-10.5	401.3	7.8	-35.0	1	1
7.8	-11.2	401.4	7.9	-35.1	1	1
7.9	-11.8	401.4	8.0	-35.3	1	1
8.0	-12.4	401.4	8.1	-35.5	1	1
8.1	-13.0	401.4	8.2	-35.6	1	1
8.2	-13.6	401.5	8.3	-35.7	1	1
8.3	-14.1	401.5	8.4	-35.7	1	1
8.4	-14.6	401.5	8.5	-35.7	1	1
8.5	-15.1	401.5	8.6	-35.6	1	1

8.6	-15.5	401.5	8.6	-35.5	1	1
8.7	-15.9	401.4	8.7	-35.3	1	1
8.8	-16.2	401.4	8.8	-35.0	1	1
8.9	-16.5	401.4	8.8	-34.7	1	1
9.0	-16.7	401.4	8.8	-34.4	1	1
9.1	-16.9	401.3	8.8	-34.1	1	1
9.2	-17.1	401.3	8.9	-33.8	1	1
9.3	-17.1	401.2	8.9	-33.6	1	1
9.4	-17.2	401.2	8.9	-30.8	1	1
9.5	-17.1	401.1	8.8	-33.2	1	1
9.6	-17.1	401.1	8.8	-33.1	1	1
9.7	-16.9	401.0	8.8	-33.1	1	1
9.8	-16.7	401.0	8.8	-33.3	1	1
9.9	-16.5	400.9	8.7	-33.7	1	1
10.0	-16.2	400.8	8.7	-34.0	1	1
10.1	-15.8	400.8	8.7	-34.1	1	1
10.2	-15.5	400.7	8.7	-34.0	1	1
10.3	-15.1	400.6	8.8	-33.6	1	1
10.4	-14.6	400.6	8.9	-33.1	1	1
10.5	-14.1	400.5	8.9	-32.3	1	1
10.6	-13.6	400.4	9.0	-31.4	1	1
10.7	-13.1	400.4	9.1	-30.3	1	1
10.8	-12.6	400.3	9.2	-29.1	1	1
10.9	-12.0	400.3	9.3	-27.8	1	1
11.0	-11.5	400.2	9.4	-26.4	1	1
11.1	-10.9	400.2	9.4	-24.9	1	1
11.2	-10.3	400.1	9.5	-23.4	1	1
11.3	-9.7	400.1	9.5	-21.8	1	1
11.4	-9.1	400.0	9.6	-20.2	1	1
11.5	-8.5	400.0	9.6	-18.6	1	1
11.6	-7.9	399.9	9.6	-17.0	1	1
11.7	-7.3	399.9	9.7	-15.5	1	1
11.8	-6.7	399.9	9.7	-14.0	1	1
11.9	-6.1	399.8	9.7	-12.5	1	1
12.0	-5.5	399.8	9.7	-11.1	1	1
12.1	-4.9	399.8	9.7	-9.7	1	1
12.2	-4.3	399.7	9.7	-8.4	1	1
12.3	-3.7	399.7	9.7	-7.2	1	1
12.4	-3.1	399.7	9.7	-6.1	1	1
12.5	-2.6	399.7	9.7	-5.1	1	1
12.6	-2.0	399.6	9.7	-4.2	1	1
12.7	-1.5	399.6	9.7	-3.5	1	1
12.8	-0.9	399.6	9.7	-2.8	1	1
12.9	-0.4	399.6	9.7	-2.3	1	1
13.0	0.1	399.6	9.7	-1.9	1	1

13.1	0.6	399.6	9.7	-1.7	1	1
13.2	1.1	399.6	9.7	-1.6	1	1
13.3	1.5	399.5	9.7	-1.7	1	1
13.4	2.0	399.5	9.7	-1.9	1	1
13.5	2.4	399.5	9.7	-2.3	1	1
13.6	2.8	399.5	9.6	-2.4	1	1
13.7	3.2	399.5	9.6	-2.1	1	1
13.8	3.5	399.5	9.6	-1.6	1	1
13.9	3.9	399.5	9.5	-0.7	1	1
14.0	4.2	399.5	9.3	0.4	1	1
14.1	4.6	399.5	9.2	1.9	1	1
14.2	4.8	399.5	9.0	3.6	1	1
14.3	5.1	399.5	8.8	5.7	1	1
14.4	5.4	399.5	8.5	8.2	1	1
14.5	5.6	399.5	8.3	11.1	1	1
14.6	5.8	399.5	8.0	14.4	1	1
14.7	6.0	399.5	7.7	18.2	1	1
14.8	6.1	399.5	7.4	22.6	1	1
14.9	6.3	399.6	7.1	27.6	1	1
15.0	6.3	399.6	6.9	33.4	1	1
15.1	6.3	399.6	6.7	39.8	1	1
15.2	6.3	399.6	6.5	46.9	1	1
15.3	6.1	399.7	6.5	54.6	1	1
15.4	5.9	399.7	6.5	62.6	0	1
15.5	5.6	399.7	6.7	71.0	0	1
15.6	5.3	399.7	7.0	78.8	0	1
15.7	4.9	399.8	7.4	85.8	0	1
15.8	4.4	399.8	8.0	91.8	0	1
15.9	3.9	399.8	8.7	96.8	0	1
16.0	3.4	399.8	9.4	101.1	0	1
16.1	2.8	399.8	10.2	104.7	0	1
16.2	2.3	399.9	11.1	107.8	0	1
16.3	1.7	399.9	11.9	110.5	0	1
16.4	1.1	399.9	12.9	113.0	0	1
16.5	0.6	400.0	13.8	115.2	0	1
16.6	0.1	400.0	14.8	117.2	0	1

CM IN RADAR CONE 92.16868 PERCENT
CMMCA W/IN STRUCTURAL LIMITS 100.0000 PERCENT

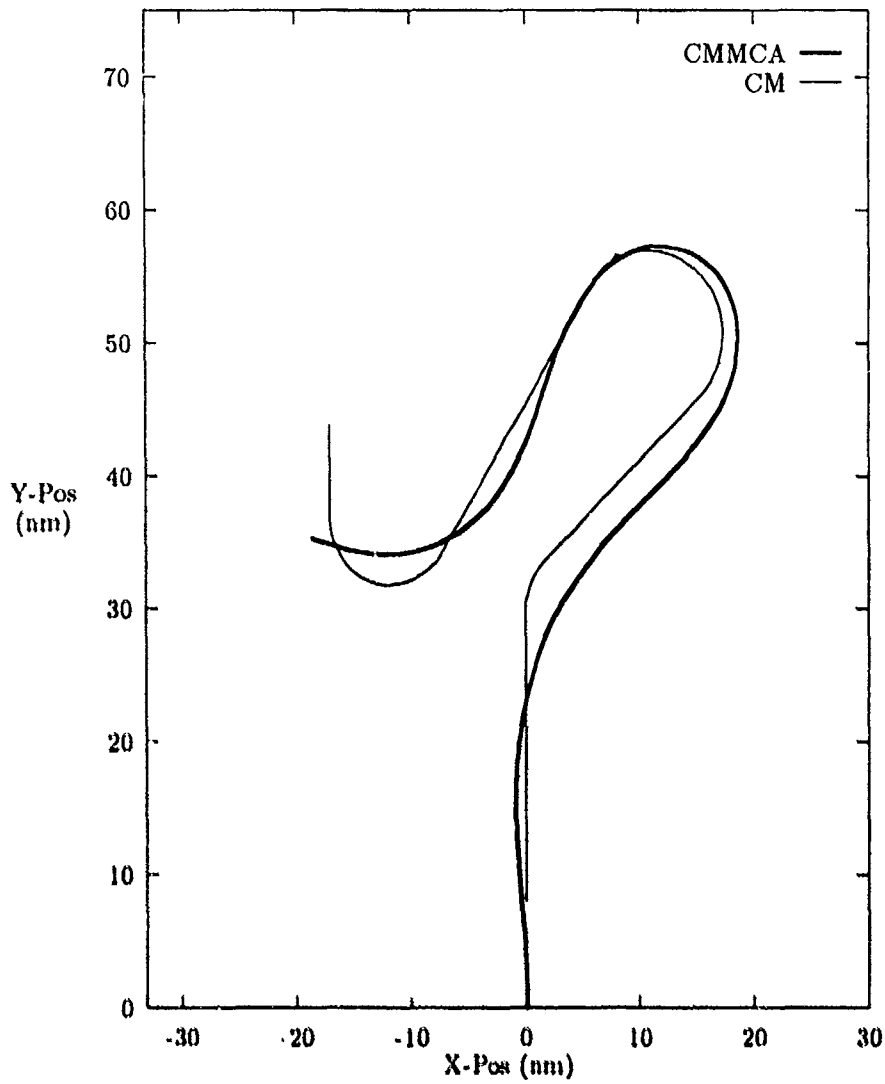

Figure 49. Section 1 CMMCA and CM Paths, CMMCA Starting Straight

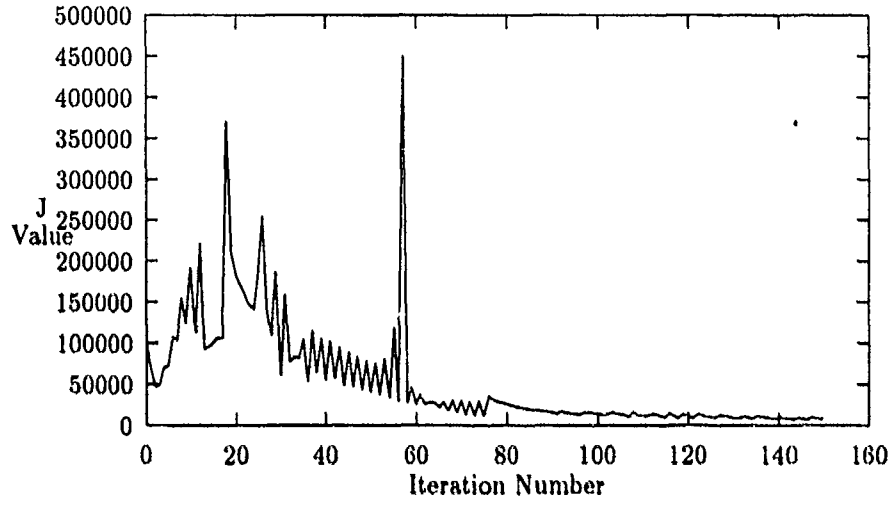

Figure 50. Plot of J Value versus Iteration Number

JSTOP = 6857.492
# ITERATIONS = 150

T	BANK	SPEED	RANGE	THETA	RADAR	STRUCT
0.1	-3.0	401.0	8.0	0.4	1	1
0.2	-2.8	401.0	8.0	1.3	1	1
0.3	-2.5	401.0	8.0	2.2	1	1
0.4	-2.3	401.0	8.0	3.1	1	1
0.5	-2.0	401.0	8.0	4.0	1	1
0.6	-1.7	401.0	8.0	4.8	1	1
0.7	-1.4	400.9	8.0	5.6	1	1
0.8	-1.1	400.9	8.0	6.3	1	1
0.9	-0.8	400.9	8.0	7.0	1	1
1.0	-0.5	400.9	8.0	7.6	1	1
1.1	-0.2	400.8	8.0	8.1	1	1
1.2	0.1	400.8	8.0	8.5	1	1
1.3	0.4	400.7	8.0	8.9	1	1
1.4	0.7	400.7	8.0	9.2	1	1
1.5	0.9	400.7	8.0	9.4	1	1
1.6	1.2	400.6	8.0	9.4	1	1
1.7	1.5	400.6	8.0	9.4	1	1
1.8	1.7	400.6	8.0	9.3	1	1
1.9	2.0	400.6	8.0	9.0	1	1
2.0	2.3	400.5	8.1	8.6	1	1
2.1	2.5	400.5	8.1	8.1	1	1
2.2	2.8	400.5	8.1	7.5	1	1
2.3	3.0	400.5	8.1	6.7	1	1
2.4	3.2	400.4	8.1	5.8	1	1
2.5	3.5	400.4	8.1	4.7	1	1
2.6	3.7	400.4	8.0	3.5	1	1
2.7	3.9	400.4	8.0	2.2	1	1
2.8	4.1	400.4	8.0	0.7	1	1
2.9	4.3	400.4	8.0	-1.0	1	1
3.0	4.5	400.4	8.0	-2.8	1	1
3.1	4.7	400.4	8.0	-4.8	1	1
3.2	4.9	400.4	8.0	-6.9	1	1
3.3	5.1	400.4	8.0	-9.3	1	1
3.4	5.2	400.4	8.0	-11.1	1	1
3.5	5.4	400.5	8.0	-12.6	1	1
3.6	5.5	400.5	8.0	-13.6	1	1
3.7	5.6	400.5	8.0	-14.3	1	1
3.8	5.7	400.5	7.9	-14.6	1	1
3.9	5.8	400.6	7.8	-14.5	1	1

4.0	5.8	400.6	7.6	-14.1	1	1
4.1	5.8	400.6	7.5	-13.9	1	1
4.2	5.8	400.7	7.4	-13.7	1	1
4.3	5.8	400.7	7.3	-13.6	1	1
4.4	5.7	400.8	7.2	-13.7	1	1
4.5	5.6	400.8	7.1	-13.8	1	1
4.6	5.5	400.9	7.1	-13.9	1	1
4.7	5.4	400.9	7.0	-14.2	1	1
4.8	5.2	401.0	6.9	-14.6	1	1
4.9	5.0	401.0	6.9	-15.0	1	1
5.0	4.8	401.1	6.9	-15.5	1	1
5.1	4.6	401.2	6.8	-16.0	1	1
5.2	4.4	401.2	6.8	-16.6	1	1
5.3	4.1	401.3	6.8	-17.2	1	1
5.4	3.8	401.4	6.7	-17.9	1	1
5.5	3.5	401.5	6.7	-18.6	1	1
5.6	3.1	401.6	6.7	-19.3	1	1
5.7	2.8	401.6	6.7	-19.9	1	1
5.8	2.4	401.7	6.7	-20.5	1	1
5.9	2.0	401.8	6.7	-21.1	1	1
6.0	1.6	401.9	6.7	-21.6	1	1
6.1	1.1	402.0	6.7	-22.1	1	1
6.2	0.6	402.1	6.7	-22.4	1	1
6.3	0.1	402.2	6.7	-22.6	1	1
6.4	-0.4	402.3	6.7	-22.6	1	1
6.5	-1.0	402.5	6.7	-22.5	1	1
6.6	-1.6	402.6	6.7	-22.2	1	1
6.7	-2.2	402.7	6.7	-21.7	1	1
6.8	-2.8	402.8	6.7	-21.5	1	1
6.9	-3.5	402.9	6.7	-21.7	1	1
7.0	-4.2	403.0	6.8	-22.1	1	1
7.1	-5.0	403.1	6.8	-22.7	1	1
7.2	-5.7	403.3	6.8	-23.6	1	1
7.3	-6.5	403.4	6.9	-24.7	1	1
7.4	-7.3	403.5	6.9	-25.9	1	1
7.5	-8.1	403.6	7.0	-27.2	1	1
7.6	-8.9	403.7	7.1	-28.6	1	1
7.7	-9.8	403.8	7.1	-30.0	1	1
7.8	-10.6	403.9	7.2	-31.4	1	1
7.9	-11.4	404.0	7.2	-32.8	1	1
8.0	-12.3	404.1	7.3	-34.1	1	1
8.1	-13.1	404.1	7.4	-35.4	1	1
8.2	-13.9	404.2	7.4	-36.5	1	1
8.3	-14.7	404.2	7.5	-37.5	1	1
8.4	-15.4	404.3	7.6	-38.3	1	1

8.5	-16.1	404.3	7.7	-39.0	1	1
8.6	-16.8	404.2	7.7	-39.5	1	1
8.7	-17.5	404.2	7.8	-39.9	1	1
8.8	-18.1	404.2	7.9	-40.0	1	1
8.9	-18.6	404.1	8.0	-40.0	1	1
9.0	-19.0	404.0	8.1	-39.8	1	1
9.1	-19.4	403.9	8.1	-39.5	1	1
9.2	-19.8	403.8	8.2	-39.0	1	1
9.3	-20.0	403.6	8.2	-38.4	1	1
9.4	-20.2	403.4	8.3	-35.0	1	1
9.5	-20.2	403.3	8.3	-37.0	1	1
9.6	-20.2	403.1	8.3	-36.2	1	1
9.7	-20.1	402.8	8.3	-35.5	1	1
9.8	-19.9	402.6	8.3	-34.8	1	1
9.9	-19.6	402.4	8.3	-34.3	1	1
10.0	-19.3	402.2	8.3	-33.6	1	1
10.1	-18.9	402.0	8.4	-32.5	1	1
10.2	-18.4	401.7	8.4	-31.2	1	1
10.3	-17.8	401.5	8.5	-29.7	1	1
10.4	-17.2	401.3	8.5	-27.9	1	1
10.5	-16.5	401.1	8.6	-25.9	1	1
10.6	-15.8	400.9	8.6	-23.7	1	1
10.7	-15.1	400.7	8.7	-21.5	1	1
10.8	-14.3	400.5	8.7	-19.1	1	1
10.9	-13.5	400.4	8.7	-16.6	1	1
11.0	-12.7	400.2	8.8	-14.1	1	1
11.1	-11.8	400.1	8.8	-11.6	1	1
11.2	-11.0	399.9	8.8	-9.0	1	1
11.3	-10.1	399.8	8.8	-6.5	1	1
11.4	-9.3	399.7	8.8	-3.9	1	1
11.5	-8.4	399.6	8.8	-1.5	1	1
11.6	-7.6	399.5	8.8	0.9	1	1
11.7	-6.7	399.4	8.8	3.2	1	1
11.8	-5.8	399.4	8.8	5.4	1	1
11.9	-5.0	399.3	8.8	7 5	1	1
12.0	-4.2	399.3	8.8	9.5	1	1
12.1	-3.3	399.2	8.8	11.3	1	1
12.2	-2.5	399.2	8.9	12.9	1	1
12.3	-1.7	399.1	8.9	14.3	1	1
12.4	-0.9	399.1	8.9	15.3	1	1
12.5	-0.1	399.1	8.9	16.6	1	1
12.6	0.7	399.1	9.0	17.4	1	1
12.7	1.4	399.0	9.0	17.9	1	1
12.8	2.2	399.0	9.0	18.3	1	1
12.9	2.9	399.0	9.0	18.3	1	1

13.0	3.6	399.0	9.1	18.1	1	1
13.1	4.3	399.0	9.1	17.6	1	1
13.2	5.0	399.0	9.1	16.8	1	1
13.3	5.6	399.0	9.1	15.8	1	1
13.4	6.3	399.0	9.2	14.4	1	1
13.5	6.9	399.1	9.2	12.7	1	1
13.6	7.6	399.1	9.2	11.2	1	1
13.7	8.2	399.1	9.2	9.9	1	1
13.8	8.7	399.1	9.2	8.7	1	1
13.9	9.2	399.1	9.2	7.8	1	1
14.0	9.7	399.1	9.1	7.0	1	1
14.1	10.2	399.1	9.1	6.3	1	1
14.2	10.6	399.1	9.0	5.9	1	1
14.3	10.9	399.2	8.9	5.6	1	1
14.4	11.2	399.2	8.8	5.5	1	1
14.5	11.4	399.2	8.6	5.7	1	1
14.6	11.5	399.2	8.4	6.0	1	1
14.7	11.6	399.3	8.2	6.7	1	1
14.8	11.6	399.3	7.9	7.7	1	1
14.9	11.5	399.3	7.6	9.1	1	1
15.0	11.4	399.4	7.3	11.0	1	1
15.1	11.1	399.4	7.0	13.4	1	1
15.2	10.8	399.4	6.7	16.5	1	1
15.3	10.5	399.5	6.4	20.3	1	1
15.4	10.0	399.6	6.1	25.0	1	1
15.5	9.4	399.6	5.8	30.9	1	1
15.6	8.8	399.6	5.7	37.4	1	1
15.7	8.1	399.7	5.6	44.1	1	1
15.8	7.4	399.7	5.7	50.7	1	1
15.9	6.6	399.8	5.9	57.0	1	1
16.0	5.7	399.8	6.2	62.7	0	1
16.1	4.8	399.9	6.6	67.8	0	1
16.2	3.9	399.9	7.0	72.4	0	1
16.3	3.0	399.9	7.5	76.5	0	1
16.4	2.0	399.9	8.1	80.2	0	1
16.5	1.0	400.0	8.6	83.6	0	1
16.6	0.3	400.0	9.2	86.8	0	1

CM IN RADAR CONE 95.78313 PERCENT
CMMCA W/IN STRUCTURAL LIMITS 100.0000 PERCENT

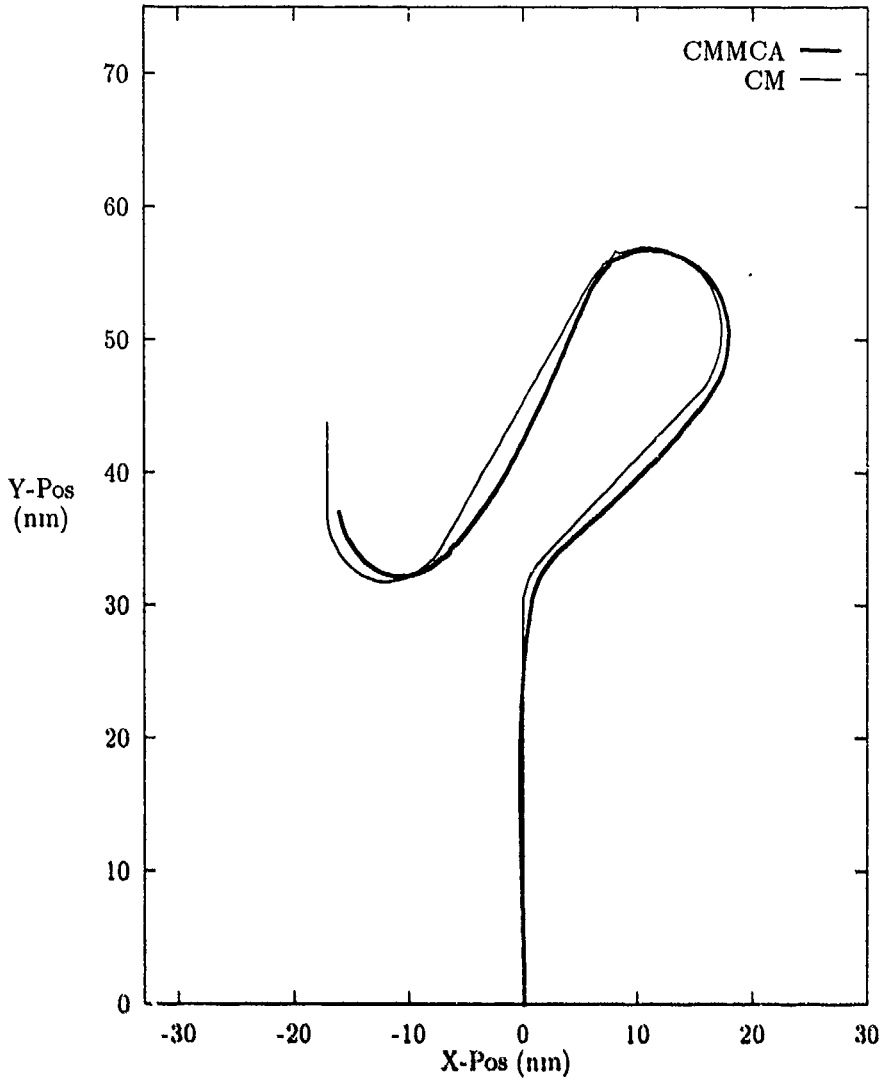

Figure 51. Section 1 CMMCA and CM Paths, CMMCA Starting Trailing

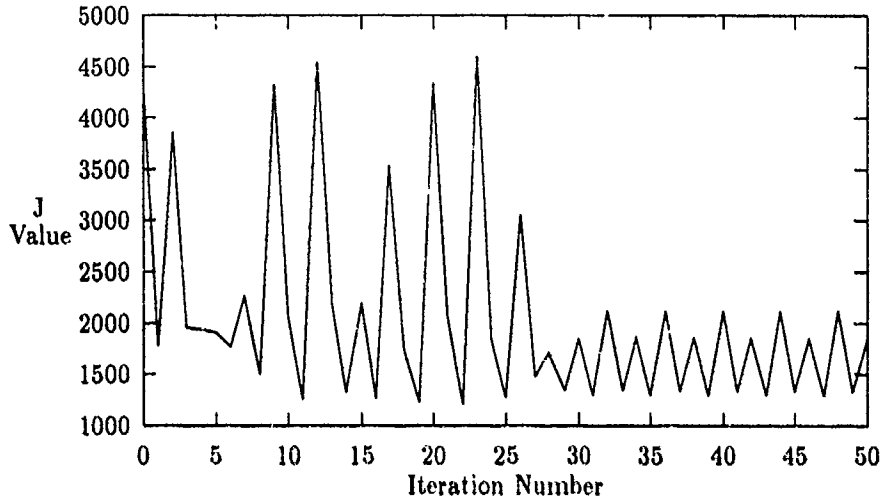

Figure 52. Plot of J Value versus Iteration Number

JSTOP = 3026.580
# ITERATIONS = 150

T	BANK	SPEED	RANGE	THETA	RADAR	STRUCT
0.1	-1.0	401.0	8.0	0.1	1	1
0.2	-0.9	401.0	8.0	0.4	1	1
0.3	-0.8	400.9	8.0	0.7	1	1
0.4	-0.8	400.9	8.0	1.0	1	1
0.5	-0.7	400.9	8.0	1.3	1	1
0.6	-0.6	400.8	8.0	1.6	1	1
0.7	-0.5	400.8	8.0	1.9	1	1
0.8	-0.4	400.8	8.0	2.1	1	1
0.9	-0.4	400.8	8.0	2.4	1	1
1.0	-0.3	400.7	8.0	2.6	1	1
1.1	-0.2	400.7	8.0	2.8	1	1
1.2	-0.1	400.7	8.0	3.0	1	1
1.3	0.0	400.7	8.0	3.2	1	1
1.4	0.1	400.6	8.0	3.4	1	1
1.5	0.1	400.6	8.0	3.5	1	1
1.6	0.2	400.6	8.0	3.6	1	1
1.7	0.3	400.6	8.0	3.7	1	1
1.8	0.4	400.6	8.0	3.7	1	1
1.9	0.5	400.6	8.0	3.7	1	1
2.0	0.6	400.6	8.0	3.7	1	1
2.1	0.7	400.5	8.0	3.6	1	1
2.2	0.8	400.5	8.0	3.5	1	1
2.3	0.8	400.5	8.0	3.3	1	1
2.4	0.9	400.5	8.0	3.1	1	1
2.5	1.0	400.5	8.0	2.9	1	1
2.6	1.1	400.5	8.0	2.6	1	1
2.7	1.2	400.5	8.0	2.2	1	1
2.8	1.3	400.5	8.0	1.8	1	1
2.9	1.4	400.5	8.0	1.3	1	1
3.0	1.5	400.5	8.0	0.8	1	1
3.1	1.6	400.5	8.0	0.2	1	1
3.2	1.7	400.5	8.0	-0.4	1	1
3.3	1.8	400.5	8.0	-1.2	1	1
3.4	1.9	400.5	8.0	-1.4	1	1
3.5	2.0	400.5	8.0	-1.1	1	1
3.6	2.1	400.5	7.9	-0.2	1	1
3.7	2.1	400.5	7.9	1.1	1	1
3.8	2.1	400.5	7.8	3.0	1	1
3.9	2.1	400.5	7.7	5.4	1	1

4.0	2.1	400.6	7.6	8.2	1	1
4.1	2.0	400.6	7.5	11.1	1	1
4.2	2.0	400.6	7.4	13.9	1	1
4.3	1.8	400.7	7.4	16.9	1	1
4.4	1.7	400.7	7.4	19.8	1	1
4.5	1.5	400.8	7.4	22.7	1	1
4.6	21.7	395.9	7.4	22.4	1	1
4.7	21.1	396.2	7.5	18.6	1	1
4.8	21.5	396.2	7.5	14.3	1	1
4.9	20.8	396.4	7.5	9.5	1	1
5.0	20.7	396.5	7.5	4.3	1	1
5.1	20.6	396.5	7.5	-1.4	1	1
5.2	13.3	398.2	7.5	-6.4	1	1
5.3	0.3	401.0	7.5	-8.7	1	1
5.4	-0.2	401.1	7.5	-9.1	1	1
5.5	1.8	400.7	7.6	-9.7	1	1
5.6	-3.8	401.9	7.6	-9.8	1	1
5.7	1.3	400.8	7.6	-9.9	1	1
5.8	-0.3	401.1	7.6	-10.3	1	1
5.9	-0.6	401.2	7.6	-10.6	1	1
6.0	-1.0	401.2	7.6	-10.7	1	1
6.1	-0.9	401.2	7.6	-10.7	1	1
6.2	-1.1	401.2	7.6	-10.7	1	1
6.3	-1.1	401.2	7.6	-10.7	1	1
6.4	-1.6	401.3	7.6	-10.5	1	1
6.5	-1.6	401.3	7.6	-10.3	1	1
6.6	-1.6	401.3	7.6	-10.0	1	1
6.7	-2.1	401.4	7.6	-9.6	1	1
6.8	-2.1	401.4	7.6	-9.6	1	1
6.9	-2.1	401.4	7.6	-10.0	1	1
7.0	-2.7	401.5	7.6	-10.9	1	1
7.1	-2.5	401.5	7.6	-12.1	1	1
7.2	-2.8	401.6	7.6	-13.8	1	1
7.3	-3.1	401.6	7.6	-15.9	1	1
7.4	-3.1	401.6	7.6	-18.3	1	1
7.5	-3.0	401.6	7.6	-21.2	1	1
7.6	-3.4	401.7	7.5	-24.4	1	1
7.7	-3.3	401.7	7.5	-28.1	1	1
7.8	-3.3	401.7	7.5	-32.1	1	1
7.9	-3.1	401.6	7.6	-36.6	1	1
8.0	-20.9	407.1	7.6	-38.7	1	1
8.1	-20.5	407.1	7.6	-38.3	1	1
8.2	-20.5	407.3	7.7	-38.0	1	1
8.3	-20.7	407.5	7.7	-37.6	1	1
8.4	-20.6	407.6	7.8	-37.2	1	1

8.5	-20.2	407.5	7.8	-36.8	1	1
8.6	-20.7	407.7	7.8	-36.4	1	1
8.7	-20.5	407.7	7.8	-35.9	1	1
8.8	-20.3	407.6	7.8	-35.5	1	1
8.9	-20.4	407.6	7.8	-35.1	1	1
9.0	-20.4	407.5	7.8	-34.7	1	1
9.1	-20.7	407.4	7.8	-34.2	1	1
9.2	-20.0	407.1	7.8	-33.9	1	1
9.3	-20.5	407.1	7.8	-33.5	1	1
9.4	-20.1	406.8	7.8	-30.2	1	1
9.5	-20.3	406.6	7.7	-32.9	1	1
9.6	-20.3	406.4	7.7	-32.6	1	1
9.7	-20.0	406.0	7.7	-32.3	1	1
9.8	-19.8	405.7	7.6	-32.2	1	1
9.9	-19.7	405.5	7.6	-32.3	1	1
10.0	-19.7	405.2	7.5	-32.1	1	1
10.1	-19.3	404.8	7.6	-31.5	1	1
10.2	-19.2	404.5	7.6	-30.4	1	1
10.3	-18.8	404.1	7.6	-29.0	1	1
10.4	-18.8	403.9	7.7	-27.2	1	1
10.5	-18.4	403.5	7.7	-25.0	1	1
10.6	48.4	385.2	7.8	-35.0	1	0
10.7	-74.0	430.3	7.9	-20.9	1	0
10.8	35.8	391.6	7.9	-1.7	1	0
10.9	-17.3	402.4	7.9	-5.8	1	1
11.0	-17.9	402.3	7.9	-1.1	1	1
11.1	-23.5	403.1	7.9	5.1	1	1
11.2	-0.2	399.3	7.9	9.0	1	1
11.3	0.0	399.2	7.9	9.6	1	1
11.4	-0.2	399.3	7.9	10.2	1	1
11.5	0.0	399.3	7.9	10.8	1	1
11.6	0.1	399.3	7.9	11.3	1	1
11.7	0.2	399.3	8.0	11.8	1	1
11.8	0.5	399.2	8.0	12.3	1	1
11.9	0.4	399.3	8.0	12.7	1	1
12.0	0.4	399.3	8.0	13.1	1	1
12.1	0.7	399.3	8.0	13.4	1	1
12.2	0.8	399.3	8.0	13.7	1	1
12.3	0.9	399.3	8.0	13.9	1	1
12.4	1.0	399.3	8.1	14.1	1	1
12.5	1.3	399.2	8.1	14.2	1	1
12.6	1.2	399.3	8.1	14.2	1	1
12.7	1.5	399.3	8.1	14.2	1	1
12.8	1.6	399.3	8.1	14.1	1	1
12.9	1.8	399.3	8.1	13.9	1	1

13.0	2.0	399.3	8.1	13.6	1	1
13.1	2.3	399.2	8.1	13.2	1	1
13.2	2.2	399.3	8.1	12.7	1	1
13.3	2.8	399.2	8.1	12.0	1	1
13.4	2.5	399.3	8.1	11.3	1	1
13.5	3.0	399.2	8.1	10.5	1	1
13.6	3.2	399.2	8.2	10.1	1	1
13.7	3.5	399.2	8.2	10.1	1	1
13.8	3.5	399.2	8.2	10.6	1	1
13.9	3.8	399.2	8.2	11.6	1	1
14.0	4.0	399.2	8.1	13.0	1	1
14.1	4.1	399.2	8.1	14.8	1	1
14.2	4.4	399.2	8.1	17.0	1	1
14.3	4.2	399.3	8.0	19.7	1	1
14.4	4.4	399.3	7.9	22.8	1	1
14.5	4.5	399.3	7.9	26.4	1	1
14.6	4.5	399.3	7.8	30.4	1	1
14.7	4.4	399.3	7.8	35.0	1	1
14.8	25.3	398.4	7.7	36.6	1	1
14.9	25.3	398.4	7.7	35.0	1	1
15.0	25.0	398.5	7.6	33.5	1	1
15.1	24.7	398.5	7.5	32.1	1	1
15.2	24.3	398.6	7.4	30.9	1	1
15.3	24.2	398.7	7.3	29.8	1	1
15.4	23.9	398.8	7.2	28.9	1	1
15.5	23.3	398.9	7.1	28.4	1	1
15.6	23.2	399.0	7.0	27.7	1	1
15.7	22.6	399.1	6.9	26.6	1	1
15.8	22.2	399.2	6.9	25.3	1	1
15.9	21.7	399.4	6.8	23.5	1	1
16.0	21.7	399.5	6.8	21.2	1	1
16.1	20.7	399.6	6.9	18.5	1	1
16.2	20.7	399.7	6.9	15.4	1	1
16.3	20.6	399.8	6.9	11.7	1	1
16.4	20.2	399.9	6.9	7.5	1	1
16.5	19.9	399.9	6.9	2.9	1	1
16.6	22.3	400.0	6.9	-2.7	1	1

CM IN RADAR CONE 100.0000 PERCENT
CMMCA W/IN STRUCTURAL LIMITS 99.19277 PERCENT

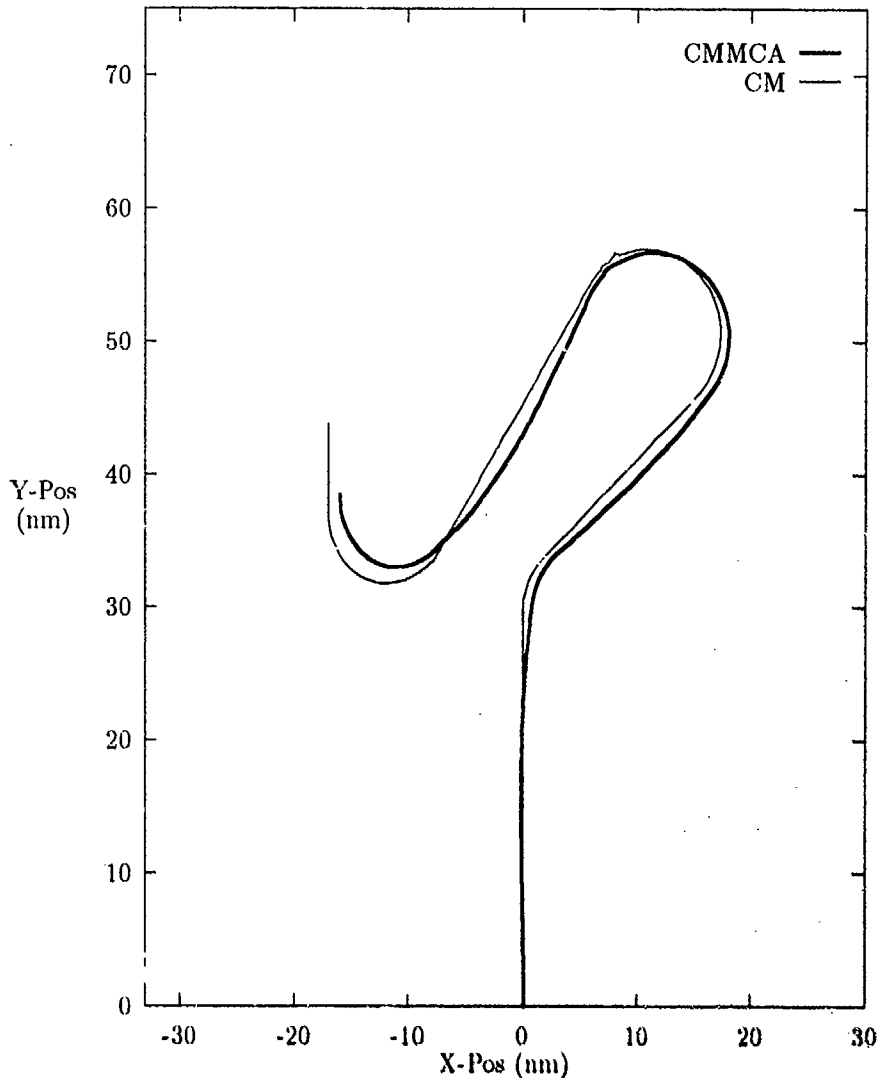

Figure 53. Section 1 CMMCA and CM Paths, CMMCA Starting Trailing

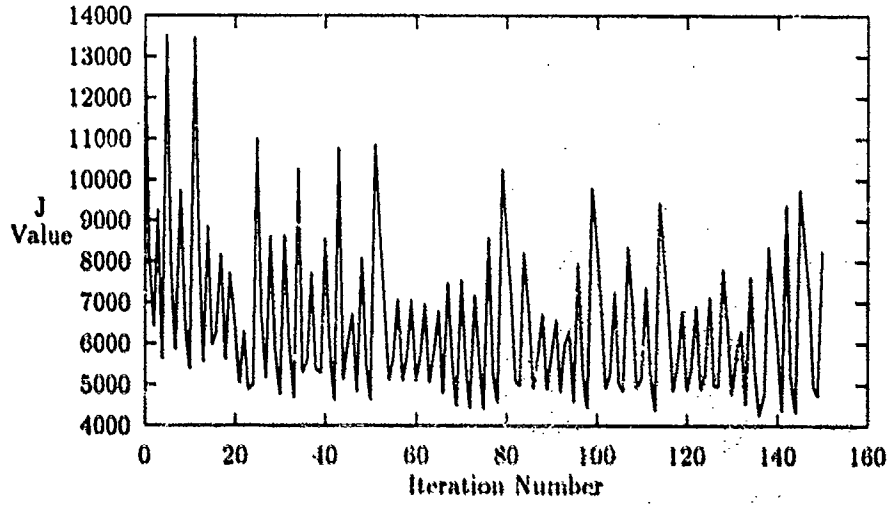

Figure 54. Plot of J Value versus Iteration Number

JSTOP = 8274.818
# ITERATIONS = 150

T	BANK	SPEED	RANGE	THETA	RADAR	STRUCT
0.1	-0.7	401.1	8.0	0.1	1	1
0.2	-0.6	401.1	8.0	0.3	1	1
0.3	-0.6	401.0	8.0	0.5	1	1
0.4	-0.5	401.0	8.0	0.7	1	1
0.5	-0.4	401.0	8.0	0.9	1	1
0.6	-0.4	401.0	8.0	1.1	1	1
0.7	-0.3	400.9	8.0	1.3	1	1
0.8	-0.3	400.9	8.0	1.4	1	1
0.9	-0.2	400.9	8.0	1.6	1	1
1.0	-0.1	400.9	8.0	1.7	1	1
1.1	-0.1	400.9	8.0	1.8	1	1
1.2	0.0	400.9	8.0	2.0	1	1
1.3	0.1	400.8	8.0	2.0	1	1
1.4	0.1	400.8	8.0	2.1	1	1
1.5	0.2	400.8	8.0	2.2	1	1
1.6	0.2	400.8	8.0	2.2	1	1
1.7	0.3	400.8	8.0	2.2	1	1
1.8	0.4	400.8	8.0	2.2	1	1
1.9	0.4	400.8	8.0	2.1	1	1
2.0	0.5	400.8	8.0	2.1	1	1
2.1	0.6	400.8	8.0	2.0	1	1
2.2	0.6	400.8	8.0	1.8	1	1
2.3	0.7	400.8	8.0	1.6	1	1
2.4	0.8	400.8	8.0	1.4	1	1
2.5	0.9	400.7	8.0	1.2	1	1
2.6	0.9	400.7	8.0	0.9	1	1
2.7	1.0	400.7	8.0	0.5	1	1
2.8	1.1	400.7	8.0	0.2	1	1
2.9	1.1	400.7	8.0	-0.3	1	1
3.0	1.2	400.7	8.0	-0.7	1	1
3.1	1.3	400.7	8.0	-1.3	1	1
3.2	1.4	400.7	8.0	-1.8	1	1
3.3	1.4	400.7	8.0	-2.5	1	1
3.4	1.5	400.7	8.0	-2.5	1	1
3.5	1.6	400.7	7.9	-2.1	1	1
3.6	1.6	400.7	7.9	-1.1	1	1
3.7	1.6	400.8	7.8	0.4	1	1
3.8	1.6	400.8	7.7	2.5	1	1
3.9	1.6	400.8	7.6	5.2	1	1

4.0	1.5	400.8	7.5	8.2	1	1
4.1	1.4	400.9	7.4	11.3	1	1
4.2	1.3	400.9	7.4	14.5	1	1
4.3	1.1	400.9	7.3	17.8	1	1
4.4	0.9	401.0	7.3	21.1	1	1
4.5	0.7	401.0	7.3	24.4	1	1
4.6	22.9	395.1	7.4	24.2	1	1
4.7	22.2	395.5	7.4	20.2	1	1
4.8	22.6	395.5	7.5	15.6	1	1
4.9	22.0	395.7	7.5	10.5	1	1
5.0	21.9	395.8	7.5	5.0	1	1
5.1	21.8	395.8	7.5	-1.2	1	1
5.2	13.9	397.8	7.5	-6.5	1	1
5.3	-0.3	401.3	7.5	-8.8	1	1
5.4	-0.8	401.4	7.5	-9.1	1	1
5.5	1.5	400.9	7.5	-9.6	1	1
5.6	-4.7	402.3	7.5	-9.6	1	1
5.7	1.1	400.9	7.5	-9.4	1	1
5.8	-0.7	401.4	7.5	-9.8	1	1
5.9	-0.9	401.4	7.5	-9.9	1	1
6.0	-1.2	401.5	7.5	-9.9	1	1
6.1	-1.1	401.5	7.5	-9.8	1	1
6.2	-1.2	401.5	7.5	-9.8	1	1
6.3	-1.1	401.4	7.6	-9.6	1	1
6.4	-1.6	401.6	7.6	-9.5	1	1
6.5	-1.5	401.5	7.6	-9.2	1	1
6.6	-1.4	401.5	7.6	-8.9	1	1
6.7	-2.0	401.6	7.6	-8.5	1	1
6.8	-1.9	401.6	7.6	-8.5	1	1
6.9	-1.8	401.6	7.6	-9.0	1	1
7.0	-2.4	401.7	7.6	-9.9	1	1
7.1	-2.1	401.7	7.6	-11.3	1	1
7.2	-2.3	401.7	7.5	-13.1	1	1
7.3	-2.6	401.8	7.5	-15.3	1	1
7.4	-2.5	401.8	7.5	-17.9	1	1
7.5	-2.3	401.7	7.5	-21.1	1	1
7.6	-2.7	401.9	7.5	-24.6	1	1
7.7	-2.5	401.8	7.4	-28.6	1	1
7.8	-2.4	401.8	7.5	-33.0	1	1
7.9	-2.1	401.7	7.5	-37.8	1	1
8.0	-21.6	408.3	7.5	-40.1	1	1
8.1	-21.1	408.3	7.6	-39.7	1	1
8.2	-21.0	408.5	7.6	-39.3	1	1
8.3	-21.3	408.8	7.7	-38.9	1	1
8.4	-21.1	408.8	7.7	-38.4	1	1

8.5	-20.6	408.7	7.8	-37.9	1	1
8.6	-21.1	408.9	7.8	-37.4	1	1
8.7	-21.0	408.9	7.8	-36.9	1	1
8.8	-20.7	408.8	7.8	-36.4	1	1
8.9	-20.8	408.7	7.8	-35.9	1	1
9.0	-20.8	408.6	7.9	-35.3	1	1
9.1	-21.1	408.6	7.9	-34.8	1	1
9.2	-20.5	408.2	7.8	-34.2	1	1
9.3	-21.1	408.2	7.8	-33.7	1	1
9.4	-20.6	407.8	7.9	-30.2	1	1
9.5	-20.9	407.6	7.8	-32.6	1	1
9.6	-20.9	407.4	7.7	-32.0	1	1
9.7	-20.7	407.0	7.7	-31.4	1	1
9.8	-20.5	406.7	7.7	-31.0	1	1
9.9	-20.5	406.3	7.6	-30.7	1	1
10.0	-20.6	406.0	7.6	-30.1	1	1
10.1	-20.3	405.6	7.6	-29.1	1	1
10.2	-20.2	405.3	7.6	-27.6	1	1
10.3	-19.8	404.9	7.6	-25.7	1	1
10.4	-19.9	404.6	7.6	-23.3	1	1
10.5	-19.6	404.2	7.7	-20.5	1	1
10.6	55.3	379.9	7.7	-33.1	1	0
10.7	-74.8	437.0	7.8	-20.7	1	0
10.8	40.6	389.2	7.8	-1.8	1	0
10.9	-18.6	402.9	7.8	-6.9	1	1
11.0	-19.2	402.8	7.8	-2.0	1	1
11.1	-25.5	403.9	7.8	4.6	1	1
11.2	0.2	399.1	7.8	8.8	1	1
11.3	0.4	399.0	7.8	9.2	1	1
11.4	0.2	399.1	7.8	9.5	1	1
11.5	0.5	399.1	7.8	9.9	1	1
11.6	0.5	399.1	7.8	10.2	1	1
11.7	0.6	399.1	7.8	10.5	1	1
11.8	1.0	399.0	7.8	10.7	1	1
11.9	0.8	399.1	7.9	10.9	1	1
12.0	0.8	399.1	7.9	11.0	1	1
12.1	1.1	399.1	7.9	11.1	1	1
12.2	1.2	399.1	7.9	11.1	1	1
12.3	1.3	399.1	7.9	11.1	1	1
12.4	1.4	399.1	7.9	11.0	1	1
12.5	1.7	399.1	7.9	10.8	1	1
12.6	1.6	399.1	7.9	10.5	1	1
12.7	1.9	399.1	7.9	10.2	1	1
12.8	2.0	399.1	7.9	9.7	1	1
12.9	2.2	399.1	7.9	9.2	1	1

13.0	2.3	399.1	7.9	8.6	1	1
13.1	2.7	399.1	7.9	7.8	1	1
13.2	2.5	399.1	7.9	7.0	1	1
13.3	3.1	399.1	7.9	6.0	1	1
13.4	2.8	399.1	7.9	5.0	1	1
13.5	3.2	399.1	7.9	3.8	1	1
13.6	3.4	399.1	7.9	3.1	1	1
13.7	3.8	399.1	7.9	2.8	1	1
13.8	3.6	399.1	7.9	3.0	1	1
13.9	4.0	399.1	7.9	3.6	1	1
14.0	4.1	399.1	7.8	4.7	1	1
14.1	4.2	399.1	7.8	6.3	1	1
14.2	4.5	399.1	7.7	8.3	1	1
14.3	4.2	399.1	7.5	10.8	1	1
14.4	4.4	399.1	7.4	13.9	1	1
14.5	4.4	399.1	7.3	17.5	1	1
14.6	4.3	399.1	7.1	21.6	1	1
14.7	4.2	399.2	7.0	26.5	1	1
14.8	27.1	397.9	6.9	28.1	1	1
14.9	27.0	398.0	6.7	26.3	1	1
15.0	26.7	398.1	6.6	24.7	1	1
15.1	26.3	398.2	6.4	23.2	1	1
15.2	25.9	398.3	6.3	21.9	1	1
15.3	25.7	398.4	6.1	20.8	1	1
15.4	25.4	398.5	5.9	19.9	1	1
15.5	24.7	398.7	5.7	19.6	1	1
15.6	24.6	398.8	5.6	19.0	1	1
15.7	24.0	399.0	5.5	18.1	1	1
15.8	23.7	399.1	5.4	16.6	1	1
15.9	23.2	399.3	5.3	14.5	1	1
16.0	23.3	399.4	5.3	11.8	1	1
16.1	22.3	399.6	5.3	8.3	1	1
16.2	22.4	399.7	5.3	4.2	1	1
16.3	22.5	399.8	5.3	-0.8	1	1
16.4	22.1	399.9	5.3	-6.6	1	1
16.5	21.9	399.9	5.3	-13.1	1	1
16.6	23.4	400.0	5.3	-20.6	1	1

CM IN RADAR CONE 100.0000 PERCENT
CMMCA W/IN STRUCTURAL LIMITS 98.19277 PERCENT

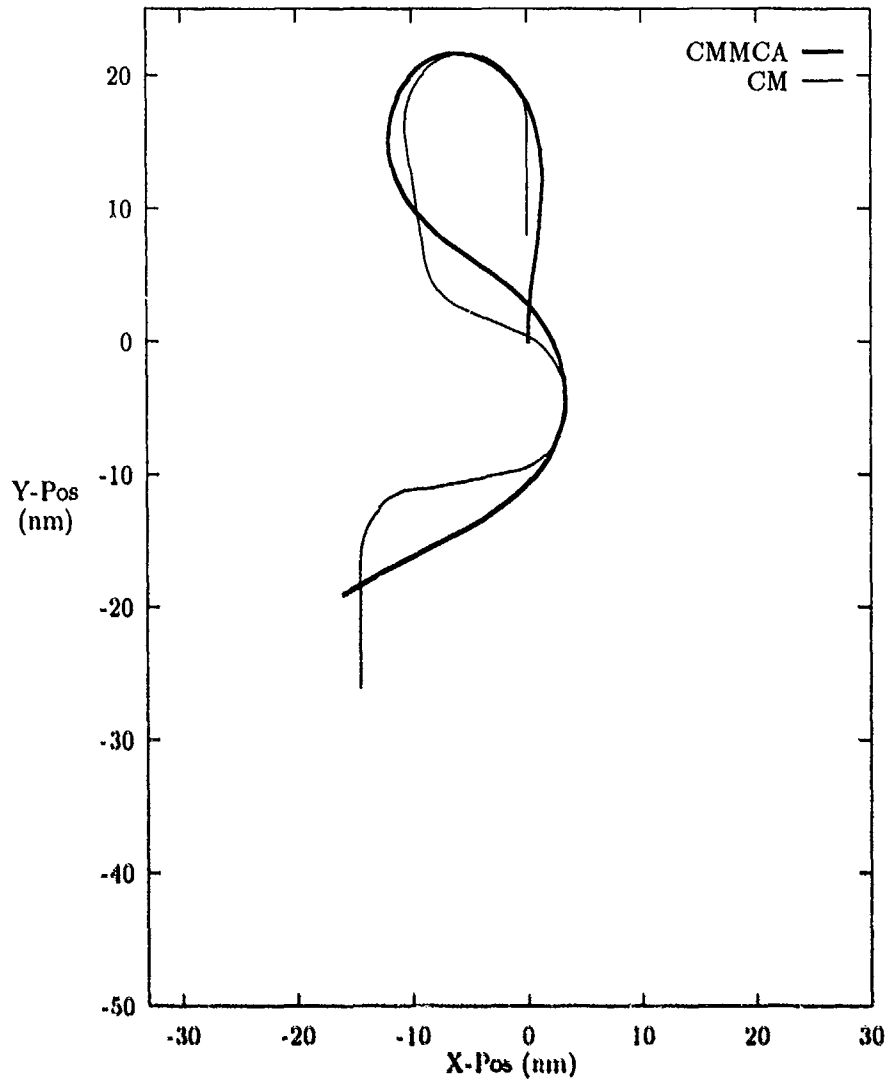

Figure 55. Section 2 CMMCA and CM Paths, CMMCA Starting Straight

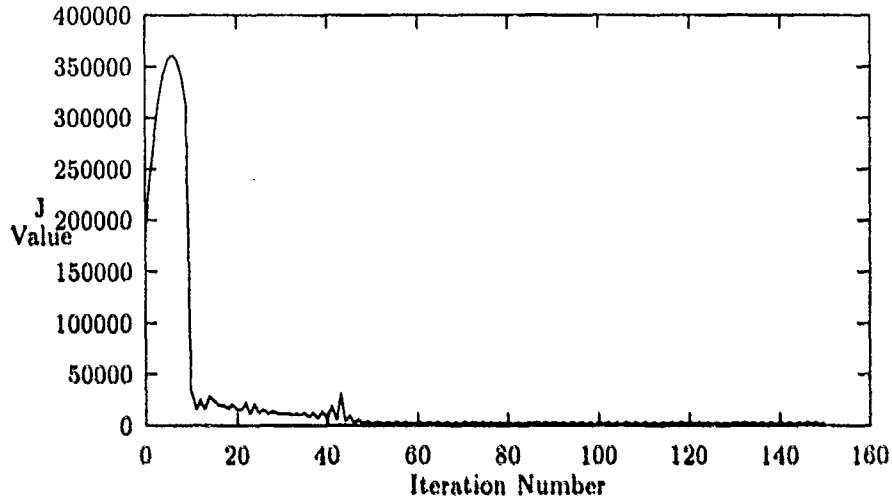

Figure 56. Plot of J Value versus Iteration Number

JSTOP = 2529.672
# ITERATIONS = 150

T	BANK	SPEED	RANGE	THETA	RADAR	STRUCT
0.1	7.1	398.6	8.0	-1.1	1	1
0.2	6.1	398.7	8.0	-3.1	1	1
0.3	5.2	398.9	8.0	-5.1	1	1
0.4	4.4	399.1	8.0	-6.9	1	1
0.5	3.5	399.3	8.0	-8.5	1	1
0.6	2.7	399.5	8.0	-10.1	1	1
0.7	1.9	399.6	8.0	-11.4	1	1
0.8	1.1	399.8	8.1	-12.5	1	1
0.9	0.3	400.0	8.1	-13.5	1	1
1.0	-0.5	400.3	8.1	-14.2	1	1
1.1	-1.3	400.5	8.1	-14.6	1	1
1.2	-2.2	400.7	8.1	-14.8	1	1
1.3	-3.0	401.0	8.1	-14.7	1	1
1.4	-3.8	401.3	8.2	-14.9	1	1
1.5	-4.7	401.6	8.2	-15.4	1	1
1.6	-5.5	401.9	8.2	-16.1	1	1
1.7	-6.4	402.2	8.2	-16.9	1	1
1.8	-7.3	402.5	8.2	-18.0	1	1
1.9	-8.1	402.9	8.1	-19.2	1	1
2.0	-9.0	403.3	8.1	-20.5	1	1
2.1	-9.9	403.7	8.1	-22.0	1	1
2.2	-10.8	404.1	8.0	-23.5	1	1
2.3	-11.6	404.5	7.9	-25.1	1	1
2.4	-12.5	405.0	7.8	-26.8	1	1
2.5	-13.4	405.4	7.7	-28.6	1	1
2.6	-14.2	405.9	7.7	-30.4	1	1
2.7	-15.1	406.3	7.6	-32.3	1	1
2.8	-15.9	406.8	7.5	-34.2	1	1
2.9	-16.7	407.3	7.4	-36.1	1	1
3.0	-17.5	407.7	7.3	-38.0	1	1
3.1	-18.3	408.2	7.3	-39.9	1	1
3.2	-19.0	408.6	7.2	-41.8	1	1
3.3	-19.7	409.0	7.2	-43.6	1	1
3.4	-20.4	409.3	7.2	-45.3	1	1
3.5	-21.0	409.6	7.2	-46.9	1	1
3.6	-21.6	409.8	7.2	-48.4	1	1
3.7	-22.0	410.0	7.2	-49.8	1	1
3.8	-22.4	410.1	7.3	-51.0	1	1
3.9	-22.6	410.1	7.3	-52.3	1	1
4.0	-22.7	410.0	7.4	-53.0	1	1

4.1	-22.7	409.8	7.6	-53.1	1	1
4.2	-22.6	409.6	7.8	-52.4	1	1
4.3	-22.5	409.3	8.0	-51.2	1	1
4.4	-22.3	408.9	8.2	-49.4	1	1
4.5	-22.0	408.5	8.4	-47.0	1	1
4.6	-21.7	408.1	8.6	-44.2	1	1
4.7	-21.3	407.6	8.8	-41.0	1	1
4.8	-20.9	407.1	8.9	-37.5	1	1
4.9	-20.5	406.6	9.0	-33.6	1	1
5.0	-20.0	406.1	9.1	-29.5	1	1
5.1	-19.5	405.6	9.2	-25.1	1	1
5.2	-19.0	405.1	9.2	-20.4	1	1
5.3	-18.4	404.6	9.2	-15.5	1	1
5.4	-17.8	404.1	9.3	-11.0	1	1
5.5	-17.2	403.7	9.3	-6.8	1	1
5.6	-16.5	403.2	9.2	-2.9	1	1
5.7	-15.7	402.8	9.2	0.6	1	1
5.8	-14.9	402.4	9.2	3.7	1	1
5.9	-14.1	402.1	9.1	6.3	1	1
6.0	-13.2	401.7	9.0	8.5	1	1
6.1	-12.2	401.4	8.9	10.2	1	1
6.2	-11.2	401.0	8.7	11.7	1	1
6.3	-10.1	400.7	8.6	13.1	1	1
6.4	-9.0	400.5	8.5	14.3	1	1
6.5	-7.8	400.2	8.4	15.3	1	1
6.6	-6.6	399.9	8.3	16.2	1	1
6.7	-5.4	399.6	8.3	16.8	1	1
6.8	-4.2	399.4	8.2	17.2	1	1
6.9	-2.9	399.1	8.1	17.3	1	1
7.0	-1.6	398.9	8.1	17.0	1	1
7.1	-0.4	398.6	8.1	17.0	1	1
7.2	0.9	398.4	8.1	17.2	1	1
7.3	2.2	398.2	8.1	17.6	1	1
7.4	3.4	397.9	8.2	18.2	1	1
7.5	4.7	397.7	8.2	18.9	1	1
7.6	5.8	397.5	8.2	19.7	1	1
7.7	7.0	397.2	8.2	20.6	1	1
7.8	8.1	397.0	8.3	21.6	1	1
7.9	9.2	396.8	8.3	22.6	1	1
8.0	10.2	396.7	8.2	23.6	1	1
8.1	11.1	396.5	8.2	24.6	1	1
8.2	12.0	396.3	8.2	25.7	1	1
8.3	12.8	396.2	8.1	26.8	1	1
8.4	13.5	396.1	8.1	27.9	1	1
8.5	14.2	396.0	8.0	29.1	1	1

8.6	14.7	395.9	8.0	30.3	1	1
8.7	15.2	395.9	7.9	31.6	1	1
8.8	15.5	395.9	7.8	33.1	1	1
8.9	15.8	395.9	7.7	34.6	1	1
9.0	15.9	396.0	7.6	36.4	1	1
9.1	16.0	396.0	7.6	38.2	1	1
9.2	15.9	396.2	7.6	39.8	1	1
9.3	15.7	396.3	7.7	41.1	1	1
9.4	15.5	396.4	7.8	42.0	1	1
9.5	15.1	396.6	7.9	42.6	1	1
9.6	14.6	396.8	8.0	42.8	1	1
9.7	14.1	397.0	8.2	42.8	1	1
9.8	13.5	397.2	8.4	42.6	1	1
9.9	12.8	397.4	8.5	42.1	1	1
10.0	12.1	397.6	8.7	41.6	1	1
10.1	11.4	397.8	8.9	40.9	1	1
10.2	10.6	398.0	9.1	40.2	1	1
10.3	9.8	398.2	9.2	40.4	1	1
10.4	9.0	398.3	9.4	40.0	1	1
10.5	8.2	398.5	9.5	39.2	1	1
10.6	7.4	398.6	9.6	38.0	1	1
10.7	6.6	398.8	9.7	36.4	1	1
10.8	5.8	398.9	9.7	34.6	1	1
10.9	5.0	399.0	9.6	32.5	1	1
11.0	4.3	399.1	9.4	30.1	1	1
11.1	3.6	399.2	9.2	27.6	1	1
11.2	3.0	399.3	8.9	24.8	1	1
11.3	2.4	399.4	8.6	21.7	1	1
11.4	1.8	399.5	8.2	18.3	1	1
11.5	1.3	399.5	7.7	14.6	1	1
11.6	0.8	399.6	7.2	10.4	1	1
11.7	0.3	399.6	6.7	5.7	1	1
11.8	-0.1	399.7	6.3	0.5	1	1
11.9	-0.4	399.8	5.9	-5.3	1	1
12.0	-0.8	399.8	5.6	-11.7	1	1
12.1	-1.0	399.8	5.4	-18.7	1	1
12.2	-1.2	399.9	5.3	-26.0	1	1
12.3	-1.3	399.9	5.2	-33.5	1	1
12.4	-1.4	399.9	5.3	-40.9	1	1
12.5	-1.3	400.0	5.4	-48.0	1	1
12.6	-1.3	400.0	5.7	-54.5	1	1
12.7	-1.1	400.0	6.0	-60.4	0	1
12.8	-0.9	400.0	6.3	-65.7	0	1
12.9	-0.7	400.0	6.8	-70.4	0	1
13.0	-0.3	400.0	7.2	-74.6	0	1

13.1	-0.1	400.0	7.7	-78.3	0	1

CM IN RADAR CONE	96.18320	PERCENT
CMMCA W/IN STRUCTURAL LIMITS	100.0000	PERCENT

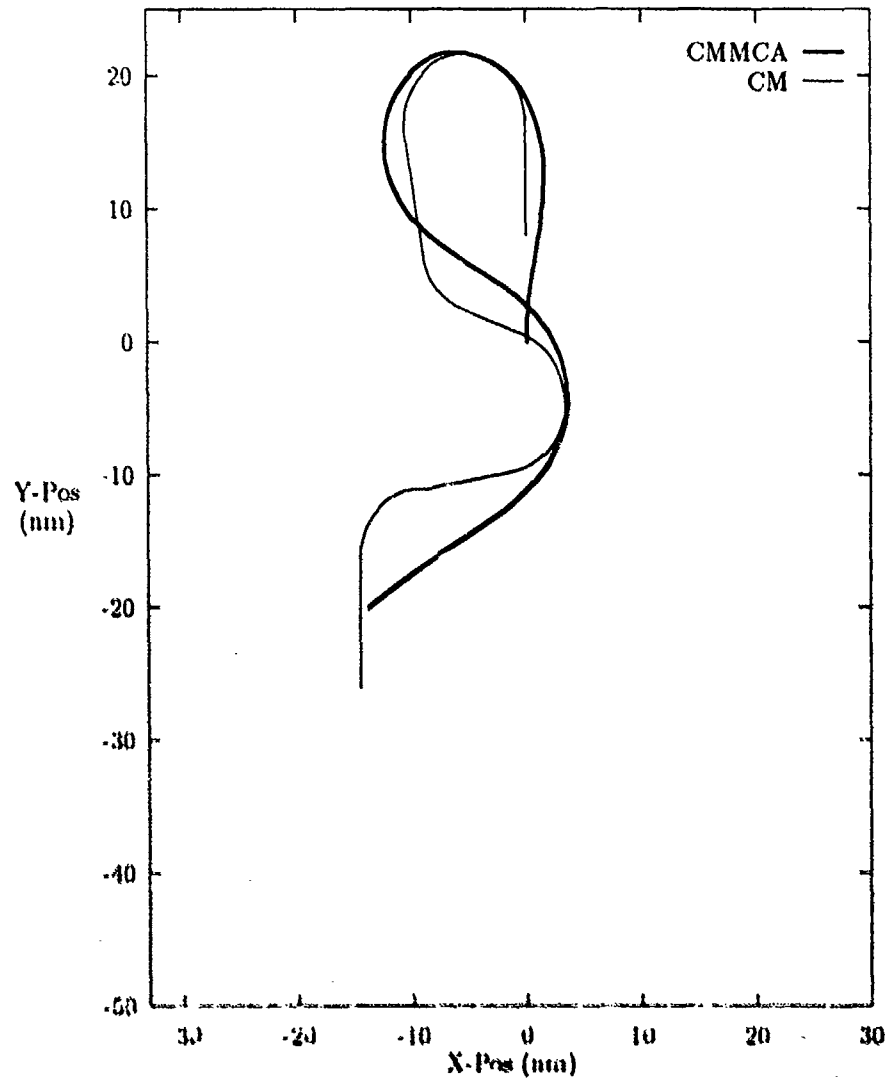

Figure 57. Section 2 CMMCA and CM Paths, CMMCA Starting Straight

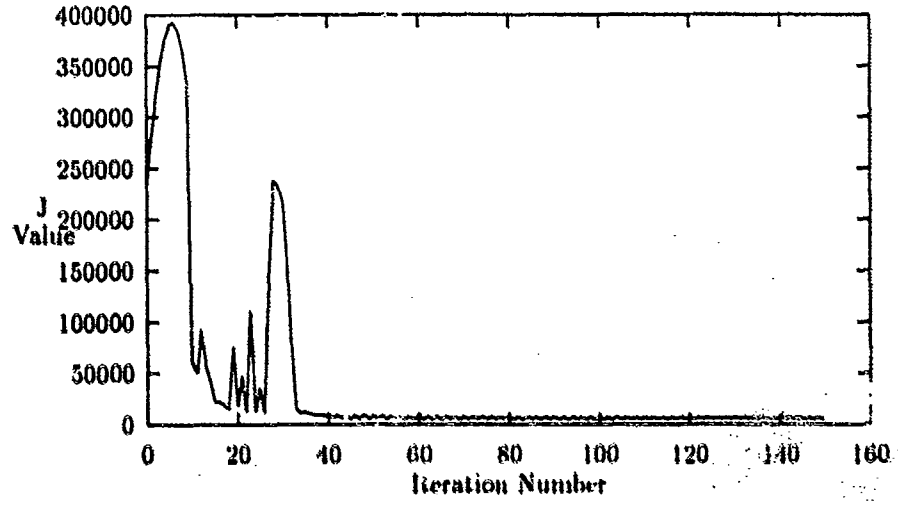

Figure 58. Plot of J Value versus Iteration Number

JSTOP = 6655.606
# ITERATIONS = 150

T	BANK	SPEED	RANGE	THETA	RADAR	STRUCT
0.1	8.0	396.9	8.0	-1.2	1	1
0.2	7.0	397.3	8.0	-3.6	1	1
0.3	6.0	397.6	8.0	-5.8	1	1
0.4	5.0	397.9	8.0	-7.9	1	1
0.5	4.1	398.3	8.0	-9.8	1	1
0.6	3.2	398.6	8.0	-11.5	1	1
0.7	2.3	399.0	8.1	-13.1	1	1
0.8	1.4	399.4	8.1	-14.4	1	1
0.9	0.5	399.8	8.1	-15.6	1	1
1.0	-0.4	400.2	8.1	-16.5	1	1
1.1	-1.2	400.6	8.2	-17.1	1	1
1.2	-2.1	401.0	8.2	-17.4	1	1
1.3	-3.0	401.5	8.2	-17.5	1	1
1.4	-4.0	402.0	8.2	-17.8	1	1
1.5	-4.9	402.6	8.3	-18.3	1	1
1.6	-5.8	403.1	8.3	-19.0	1	1
1.7	-6.7	403.7	8.3	-19.9	1	1
1.8	-7.7	404.3	8.3	-20.9	1	1
1.9	-8.6	404.9	8.3	-22.0	1	1
2.0	-9.5	405.6	8.3	-23.3	1	1
2.1	-10.4	406.2	8.2	-24.6	1	1
2.2	-11.3	406.9	8.2	-26.0	1	1
2.3	-12.2	407.6	8.1	-27.5	1	1
2.4	-13.0	408.3	8.1	-29.0	1	1
2.5	-13.8	409.0	8.0	-30.5	1	1
2.6	-14.7	409.7	7.9	-32.2	1	1
2.7	-15.4	410.4	7.8	-33.8	1	1
2.8	-16.2	411.1	7.8	-35.5	1	1
2.9	-17.0	411.8	7.7	-37.2	1	1
3.0	-17.7	412.4	7.6	-38.9	1	1
3.1	-18.3	413.0	7.6	-40.6	1	1
3.2	-19.0	413.6	7.5	-42.3	1	1
3.3	-19.5	414.1	7.5	-44.0	1	1
3.4	-20.1	414.6	7.5	-45.6	1	1
3.5	-20.6	415.0	7.5	-47.2	1	1
3.6	-21.0	415.3	7.5	-48.8	1	1
3.7	-21.3	415.5	7.5	-50.3	1	1
3.8	-21.6	415.7	7.6	-51.7	1	1
3.9	-21.7	415.7	7.6	-53.2	1	1
4.0	-21.8	415.6	7.7	-54.3	1	1

4.1	-21.7	415.4	7.9	-54.7	1	1
4.2	-21.7	415.2	8.1	-54.5	1	1
4.3	-21.5	414.8	8.3	-53.7	1	1
4.4	-21.3	414.5	8.5	-52.4	1	1
4.5	-21.1	414.0	8.8	-50.6	1	1
4.6	-20.9	413.5	9.0	-48.3	1	1
4.7	-20.6	413.0	9.2	-45.6	1	1
4.8	-20.3	412.4	9.3	-42.6	1	1
4.9	-20.0	411.8	9.5	-39.2	1	1
5.0	-19.7	411.1	9.6	-35.5	1	1
5.1	-19.3	410.5	9.7	-31.6	1	1
5.2	-19.0	409.9	9.8	-27.4	1	1
5.3	-18.6	409.2	9.8	-22.9	1	1
5.4	-18.2	408.6	9.8	-18.7	1	1
5.5	-17.7	407.9	9.8	-14.7	1	1
5.6	-17.3	407.3	9.8	-11.1	1	1
5.7	-16.7	406.7	9.8	-7.7	1	1
5.8	-16.1	406.1	9.8	-4.6	1	1
5.9	-15.5	405.5	9.7	-1.9	1	1
6.0	-14.7	404.9	9.6	0.5	1	1
6.1	-13.9	404.4	9.5	2.4	1	1
6.2	-13.0	403.8	9.4	4.2	1	1
6.3	-12.1	403.3	9.3	6.0	1	1
6.4	-11.0	402.8	9.2	7.6	1	1
6.5	-9.9	402.3	9.1	9.2	1	1
6.6	-8.8	401.9	9.0	10.6	1	1
6.7	-7.6	401.4	8.9	11.9	1	1
6.8	-6.4	401.0	8.9	12.9	1	1
6.9	-5.1	400.6	8.8	13.7	1	1
7.0	-3.8	400.2	8.8	14.3	1	1
7.1	-2.5	399.7	8.8	15.0	1	1
7.2	-1.2	399.3	8.8	16.0	1	1
7.3	0.1	399.0	8.8	17.1	1	1
7.4	1.5	398.6	8.9	18.4	1	1
7.5	2.8	398.2	8.9	19.8	1	1
7.6	4.1	397.8	8.9	21.3	1	1
7.7	5.3	397.5	9.0	22.8	1	1
7.8	6.6	397.1	9.0	24.4	1	1
7.9	7.7	396.8	9.0	26.0	1	1
8.0	8.9	396.5	9.0	27.5	1	1
8.1	9.9	396.2	8.9	29.0	1	1
8.2	11.0	395.9	8.9	30.5	1	1
8.3	11.9	395.6	8.9	32.0	1	1
8.4	12.8	395.4	8.8	33.4	1	1
8.5	13.5	395.2	8.8	34.8	1	1

8.6	14.2	395.0	8.7	36.2	1	1
8.7	14.8	394.9	8.7	37.7	1	1
8.8	15.3	394.8	8.6	39.1	1	1
8.9	15.7	394.7	8.6	40.6	1	1
9.0	16.0	394.7	8.5	42.1	1	1
9.1	16.1	394.7	8.5	43.7	1	1
9.2	16.1	394.7	8.5	45.1	1	1
9.3	16.1	394.8	8.6	46.1	1	1
9.4	15.9	394.9	8.7	46.7	1	1
9.5	15.6	395.0	8.9	47.0	1	1
9.6	15.2	395.2	9.0	47.0	1	1
9.7	14.7	395.3	9.2	46.8	1	1
9.8	14.2	395.5	9.4	46.3	1	1
9.9	13.6	395.8	9.6	45.7	1	1
10.0	12.9	396.0	9.8	44.9	1	1
10.1	12.2	396.2	10.0	44.0	1	1
10.2	11.5	396.5	10.2	43.1	1	1
10.3	10.7	396.7	10.4	43.0	1	1
10.4	9.8	397.0	10.6	42.4	1	1
10.5	9.0	397.2	10.7	41.5	1	1
10.6	8.1	397.5	10.9	40.2	1	1
10.7	7.2	397.7	11.0	38.7	1	1
10.8	6.3	398.0	11.0	36.9	1	1
10.9	5.4	398.2	10.9	35.0	1	1
11.0	4.5	398.4	10.8	32.9	1	1
11.1	3.7	398.6	10.7	30.7	1	1
11.2	2.8	398.8	10.4	28.4	1	1
11.3	2.0	399.0	10.1	26.0	1	1
11.4	1.3	399.1	9.7	23.5	1	1
11.5	0.6	399.3	9.2	20.8	1	1
11.6	0.0	399.4	8.7	17.9	1	1
11.7	-0.6	399.5	8.2	14.9	1	1
11.8	-1.1	399.6	7.8	11.6	1	1
11.9	-1.5	399.7	7.4	8.1	1	1
12.0	-1.9	399.8	7.0	4.3	1	1
12.1	-2.1	399.8	6.6	0.1	1	1
12.2	-2.3	399.9	6.3	-4.4	1	1
12.3	-2.4	399.9	6.1	-9.3	1	1
12.4	-2.4	400.0	5.9	-14.5	1	1
12.5	-2.3	400.0	5.8	-19.9	1	1
12.6	-2.1	400.0	5.7	-25.5	1	1
12.7	-1.8	400.0	5.7	-31.2	1	1
12.8	-1.5	400.0	5.8	-36.8	1	1
12.9	-1.1	400.0	5.9	-42.3	1	1
13.0	-0.6	400.0	6.1	-47.6	1	1

13.1	-0.2	400.0	6.3	-52.6	1	1

CM IN RADAR CONE	100.0000	PERCENT
CMMCA W/IN STRUCTURAL LIMITS	100.0000	PERCENT

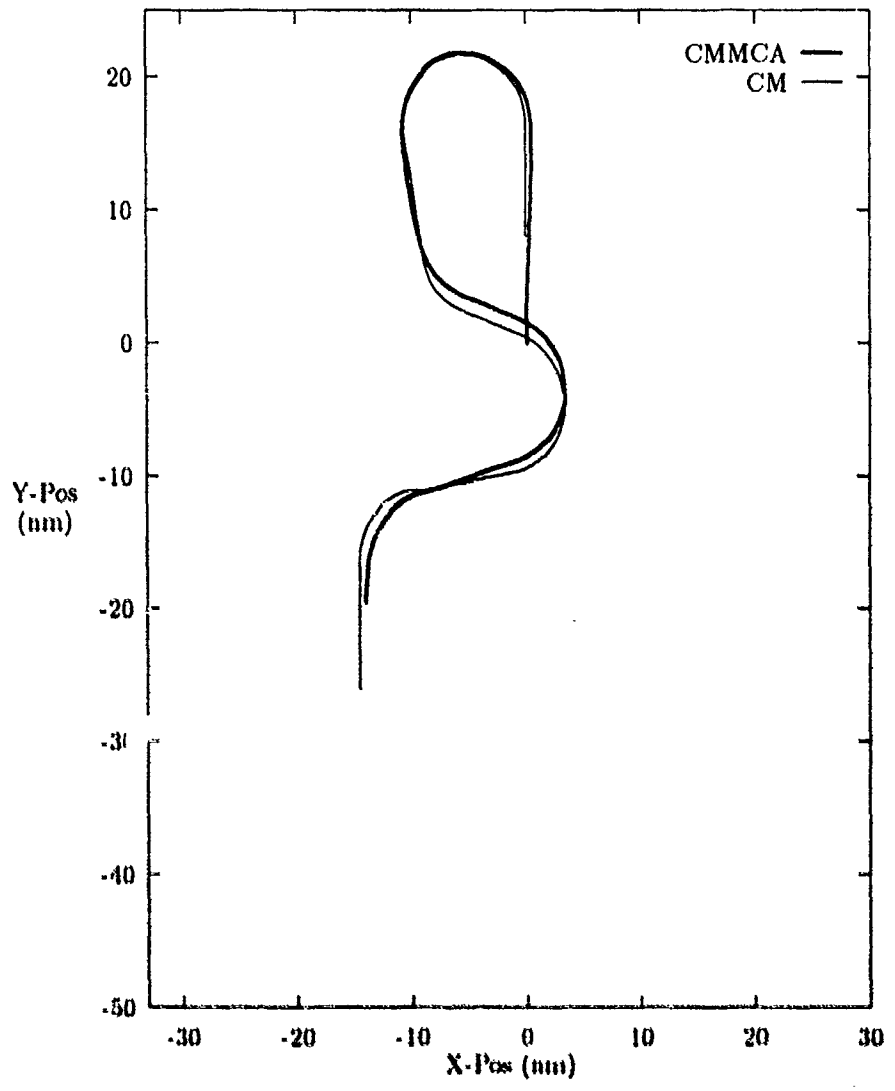

Figure 59. Section 2 CMMCA and CM Paths, CMMCA Starting Trailing

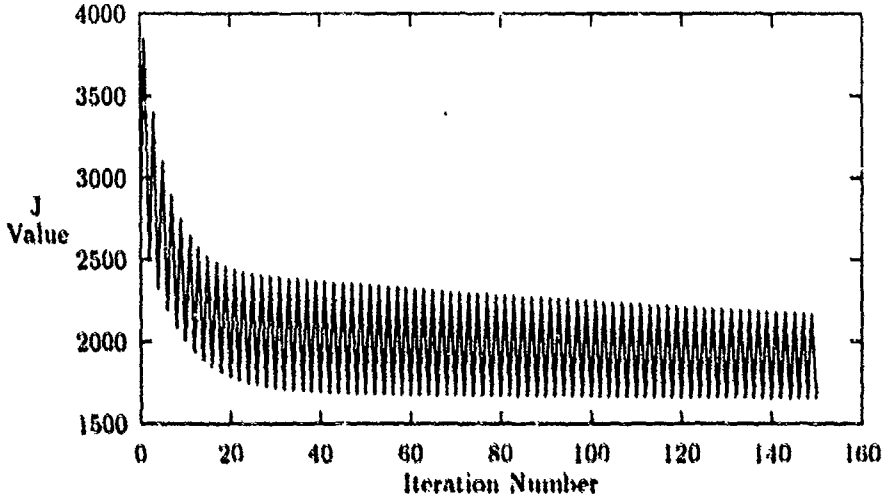

Figure 60. Plot of J Value versus Iteration Number

JSTOP = 1654.592
# ITERATIONS = 150

T	BANK	SPEED	RANGE	THETA	RADAR	STRUCT
0.1	1.8	400.9	8.0	-0.3	1	1
0.2	1.6	400.9	8.0	-0.8	1	1
0.3	1.4	400.9	8.0	-1.3	1	1
0.4	1.2	400.9	8.0	-1.8	1	1
0.5	1.0	400.9	8.0	-2.2	1	1
0.6	0.8	401.0	8.0	-2.6	1	1
0.7	0.7	401.0	8.0	-3.0	1	1
0.8	0.5	401.0	8.0	-3.4	1	1
0.9	0.3	401.0	8.0	-3.7	1	1
1.0	0.1	401.0	8.0	-4.0	1	1
1.1	-0.1	401.1	8.0	-4.2	1	1
1.2	-0.2	401.1	8.0	-4.4	1	1
1.3	-0.4	401.1	8.0	-4.5	1	1
1.4	-0.6	401.1	8.0	-5.2	1	1
1.5	-0.8	401.1	8.0	-6.4	1	1
1.6	-0.9	401.2	8.0	-8.1	1	1
1.7	-1.1	401.2	7.9	-10.4	1	1
1.8	-1.2	401.2	7.9	-13.1	1	1
1.9	-1.3	401.2	7.8	-16.5	1	1
2.0	-1.3	401.2	7.7	-20.3	1	1
2.1	-1.4	401.2	7.6	-24.7	1	1
2.2	-1.4	401.2	7.6	-29.7	1	1
2.3	-1.3	401.2	7.5	-35.2	1	1
2.4	-1.3	401.1	7.5	-41.3	1	1
2.5	-21.9	411.2	7.5	-44.8	1	1
2.6	-21.4	411.3	7.5	-45.5	1	1
2.7	-30.3	416.7	7.6	-44.8	1	0
2.8	-30.1	417.0	7.6	-42.6	1	0
2.9	-21.8	412.5	7.5	-41.7	1	1
3.0	-22.3	412.9	7.5	-42.2	1	1
3.1	-21.9	412.7	7.5	-42.7	1	1
3.2	-22.5	413.1	7.5	-43.2	1	1
3.3	-22.7	413.2	7.5	-43.7	1	1
3.4	-23.1	413.3	7.5	-44.1	1	1
3.5	-22.9	413.1	7.5	-44.5	1	1
3.6	-23.5	413.2	7.5	-44.9	1	1
3.7	-23.5	413.0	7.5	-45.2	1	1
3.8	-24.1	413.0	7.5	-45.4	1	1
3.9	-24.1	412.7	7.5	-45.7	1	1
4.0	-24.5	412.5	7.5	-45.5	1	1

4.1	-24.3	412.0	7.6	-44.6	1	1
4.2	-24.6	411.7	7.7	-43.1	1	1
4.3	-25.1	411.5	7.8	-40.8	1	1
4.4	-24.4	410.6	7.9	-37.9	1	1
4.5	-25.2	410.5	8.0	-34.4	1	1
4.6	-24.9	409.8	8.1	-30.2	1	1
4.7	-25.2	409.4	8.2	-25.3	1	1
4.8	-24.9	408.8	8.2	-19.9	1	1
4.9	-32.4	411.5	8.2	-12.5	1	0
5.0	-3.6	399.9	8.2	-7.8	1	1
5.1	-4.0	400.0	8.2	-7.2	1	1
5.2	-3.8	399.9	8.3	-6.5	1	1
5.3	-3.7	399.9	8.3	-5.8	1	1
5.4	-3.5	399.8	8.3	-5.6	1	1
5.5	-3.9	399.9	8.2	-5.9	1	1
5.6	-3.7	399.8	8.2	-6.6	1	1
5.7	-3.6	399.7	8.2	-7.9	1	1
5.8	-3.3	399.6	8.1	-9.7	1	1
5.9	-3.6	399.7	8.0	-12.0	1	1
6.0	-3.3	399.6	7.9	-14.7	1	1
6.1	-3.1	399.5	7.8	-18.1	1	1
6.2	-2.7	399.4	7.8	-21.8	1	1
6.3	-3.0	399.5	7.7	-25.5	1	1
6.4	-23.2	404.3	7.7	-26.0	1	1
6.5	-23.0	404.0	7.7	-23.0	1	1
6.6	-22.8	403.7	7.7	-19.6	1	1
6.7	-22.2	403.5	7.7	-15.7	1	1
6.8	-21.4	403.2	7.7	-11.4	1	1
6.9	-21.7	403.2	7.7	-6.8	1	1
7.0	-21.0	403.1	7.7	-1.6	1	1
7.1	-20.5	403.0	7.7	4.6	1	1
7.2	-7.0	400.1	7.7	9.6	1	1
7.3	0.4	398.7	7.7	12.5	1	1
7.4	0.8	398.6	7.7	14.8	1	1
7.5	0.9	398.6	7.7	17.7	1	1
7.6	1.3	398.6	7.7	21.0	1	1
7.7	1.3	398.6	7.6	24.9	1	1
7.8	1.6	398.6	7.6	29.2	1	1
7.9	1.6	398.6	7.6	34.0	1	1
8.0	1.9	398.6	7.7	39.3	1	1
8.1	22.7	393.7	7.7	41.6	1	1
8.2	22.5	393.7	7.7	40.8	1	1
8.3	22.9	393.6	7.8	40.0	1	1
8.4	22.9	393.5	7.8	39.1	1	1
8.5	22.8	393.5	7.8	38.2	1	1

8.6	22.7	393.7	7.8	37.3	1	1
8.7	23.0	393.7	7.8	36.5	1	1
8.8	22.9	393.9	7.7	35.7	1	1
8.9	22.9	394.1	7.7	34.9	1	1
9.0	22.6	394.3	7.6	34.2	1	1
9.1	22.8	394.5	7.5	33.6	1	1
9.2	22.4	394.8	7.5	32.5	1	1
9.3	22.4	395.1	7.5	31.1	1	1
9.4	22.0	395.4	7.5	29.1	1	1
9.5	22.2	395.7	7.6	26.7	1	1
9.6	21.6	396.1	7.6	23.8	1	1
9.7	21.6	396.4	7.6	20.5	1	1
9.8	21.5	396.6	7.7	16.6	1	1
9.9	21.1	397.0	7.7	12.2	1	1
10.0	21.2	397.2	7.7	7.4	1	1
10.1	17.5	398.0	7.7	2.6	1	1
10.2	0.4	400.3	7.7	0.6	1	1
10.3	-0.1	400.4	7.7	2.2	1	1
10.4	-0.1	400.4	7.7	3.3	1	1
10.5	-0.2	400.4	7.7	3.8	1	1
10.6	-0.1	400.3	7.6	3.6	1	1
10.7	-0.7	400.4	7.6	2.9	1	1
10.8	-0.7	400.4	7.6	1.7	1	1
10.9	-0.7	400.4	7.5	-0.2	1	1
11.0	-0.6	400.4	7.5	-2.6	1	1
11.1	-1.1	400.4	7.3	-5.6	1	1
11.2	-0.9	400.4	7.2	-9.1	1	1
11.3	31.6	398.1	7.1	-13.8	1	0
11.4	-21.6	401.7	7.0	-26.4	1	1
11.5	-21.0	401.5	6.8	-26.3	1	1
11.6	-21.1	401.4	6.7	-26.3	1	1
11.7	-20.8	401.2	6.7	-26.1	1	1
11.8	-20.7	401.0	6.6	-25.4	1	1
11.9	-20.6	400.9	6.6	-24.2	1	1
12.0	-20.2	400.8	6.6	-22.8	1	1
12.1	-20.4	400.6	6.6	-20.3	1	1
12.2	-20.1	400.5	6.7	-17.5	1	1
12.3	-19.9	400.4	6.7	-14.2	1	1
12.4	-20.0	400.3	6.7	-10.3	1	1
12.5	-20.1	400.2	6.7	-5.8	1	1
12.6	-17.9	400.1	6.7	-1.1	1	1
12.7	0.3	399.9	6.7	1.0	1	1
12.8	0.2	400.0	6.7	0.6	1	1
12.9	0.1	400.0	6.7	0.1	1	1
13.0	0.1	400.0	6.7	-0.3	1	1

13.1	0.0	400.0	6.7	-0.7	1	1

CM IN RADAR CONE	100.0000	PERCENT
CMMCA W/IN STRUCTURAL LIMITS	96.94656	PERCENT

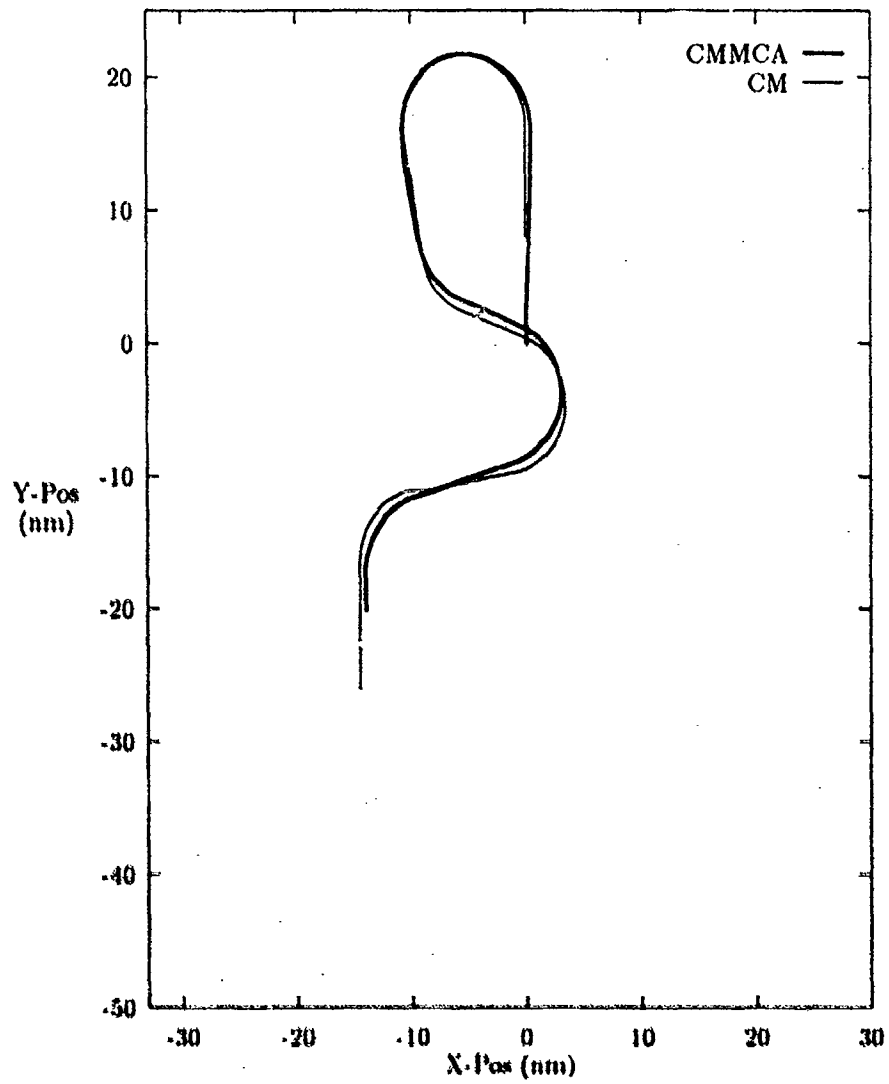

Figure 61. Section 2 CMMCA and CM Paths, CMMCA Starting Trailing

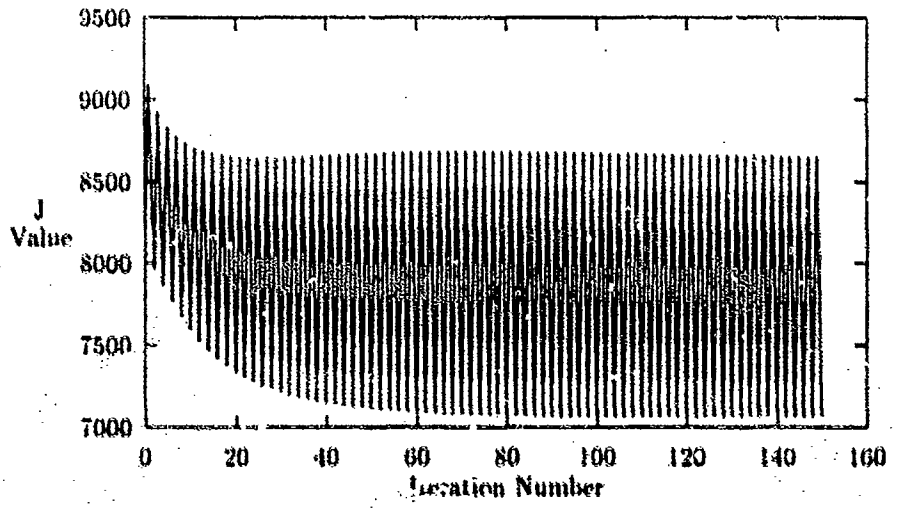

Figure 62. Plot of J Value versus Iteration Number

JSTOP = 7064.657
# ITERATIONS = 150

T	BANK	SPEED	RANGE	THETA	RADAR	STRUCT
0.1	1.6	401.1	8.0	-0.2	1	1
0.2	1.4	401.1	8.0	-0.7	1	1
0.3	1.2	401.1	8.0	-1.1	1	1
0.4	1.1	401.1	8.0	-1.6	1	1
0.5	0.9	401.1	8.0	-2.0	1	1
0.6	0.7	401.2	8.0	-2.4	1	1
0.7	0.6	401.2	8.0	-2.7	1	1
0.8	0.4	401.2	8.0	-3.0	1	1
0.9	0.2	401.2	8.0	-3.3	1	1
1.0	0.1	401.3	8.0	-3.5	1	1
1.1	-0.1	401.3	8.0	-3.7	1	1
1.2	-0.2	401.3	8.0	-3.9	1	1
1.3	-0.4	401.3	8.0	-4.0	1	1
1.4	-0.6	401.4	8.0	-4.6	1	1
1.5	-0.7	401.4	8.0	-5.8	1	1
1.6	-0.9	401.4	7.9	-7.5	1	1
1.7	-1.0	401.5	7.9	-9.8	1	1
1.8	-1.1	401.5	7.8	-12.5	1	1
1.9	-1.1	401.5	7.8	-15.9	1	1
2.0	-1.1	401.5	7.7	-19.8	1	1
2.1	-1.1	401.5	7.6	-24.3	1	1
2.2	-1.0	401.4	7.5	-29.4	1	1
2.3	-0.9	401.4	7.5	-35.0	1	1
2.4	-0.8	401.3	7.5	-41.3	1	1
2.5	-22.9	414.6	7.5	-44.7	1	1
2.6	-22.2	416.0	7.5	-45.3	1	1
2.7	-31.6	422.2	7.5	-44.4	1	0
2.8	-31.3	422.5	7.5	-42.0	1	0
2.9	-22.5	416.5	7.5	-40.9	1	1
3.0	-22.9	417.0	7.4	-41.3	1	1
3.1	-22.4	416.8	7.4	-41.8	1	1
3.2	-23.0	417.3	7.4	-42.3	1	1
3.3	-23.2	417.4	7.4	-42.7	1	1
3.4	-23.6	417.6	7.4	-43.1	1	1
3.5	-23.3	417.3	7.3	-43.5	1	1
3.6	-23.9	417.4	7.3	-44.0	1	1
3.7	-23.8	417.1	7.3	-44.3	1	1
3.8	-24.4	417.1	7.3	-44.6	1	1
3.9	-24.4	416.7	7.3	-44.9	1	1
4.0	-24.8	416.5	7.3	-44.7	1	1

4.1	-24.6	415.7	7.4	-43.9	1	1
4.2	-24.9	415.4	7.5	-42.4	1	1
4.3	-25.4	415.1	7.6	-40.1	1	1
4.4	-24.6	414.0	7.7	-37.2	1	1
4.5	-25.5	413.8	7.8	-33.6	1	1
4.6	-25.1	412.9	7.9	-29.4	1	1
4.7	-25.5	412.4	8.0	-24.4	1	1
4.8	-25.2	411.6	8.0	-18.9	1	1
4.9	-33.0	415.3	8.0	-11.3	1	0
5.0	-2.5	399.7	8.0	-6.5	1	1
5.1	-3.0	399.9	8.0	-6.1	1	1
5.2	-2.8	399.7	8.0	-5.6	1	1
5.3	-2.8	399.7	8.0	-5.0	1	1
5.4	-2.6	399.6	8.0	-5.0	1	1
5.5	-3.1	399.7	8.0	-5.6	1	1
5.6	-2.9	399.6	8.0	-6.6	1	1
5.7	-2.7	399.5	7.9	-8.1	1	1
5.8	-2.5	399.4	7.9	-10.3	1	1
5.9	-2.9	399.5	7.8	-12.9	1	1
6.0	-2.5	399.4	7.7	-16.1	1	1
6.1	-2.3	399.3	7.6	-19.9	1	1
6.2	-1.8	399.2	7.5	-24.1	1	1
6.3	-2.1	399.3	7.5	-28.2	1	1
6.4	-23.8	405.9	7.5	-28.9	1	1
6.5	-23.5	405.5	7.6	-26.0	1	1
6.6	-23.3	405.1	7.6	-22.5	1	1
6.7	-22.8	404.7	7.6	-18.6	1	1
6.8	-22.0	404.3	7.6	-14.3	1	1
6.9	-22.3	404.4	7.6	-9.5	1	1
7.0	-21.6	404.1	7.6	-4.2	1	1
7.1	-21.2	404.0	7.6	2.1	1	1
7.2	-6.8	400.1	7.6	7.2	1	1
7.3	1.1	398.1	7.6	10.0	1	1
7.4	1.4	398.1	7.6	12.1	1	1
7.5	1.4	398.1	7.5	14.8	1	1
7.6	1.7	398.0	7.5	18.0	1	1
7.7	1.6	398.1	7.5	21.8	1	1
7.8	1.9	398.0	7.4	26.1	1	1
7.9	1.7	398.1	7.4	30.9	1	1
8.0	1.8	398.1	7.4	36.3	1	1
8.1	24.1	391.6	7.4	38.5	1	1
8.2	23.8	391.6	7.4	37.4	1	1
8.3	24.0	391.5	7.4	36.2	1	1
8.4	23.8	391.6	7.4	35.0	1	1
8.5	23.6	391.7	7.4	34.0	1	1

8.6	23.3	391.9	7.3	33.0	1	1
8.7	23.4	392.0	7.2	32.1	1	1
8.8	23.1	392.3	7.2	31.3	1	1
8.9	23.0	392.6	7.1	30.6	1	1
9.0	22.5	393.0	7.0	30.2	1	1
9.1	22.6	393.3	6.9	29.8	1	1
9.2	22.1	393.7	6.9	29.1	1	1
9.3	22.0	394.1	6.9	27.9	1	1
9.4	21.5	394.5	6.9	26.3	1	1
9.5	21.7	394.9	6.9	24.2	1	1
9.6	21.0	395.4	6.9	21.6	1	1
9.7	20.9	395.7	6 9	18.5	1	1
9.8	20.9	396.1	7.0	14.8	1	1
9.9	20.5	396.5	7.0	10.6	1	1
10.0	20.8	396.8	7.0	5.9	1	1
10.1	16.9	397.8	7.0	1.2	1	1
10.2	-1.2	400.6	7.0	-0.6	1	1
10.3	-1.7	400.7	7.0	1.5	1	1
10.4	-1.6	400.7	6.9	3.0	1	1
10.5	-1.6	400.7	6.9	3.9	1	1
10.6	-1.4	400.6	6.9	4.0	1	1
10.7	-1.9	400.7	6.9	3.6	1	1
10.8	-1.8	400.7	6.9	2.6	1	1
10.9	-1.7	400.7	6.8	1.0	1	1
11.0	-1.5	400.6	6.7	-1.3	1	1
11.1	-1.8	400.7	6.6	-4.3	1	1
11.2	-1.5	400.6	6.5	-7.9	1	1
11.3	33.4	397.7	6.4	-18.3	1	0
11.4	-23.7	402.3	6.3	-26.4	1	1
11.5	-22.8	402.0	6.2	-26.2	1	1
11.6	-22.7	401.9	6.1	-26.3	1	1
11.7	-22.2	401.6	6.0	-26.0	1	1
11.8	-21.9	401.5	6.0	-25.2	1	1
11.9	-21.7	401.3	6.0	-23.8	1	1
12.0	-21.1	401.1	6.0	-21.8	1	1
12.1	-21.4	400.9	6.0	-19.2	1	1
12.2	-20.9	400.7	6.1	-16.0	1	1
12.3	-20.8	400.6	6.1	-12.1	1	1
12.4	-20.9	400.5	6.1	-7.6	1	1
12.5	-21.1	400.4	6.1	-2.4	1	1
12.6	-18.8	400.2	6.1	3.2	1	1
12.7	0.7	399.9	6.1	6.0	1	1
12.8	0.5	400.0	6.1	6.1	1	1
12.9	0.3	400.0	6.1	6.2	1	1
13.0	0.2	400.0	6.1	6.3	1	1

13.1	0.0	400.0	6.1	6.5	1	1

CM IN RADAR CONE	100.0000	PERCENT
CMMCA W/IN STRUCTURAL LIMITS	96.94656	PERCENT

Bibliography

1. Baker, Lt Col W. P. Deputy Department Head and Assistant Professor, Department of Mathematics and Statistics. Personal Interviews. Air Force Institute of Technology (AU), Wright-Patterson AFB OH, December 1991 through January 1992.
2. Baker, W. P. *CMMCA Cost Functional.* Unpublished report. Air Force Institute of Technology (AU), Wright-Patterson AFB OH, 1988.
3. Bekey, George A. *Simulability of Dynamical Systems*, Transactions of the Society for Computer Simulation, 2:57-70 (May 1985).
4. Garton, Capt Antoine M. ARIA/CMMCA Programs Division. Personal Interviews. 4950th Test Wing, Wright-Patterson AFB OH, August 1991 through March 1992.
5. Garton, Capt Antoine M. Using Simulation to Determine a Strategy for Positively Tracking a Cruise Missile by CMMCA. MS Thesis, AFIT/GST/ENS/90M-6. School of Engineering, Air Force Institute of Technology (AU), Wright Patterson AFB OH, March 1990. (AD-A220526)
6. Guelman, M. *Proportional Navigation with a Maneuvering Target*, IEEE Transactions on Aerospace and Electronic Systems, 8:364-371 (May 1972).
7. Heavner, Capt Leonard G. An Investigation into the Application of Dynamic Programming to Determine the Optimal Controls for Tracking a Cruise Missile Maneuver by CMMCA. MS Thesis, AFIT/GST/ENS/89M-6. School of Engineering, Air Force Institute of Technology (AU), Wright Patterson AFB OH, March 1989.
8. Kirk, Donald E. Optimal Control Theory. Englewood Cliffs, NJ: Prentice-Hall, Inc. 1970
9. Mahapatra, P.R. and U.S. Shukla. *Accurate Solution of Proportional Navigation for Maneuvering Targets*, IEEE Transactions on Aerospace and Electronic Systems, 25:81-88 (January 1989).
10. Pritsker, A. Alan B. Introduction to Simulation and SLAM II (Third Edition). New York: Halsted Press, 1986.
11. Sargent, Robert G. *A Tutorial on Validation and Verification of Simulation Models*, Proceedings of the 1988 Winter Simulation Conference. 33-39. San Diego CA, 1988.
12. Schuppe, Col Thomas F. Department Head and Assistant Professor, Department of Operational Sciences. Personal Interviews. Air Force Institute of Technology (AU), Wright-Patterson AFB OH, August 1991 through March 1992.

13. Stanislaw, Harold. *Tests of Computer Simulation Validity*, Simulation and Games, 17:173-191 (June 1986).

14. Stewart, Stephen J. *Flight Simulation for Museums*, Simulation, 51:235-241 (December 1988).

15. Walls, Justin and others. *A Mathematical Model of the Orbital Maneuvering Vehicle*, Simulation, 48:98-102 (March 1987).

Vita

Captain Andrew C. Hachman was born on 2 October 1964 in Salt Lake City, Utah. He graduated from Skyline High School in Salt Lake City in 1982 and Attended Washington State University, graduating with a Bachelor of Science in Electrical Engineering in May 1986. Upon graduation he received a commission in the US Air Force through ROTC and served his first tour of duty at Kelly AFB, Texas. Captain Hachman served as an Electronic Warfare Test Engineer and Radar Systems Analyst for the Air Force Electronic Warfare Center (AFEWC), where he organized and directed tests of Air Force aircrew training devices and electronic warfare ground threat simulator systems. He also supervised AFEWC test teams providing electronic test and measurement support to various Air Force major commands and other DoD agencies, until entering the School of Engineering, Air Force Institute of Technology, in August 1990.

Capt Hachman is married to the former Shelley Lee DiStasio of Campton, New Hampshire.

Permanent address: N.E. 435 Campus St
Pullman, WA 99163